University of New Orleans

ScholarWorks@UNO

University of New Orleans Theses and Dissertations

Dissertations and Theses

Spring 5-16-2014

One-Dimensional Dynamic Modeling of the Lower Mississippi River

Tshering T. Gurung
Civil & Environmental Engineering Department, ttgurung@uno.edu

Follow this and additional works at: https://scholarworks.uno.edu/td

Part of the Civil Engineering Commons, Environmental Engineering Commons, and the Hydraulic Engineering Commons

Recommended Citation

Gurung, Tshering T., "One-Dimensional Dynamic Modeling of the Lower Mississippi River" (2014). *University of New Orleans Theses and Dissertations*. 1804.
https://scholarworks.uno.edu/td/1804

This Thesis is protected by copyright and/or related rights. It has been brought to you by ScholarWorks@UNO with permission from the rights-holder(s). You are free to use this Thesis in any way that is permitted by the copyright and related rights legislation that applies to your use. For other uses you need to obtain permission from the rights-holder(s) directly, unless additional rights are indicated by a Creative Commons license in the record and/or on the work itself.

This Thesis has been accepted for inclusion in University of New Orleans Theses and Dissertations by an authorized administrator of ScholarWorks@UNO. For more information, please contact scholarworks@uno.edu.

One-Dimensional Dynamic Modeling of the Lower Mississippi River

A Thesis

Submitted to the Graduate Faculty of the
University of New Orleans
in partial fulfillment of the
requirements for the degree of

Master of Science
In
Civil & Environmental Engineering
(Water Resources)

by

Tshering T. Gurung

B.Sc. University of New Orleans, 2012

May 2014

© 2014, Tshering Gurung

Dedications

In the memory of my loving mother

Sermu Gurung

Acknowledgements

I would like to foremost thank Dr. J. Alex McCorquodale for giving me the opportunity to be a part of this research. His guidance and support provided during this study has made this research possible.

I would also like to thank the Lake Pontchartrain Basin Foundation for funding part of the research. Dr. John Lopez and Dr. Ezra Boyd from LPBF provided data such as flow estimates and height of land survey data around Bohemia reach including channel dimension surveys for Mardi Gras Pass.

This research was funded in part by National Science Foundation (NSF) as a part of the Northern Gulf Coastal Hazards Collaboratory (NG-CHC; http:\\ngchc.org).

I would also like to thank Mississippi Hydro-study, and Coastal Protection and Restoration Authority (CPRA) for financially assisting the study.

I would like to thank Dr. Forrest Holly for giving permission to use the CHARIMA model for free of cost. Without his documentation and development of the model, this study would not have been possible.

I would like to thank Dr. Mead Allison for making available the field data that was used extensively for sand transport modeling.

I would like to thank the LSU research group working on ADCIRC model of the Gulf which provided with important data for Hurricane simulation.

I would like to thank Dr. Joao Pereira for his guidance and support during my initial phase of the research. His availability to help promptly for any issues related to the study was a big help.

I would like to thank the committee members, Dr. Malay G. Hajra and Dr. Gianna M. Cothren for their help and suggestions.

I would like to thank my co-workers at the University of New Orleans during my study: Ms. Grecia Teran, Ms. Tatiana Pavlyukova, Mr. Sina Amini, Mr. John Edgar Dimitri Filostrat and Mrs. Nina Reins.

I would also like to thank my roommates in Pasteur Blvd for their company and support during my stay in New Orleans for the study.

Finally, I would like to thank my parents and sisters for enduring me for all these years and supporting my choice to continue my studies. I would like to thank my grandmother for all the love and prayers.

Table of Contents

List of Figures viii
List of Tables xi
Nomenclature xii
Abstract xiv
Chapter 1: Introduction 1
1.1 Background 1
1.2 Objectives 2
1.3 General Approach 3
Chapter 2: Literature Review 5
2.1 Description of Numerical Models 5
2.2 Parameters for Numerical model selection 6
2.3 Numerical modeling of Mississippi River 7
Chapter 3: Existing and Future Conditions of the Mississippi River Domain 9
3.1 Modeled Reach 9
3.2 Existing Diversions 9
3.3 Future MLODS Diversions 10
2.1.2 Scenarios considered for model simulation 11
Chapter 4: Description of the Models 12
4.1 Description of HEC-RAS 12
4.1.1 Geometric Data Editor 12
4.1.2 Unsteady Flow Data Editor 13
4.1.3 Unsteady Flow Analysis Editor 14
4.2 Governing Equations 14
4.2.1 Conservation of Mass (Continuity) 14
4.2.2 Conservation of Momentum 17
4.3 Finite Difference Method 21
4.4 Description of CHARIMA 22
4.4.1 Components of Geometry of CHARIMA 23

4.4.2 Data Input Files 23
4.4.3 Result Output Files 24
4.4.4 Governing Equations for CHARIMA 24
4.4.5 The sediment Transport Formula 26
Chapter 5: Model Development 28
5.1 HEC-RAS Model Development 28
5.1.1 Geometry Data 28
5.1.2 Channel Roughness 37
5.1.3 Boundary Conditions 39
5.2 CHARIMA Model Development 41
5.2.1 Geometry Data 41
5.2.2 Channel Roughness 44
5.2.3 Boundary Conditions for CHARIMA 45
Chapter 6: Calibration and Validation 48
6.1 HEC-RAS Model Calibration 48
6.2 HEC-RAS Model Validation 52
6.3 CHARIMA Model Calibration 54
6.4 CHARIMA Model Validation 59
Chapter 7: Applications 62
7.1 Hurricane Surge Calculation 62
7.1.1 Surge Calculation 67
7.2 Surge for different flow scenarios 68
7.3 Simulations with addition of MLODS diversions and Pass Closure 70
7.3.1 Existing and future MLODS diversions with Pass Closure (HEC-RAS) 70
7.3.2 Existing and future MLODS diversions with Pass Closure (CHARIMA) 73
7.4 Mardi Gras Pass Simulations 81
Chapter 8: Summary of Findings and Discussion 84
Chapter 9: Conclusions 86
References 87
Appendix A: 90
Boundary Condition: 90
Appendix B: 97

Calibration and Validation Results 97
Appendix C 137
Manning's n Values in HEC-RAS model 137
Appendix D 177
Flow Roughness Factor in HEC-RAS model 177
Appendix E 179
Strickler's Coefficient Values in CHARIMA model 179
VITA 202

List of Figures

Figure 1-1: Google Earth image of the Model domain. 2
Figure 1-2: HEC-RAS Model Schematic Overlaying Satellite Imagery (Pereira et al.2010). 4
Figure 2-1: Existing and future diversions in the model domain. (Google Earth Imagery, 2013) 10
Figure 3-1: Representative Control Volume for derivation of Continuity equations. 15
Figure 3-2: Representative Control Volume for Conservation of Momentum. 17
Figure 4-3: Computational Grid for the box scheme. 22
Figure 5-1: Existing Outflows located in Lower Mississippi River marked in Google Earth image. 28
Figure 5-2: LPBF Survey for Bohemia Reach where the distance is measured from upriver (RM 44) to downriver (RM 31). 29
Figure 5-3: Bohemia weirs installed in HEC-RAS Model corresponding to LPBF Survey Data. 31
Figure 5-4: Bohemia reach with the survey data path plotted in Google Earth image (RM 31 to RM 44). 31
Figure 5-5: Ostrica outlets marked on Google Earth image (RM 22 to RM 26). 33
Figure 5-6: Ostrica equivalent channel cross-section in HEC-RAS model. 33
Figure 5-7: Fort St. Philip cuts from Google Earth image(RM 18 to RM 21). 34
Figure 5-8: Fort St. Philip equivalent channel cross-section in HEC-RAS model. 34
Figure 5-9: 7 cuts weir outlets marked on Google Earth image (RM 11 to RM 18). 35
Figure 5-10: 7 cuts weir equivalent channel in HEC-RAS model. 36
Figure 5-11: Southwest pass marked with cuts on Google Earth image. 36
Figure 5-12: HEC-RAS upstream flow boundary for 2011. 39
Figure 5-13: HEC-RAS daily stage downstream stage boundary for 2011. 40
Figure 5-13: HEC-RAS hourly stage downstream stage boundary for 2011. 40
Figure 5-14: Lateral flow extraction hydrograph for Morganza and Bonnet Carré spillway for 2011(Note-Negative value indicates outflow). 41
Figure 5-15: Schematic diagram for CHARIMA model with existing diversions. 42

Figure 5-16: Existing and future diversions in the CHARIMA model domain. 43
Figure 5-17: Fort St. Philip reach showing the 3 equivalent channels used in CHARIMA model (Google Earth Image). 44
Figure 5-18: CHARIMA model upstream flow boundary for 2009 45
Figure 5-19: CHARIMA model downstream stage boundary for 2009 46
Figure 5-20: Rating Curve used for calculation of the sediment boundary in CHARIMA model. (USGS) 46
Figure 5-21: CHARIMA model upstream sediment boundary for 2011. 47
Figure 6-1: Baton Rouge comparison of stage for 2011. 49
Figure 6-2: Carrollton comparison of stage for 2011. 49
Figure 6-3: Venice comparison of stage for 2011. 50
Figure 6-4: Peak flow comparison for 2011. 51
Figure 6-5: Baton Rouge stage comparison for 2008. 52
Figure 6-6: Carrollton stage comparison for 2008. 53
Figure 6-7: Peak flow comparison for 2008 54
Figure 6-8: Alliance stage comparison for 2009 55
Figure 6-9: Bohemia outflow comparison for 2009 56
Figure 6-10: Fort St. Philip outflow comparison for 2009 56
Figure 6-11: Sediment Concentration and Load comparison for 2009 at Myrtle Grove and Magnolia. 58
Figure 6-12: Alliance stage comparison for 2008. 59
Figure 6-13: Bohemia outflow comparison for 2008. 60
Figure 6-14: Fort St. Philip outflow comparison for 2008. 60
Figure 7-1: HEC-RAS downstream boundary condition for hurricane Gustav (2008). 62
Figure 7-2: HEC-RAS upstream boundary condition for hurricane Gustav (2008). 63
Figure 7-3: Carrollton stage comparison for hurricane Gustav (2008). 63
Figure 7-4: Algiers Lock stage comparison for hurricane Gustav (2008). 64
Figure 7-5: Downstream stage boundary for Hurricane Isaac (2012). 65
Figure 7-6: Upstream flow boundary for Hurricane Isaac (2012). 65
Figure 7-7: Bohemia stage boundary-Observed stages at Shell Beach-Impact Case- Isaac (2012). 66
Figure 7-8: Bonnet Carré stage comparison for Hurricane Isaac (2012). 66

Figure 7-9: Carrollton stage comparison for Hurricane Isaac (2012). 67
Figure 7-10: Surge height comparison for Hurricanes Isaac, Gustav and Katrina. 68
Figure 7-11: Comparison of River stage with surge comparison from Hurricane Gustav for different flow scenarios..... 69
Figure 7-12: Comparison of River stage with surge comparison from Hurricane Isaac for different flow scenarios..... 70
Figure 7-13: Outflows comparison for HEC-RAS on 4/25/2008 71
Figure 7-14: Outflows comparison for HEC-RAS on 4/25/2008 72
Figure 7-15: Outflows comparison for CHARIMA on 4/25/2008 73
Figure 7-16: Outflows comparison for CHARIMA on 4/25/2008 74
Figure 7-17: Outflows comparison for CHARIMA on 4/25/2008 75
Figure 7-18: Total Sand Load for outlets from CHARIMA model on 4/25/2008 76
Figure 7-19: Sediment to water ratio for outlets from CHARIMA model on 4/25/2008 77
Figure 7-20: Sediment to water ratio for outlets from CHARIMA model on 4/25/2008 77
Figure 7-21: Total Sand concentration in the MR from CHARIMA model on 4/25/2008 78
Figure 7-22: Total Discharge in the MR from CHARIMA model on 4/25/2008 79
Figure 7-23: Total Sand Load in the MR from CHARIMA model on 4/25/2008 80
Figure 7-24: Mardi Gras Pass in Google Earth image. 82
Figure 7-25: Rating Curve for the Mardi Gras Channel based on 2013 Survey..... 82
Figure 7-26: Flow Comparison for Mardi Gras Channel based on 2013 Survey. 83
Figure 7-27: SWR in Mardi Gras Channel based on 2013 Survey. 83
Figure 7-28: Total Sediment Load in Mardi Gras Channel based on 2013 Survey. 84

List of Tables

Table 2.1: Possible 1-D models that include sediment (Papanicolaou et al. 2008)..... 6
Figure 5.1: Sand Load Boundary Condition-Existing Outflow Case – 1-D Calibration 2009.... 47
Table 6.1: Error Analysis HEC-RAS stage Calibration - 2011..... 51
Table 6.2: Error Analysis HEC-RAS stage validation - 2008..... 53
Table 6.3: Error Analysis CHARIMA stage and flow Calibration – 2009..... 55
Table 6.4: Peak flows for Bohemia and Fort St. Philip in CHARIMA for Calibration – 2009.... 56
Table 6.5: Ratio of model to observed values for sand concentration for Calibration – 2009.... 57
Table 6.6: Error Analysis CHARIMA stage validation - 2008..... 59
Table 6.7: Error Analysis CHARIMA Flow validation – 2008 61
Table 6.7: Peak Flow for Bohemia and Fort St. Philip in CHARIMA for validation - 2008..... 61
Table 7.1: Error Analysis HEC-RAS Hurricane Gustav calibration - 2008..... 64
Table 7.2: Error Analysis HEC-RAS Hurricane Isaac validation - 2012 67

Nomenclature

Symbol	Description	Units
$\overline{C}$	Mean sediment concentration of suspended sediment.	M/L^3
$\overline{C_T}$	Sediment flux concentration (sediment mass flux per unit mass flow rate).	$M/L^3/M$
R_e^*	Particle Reynolds Number.	Dimensionless
$\overline{u_i}$	Mean flow velocity.	Dimensionless
∂	Partial differential operator.	
A	Cross-sectional Area.	L^2
a	Acceleration.	L/T^2
a_T	Temporal component of acceleration.	L/T^2
a_S	Spatial component of acceleration.	L/T^2
B	Top width of the cross-section.	L
C	Suspended Load Concentration.	M/L^3
C	Chezy coefficient.	$L^{1/2}/T$
c_1,c_2,c_3,c_4	Coefficients in Ackers-White Total-Load Predictor.	Dimensionless
c’	Conversion factor for Manning’s formula.	Dimensionless
C_D	Drag Coefficient.	Dimensionless
d	Particle diameter.	L
D	Total water column depth.	L
d_*	Dimensionless grain diameter.	Dimensionless
D_{50}	Median diameter of sediment.	L
d_{gr}	Dimensionless grain diameter.	Dimensionless
F_{gr}	Sediment mobility number.	Dimensionless
f_s	Silt factor.	
G	Acceleration due to gravity.	L/T^2
K	Conveyance.	L^3/T
K_s	Manning-Strickler Coefficient.	L^3T
n	Manning’s coefficient.	Dimensionless
P	Pressure.	$M/L/T^2$

P_w	Wetted Perimeter.	L
Q	Water discharge.	L^3/T
q	Lateral inflow.	$L^3/T/L$
R	Hydraulic radius.	L
s	Specific gravity of the particles.	Dimensionless
S	Sediment source or sink within the solution domain other than the boundaries.	$M/L^3/T$
S_f	Steady-state energy or Friction slope.	Dimensionless
T	Time.	T
u	Velocity component in the x-direction.	L/T
u_*	Shear velocity.	L/T
V	Mean velocity.	L/T
x	Abscissa measured along the river; spatial component.	L
y	Water surface elevation; spatial component.	L
z	Bed elevation; Spatial vertical component.	L
α	Momentum correction factor.	Dimensionless
γ	Specific weight of water.	$ML/T^2/M^3$
γ_s	Specific weight of sediment.	$ML/T^2/M^3$
Δt	Time step.	T
Δx	Horizontal grid spacing in the x-direction.	L
Δy	Horizontal grid spacing in the y-direction.	L
ε_j	Exposure correction factor.	M/L^2
υ	Kinematic viscosity.	L^2/T
ρ	Fluid density.	L/M^3
ρ_s	Sediment density.	L/M^3
τ_o	Total bottom shear stress.	$M/L/T^2$

Abstract

The Mississippi River (MR) has been engineered with the development of the levee system, dams for flood control measures, jetties, revetments and dredging of the navigation channel. These alterations have reduced the replenishment of the sediment to the Louisiana Coastal area. To aid in the restoration planning, 1-D numerical models have been calibrated and validated to predict the river response to various changes such as channel modifications, varied flow conditions and hurricane situations. This study utilized the HEC-RAS 4.1 and the CHARIMA (Dr. Forrest Holly, University of Iowa). The models were calibrated for hydrodynamics and sediment using Tarbert Landing discharges (HEC-RAS), Belle Chasse sand concentrations (CHARIMA), and Gulf of Mexico (GOM) stages. The models showed that a large percentage of the river flow is lost over the East Bank downstream of Bohemia which reduces the sand transport capacity of the river. This reach is subject to flow reversals during hurricanes.

Keywords: Lower Mississippi River, Unsteady Hydrodynamics, MLODS, HEC-RAS model, CHARIMA model, sand load, Hurricane surge, Isaac, Gustav

Chapter 1: Introduction

1.1 Background

The Mississippi River (MR) has been a major natural, economic, and industrial resource for the United States since the 1800s. The MR was a major source of sediment, freshwater and nutrients to the Louisiana Coast. However, due to the development of the levee system, dams, jetties and non-beneficial dredging of the navigation channel, the replenishment of the sediment to the delta has been drastically reduced. The Louisiana's coastal wetlands have been deprived of the most of their historic sediment load of about 120 million tons annually. The MR river transports these sediments to the Gulf of Mexico (GOM) (Allison and Meselhe, 2010; Parker and Sequerios 2006).

The Mississippi River (MR) has an average annual discharge of around 540,000 cubic feet per second (CFS) (2007-2013). The peak discharge of around 1.5 million CFS was measured at Tarbert Landing gage (RM 306) in 2011. During high flows, the chances of flooding by topping the levees or breaching are high. Spillways such as Bonnet Carré and Morganza are opened in order to control the high flows in Lower MR in New Orleans. The hurricane season extends from June to September in New Orleans area. In 2011, the peak MR discharge overlapped with the beginning of the hurricane season which means that it is feasible for a flood on the MR coinciding with a hurricane surge. Also with flows entering the MR from the Gulf and un-leveed outflows such as Bohemia pushes more flow into MR leading to higher risk of flooding and breach of levees.

In order to restore the sediments and freshwater from MR to the Louisiana Coastal areas, a better understanding of working of the system hydrodynamics and sediment transport is necessary. The numerical modeling of hydrodynamics and sediment transport of the MR can be very useful in assessing potential impacts of restoration projects or future sea level or climatological conditions. This study includes 1-D dynamic modeling of the Lower MR reach from Tarbert Landing (RM 306.2) to GOM for hydrodynamics in HEC-RAS. The sediment transport model has been developed in CHARIMA with a domain from Belle Chasse (RM 76) to GOM. The following figure shows the Lower Mississippi River with the location of the reaches modeled.

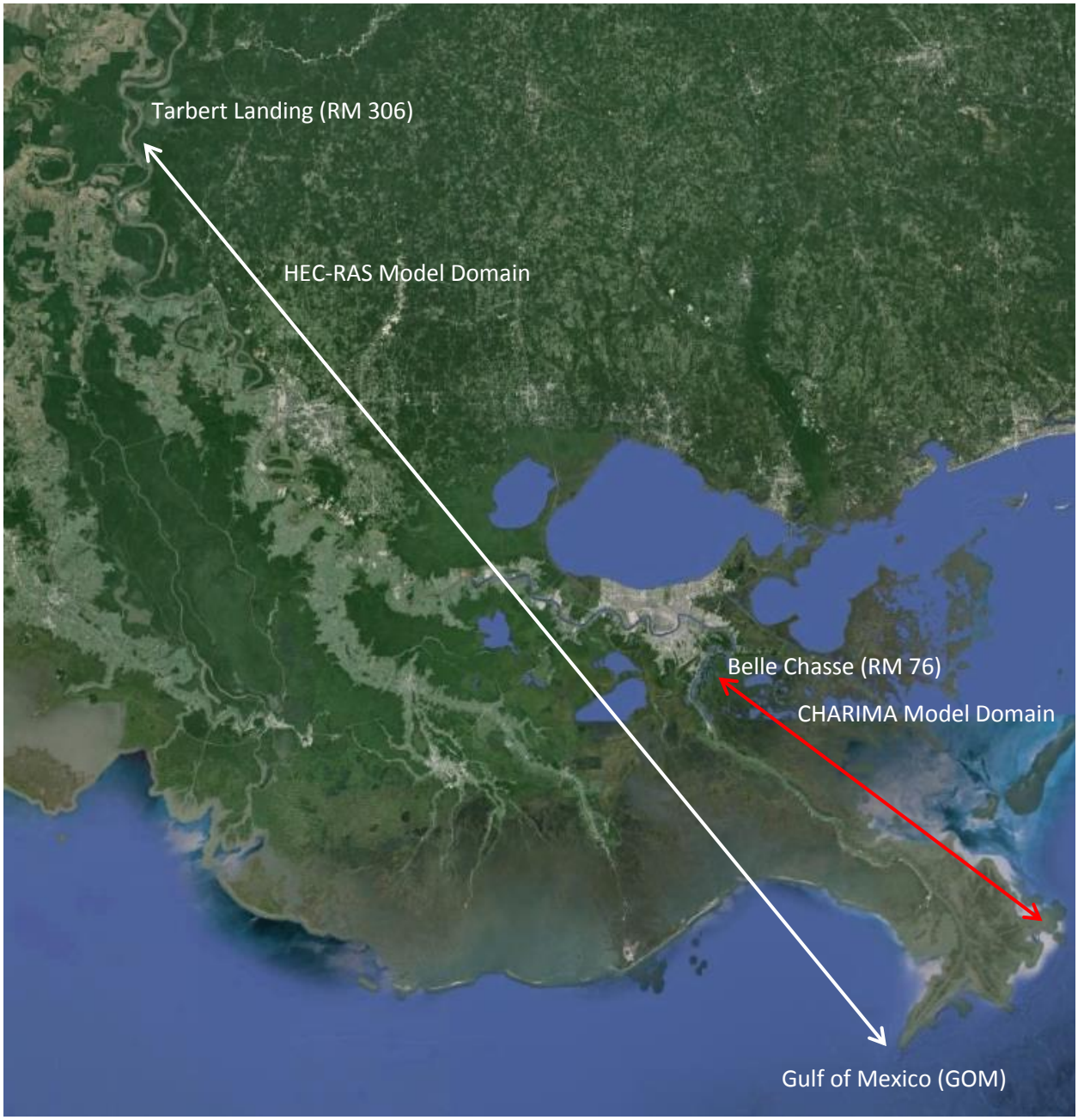

Figure 1-1: Google Earth image of the Model domain.

1.2 Objectives

The purpose of this study is to investigate the inflows and outflows from MR for normal (existing), altered (e.g. diversions) and hurricane conditions. A 1-dimensional numerical model

was needed to simulate the hydrodynamics of the river and its existing diversions. The lower Mississippi River model developed by Davis was recalibrated using HEC-RAS 4.1 with the updated elevations in Bohemia Spillway, Ostrica, Fort St. Philip, and the passes. The survey data from the Lake Pontchartrain Basin Foundation (LPBF) were used for the reach from Bohemia to Fort St. Philip. Additional data for Fort St. Philip were obtained from the Mississippi Hydro Study (Dr. Thad Pratt).

Re-calibration and validation were needed to ensure the accuracy of the model. After validation, model was used to quantify the outflows in un-leveed region such as Bohemia since they represent a significant part of the water and sediment extraction in the Lower River. The model was used to simulate hurricanes. The model was used to estimate the surge propagation in MR due to hurricanes such as Isaac, Gustav and Katrina. These river surges can travel hundreds of miles up the river and may result in flow reversals and added hydrostatic pressures on the levees. The HEC-RAS model calibrated for hydrodynamics was used as a source for stage and flow data to calibrate the CHARIMA model. Then the calibrated CHARIMA model was used to simulate sediment (sand) transport in MR and calculate the sediment to water ratio (SWR) for outflows which assisted in identifying if the diversions are likely to cause shoaling or erosion in the main stem of the river.

1.3 General Approach

HEC-RAS 4.1 developed by USACE was chosen for the 1-d numerical modeling for hydrodynamics because of the large spatial domain of the River and long-term time predictions that were required. The cross-sectional data from various sources, including the 2003-2004 Hydrodynamics Survey (USACE NOD, 2007), were used to replicate the channel geometry in the model. Equivalent channels were developed to account for unknown survey data at several locations. Inline and lateral structures were inputted to imitate the existing diversion structures. Discharge and stage data were used as boundary conditions. Model parameters such as discharge coefficients and flow roughness factors were altered for the calibration of the model based on measured data. The model was run from 2007 until 2013 for calibration and validation purposes. Figure 1-2 shows the schematic of the HEC-RAS model overlaying a satellite view of the southern Louisiana (Pereira *et al*. 2009).

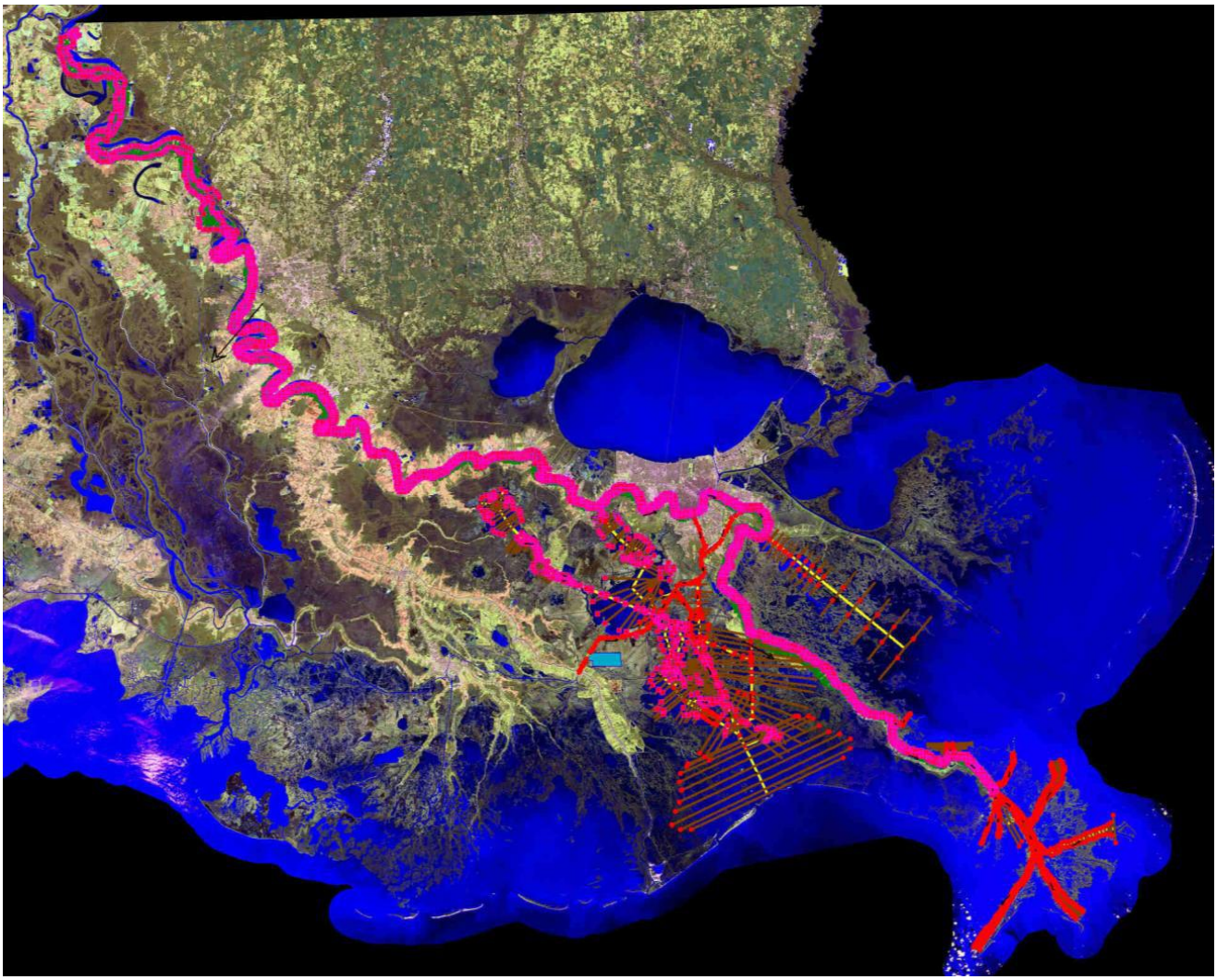

Figure 1-2: HEC-RAS Model Schematic Overlaying Satellite Imagery (Pereira et al.2010).

Chapter 2: Literature Review

Numerical models are becoming popular alternative for designing and modeling a hydraulic system. Numerical models are typically inexpensive compared to physical models. It is easier to change system parameters, has the ability to simulate realistic and/or ideal conditions, and also provides for the exploration of hypothetical events (Waldron, 2008). On the other hand, physical models are being abandoned due to geometry constraints and lack of applicability to alternate problems (Papanicolau *et al*.2008). Louisiana State University's (LSU) Small Scale Physical Model (SSPM) of the Lower Mississippi River (MR) was tested to examine the possibility for freshwater and sediment diversions in 2008. The first problem with the SSPM is that the vertical scale (1:500) is much smaller than the length scale (1:12000). This represents a distorted scale of 24, which changes some river processes such as secondary currents which makes it difficult to perfectly quantify mobile bed processes (Waldron 2008). The necessary space required for a reliable SSPM could possibly take up an entire street block. The second problem with LSU's SSPM is viscosity and surface tension scale effects which reduce the accuracy of the model especially for small diversions. For example 1 mm in the model corresponds to 1.7 prototype feet which limit the results due to the precision of the measurements.

2.1 Description of Numerical Models

There are many 1, 2 and 3-Dimensional numerical models available for use, depending upon the spatial-temporal capabilities necessary. For example, Table 2.1 shows some possible 1-D models that have been used in river modeling (after Papanicolaou *et al.* 2008). A 1-D numerical model has one spatial dimension either along the channel or water column with the capability to simulate both steady and unsteady state flows. Most of the 1-D models are formulated in a rectilinear co-ordinates system and solve the differential conservation equations of mass and momentum of flow (the St. Venant flow equations) along with the sediment mass continuity equation (the Exner equation) by using finite difference schemes. The 2-D numerical model has two spatial dimensions where one is along the channel and the other along the water column. 2-D models can simulate both steady and unsteady state flows, as well as solve steady and unsteady state mass equations. Most 2-D models solve the depth-averaged continuity and Navier-Stokes equations along with the sediment mass balance equation with the methods of finite difference, finite element, or finite volume (Papanicolaou *et al*. 2008). 3-D numerical model has 3 spatial dimensions, where one is along the channel (x), one is along the water column (z), and the other is across the channel (y). 3-D models are advanced mechanistic models that can simulate steady and unsteady state flows and can make steady and unsteady state mass computations. Most 3-D models solve the continuity and the Navier-Stokes equations, along with the sediment mass balance equations through the methods of finite difference, finite element, or finite-volume. The Reynolds average Navier-Stokes (RANS) approach has been employed to

solve the governing equations. 3-D models are mostly used for the unsteady conditions (McCorquodale and Georgiou, 2006).

Table 2.1: Possible 1-D models that include sediment (Papanicolaou et al. 2008)

Table 1. Summary of Selected 1D Models

Model and references	Last update	Flow	Bed sediment transport	Suspended sediment transport	Sediment mixtures	Cohesive sediment	Sediment exchange processes	Executable	Source code	Language
HEC-6: Hydraulic Engineering Center; Thomas and Prashum (1977)	V. 4.2 (2004)	Steady	Yes	Yes	Yes	No	Entrainment and deposition	PD	PD	F77
MOBED: MObile BED; Krishnappan (1981)	—	Unsteady	Yes	Yes	Yes	No	Entrainment and deposition	C	C	F90
IALLUVIAL: Iowa ALLUVIAL; Karim and Kennedy (1982)	—	Quasi-steady	Yes	Yes	Yes	No	Entrainment and deposition	C	C	FIV
FLUVIAL 11; Chang (1984)	—	Unsteady	Yes	Yes	Yes	No	Entrainment and deposition	C	P	FIV
GSTARS: Generalized sediment transport models for alluvial River simulation (Molinas and Yang, 1986)	V. 3 (2002)	Unsteady	Yes	Yes	Yes	No	Entrainment and deposition	PD	PD	F90/95
CHARIMA: Acronym of the word CHARiage which means bedload in French Holly et al. (1990)	—	Unsteady	Yes	Yes	Yes	Yes	Entrainment and deposition	C	C	F 77
SEDICOUP: SEDIment COUPled; Holly and Rahuel (1990)	—	Unsteady	Yes	Yes	Yes	No	Entrainment and deposition	C	C	F77
OTIS: One-dimensional transport with inflow and storage; Runkel and Broshears (1991)	V. OTIS-P (1998)	Unsteady	No	Yes	No	No	Advection-diffusion	PD	PD	F 77
EFDC1D: Environmental fluid dynamics code; Hamrick (2001)	—	Unsteady	Yes	Yes	Yes	Yes	Entrainment and deposition	PD	PD	F77
3STD1, steep stream sediment Transport 1D model; Papanicolaou et al. (2004)	—	Unsteady	[a]Yes	[a]Yes	Yes	No	Entrainmentand deposition	C	P	F90

Note: V=version; C=copyrighted; LD=limited distribution; P=proprietary; PD=public domain; and F=FORTRAN.

[a]Treated as a total load without separation.

2.2 Parameters for Numerical model selection

The selection of a suitable numerical model depends on various factors ranging from cost to availability of the model. Based on a comprehensive list of model parameters listed by McCorquodale and Georgiou (2006), the following attributes have been considered for the selection of the model for this study.

- Availability of the model
- Dimensionality of the model
- Cost of obtaining and implementing the code
- Hardware and Software requirements
- Execution efficiency

- Data requirement for the calibration, validation and application of the model
- Precedence for using this model at the site for similar site and the quality of the outcome

The numerical models selected for the study based on above mentioned criteria were HEC-RAS and CHARIMA. Davis (2010) used HEC-RAS for the hydrodynamics of the Lower Mississippi River including confluences and flow splits. The model was improved and recalibrated based on improved field data for outflows such as Fort St. Philip and Bohemia. Pereira *et al.* (2009) applied HEC-RAS to study the sand transport in the main stem of the Lower Mississippi River. However, HEC-RAS does not have the capability to model sand transport at confluences and flow splits. So, CHARIMA was used for simulation of the sand transport. CHARIMA was selected over HEC-RAS because it allows the simulation of sediment transport with fully unsteady flows and computes the sediment exchanges at junctions. It also allows the user to input/change more parameters than HEC-RAS permitting a better calibration. In addition, Dr. Holly provided access to the source code of CHARIMA.

2.3 Numerical modeling of Mississippi River

Previously 1-D modeling of the MR was conducted for the reach between Tarbert Landing (RM 306) and East Jetty (RM -20) using the Waterways Experiment Station's (WES) TABS-1 model (Copeland and Thomas, 1992). The study investigated the effects of diversions have on dredging the MR. The sediment transport module was used to predict the patterns of sand deposition downstream of a diversion by changing the concentration of sediment diverted from the river. Several diversion site alternatives were tested to compare the river's response to the location of a diversion. The results of the study indicated that the further upstream the diversion is located, the less dredging will be required because the flow would be high enough to re-suspend the recently deposited sediment just downstream of the diversion. The study also showed that the amount of sediment diverted plays an even bigger role in the resulting water surface and bed deposition because if no sediment were diverted there would not be enough flow to entrain the deposited sediment and dredging would be increased.

Another 1-D model for MR was developed in 2010 and the modeled reach extended from Tarbert Landing to Gulf of Mexico (GOM) using the HEC-RAS numerical model (Davis *et al.* 2010). This study investigated the hydrodynamics of the river and its existing diversions and distributaries. The river response model was needed to investigate the impacts of proposed freshwater diversions as well as proposed distributary modifications. The model was considered suitable for application because it was validated with relatively small errors. The model was then used to simulate conditions such as closing of West Bay, South Pass and Southwest Pass individually and observe the changes in flow distribution in the remaining outlets.

In 2011, 1-D model was developed in CHARIMA for the reach extending from Belle Chasse to downstream of Main Pass (Pereira *et al.* 2011). The model simulated the hydrodynamics and suspended sand transport. The sediment data was obtained from Nittrouer *et al*. (2008) and Allison (2010). Hydrodynamics data for the model was obtained from the Davis (2010) study in which HEC-RAS was applied to model the Lower MR from Tarbert Landing to the Gulf of Mexico. The model could simulate the suspended sand transport but it was found to be time-step dependent contradicting the theory.

Chapter 3: Existing and Future Conditions of the Mississippi River Domain

3.1 Modeled Reach

The current study incorporated Davis *et al.*'s (2010) channel geometry of the MR from Tarbert Landing (RM 306) to GOM (RM -18) with the improvements in Bohemia and Fort St. Philip reach due to availability of survey data from LPBF for the HEC-RAS model. For the CHARIMA model, Pereira *et al.*'s (2011) model from Belle Chasse to HOP was extended to the GOM.

3.2 Existing Diversions

There are several existing freshwater and sediment diversions along the MR from Tarbert Landing to the GOM. These diversions are primarily designed for land building purposes and some are used for the dissipation of high floods. Some manmade channels along the river are designed for navigational purposes. The following is the list of all the outflow channels, diversions, and spillway that were included in the model under existing diversions.

1. Morganza Spillway (RM 280)
2. Bonnet Carré Spillway (129)
3. Davis Pond (118)
4. ICCW at Harvey (RM 99)
5. IHNC at Chalmette (RM 92)
6. ICCW at Algiers (RM 88)
7. Violet (RM 84)
8. Caernarvon Diversion (RM 82)
9. White Ditch (RM 65)
10. West Pointe A-La-Hache (RM 49)
11. Bohemia U/S (RM 34)
12. Bohemia Intermediate (RM 32.5)
13. Bohemia D/S (RM 31)
14. Bayou Lamoque N (RM 33)
15. Bayou Lamoque S (RM 32)
16. Fort St. Philip (RM 20)
17. Baptiste Collette (RM 12)
18. Grand Pass (RM 10)
19. Tiger Pass (RM 10)
20. West Bay (RM 4)

21. Main Pass (RM 4)

Figure 2-1 shows the existing outflow channels and diversion in both HEC-RAS and CHARIMA model domain.

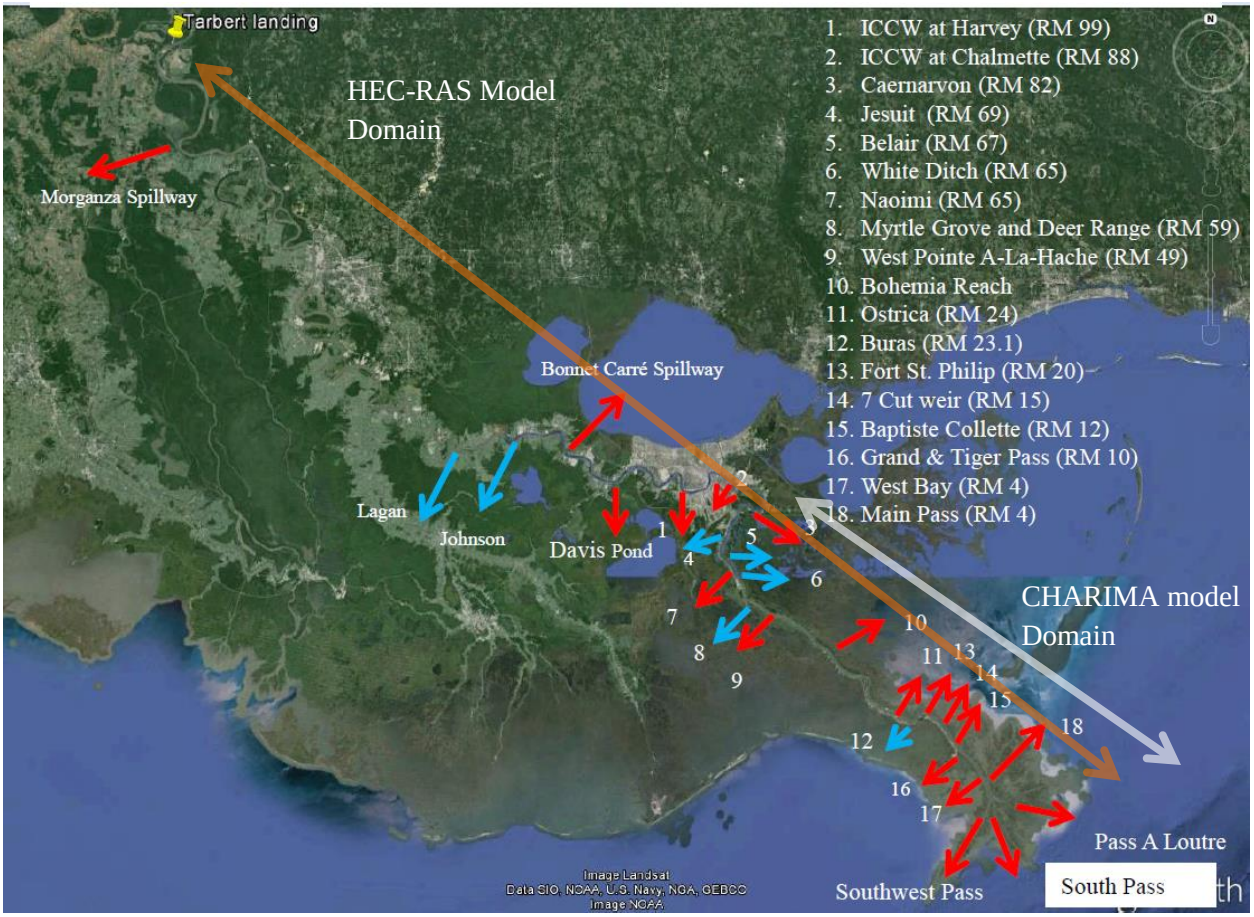

Figure 2-1: Existing and future diversions in the model domain. (Google Earth Imagery, 2013)

3.3 Future MLODS Diversions

The MLODS (LPBF 2008) outlines several proposed diversions along the MR which are intended to reintroduce freshwater and sediment into the coastal area. Following are the list of proposed diversions in the Lower Mississippi River.

a) Lagan (RM)
b) Johnson (RM)
c) Jesuit (RM 69.1)
d) Belair (RM 67.1)
e) Myrtle Grove and Deer Range (RM 59.1)
f) Buras (RM 23.1)

Figure 2-1 shows the HEC-RAS model domain with both existing and future diversions and outflow channels. Figure 2-1 also shows the CHARIMA model domain with both existing and future diversions and outflows channels.

3.1.2 Scenarios considered for model simulation

Both HEC-RAS and CHARIMA models were simulated for following cases:

1) Existing Diversions
2) Addition of MLODS (Multiple Lines of Defense Strategy) diversions
3) Addition of MLODS diversions with dredged Pass-A-Loutre
4) Addition of MLODS diversions, dredged Pass A-Loutre and Southwest pass closure
5) Addition of MLODS diversions, dredged Pass A-Loutre and South pass closure
6) Addition of MLODS diversions, dredged Pass A-Loutre with both South & Southwest pass closure

The results of discharge load, sand load and sand concentration in MR and outflows from HEC-RAS and CHARIMA model can be found in the application section.

Chapter 4: Description of the Models

The two models used for this study were HEC-RAS 4.1 and CHARIMA.

4.1 Description of HEC-RAS

In this study, HEC-RAS 4.1, a 1-D numerical model, was used to simulate the hydrodynamics of the Lower MR under unsteady flow and fixed-bed conditions (USACE HEC, 2010, http://www.hec.usace.army.mil/software/hec-ras/downloads.aspx). HEC-RAS is a public domain model created by the Hydrologic Engineering Center (HEC) of the U.S. Army Corps of Engineers. It is an upgrade of its predecessors HEC-2 and HEC-6 because it includes a user interface and graphical outputs. From the output tables, hydrodynamic features such as stages, discharges, velocities, water surface elevations, shear stresses etc. can be accessed for each cross-section at each user specified time interval. Other outputs include stage and discharge hydrographs, longitudinal flow profiles, rating curves and cross-sectional flow profiles. The graphical outputs can also be animated to show how the parameters change at every user-specified time step. The user interface includes colored icon buttons for to access various functions of the model, a drawing area for river schematics, legends for plots, zooming and panning options, identification labels for reaches, junctions, storage areas and cross-sections, flow directionality arrows, and multiple windows for view purposes. HEC-RAS can make long-term predictions and can handle large scale project areas. Also, tributary and distributary systems can be modeled as network. The model has the options for U.S. Customary and System International (SI) units. The model can simulate steady and unsteady hydrodynamics. It can also simulate sediment transport under quasi-steady flow regimes, i.e. the hydrograph is assumed to vary stepwise from one steady state to the next steady state. The code does not permit modeling of sediment diversions.

4.1.1 Geometric Data Editor

A *reach* is described as a river, lake, stream, channel or a portion of these drawn in the geometry interface window. A reach is comprised of at least two cross-sections inputted by the user. Cross-sections can be depicted by a maximum of 500 station and elevation co-ordinates with the first station being zero. All stations are entered from left to right looking downstream. Data such as Manning's n values, bank stations, reach lengths and expansion/contraction coefficients are required for each cross-section. The Manning's n can be varied vertically or horizontally. They can also be a varied based on the flow rate in the channel by entering flow roughness factors that will be multiplied by the n values for individual flow rates. Manning's n values are used as a parameter for calibration purposes.

A *junction* is defined as a connection of two or more reaches for either split flows or flow confluences.

The model is capable of estimating flow through, over, and/or around hydraulic structures such as weirs, gates, spillways, storage areas, levees, pumps, culverts and bridges. The structures are specified as inline structures, lateral structures, bridges/culverts, storage areas and pumps. An inline structure can be modeled as a weir or a weir with gates (spillway). A lateral structure can be modeled as weirs, weirs with culverts, weir with gates and culverts or a lateral diversion rating curve. Lateral structures also have the option to divert flow out of the system into a storage area or into a cross-section or range of cross-sections. Lateral structures can be placed on the left or right bank or next to the left or right bank station. Stations, elevations, weir coefficient, weir width, weir crest shape and the distance to the upstream cross-section are needed for all lateral and inline structures. The data required for gates are width, height, invert, centerline stations, type, submerged orifice coefficient, overflow weir shape and coefficient. Storage areas in the model are considered to be offline storage and require a lateral structural to connect to a reach. Multiple storage areas can be connected to each other via storage area connections. Inputting a storage area requires a representative area and a minimum elevation or an elevation versus volume curve.

4.1.2 Unsteady Flow Data Editor

Boundary conditions and initial conditions are required to simulate unsteady flows. Upstream and downstream boundaries are required for all model reaches except for junctions. If the upstream boundary of the reach is a junction, then only a downstream boundary is needed. No boundary conditions are needed for a reach with both boundaries as junctions. The boundary conditions for reaches consist of stage hydrographs, flow hydrographs, stage/flow hydrographs, rating curves and normal depths. The possible boundary conditions for lateral structures with gates are elevation controlled gates, time series gate openings and rules. Inline structures have similar boundary conditions as lateral structures with the addition of navigation dams. The program has the option to add an internal boundary condition too. The internal boundary condition consists of lateral inflow hydrographs, uniform lateral flow, groundwater interflow and internal boundary stage/flow hydrographs. Lateral inflow hydrograph can also be added as a boundary condition for storage areas. Flow change locations can be added for any cross-section (except for the first of the reach) or any lateral or inline structures of any reach. Flows entered with a negative sign are considered outflows and the ones with positive signs are considered inflows. Initial conditions consist of the initial flow distribution for the upstream cross-section of each reach and the initial elevation of water in each storage area.

4.1.3 Unsteady Flow Analysis Editor

A *plan* is a simulation setup file with a specific geometry file and unsteady flow data file with a specific date and time defined for the start and end of the simulation. The user must define which plan to simulate or else the most recent plan will be executed by the program. The model offers the option of selecting the program to run which includes Geometry Preprocessor, Unsteady Flow Simulation and Post Processor. The user need to select the computation time interval, hydrograph output interval and detailed output interval. Some other simulation options available include mixed flow options, initial backwater flow optimizations, calculation options and tolerances and runtime computational options. The program checks if all boundary and initial conditions that were entered, the geometry requirements were satisfied and that all necessary data was provided before running the simulation. The program stops running and provides a detailed error message indicating the problem in a separate window when any errors or missing input data occurs. During simulation, additional window opens and displays the status of the simulation. After the program stops running, all graphical and tabular outputs are available to check the results.

4.2 Governing Equations

The flow in the MR is considered unsteady as the velocity in the channel changes with time. Since, the flow is free from hydraulic drops or jumps in the considered reach, it can be assumed to be gradually varied and unsteady flow. HEC-RAS solves two unsteady equations which are the conservation of mass (continuity) and the conservation of momentum. These two equations were first introduced in their partial differential form by de St. Venant in 1871 (Mahmood and Yevjevich, 1975). Due to the complexity of the equations, exact integration is not possible unless step methods or simplifying assumptions are used (Chow, 1959). The unsteady flow routing of HEC-RAS is based on Liggett's derivations of the de St. Venant unsteady flow equations (USACE HEC -2008).

4.2.1 Conservation of Mass (Continuity)

The law of conservation of mass states that for a closed system, the mass must remain constant over time. So, the mass flowing into a control volume (CV) has to come out. Therefore, the net rate of inflow should be equal to the rate of change in storage in the CV. Consider the CV shown below (Figure 3-1). The co-ordinate system used herein designates x as the horizontal (longitudinal) direction of the primary flow, y as the horizontal (lateral) direction normal to the primary flow, and z as the vertical direction.

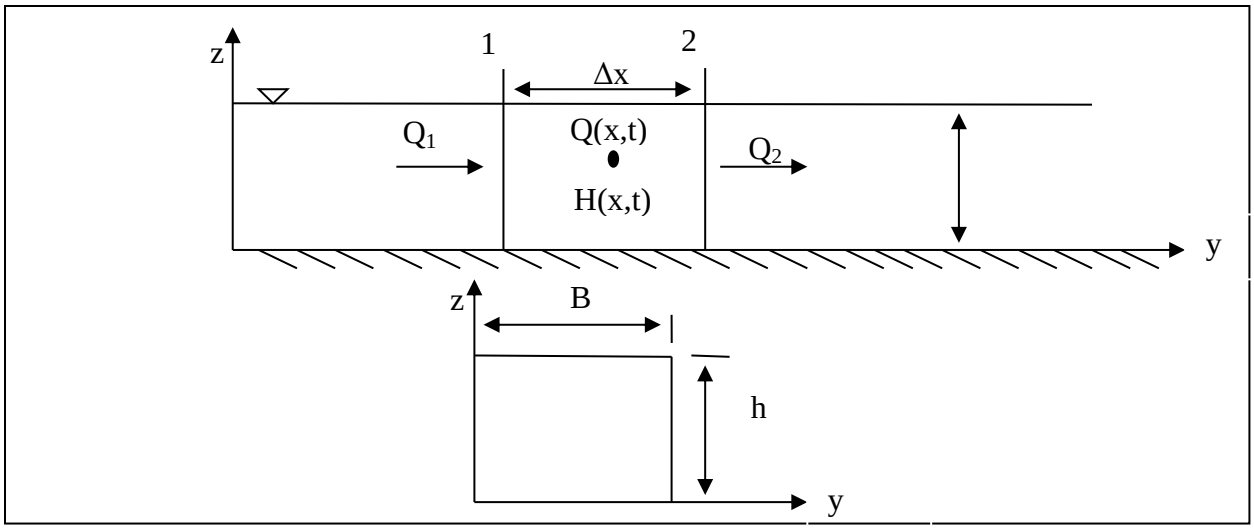

Figure 3-1: Representative Control Volume for derivation of Continuity equations.

The flow rate Q is the function of channel area and fluid velocity. As the flow travels along the cross-sections across a distance Δx, the area is considered to be changing with respect to the x-axis. As a result, the flow rate is also changing over the distance Δx. The change in flow over distance is represented by $\partial Q/\partial x$. The net inflow rate Q_1 is equal to the flow at the centroid of the CV minus the change in flow at the centroid with respect to the distance between face 1 and the centroid.

$$Q_1 = Q - \frac{\partial Q}{\partial x}\frac{\Delta x}{2} \qquad \text{Equation 4.1}$$

Similarly, the rate of outflows Q_2 is equal to the flow at the centroid of the CV plus the change in flow at the centroid with respect to the distance between the centroid and face 2.

$$Q_2 = Q + \frac{\partial Q}{\partial x}\frac{\Delta x}{2} \qquad \text{Equation 4.2}$$

The rate of change in storage ΔS is equal to the change in volume over time. As x is an independent variable, the change is storage become $\partial A \Delta x$. The rate of change in storage is given by:

$$\Delta S = \frac{\partial V}{\partial t} = \frac{\partial A}{\partial t}\Delta x \qquad \text{Equation 4.3}$$

So, the equation of conservation of mass can be written as:

$$\rho\frac{\partial A}{\partial t}\Delta x = \rho\left[\left(Q - \frac{\partial Q}{\partial x}\frac{\Delta x}{2}\right) - \left(Q + \frac{\partial Q}{\partial x}\frac{\Delta x}{2}\right)\right] \qquad \text{Equation 4.4}$$

Flow entering the channel through runoff, precipitation and other means must be accounted too when considering the continuity. As a representation of these lateral flows, Q_L is added to the above equation.

$$\rho \frac{\partial A}{\partial t} \Delta x = \rho \left[\left(Q - \frac{\partial Q}{\partial x} \frac{\Delta x}{2} \right) - \left(Q + \frac{\partial Q}{\partial x} \frac{\Delta x}{2} \right) + Q_L \right]$$

Or, $$\rho \frac{\partial A}{\partial t} \Delta x = \rho \left[Q_L - \frac{\partial Q}{\partial x} \Delta x \right]$$ Equation 4.5

Assuming the fluid is incompressible, the density (ρ) is constant. Dividing by ρΔx,

$$\frac{\partial A}{\partial t} = \frac{Q_L}{\Delta x} - \frac{\partial Q}{\partial x}$$

Or, $$\frac{\partial A}{\partial t} + \frac{\partial Q}{\partial x} - q_L = 0$$ Equation 4.6

Equation 3.6 represents the simplified version of the conservation of mass equation where:

Q_1 = Net inflow rate

Q_2 = Net outflow rate

Q = Flow rate at the centroid of the CV

Δx = Differential longitudinal width of the CV

ΔS = Rate of change of storage

B = Top Width of the CV

h = Depth of the CV

t = time

ρ = Density of the water

Q_L = Lateral inflow in the CV

q_L = Lateral inflow per unit length of the CV

∂ = Partial derivative function

4.2.2 Conservation of Momentum

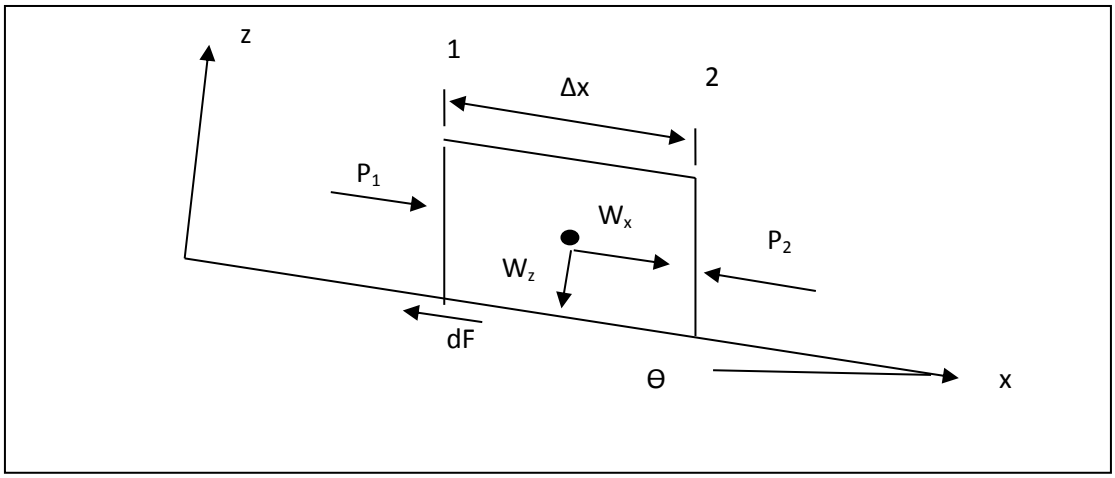

Figure 3-2: Representative Control Volume for Conservation of Momentum.

The conservation of momentum based on Newton's second law of motion states that the rate of change of momentum of a fluid in control volume (CV) is equal to the sum of the external forces acting on the CV. HEC-RAS solves the momentum equation only in the x-direction and the external forces acting on the CV are pressure, gravity and friction.

The conservation of momentum is expressed as:

$\sum F_x = dm\ a$ Equation 4.7

Considering the external forces, the momentum equation is represented by:

$$P_1 - P_2 + W_x - d_F = dma$$ Equation 4.8

Where:

P_1 = Pressure force along face 1 of the CV

P_2 = Pressure force along face 2 of the CV

W = Weight of the water in the CV = γ V

W_x = Weight of the water in the CV along the x-axis = W sinΘ

W_z = Weight of the water in the CV along the z-axis = W cosΘ

dF = friction force along the bed of the CV = γ A S_f Δx

dm = Change in mass in the CV = ρ A Δx

a = Acceleration of the control volume

ρ = Density of the water

A = Cross-sectional area of the CV

Δx = Differential longitudinal width of the CV

γ = Specific weight of water = 62.42 lbs/ft^3 = 9.806 kN/m^3

V = Volume of water in Cv = A Δx

The acceleration term 'a' has two components. The temporal component 'a_T' represents the change in velocity in time at the centroid of the CV.

$$a_T = \frac{\partial v}{\partial t} \qquad \text{Equation 4.9}$$

The spatial component 'a_S' represents the change in the velocity with respect to the distance between the face and the centroid of the CV.

$$a_S = v\frac{\partial v}{\partial x} \qquad \text{Equation 4.10}$$

So,

$a = a_T + a_S$

Or, $$a = \frac{\partial v}{\partial t} + v\frac{\partial v}{\partial x} \qquad \text{Equation 4.11}$$

Where:

V = Velocity in the CV

t = time

With the acceleration term, the new equation is represented by:

$$P_1 - P_2 + W_x - d_F = dm\left(\frac{\partial v}{\partial t} + v\frac{\partial v}{\partial x}\right) \qquad \text{Equation 4.12}$$

The mass in a CV is given by:

$$dm = \rho V \qquad \text{Equation 4.13}$$

Volume is the product of length, width and height of a CV. The length in the CV is designated as Δx. The cross-sectional area 'A' represents the product of the width and height of the CV. So,

$$dm = \rho A \Delta x$$ Equation 4.14

The conservation of momentum equation can be represented as:

$$P_1 - P_2 + W_x - d_F = \rho A \Delta x \left(\frac{\partial v}{\partial t} + v \frac{\partial v}{\partial x} \right)$$ Equation 4.15

The pressure 'p' acting on the face of CV is defined as the force exerted by the surrounding water per unit area of the face. According to Liggett, shallow water theory assumes that the pressure is hydrostatic, and it therefore has a linear distribution along the depth (Mahmood and Yevjevich, 1975). The hydrostatic pressure equation is given by:

$$p = \rho g (h - z)$$ Equation 4.16

where:

p = Pressure

ρ = Density of the water

g = Acceleration due to gravity

h = Water depth

z = Vertical co-ordinate

The pressure force 'P' can be obtained by multiplying the cross-sectional area of the CV 'A',

$$P = \rho g A (h - z)$$ Equation 4.17

Let the pressure at the centroid of the CV be P. So, the pressure force at face 1 of CV 'P_1' is the pressure P minus the change in pressure P from face 1 to the centroid multiplied by the distance between face 1 and the centroid. Similarly, the pressure force at face 2 'P_2' is the pressure P plus the change in the pressure P from face 2 to the centroid multiplied by the distance between face 2 and the centroid.

$$P_1 = P - \frac{\partial P}{\partial x} \frac{\Delta x}{2}$$ Equation 4.18

$$P_2 = P + \frac{\partial P}{\partial x} \frac{\Delta x}{2}$$ Equation 4.19

Now,

$$P_1 - P_2 = \left(P - \frac{\partial P}{\partial x}\frac{\Delta x}{2} \right) - \left(P + \frac{\partial P}{\partial x}\frac{\Delta x}{2} \right)$$

Or, $P_1 - P_2 = -\frac{\partial P}{\partial x}\Delta x$ Equation 4.20

Integrating Equation 4.17 between h and z with respect to the x-axis and setting ρ, g and A as constants, Equation 4.20 becomes:

$$P_1 - P_2 = -\rho g A \Delta x \frac{\partial z}{\partial x}$$

Or, $P_1 - P_2 = -\gamma A \Delta x \frac{\partial z}{\partial x}$ Equation 4.21

So, the momentum equation becomes:

$$-\gamma A \Delta x \frac{\partial z}{\partial x} + W_x - d_F = \rho A \Delta x \left(\frac{\partial v}{\partial t} + v\frac{\partial v}{\partial x} \right)$$ Equation 4.22

We have, $W_x = WSin\theta = dmgSin\theta = \rho g A \Delta x Sin\theta = \gamma A \Delta x Sin\theta$

In natural channels, the angle θ is very small. So, Sinθ can be written as tanθ, which is the slope of the channel bed 'S_o'.

So, $-\gamma A \Delta x \frac{\partial z}{\partial x} + \gamma A \Delta x S_o - d_F = \rho A \Delta x \left(\frac{\partial v}{\partial t} + v\frac{\partial v}{\partial x} \right)$ Equation 4.23

The friction force 'dF' acting on the CV is the product of the boundary shear stress 'τ_o', the wetted perimeter 'P_w' and the length 'Δx' of the CV.

$$dF = \tau_o P_w \Delta x$$ Equation 4.24

The boundary shear stress is given by:

$$\tau_o = \rho C_D v^2$$ Equation 4.25

Where C_D is the drag coefficient, which is defined as:

$$C_D = \frac{g}{C^2}$$ Equation 4.26

C is the Chezy coefficient which is used in defining the Chezy equation:

$$v = C\sqrt{RS_f} \qquad \text{Equation 4.27}$$

where, $R = \frac{A}{P_w}$ = Hydraulic Radius

S_f = friction slope

Now,

$$dF = \rho C_D v^2 P_w \Delta x = \rho \frac{g}{C^2}\left(C\sqrt{RS_f}\right)^2 P_w \Delta x = \rho g R P_w \Delta x S_f = \gamma A \Delta x S_f \qquad \text{Equation 4.28}$$

Finally,

$$-\gamma A\Delta x\frac{\partial z}{\partial x} + \gamma A\Delta x S_o - \gamma A\Delta x S_f = \rho A\Delta x\left(\frac{\partial v}{\partial t} + v\frac{\partial v}{\partial x}\right) \qquad \text{Equation 4.29}$$

Dividing the equation with ρAΔx and simplifying the equation, we get;

$$\frac{\partial v}{\partial t} + v\frac{\partial v}{\partial x} + g\left(\frac{\partial z}{\partial x} - S_o + S_f\right) = 0 \qquad \text{Equation 4.30}$$

4.3 Finite Difference Method

A numerical method is required to solve the above equations due to the presence of non-linear terms. The HEC-RAS program uses a finite difference method which takes a channel and divides it into N reaches each with a length of Δx. Each reach is defined by an upstream node and a downstream node. For the first node of the channel defined as 1, the last node would be labeled N+1. The equations are solved at distinct instances in time, where the difference in two times is called a computational time step 'Δt' (Roberson et al. 1988). In HEC-RAS, the computational time step is defined by the user as needed. A computational grid is then created using the independent variables x and t. HEC-RAS uses the four-point implicit scheme (box scheme) to solve the equations of continuity and momentum. Figure 4-3 shows the computation grid for the box scheme.

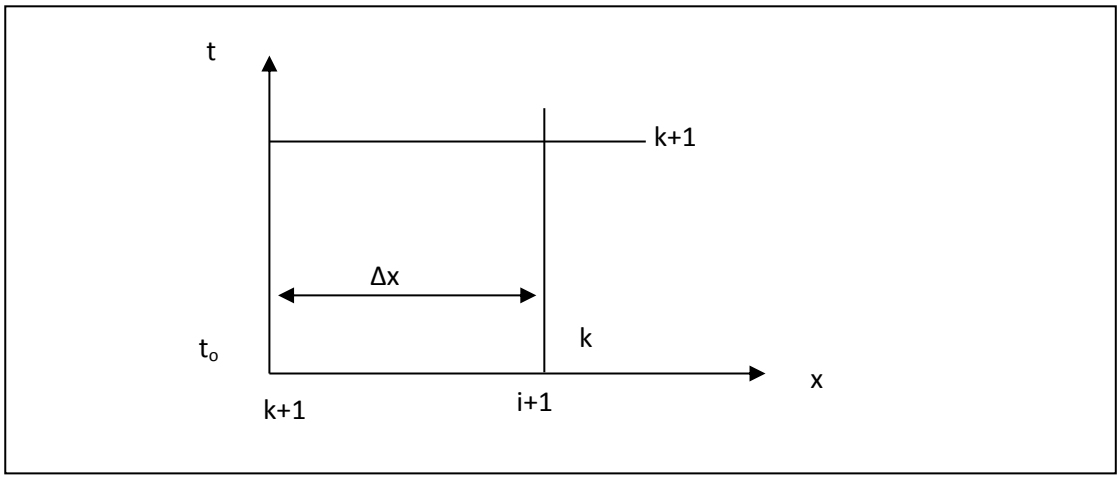

Figure 4-3: Computational Grid for the box scheme.

The partial derivatives of the governing Equation 4.6 and Equation 4.30 are substituted by finite-difference approximations, which become algebraic equations that are easier to solve. If the known variables at t_o represent the initial conditions, then the unknown variables correspond to $t_o+\Delta t$. For the implicit scheme, the algebraic equations are in terms of the unknown variables and are computed at each node simultaneously.

4.4 Description of CHARIMA

CHARIMA (Holly et al. 1990, Holly 2009) is a one-dimensional unsteady state computation model developed for simulation of steady or unsteady water, sediment and contaminant movement in simple or complex systems of channels. The model is prepared to simulate bed-load and/or suspended-load transport of mixtures of cohesive or non-cohesive sediments along with the short or long-term bed-level changes (aggradation and degradation), bed-sediment sorting and armoring. The program is written in FORTRAN 77. The model can run in both windows and LINUX/UNIX environments. The code consists of a main program (NEWMAIN) and other 85 files. A user-friendly interface developed by Visual Basic for windows environment can be found. The GUI allows the user to update the input files, check the formatting as well as running of the application. Dr. Holly provided the source code which allowed for minor changes in the code that were needed because of the large number of links and nodes in the modeled reaches.

4.4.1 Components of Geometry of CHARIMA

a) Links: A link is the flow path between two nodes which is characterized by a single hydraulic law (E.g. Weir, fluvial channel, pump etc.) A link must have at least two computation points. Various link types available in CHARIMA are: Fluvial (de St. Venant) Link, Rectangular Weir Link, Imposed Discharge (pump), Imposed Upstream Water Level Link, Thermal Power Plant, Culvert, Cooling Tower, Rectangular Orifice (gate), Imposed temperature link, Manning-Sticklers Non-Inertial Fluvial link and user-customized link.

b) Nodes: A node is a junction of two or more links. A node having only one link attached is a boundary condition for that link. The simplest model has one link and two nodes. Any node may have external water inflow specified as a time series. A discharge entering the model node is positive and a discharge taken out of the model is negative. A node may also have an imposed water-surface elevation typically at a downstream exit point of a model or exit to the open water; there can be multiple exit points.

c) Points: A point is a computation point on a link. Any link must have at least two computation points. The physical data associated with a point always include its position RM (miles or km) and its initial water-surface elevation Y (ft. or m) and initial water discharge Q (CFS or CMS).

d) Sections: A section is a cross-sectional shape that is assigned to one or more computation points. All the fluvial computation points of a model can use the same cross-sectional shape (e.g. rectangular or a trapezoid) or every fluvial computation points may have its own unique cross-section as in a river model.

4.4.2 Data Input Files

These files give the user access to model to make changes in geometry, boundary conditions and results output parameters and locations.

a) *Cardin.dat*: This is a formatted file containing the complete topological, topographical, geometrical and operational description for a model run in British units. Any changes to the model can be made through this file or this file can be accessed through the GUI also which updates the files and saves the changes made by the user.

b) *Char23.in*: This is a free-field file containing the sequential hydrological and operational time-series data sets necessary for a simulation. The file can be manually updated by the user or updated through GUI by running the CHAR23.EXE file.

c) *Rec23.dat*: This is formatted file prepared by CHAR23.EXE and contains all the simulation time series reorganized as successive time records. This file is subsequently read by CHARIMA.EXE to drive a simulation.

d) *Cusout.dat*: This is a formatted file prepared by the GUI which contains user-specified temporal and spatial output results. Some of the output parameters are water discharge (Q-CFS), water-surface elevation (Y- CFS), thalweg elevation (THAL-ft.), total bed load (QSTO- CFS), water surface velocity at a point (VEL-ft./s) and sum of suspended-load concentrations for all size classes (CSLT-lb./ft^3)

4.4.3 Result Output Files

These files are important to check the simulation and results. They can be accessed to find the errors and warnings and monitor the working of the model as well as the results.

a) *Errwar.out*: This is a text file containing one-line error warning and error messages. The numbered errors and Warning can be cross-referenced with the manual to understand these messages and make necessary changes accordingly.

b) *Printer.out*: This is a text file that echoes most input data from cardin.dat and contains multiple instantaneous snapshots of the state of the entire model as user-specified moments of time.

c) *Fate.out*: The is a text file that reports detailed water and constituent mass conservation in all links of the model and at the same user-specified moments of time that are used by *printer.out*.

d) *Tfunct.out* & *Xfunct.out*: These text files contain the time and space dependent output results as requested by the user through the cusout.dat file.

4.4.4 Governing Equations for CHARIMA

The de St. Venant (1871) equations for the unsteady flow are based on the flowing assumptions: a) the flow is one-dimensional (i.e. the velocity is uniform over the cross-section and the water level across the cross-section is horizontal); b) the streamline curvature is small and vertical accelerations are negligible hence the pressure is hydrostatic; c) the efforts of boundary friction and turbulence can be accounted for through resistance laws analogous to

those used for steady state flow; d) the average channel bed slope is small so that the cosine of the angle it makes with the horizontal may be replaced by unity.

There are many formulations expressing the interrelation of the sediment transport and water flow in unsteady situations; the simplest acceptable mathematical description is summarized by the following equations.

Water Continuity Equation:

$$\frac{\partial A}{\partial t}+\frac{\partial Q}{\partial x}=q \qquad \text{Equation 4.31}$$

Momentum Equation:

$$\frac{\partial Q}{\partial t}+\frac{\partial}{\partial x}\left(\alpha\frac{Q^2}{A}\right)+gA\frac{\partial y}{\partial x}+gA=\frac{Q|Q|}{k^2}=0 \qquad \text{Equation 4.32}$$

Continuity equation for solid discharge (modified Exner):

$$(1-n)\tilde{B}\frac{\partial z}{\partial t}+\frac{\partial Q_s}{\partial x}=S \qquad \text{Equation 4.33}$$

The suspended-sediment transport formula:

$$\frac{\partial C}{\partial t}+\frac{\partial}{\partial x}\left(\frac{QC}{A}\right)=\frac{1}{A}\frac{\partial}{\partial x}\left(AK_x\frac{\partial C}{\partial x}\right)+\frac{S}{A} \qquad \text{Equation 4.34}$$

where, Q = Water Discharge

A = Cross-sectional Area

x = Abscissa measured along the river

g = Gravitational acceleration

α = Momentum Correction Factor

t = Time

q = Lateral inflow

Q_s= Volumetric bed-load sediment discharge

$\tilde{B}$ = Water surface width of the section affected by bed load transport

K = Conveyance

C = Suspended-load concentration

S = Source-sink exchange of solid material between the bed layer and suspension.

The modified Exner and the suspended-sediment transport formulas are symbolic representation of a summation overall all sediment classes, each class being transported all or partly as suspended load or bed load, the allocation being variable in space and time. Holly and Rahuel (1990) present a more detailed description of the equations and their terms of reference.

The above equations form a non-linear partial differential system that can be solved by numerical methods of integration. The equations are complemented by empirical relations for the bed-load transport capacity, near-bed equilibrium suspended-sediment concentration, and bedload-suspended load allocation factors depending on local shear stress, for each size class.

4.4.5 The sediment Transport Formula

For the non-cohesive sediment formulation, there are four total-load predictors adopted for use in CHARIMA. They are a) Modified TLTM method (Karim 1985); (b) Modified Ackers-White Method (Proffitt and Sutherland 1983); (c) Engelund-Hansen method (1967); (d) Power-law method. For this study, Ackers-White Method was adopted for the modeling of non-cohesive suspended sand transport. Strickler coefficient (Ks) or the friction factor (f) is given as inputs (Holly et al. 1990) which is the primary parameter for calibration of the model.

The Ackers-White (1973) total-load predictor was developed for uniform sediments and has been expanded by Profitt and Sutherland (1983) to calculate the sediment transport for non-uniform sediments. The original Ackers-White (1973) formula for uniform sediment is:

$$\overline{C_T} = \frac{\gamma_s D c_2 \left(\frac{Fgr}{c3} - 1 \right)^{c_4}}{\left(u_* / U \right)^{c_1} \gamma_f d} \qquad \text{Equation 4.35}$$

With the sediment mobility number, F_{gr}, given by:

$$Fgr = \left(\frac{u_*^{c_1}}{\sqrt{(s-1) g D_{35}}} \right) \left(\frac{U}{\sqrt{32} \log(10 d / D_{35})} \right)^{1-c_1} \qquad \text{Equation 4.36}$$

and the dimensionless grain diameter, d_{gr}, is:

$$d_{gr} = \left((s-1)g/v_2\right)^{1/3} D_{35} \qquad \text{Equation 4.37}$$

For $1.0 < d_{gr} < 60.0$:

$$c_1 = 1.0 - 0.56\log d_{gr}; c_2 = 10^{\left(2.56\log d_{gr} - (\log d_{gr*})^2 - 3.53\right)}; c3 = 0.23/d_{gr}^{1/2} + 0.14; c4 = 0.966/d_{gr} + 1.34$$

For $d_{gr} > 60.0$:

$$c_1 = 0.0; c_2 = 0.025; c3 = 0.17 + 0.14; c4 = 1.5$$

where, $\overline{C_T}$ =sediment flux concentration (sediment mass flux per unit mass flow rate). To apply this formulation for non-uniform sediments, D_{35} must be replaced by each size fraction diameter and F_{gr} must be corrected by an exposure correction factor, ε_j, given as follows:

$$\varepsilon_j = \frac{F_{gr}(To \quad staisfy \quad the \quad measured\, data)}{F_{gr}(for\, uniform\, se\dim ents\, with\, D = D_j)}$$

Proffitt and Sutherland (1983) give εj as follows:

$$\varepsilon_j = 1.3 \quad D_j/D_u > 3.7$$

$$\varepsilon_j = 0.53\log(D_j/D_u) + 1.0 \quad 0.075 < D_j/D_u < 3.7$$

$$\varepsilon_j = 0.4 \quad D_j/D_u < 0.075$$

The diameter Du can be determined by a formula defined by Proffitt and Sutherland (1983):

$$\frac{D_u}{D_{50}} = f\left[u_*^2/g(s-1)D_{50}\right] \qquad \text{Equation 4.38}$$

Or D_u can simply be taken as D_{50}.

Chapter 5: Model Development

5.1 HEC-RAS Model Development

5.1.1 Geometry Data

The cross-sections of the Mississippi River (MR) from Tarbert landing to the Passes were taken from the 2010 HEC-RAS study (Davis *et al*. 2010). For components of the geometry of the model, you can refer to Mallory Davis thesis (Davis *et al*. 2010). In the previous model, the outflows such as Fort St. Philip and Bohemia Reach were using simplified rectangular cross-sections. These outflows flow estimates were not calibrated. Also, various small outflows in Ostrica reach as well as between Fort St. Philip and Baptiste Collette were not included into the model due to lack of data. These outflows were improved using survey data provided by Lake Pontchartrain Basin Foundation (LPBF) and with the use of Google Earth.

Figure 5-1: Existing Outflows located in Lower Mississippi River marked in Google Earth image.

Figure 5-1 shows the outflows in the Lower Mississippi River (LMR) with the Ostrica and 7-cut weir.

The Bohemia reach extends from RM 31 till RM 44. The Bohemia reach consists of an elevated road built on a natural levee along the east bank of MR until the Ostrica Lock. Most of the reach has irregular height of land which acts as a natural levee allowing flows to discharge during the high stages (discharges) in the Mississippi River. The Bohemia reach was surveyed by LPBF. Figure 5-2 shows the height of land survey which represents the Bohemia reach. The survey data from LPBF was imposed as weir in the Bohemia reach. The Bohemia reach was divided into 3 channels i.e. Bohemia Upstream, Bohemia Intermediate and Bohemia Downstream. The division was done in the model for easier management of the structure and also to have control over the weir coefficient. The Bohemia Upstream was further divided into 8 smaller channels which corresponded to the existing equivalent channels behind the bohemia weir as captured in the Google Earth. In the previous models, the bohemia reach was used as a lateral structure with the capability to withdraw flows from the MR however it lacked the capability to model for flows coming from the bohemia reach into the river during extreme conditions such as hurricane. Currently, the Bohemia reach has been modeled as an inline structure with the capability to allow flow in to the open water and vice versa.

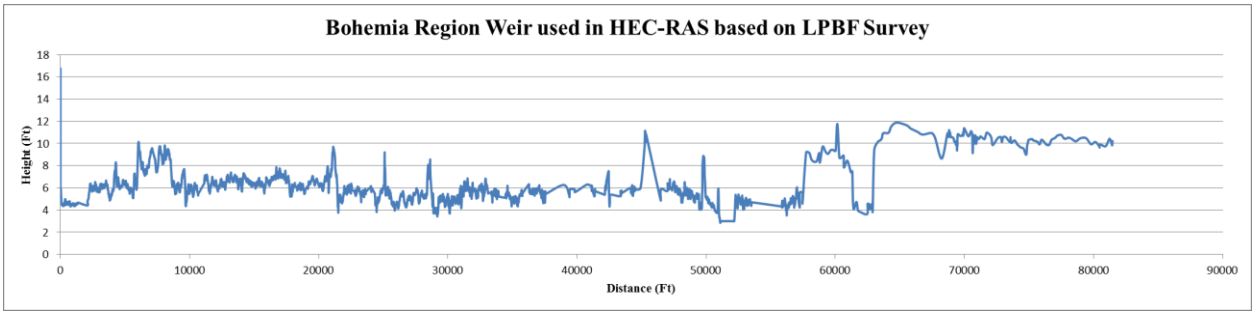

Figure 5-2: LPBF Survey for Bohemia Reach where the distance is measured from upriver (RM 44) to downriver (RM 31).

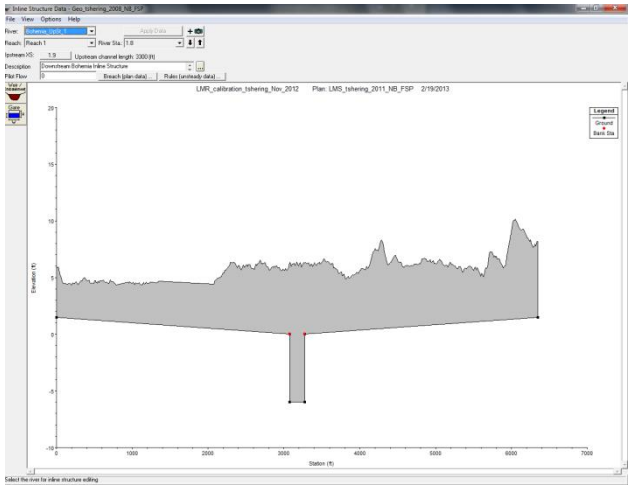

Bohemia U/S Structure 1

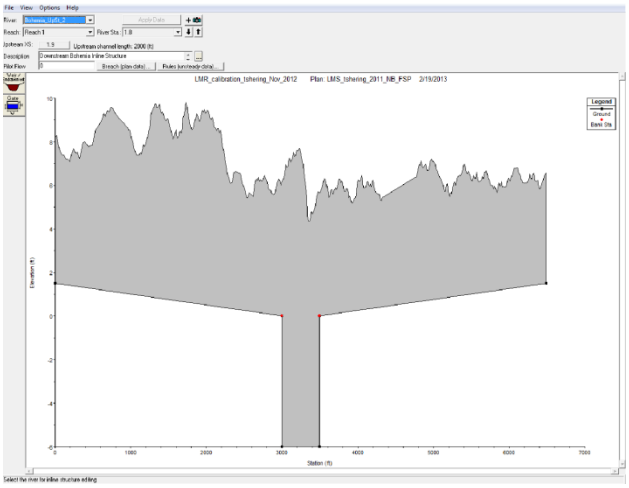

Bohemia U/S Structure 2

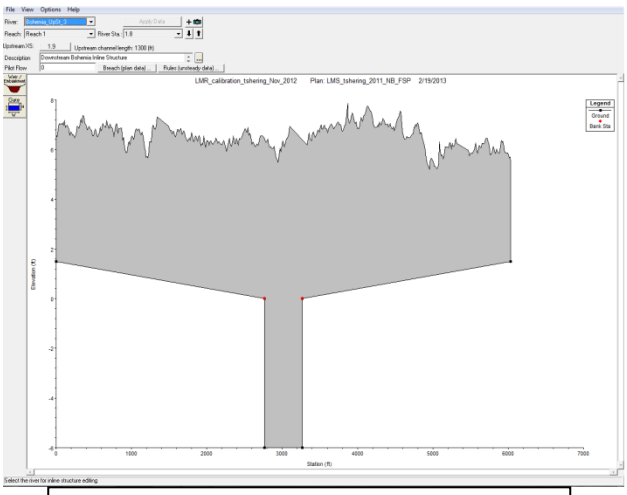

Bohemia U/S Structure 3

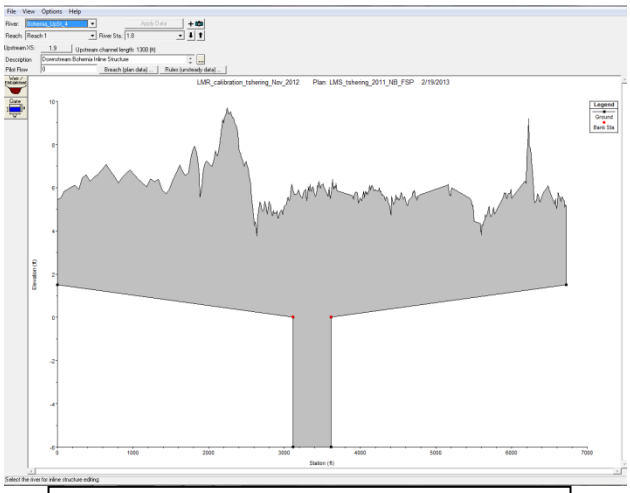

Bohemia U/S Structure 4

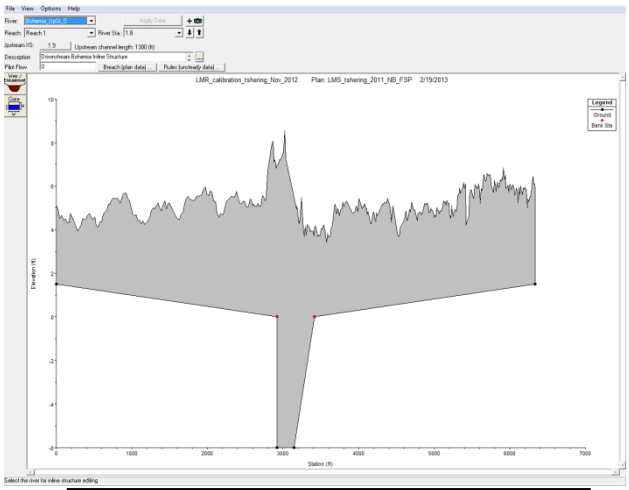

Bohemia U/S Structure 5

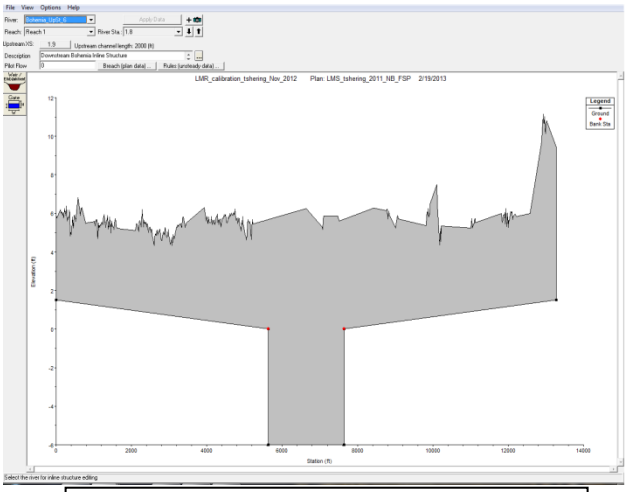

Bohemia U/S Structure 6

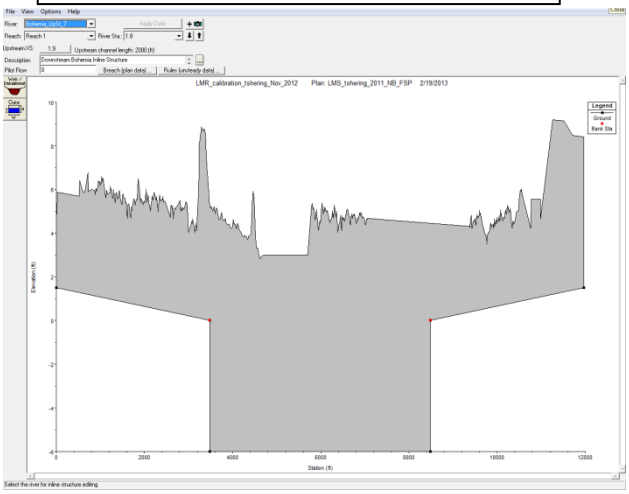

Bohemia U/S Structure 7

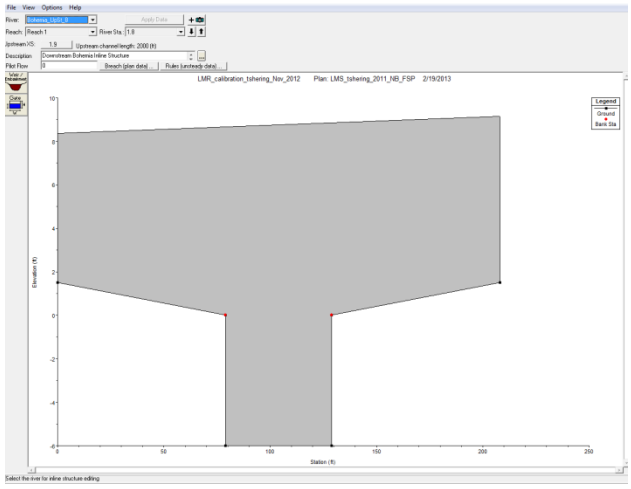

Bohemia U/S Structure 8

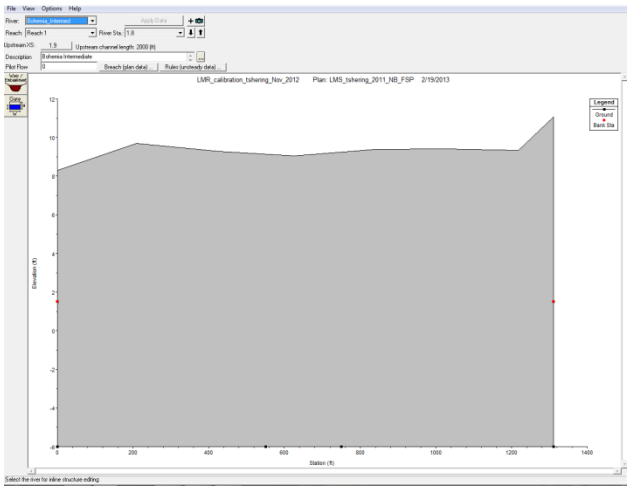

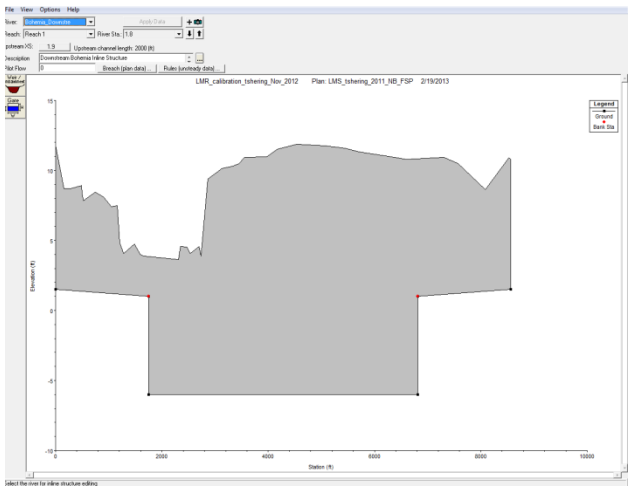

Bohemia Intermediate Structure

Bohemia D/S Structure

Figure 5-3: Bohemia weirs installed in HEC-RAS Model corresponding to LPBF Survey Data.

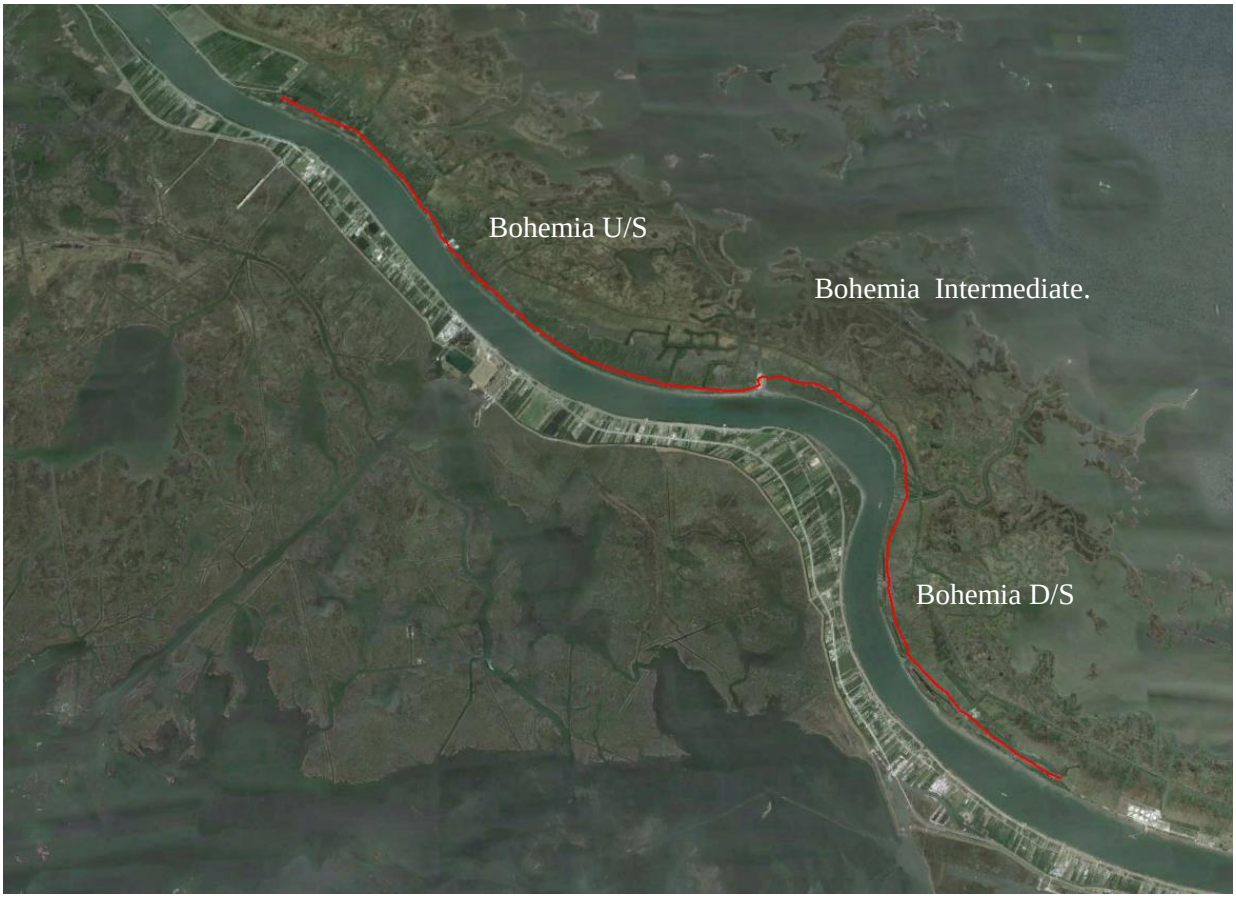

Figure 5-4: Bohemia reach with the survey data path plotted in Google Earth image (RM 31 to RM 44).

Ostrica extends from RM 22 to around 26. There are couples of cuts that branch off from the MR and have the capability to extract flows. These cuts were not included in the previous models. For the current model, the study focused on a better estimate of flows extracted from MR and thus all major cuts capable of extracting flows were included. Google Earth images were used to measure the length and width of the cuts located in these areas. Then, Lacey's Regime equations were used to calculate the depth.

In Lacey's Equation, width is represented by the wetted perimeter (P_w),

$$P_w = 2.67Q^{1/2} \qquad \text{Equation 5.1}$$

As the width is found from Google Earth, estimated discharge (Q) can be found for every cut. Lacey uses a silt factor to give the effect of sediment.

$$f_s = 8\left\{D_{50(inches)}\right\}^{1/2} \qquad \text{Equation 5.2}$$

The D_{50} is used as 0.18mm as it represents an average particle size in the LMR. The depth (D) is represented by the hydraulic radius (R) which is given by:

$$D = R = \left\{Q/\left(1.17P_w f_s^{1/2}\right)\right\}^{2/3} \qquad \text{Equation 5.3}$$

The velocity in the channel can be calculated by:

$$V = 1.17\left[f_s R\right]^{1/2} \qquad \text{Equation 5.4}$$

This form of Lacey's equations is in US customary units.

From equation of continuity, the cross-sectional area can be calculated by:

$$A = Q/V = P_w RV \qquad \text{Equation 5.5}$$

For the equivalent channel, an average length of the channel is calculated based on each individual measured data. The cumulative width and depth of the channels are calculated to achieve the equivalent channel.

Figure 4-5 shows the Google Earth image of Ostrica reach with the cuts marked. Figure 4-6 show the HEC-RAS model cross-section used to represent Ostrica.

Figure 5-5: Ostrica outlets marked on Google Earth image (RM 22 to RM 26).

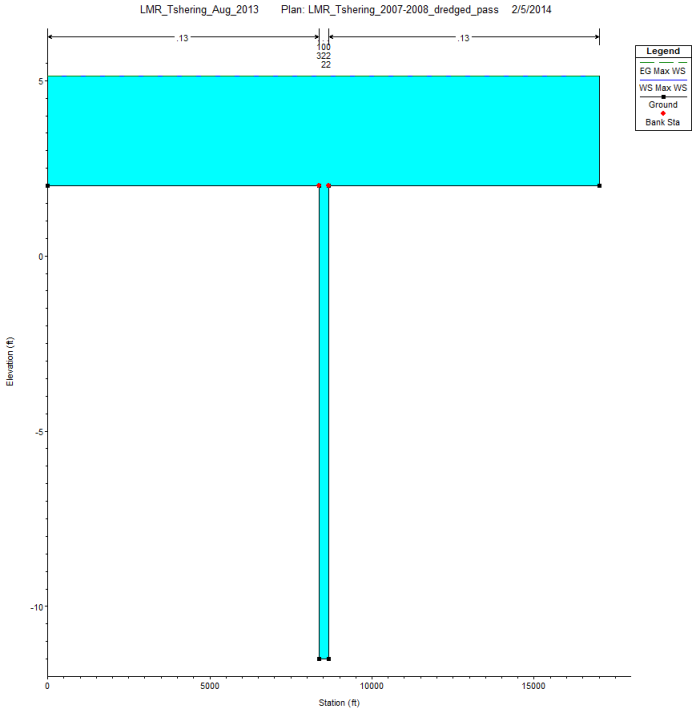

Figure 5-6: Ostrica equivalent channel cross-section in HEC-RAS model.

Figure 5-7: Fort St. Philip cuts from Google Earth image(RM 18 to RM 21).

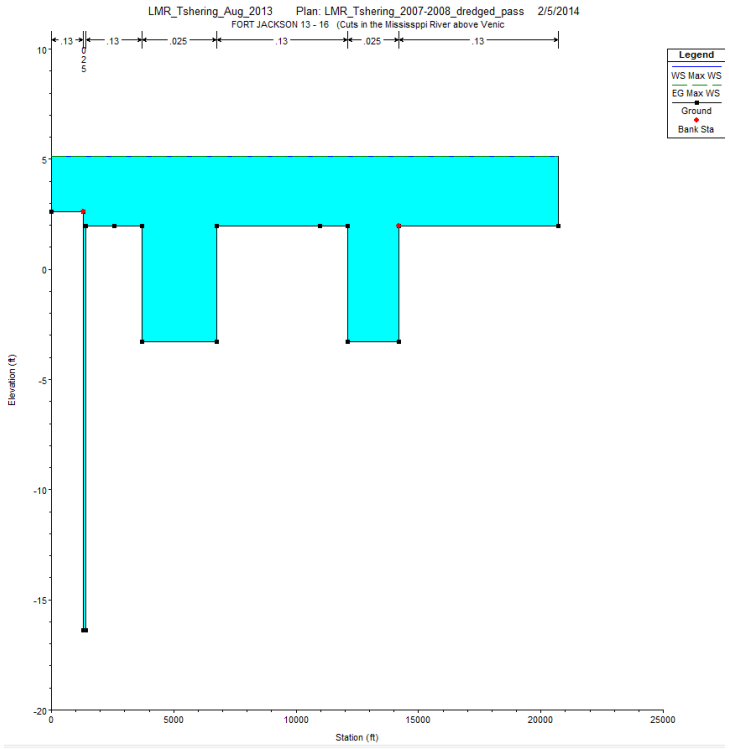

Figure 5-8: Fort St. Philip equivalent channel cross-section in HEC-RAS model.

The Fort St. Philip cuts are located around RM 18 to RM 21 in the MR. Figure 5-7 shows the Google Earth image of the cuts in the Fort St. Philip reach. The outlet was again measured for length and width using Google Earth map and the channel dimension was estimated using Lacey's regime equations. The channel was divided into 3 equivalent outlets which were compiled as a single cross-section for the HEC-RAS model. Figure 5-8 shows the cross-section of Fort St. Philip used in the HEC-RAS model.

The 7-Cut weir extend from RM 11 to RM 18. This reach located between Fort St. Philip and Baptiste Collette contains multiple cuts with 7 significantly visible channels and was thus named as 7-Cut weir. Similar approach of equivalent channels and Lacey's regime equations was applied for this channel too obtain a useable geometric cross-section in the HEC-RAS model. Figure 5-9 shows the Google Earth image of the cuts in the Fort St. Philip reach. Figure 5-10 shows the cross-section of Fort St. Philip used in the HEC-RAS model.

Figure 5-9: 7-Cut weir outlets marked on Google Earth image (RM 11 to RM 18).

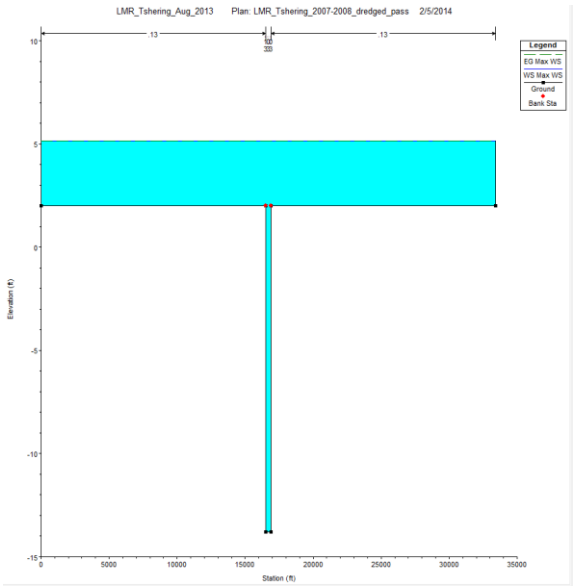

Figure 5-10: 7-Cut weir equivalent channel in HEC-RAS model.

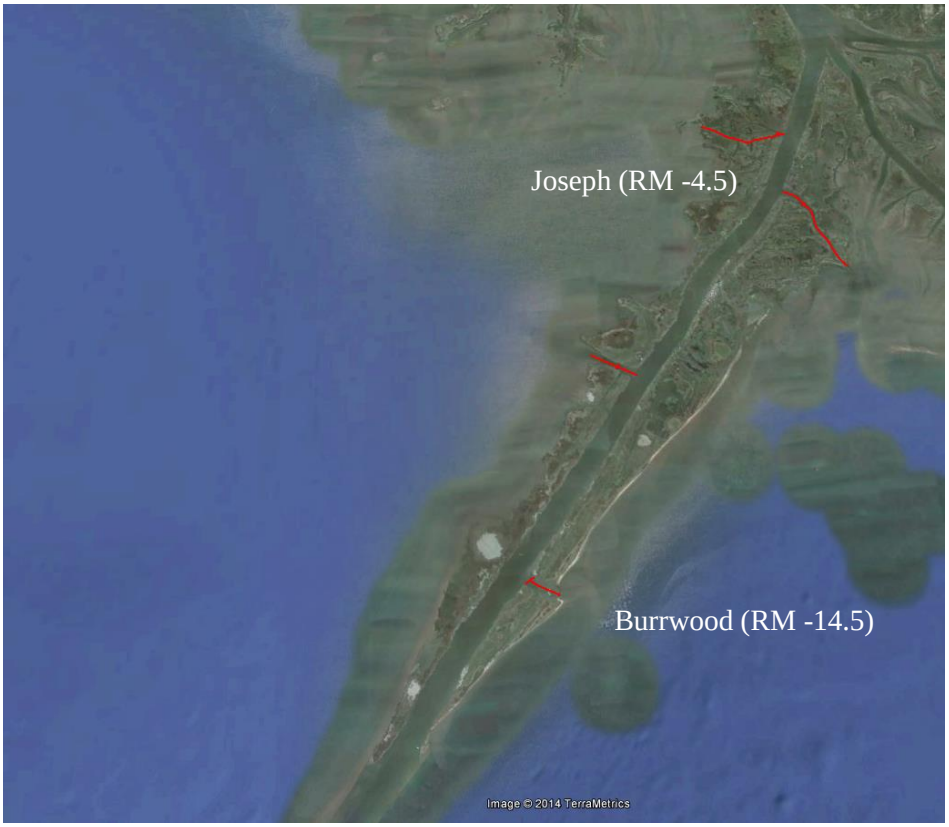

Figure 5-11: Southwest pass marked with cuts on Google Earth image.

Joseph and Burrwood cuts are equivalent channels included in the model to represent the cuts located in South-west Pass. The upper cuts were combined to form Joseph outlet which is located around 4.5 miles downstream Head of Pass (HOP). Burrwood is the equivalent channel

for cuts located at lower portion of the pass which is located at around 14.5 miles downstream of HOP. It is important to include these cuts as they extract significant amount of flow from the pass affecting the head and energy present in the pass.

5.1.2 Channel Roughness

Based on Manning's Equation, the flow of a river is dependent on the roughness of the channel. Manning defined the roughness with a coefficient '*n*' and is presented in the following equation:

$$n = \frac{c'}{Q} A R^{2/3} S^{1/2} \qquad \text{Equation 5.6}$$

where: Q = Discharge (ft^3/s or m^3/s)

c' = Conversion Factor (1.486 for U.S. units and 1 for S.I. units)

A = Cross-sectional area (ft^2 or m^2)

R = Hydraulic Radius = A/P_w (ft or m)

P_w = Wetted Perimeter (ft or m)

S = Bed Slope

n = Roughness Coefficient

There are other factors also contributing to roughness coefficient of a channel. Chow has described the following factors (Chow 1959):

1) Surface Roughness: Based on Chow (1959), it is found that the channel surface roughness is dependent upon the grain material of the wetted perimeter or the channel submerged in the water. The coarser grains lead to a higher *n* value whereas finer grains pertain to a lower *n* value. So, the *n* value is directly proportional to $D_{50}^{1/6}$ where D_{50} is the median grain size.

2) Vegetation: Presence of vegetation leads to a higher *n* value and its effects are varying based the height, density, distribution and type of vegetation. Lower discharge in the channel result in a higher *n* value for a vegetation cover compared to higher flows as it requires more energy to pass through or over the vegetation comparatively. The higher discharge tends to submerge the vegetation reducing the *n* value. Also, channels with

steeper side slopes contribute to higher velocity which compresses the vegetation and lowers the *n* value.

3) Channel Irregularities: Channel bed irregularities such as sand bars and deep holes lead to additional resistance to the following contributing to a higher *n* value.

4) Channel Alignment: Severe meandering contributes to slowing down of the flow and eventually contributing to increase in *n* value.

5) Silting and Scouring: Silting or deposition can cover the channel irregularities making a smoother surface and thus decreasing the *n* value. However, scouring does the opposite creating more irregular surfaces and eventually contributing to higher roughness factor. Finer materials like clay scour non-uniformly creating pits or holes and increase the *n* value. However, coarser materials like sand or gravel scour uniformly resulting in a uniform bed surface and reduce the *n* value.

6) Obstructions: Obstructions such as bridge piers and debris can contribute to increase in the value of *n* depending on their nature, size, shape, number and distribution.

7) Size and Shape of Channel: Shape and size of the channel also has varying affects. Channel with steeper slopes and side slopes can lead to high velocity in channel which contribute to erosion. Its affect also depend upon vegetation cover and varies with type of bed loads as discussed previously.

8) Stage and Discharge: The amount of discharge affect is discussed in the vegetation covers. The increase in stage during high discharge, inundation of the floodplains takes place which increases the composite *n* value as floodplains typically have higher *n* values than the channels.

9) Seasonal Change: Seasonal growth of vegetation in the channel and the flood plains also impact the roughness coefficient.

10) Suspended material and Bed Load: Sediment rich channels need additional energy for the transport of suspended and bed materials leading to higher value of *n*.

The lower MR channel is comprised of many meanders, bridges, bars, deep holes and some vegetation that is encountered at high flows. It also transports range of sediments from coarse sand to fine clays. These all factors combine to increase the roughness factor in the river. However, most of the river is constrained by flood protection levees on both sides leading to large depth in most places and thus decreasing resistance to the flow. The presence of bed forms or sand dunes varying in height and wave length due to changes in the bed shear in the channel complicates the calculation of a fixed roughness coefficient. The distribution of bed forms in the channel is both spatial and temporal.

Altogether, these bed forms tend to increase the effective roughness. These all variables contribute to the value of Manning's *n* not being accurately determined from the measured stages and flows for the MR. For this study, varying value of Manning's n ranging from 0.018 to 0.03 were determined by calibration based on the flow and stage data.

5.1.3 Boundary Conditions

Daily discharge measured at Tarbert Landing by USACE was used as the upstream boundary condition for the MR reach for each of the periods of simulated.

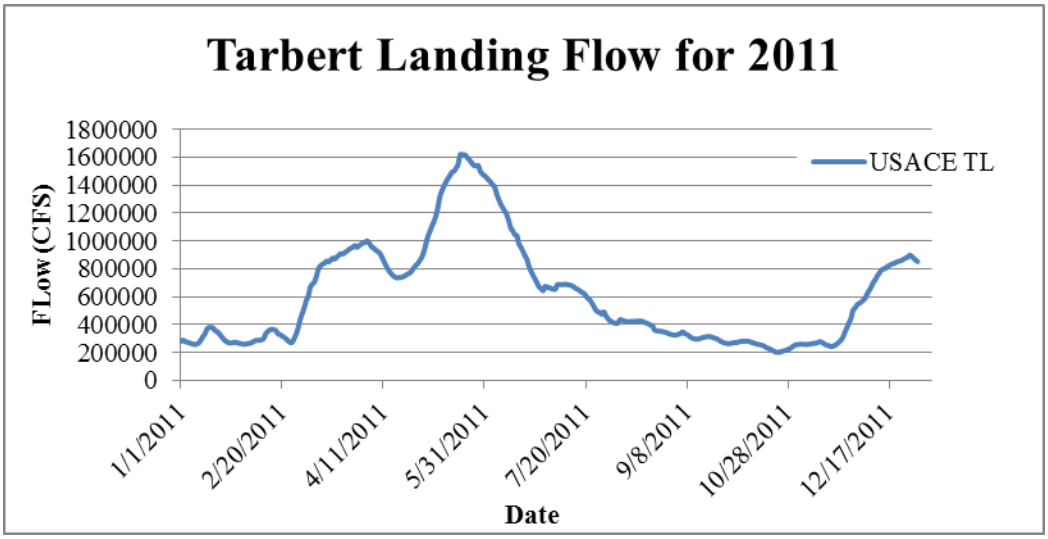

Figure 5-12: HEC-RAS upstream flow boundary for 2011.

Fig 5-12 shows the Tarbert Landing discharge for 2011. Flow boundaries used for other validation years can be found in Appendix A.

A single daily stage hydrograph at the GOM obtained from USACE website was use as the downstream boundary condition for all open water channels which include Barataria Bay, Passes, Caernarvon diversion, Bayou Lamoque, Bohemia, Ostrica, Fort St. Philip, 7-Cut weir, Baptiste Collette and West Bay. Hourly simulations were also performed for the validation process. The hourly data were obtained from NOAA's tide and current website (http://tidesandcurrents.noaa.gov/waterlevels.html?id=8760922). Figures 5-13 and 5-14 show the daily and hourly discharge in GOM. Daily and hourly stages for other years used for validation can be found in the Appendix A.

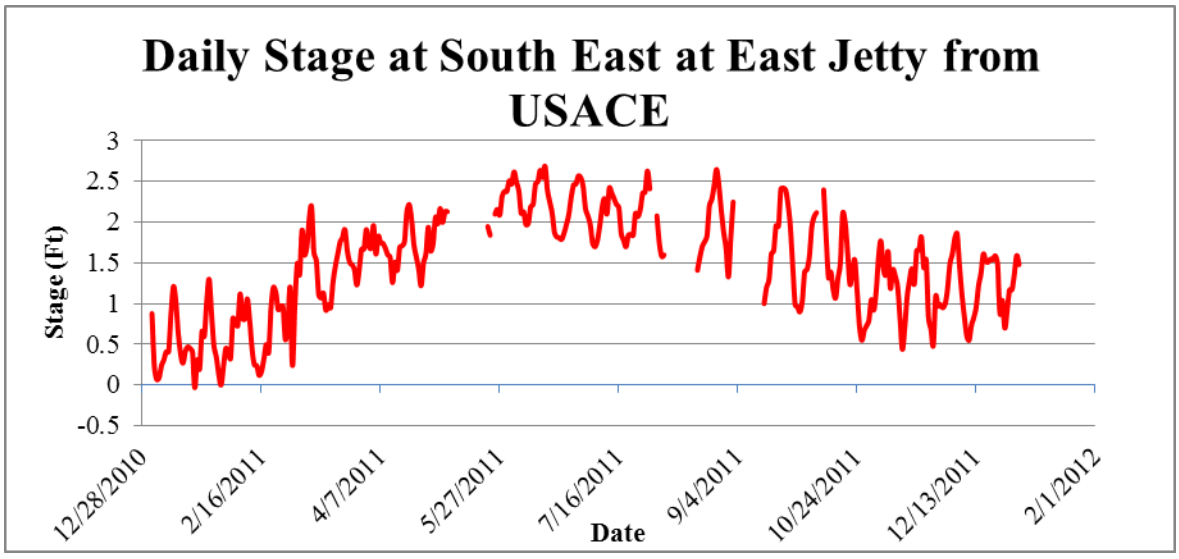

Figure 5-13: HEC-RAS daily stage downstream stage boundary for 2011.

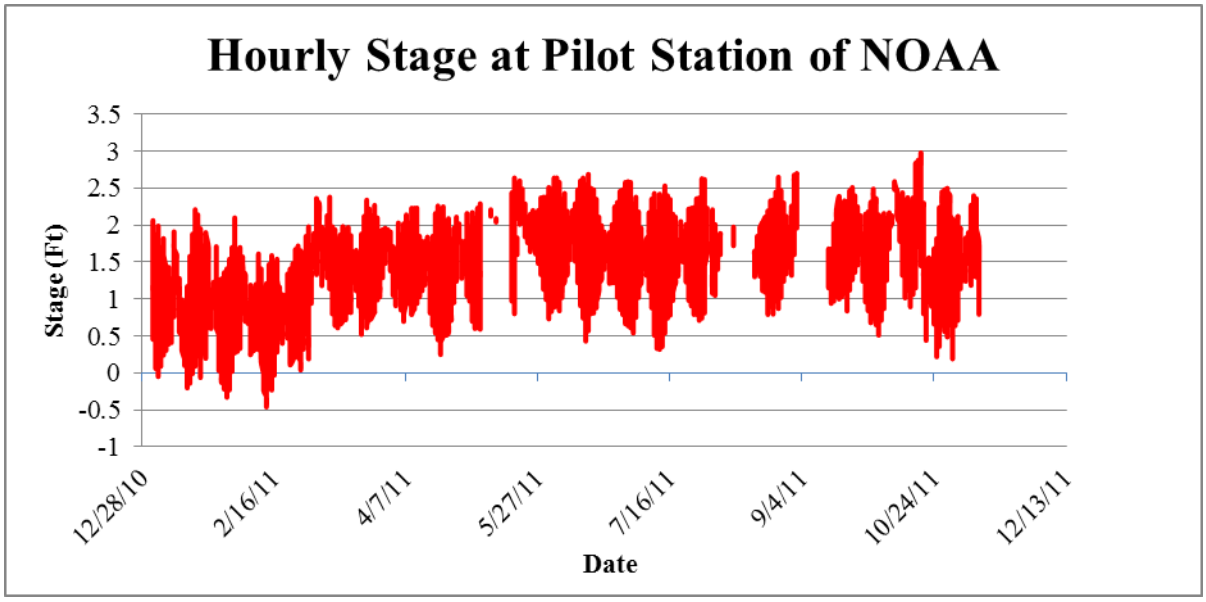

Figure 5-13: HEC-RAS hourly stage downstream stage boundary for 2011.

The Morganza (RM 280) and Bonnet Carré (RM 128) spillways were modeled as lateral flow extractions. The time series for the extraction were obtained from the estimates by the USACE. Figure 5-14 shows the Morganza and Bonnet Carré flow extraction estimates used in the model.

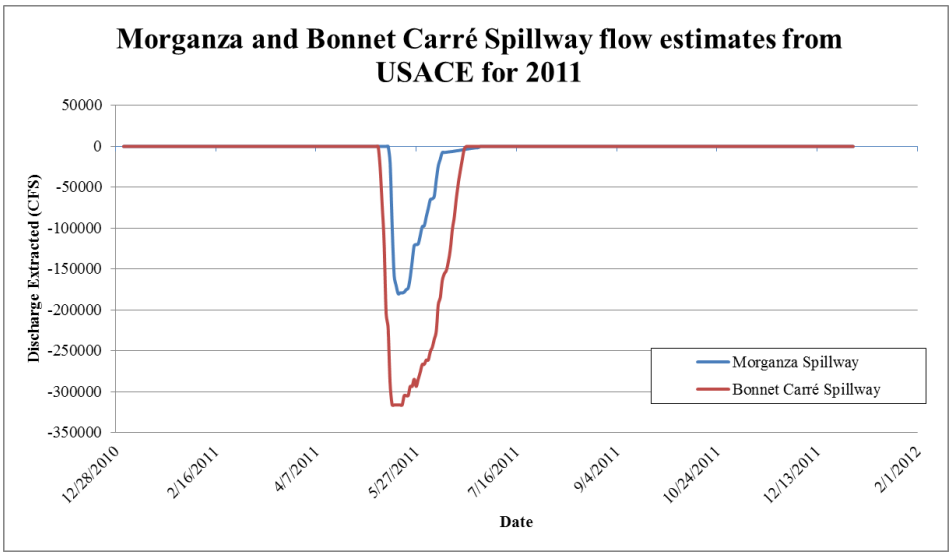

Figure 5-14: Lateral flow extraction hydrograph for Morganza and Bonnet Carré spillway for 2011(Note-Negative value indicates outflow).

The elevation controlled gates options which was chosen as boundary condition for the both the Davis Pond Freshwater Diversion and the Caernarvon Freshwater Diversion Structures. Both Bayou Lamoque North and South gated structures were given a time-series of gate opening boundary condition. The settings and boundary for these structures were unchanged and used as specified by Davis *et. al (2010)*.

5.2 CHARIMA Model Development

5.2.1 Geometry Data

The geometric sections in CHARIMA correspond to the data used in the HEC-RAS model. Previously, the model was developed by Pereira *et al* (2011) for the Lower Mississippi River. The model domain was from Belle Chasse (RM 76) to HOP (RM 0) without Ostrica and 7-Cut weir. In the study, the model was extended to the GOM by the addition of the 3 passes (Southwest, South and Pass A-Loutre). Also, the geometric cross-sections in the Bohemia Reach, Ostrica, 7-Cut weir and Fort St. Philips were improved with availability of additional data from LPBF. Figure 5-15 shows schematic diagram of the outflows topology of the current CHARIMA model for existing outlets and diversions. Figure 5-16 shows the schematic diagram of the outflows topology of the CHARIMA model for existing outlets and diversions including the future MLODS diversions. The model is defined by nodes (circles) and links (lines) as well as structures such as weirs and gates. The computational domain for existing conditions includes 990 different cross-sections organized in a structure of 54 nodes and 54 links. Chapter 4 discusses about the model components in CHARIMA.

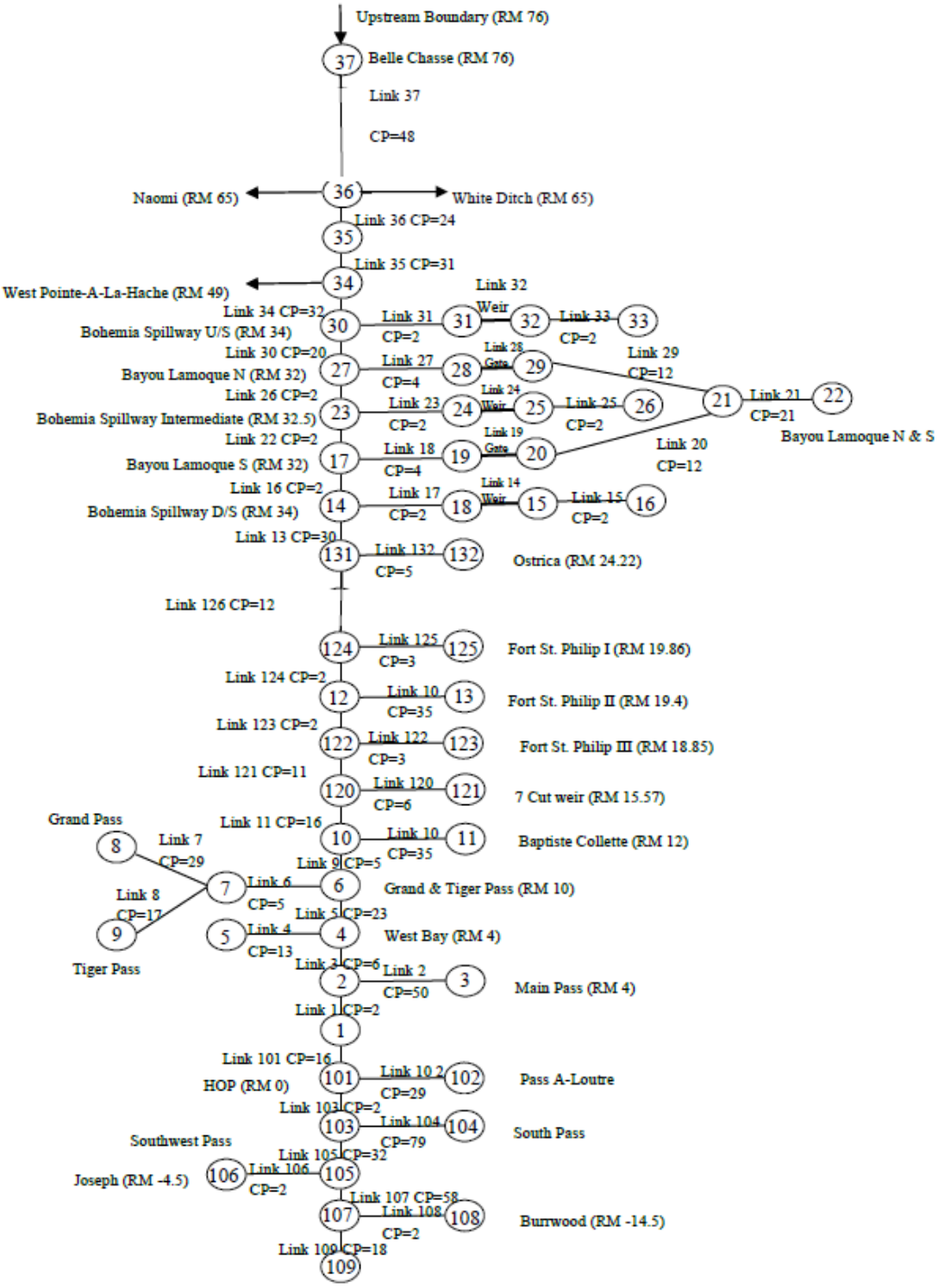

Figure 5-15: Schematic diagram for CHARIMA model with existing diversions.

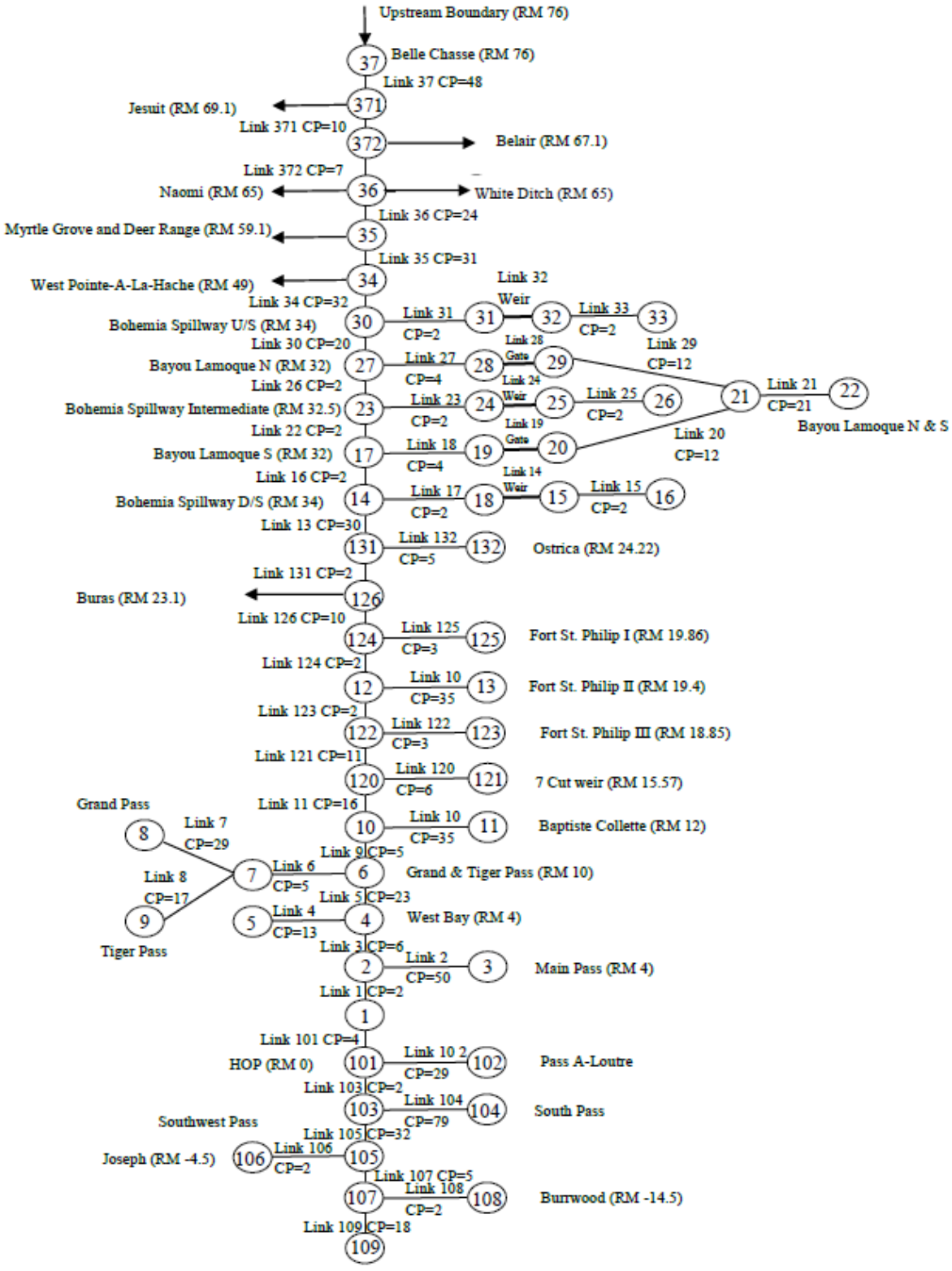

Figure 5-16: Existing and future diversions in the CHARIMA model domain.

All the geometric cross-sections used in CHARIMA model correspond to the ones used in HEC-RAS model. The only difference lies in Fort St. Philip. In HEC-RAS, three equivalent channels were installed as one cross-section as the model as option for variable values of Manning's *n* based on horizontal distance over the cross-section. This feature is not available in CHARIMA and thus the 3 equivalent channels were inserted individually and named Fort St. Philip 1, 2 and 3 respectively. Fig 5-17 shows the three separate channels present in Fort St. Philip reach.

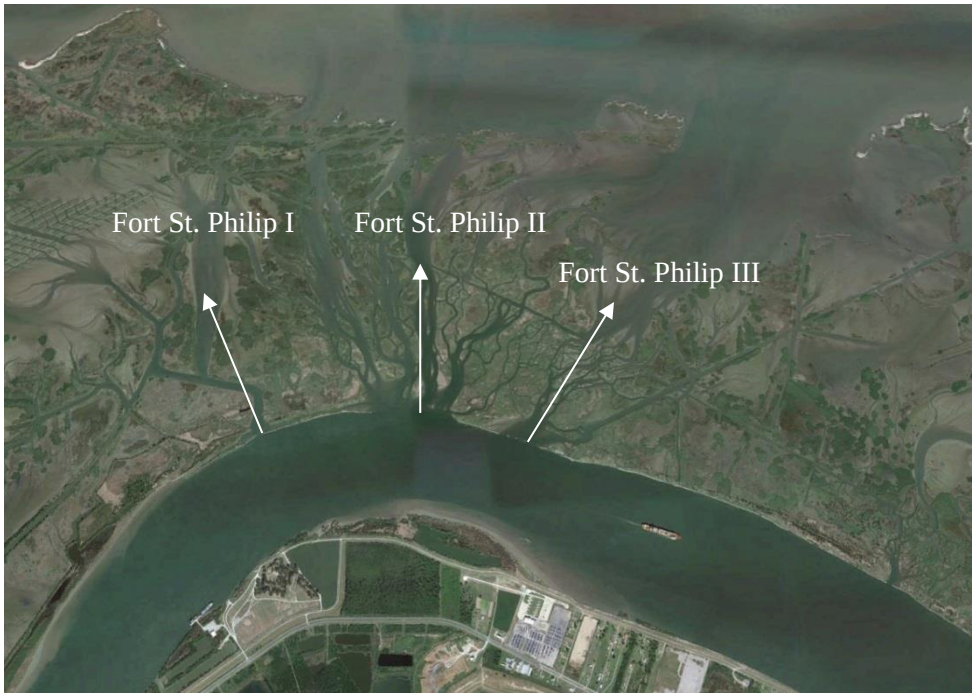

Figure 5-17: Fort St. Philip reach showing the 3 equivalent channels used in CHARIMA model (Google Earth Image).

5.2.2 Channel Roughness

To model the channel's roughness corresponding to Manning's *n* value, CHARIMA model use the Strickler's coefficient 'K_s'. This value is equal to the reciprocal of the *n* value. The model reaches use the roughness coefficient value corresponding to the range of *n* values in the main channel of the HEC-RAS model. The range of K_s value is 65 to 33 which translate to Manning's *n* value of 0.016 to 0.03. The outlets have the highest values and obtained by calibration. The MR reaches have values corresponding to Manning's coefficient of 0.018 to 0.026.

5.2.3 Boundary Conditions for CHARIMA

Daily discharge obtained from HEC-RAS model at Belle Chasse (RM 76) was used as the upstream boundary condition for the MR reach for each of the periods of simulated. Observed data at RM 76 provided by USGS (http://waterdata.usgs.gov/usa/nwis/uv?07374525) could also be used for the study however future case scenarios were also simulated using the model. So, the flow from HEC-RAS, a model with the capability to predict discharge at Belle Chasse for varying cases, was chosen.

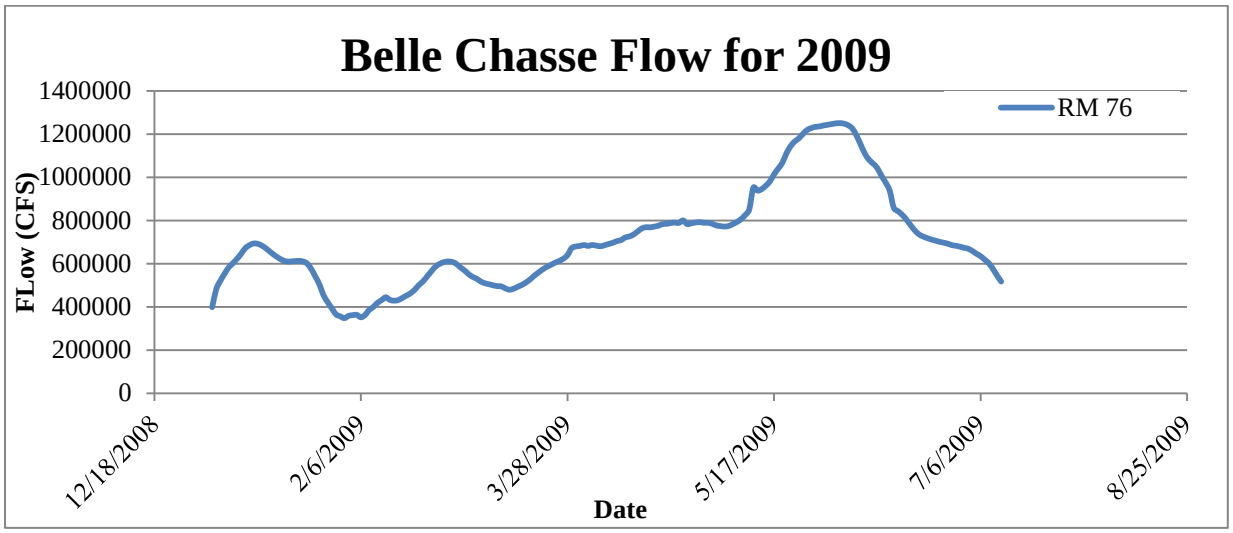

Figure 5-18: CHARIMA model upstream flow boundary for 2009

Fig 5-18 shows the Belle Chasse discharge for 2009 from HEC-RAS model. Flow boundaries used for other years for validation can be found in Appendix B.

A single daily stage hydrograph at the GOM obtained from USACE website was used as the downstream boundary condition for all open water channels which include: all the Passes, Bayou Lamoque, Bohemia, Ostrica, Fort St. Philip, 7-Cut weir, Baptiste Collette and West Bay. The stage boundary conditions in HEC-RAS and CHARIMA are same for the corresponding reaches. Figure 5-19 shows stage at GOM used for downstream boundary in CHARIMA for the period of 2009.

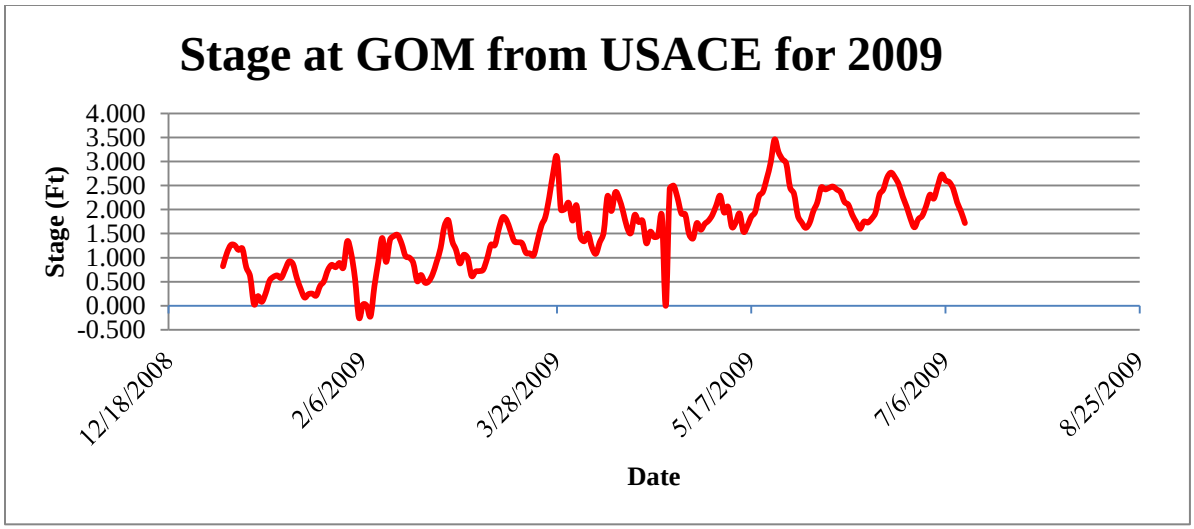

Figure 5-19: CHARIMA model downstream stage boundary for 2009

For the sediment load, the suspended sand concentration (mg/L) rating curve from USGS was used to obtain a sediment discharge boundary (Qs versus Q–CFS).

For the sediment load, the suspended sand concentration (mg/L) rating curve shown in Figure 5-20 was derived from USGS data at Belle Chasse obtained from the website (http://waterdata.usgs.gov/nwis/dv/?site_no=07374525&agency_cd=USGS&referred_module=sw) and was used to obtain a sediment discharge boundary (Qs versus Q in CFS) as shown in Figure 5-21.

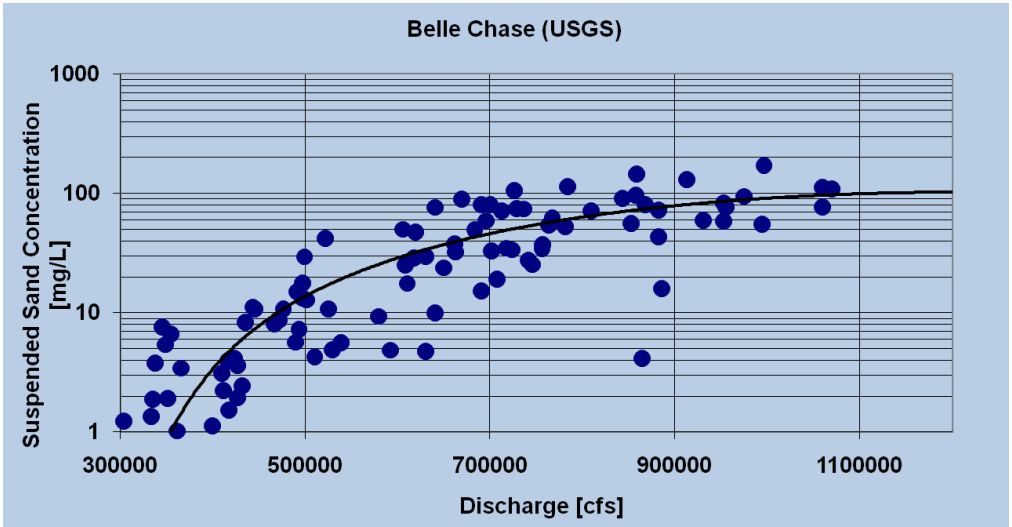

Figure 5-20: Rating Curve used for calculation of the sediment boundary in CHARIMA model. (USGS)

The Belle Chasse inflow suspended sand loads were based on the field data obtained by Nittrouer et al. (2008) and the Belle Chasse water discharge given by HEC-RAS. There was no need to give sand concentrations or loads as boundary conditions for the outflows. The formulation in CHARIMA allows the calculation of the balance of not only the water but also the sediment that is extracted at each diversion. Table 5.1 shows the maximum, minimum and average values of the sand load series given as upstream boundary condition for 2009 simulation for calibration process.

Table 5.1: Sand Load Boundary Condition-Existing Outflow Case – 1-D Calibration 2009

Site	Qs Maximum (metric tons/day, CFS)		Qs Minimum (metric tons/day, CFS)		Qs Average (metric tons/day, CFS)	
Belle Chasse (RM 76)	191,956.67	29.62	3,723.85	0.57	66,397.69	10.27

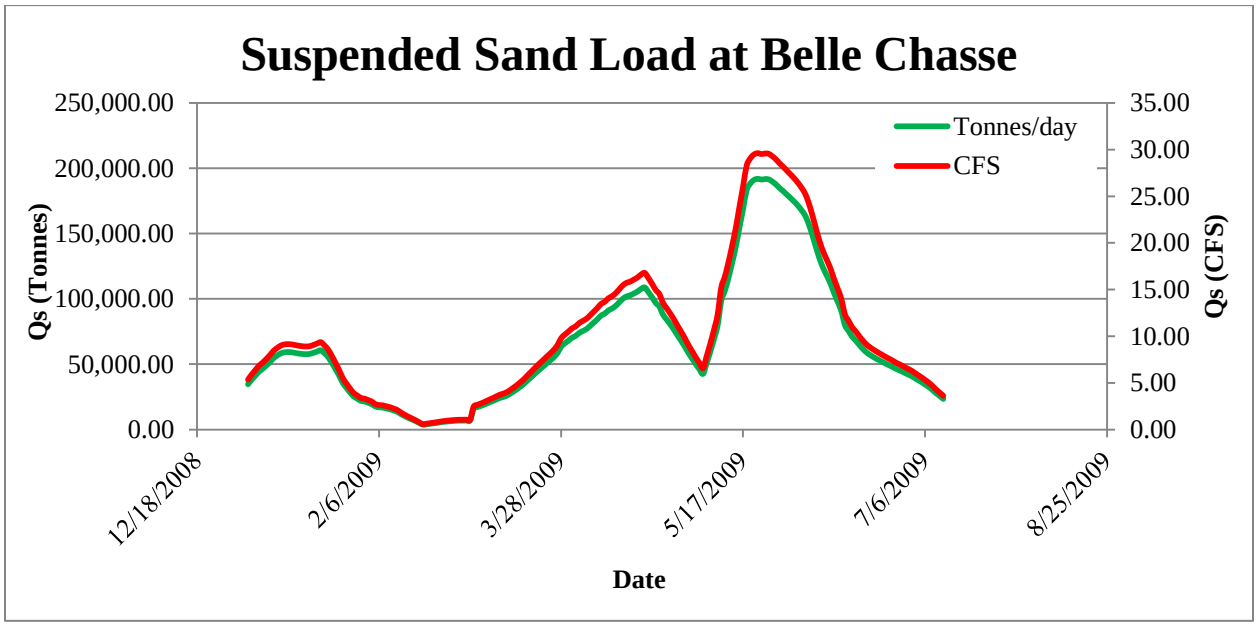

Figure 5-21: CHARIMA model upstream sediment boundary for 2011.

Chapter 6: Calibration and Validation

In order to utilize the results from the model simulations, the model had to be calibrated based on observed data for a one period and validated or checked using observed data from a different period. In the validation process the parameters that were adjusted in the calibration phase are left untouched. After calibration and validation of the model, it was considered to be serviceable for other applications.

6.1 HEC-RAS Model Calibration

For the calibration procedure, the calendar year of 2011 was used as this period comprised of peak flow over 1 million CFS and low flow closing to 200,000 CFS. The model was calibrated with the existing diversions. The Morganza and Bonnet Carré spillways were modeled as lateral flow extractions.

The stage results in the MR obtained from HEC-RAS model were compared to measured stage data from the USACE river gages website at the following locations (Mississippi River & Passes; http://rivergages.mvr.usace.army.mil/WaterControl/new/layout.cfm): Red River Landing (RM 302.4), Baton Rouge (RM 228.4), Bonnet Carré (RM 126.9), New Orleans at Carrollton (RM 102.8), Belle Chasse (RM 72.8), Alliance (RM 63.2), West Pointe A-La-Hache (RM 48.7), Empire (RM 29.5), Venice (RM 10.7) and Head of Passes (RM 0).

The Manning's *n* value was changed along several reaches of the MR for the calibration process. With the changes in the *n* value, the model was re-run until the model output gave similar results to the measured data. Appendix C shows all the *n* values used in the main MR for the calibration process. As discharge as an impact on the *n* value, roughness coefficient factor was introduced. The roughness coefficient gives the option to apply varying *n* values depending on the nature of the flow. For higher flows, the factor is reduced giving a lower *n* value and vice versa. Figures 5-1, 5-2 and 5-3 show the stages calibration for stations located at RM 228.4, 126.9 and 10.7 using the adjusted *n* values. Other calibration plots can be found in Appendix B.

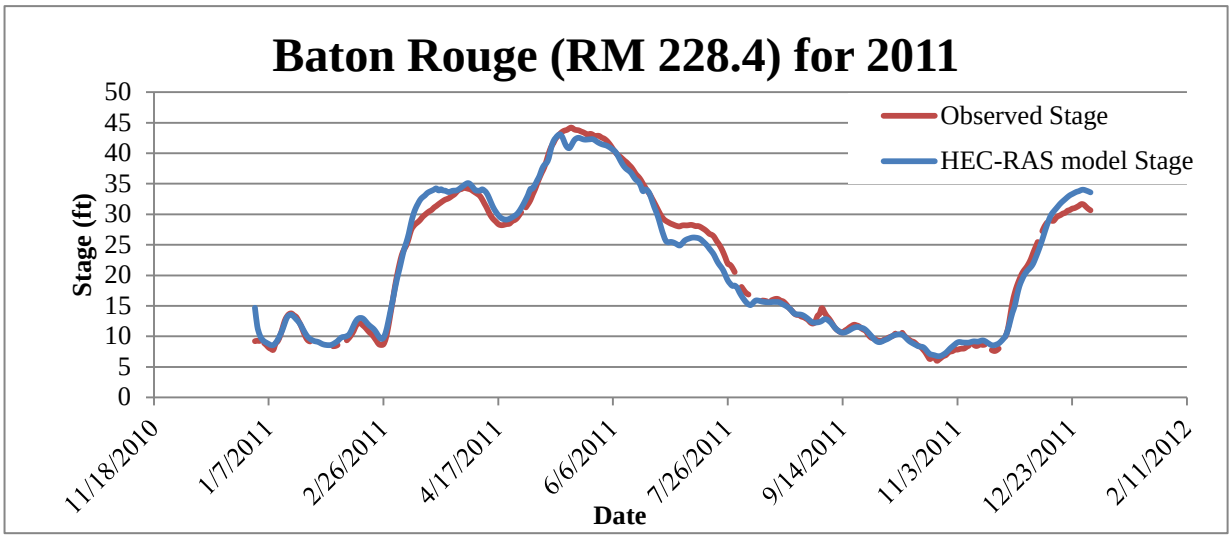

Figure 6-1: Baton Rouge comparison of stage for 2011.

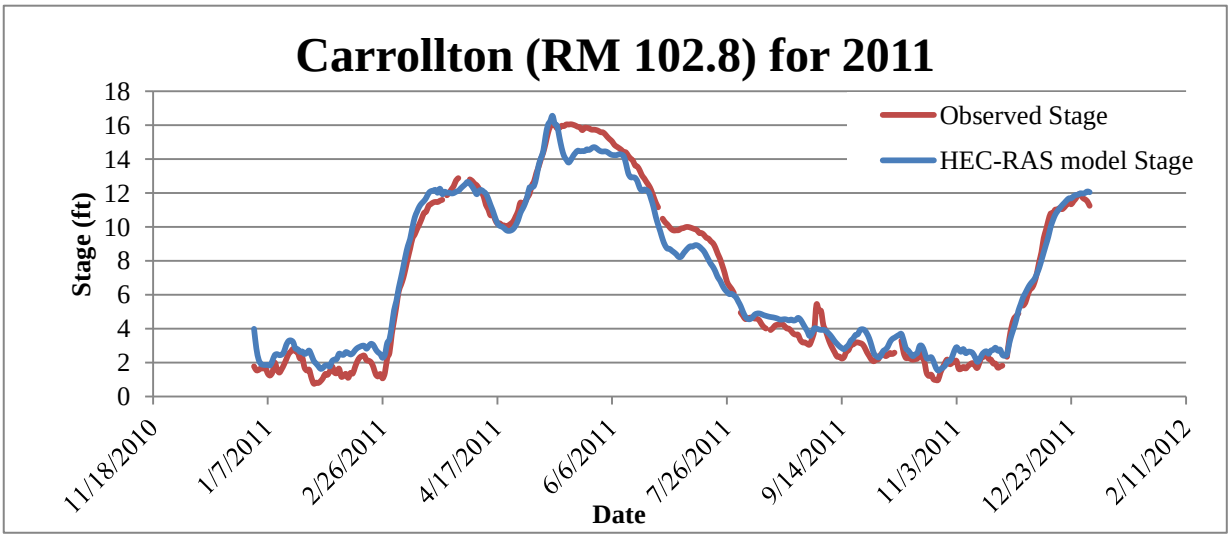

Figure 6-2: Carrollton comparison of stage for 2011.

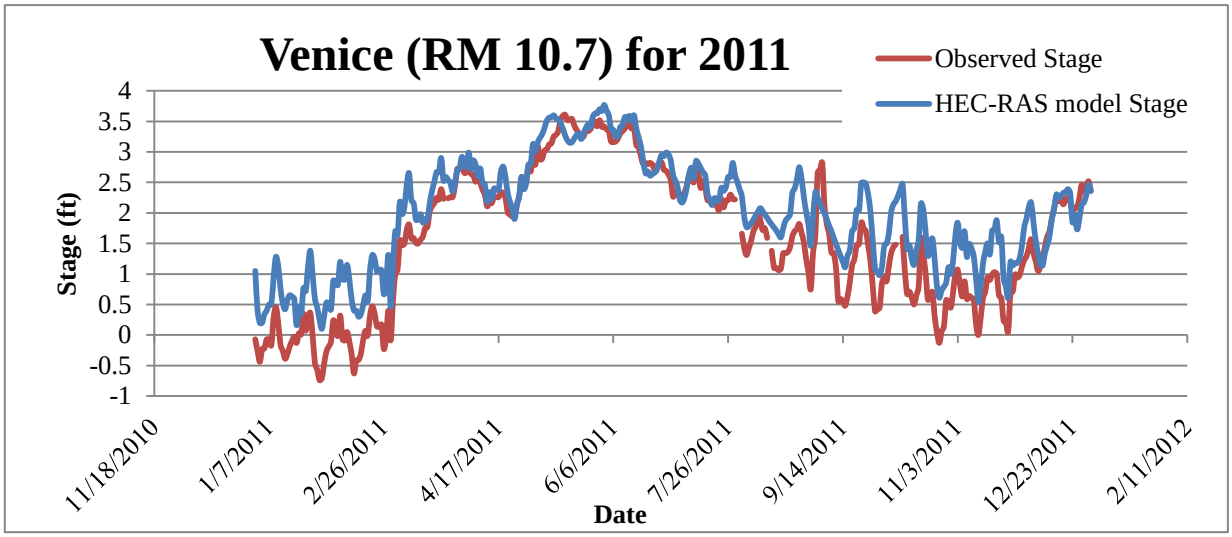

Figure 6-3: Venice comparison of stage for 2011.

Visually, there is an agreement with the stage plots for above listed stations. The stages are following the trend of the observed data.

To quantify the accuracy of the model, the root mean square error (RMSE), the coefficient of efficiency and the bias error between the model and observed data were computed. The RMSE, coefficient of efficiency and the bias error were determined by the following equations:

$$\text{Root Mean Square Error (RMSE)} = \sqrt{\frac{\sum_{i=1}^{N}(O_i - P_i)^2}{N}} \qquad \text{Equation 6.1}$$

$$\text{Coefficient of Efficiency} = 1.0 - \frac{\sum_{i=1}^{N}(O_i - P_i)^2}{\sum_{i=1}^{N}(O_i - O_{avg})^2} \qquad \text{Equation 6.2}$$

$$\text{Bias Error} = \frac{\sum_{i=1}^{N}(P_i - O_i)}{N} \qquad \text{Equation 6.3}$$

where O_i is the observed value, in this case taken as the data measured by USACE; P_i is the model predicated value; O_{avg} is the average of the observed value and N is the number of observations.

Table 6.1 shows the coefficient of efficiency and the RMSE obtained for the hydrodynamics stage calibration. These results have a good agreement between the simulations and the observed data obtained from USACE.

Table 6.1: Error Analysis HEC-RAS stage Calibration - 2011

Mississippi River Location	RMSE (ft)	Efficiency	Bias Error (ft)
Baton Rouge (RM 228)	1.44	0.98	+0.01
Bonnet Carré (RM 126.9)	0.99	0.98	+0.26
Carrollton (RM 102.8)	0.80	0.97	+0.10
West Pointe A-La-Hache (49)	0.81	0.88	+0.65
Venice (RM 10.7)	0.53	0.78	+0.40

The efficiency predicts the closeness of the model values to the observed value. The efficiency values ranging from 78% to 98% is very good. The bias error refers to the model values, minus the observed value. The bias values are very low and thus infers the model is calibrated.

For flow comparison, the observed data were plotted against HEC-RAS model results. Some of the flow estimates were provided the LPBF for various outlets which were used to compare to the model data. Other outlet flow data were obtained from the USACE.

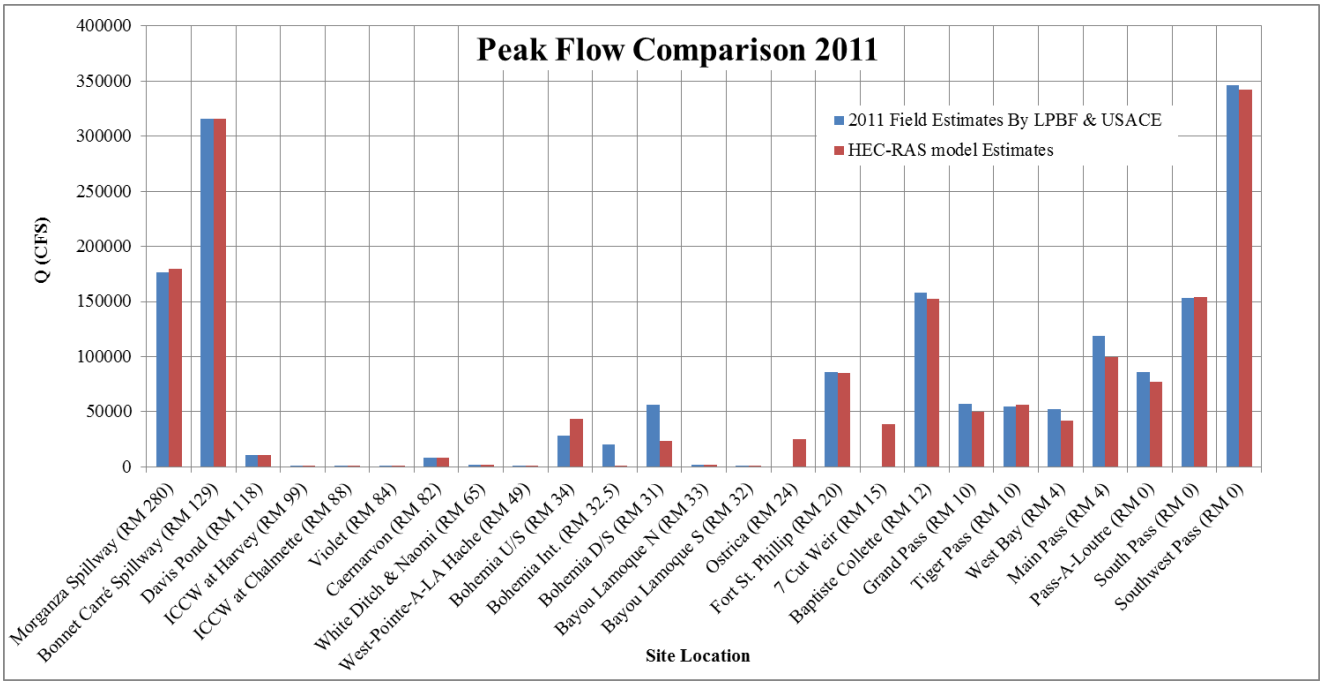

Figure 6-4: Peak flow comparison for 2011.

Figure 6-4 shows the comparison between the model flows and the flows estimated by LPBF for the calibration period of 2011. During the LPBF estimates, the Ostrica flows were included in the Bohemia reach flow. Also, parts of 7-Cut weir flow were included in Fort St. Philip and the remaining in the Baptiste Collette flow. However, the HEC-RAS model represents these flows in a separate channel. Through error analysis, it is found the calibrated model has a RMSE error of 9.3%. Also overall, the model was under predicting by 1.4% of the peak flow at Tarbert Landing.

6.2 HEC-RAS Model Validation

For the validation process, the model was given boundary conditions of the calendar year of 2008. Rest of the model parameters from the roughness factor to manning's *n* values were kept same as the calibrated model. The model was also validated for the years 2007, 2009, 2010 and 2012 for which the stage results are listed in Appendix B. The stage validation results for 2008 are listed in Figures 6-5 and 6-6.

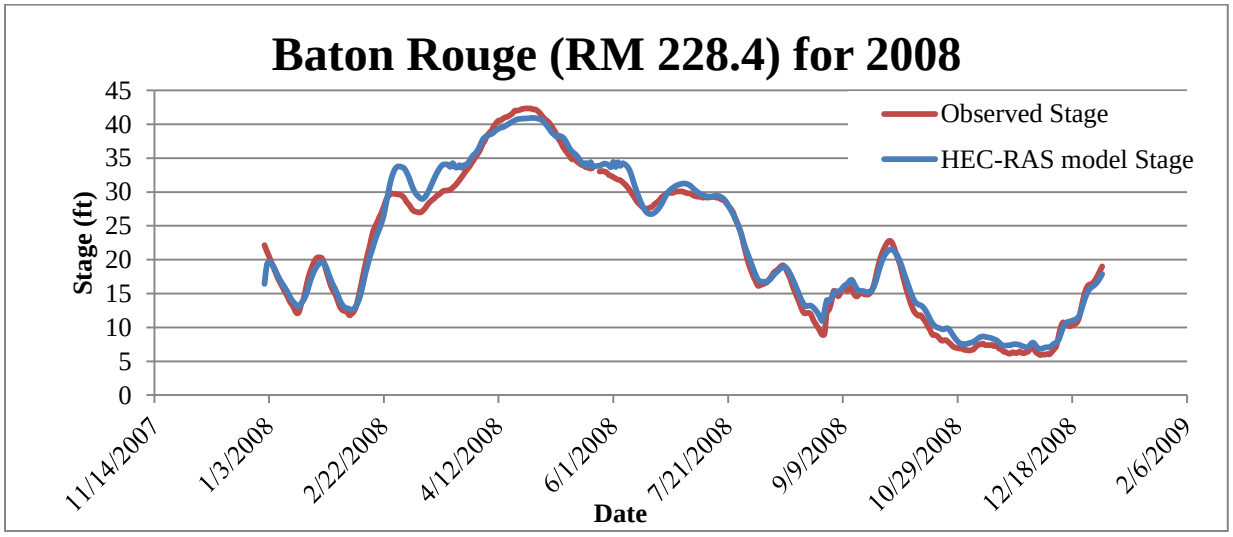

Figure 6-5: Baton Rouge stage comparison for 2008.

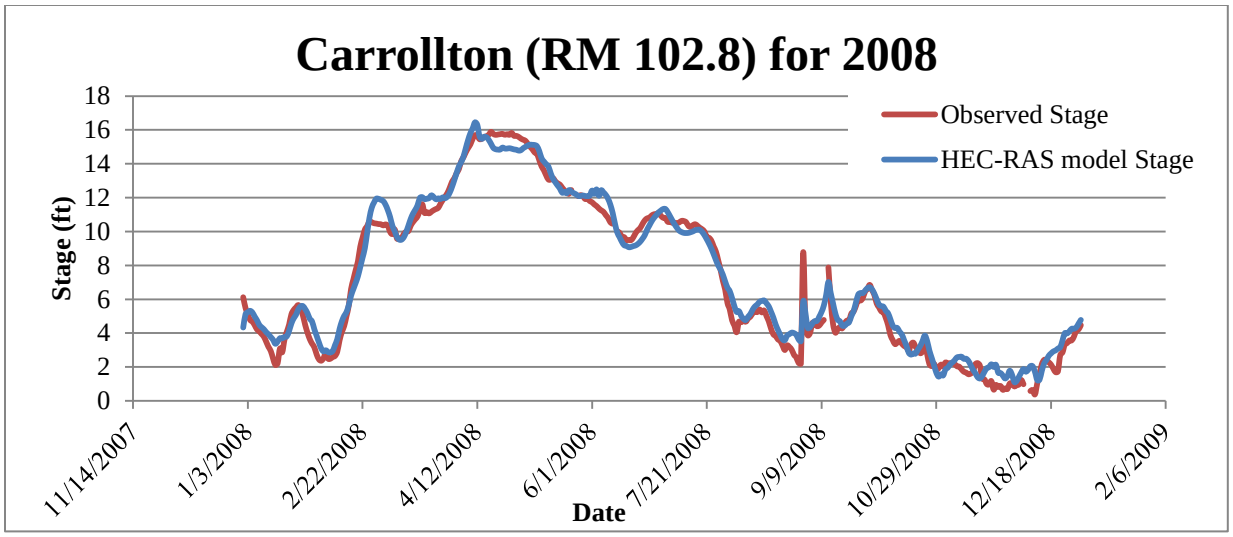

Figure 6-6: Carrollton stage comparison for 2008.

Visually, there is an agreement with the stage plots for above listed stations. The stages are following the trend of the observed data.

To access the accuracy of the model, the root mean square error (RMSE), the coefficient of efficiency and the bias error between the model and observed data was measured. Table 6.2 shows the error analysis for validation period 2008. These results have a good agreement between the simulations and the observed data obtained from USACE.

Table 6.2: Error Analysis HEC-RAS stage validation – 2008

Mississippi River Location	RMSE (ft)	Efficiency	Bias Error (ft)
Baton Rouge (RM 228)	1.44	0.98	+0.60
Bonnet Carré (RM 126.9)	0.80	0.98	+0.13
Carrollton (RM 102.8)	0.67	0.98	+0.25
West Pointe A-La-Hache (49)	1.20	0.71	+0.74
Venice (RM 10.7)	0.39	0.85	+0.23

Figure 6-7 show the comparison between the model flows and the flow estimated by LPBF and USACE for the validation period of 2008. During the LPBF estimates, the Ostrica flows were included in the Bohemia reach flow. Also, parts of 7-Cut weir flow were included in Fort St. Philip and the remaining in the Baptiste Collette flow. However, the HEC-RAS model represents these flows in a separate channel. Through error analysis, it is found the calibrated model has a RMSE error of 14.6%. Also the model was over predicting by 9% of the peak flow at Tarbert Landing.

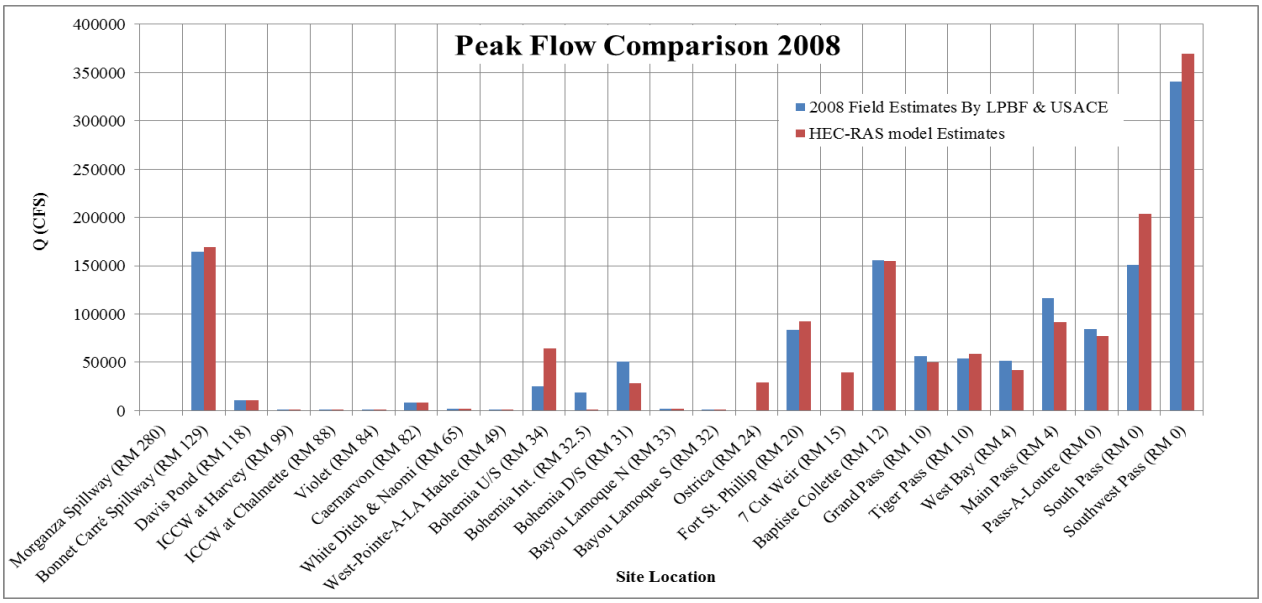

Figure 6-7: Peak flow comparison for 2008

6.3 CHARIMA Model Calibration

For the calibration procedure, the calendar year of 2009 was used as this period had measured sediment data available. The model was calibrated with the existing diversions.

The stage results in the MR obtained from CHARIMA model was compared to stage data HEC-RAS model at the following locations: Alliance (RM 62.5), Myrtle Grove (RM 59), West Pointe A-La-Hache (RM 48.7) and Empire (RM 29.5).

The Strickler's coefficient 'K_s' value was changed along several reaches of the MR for the calibration process. These values usually corresponded to the average *n* values used for HEC-RAS model calibration. With the changes in the 'K_s' value, the model was re-run until the model output gave similar results to the measured data. Appendix E shows all the 'K_s' values used in the main MR for the calibration process. The CHARIMA model does not have the flow dependent roughness factor of HEC-RAS which helps to insert varying Manning's *n* values for different discharge. The flow was calibrated solely on Strickler's Coefficient variation that was fixed in time. So, some extreme values have been used to achieve the flow calibration. Figure 6-8 shows the stages calibration for Alliance station at RM 62.5 using the adjusted *n* values. Other calibration plots can be found in Appendix B.

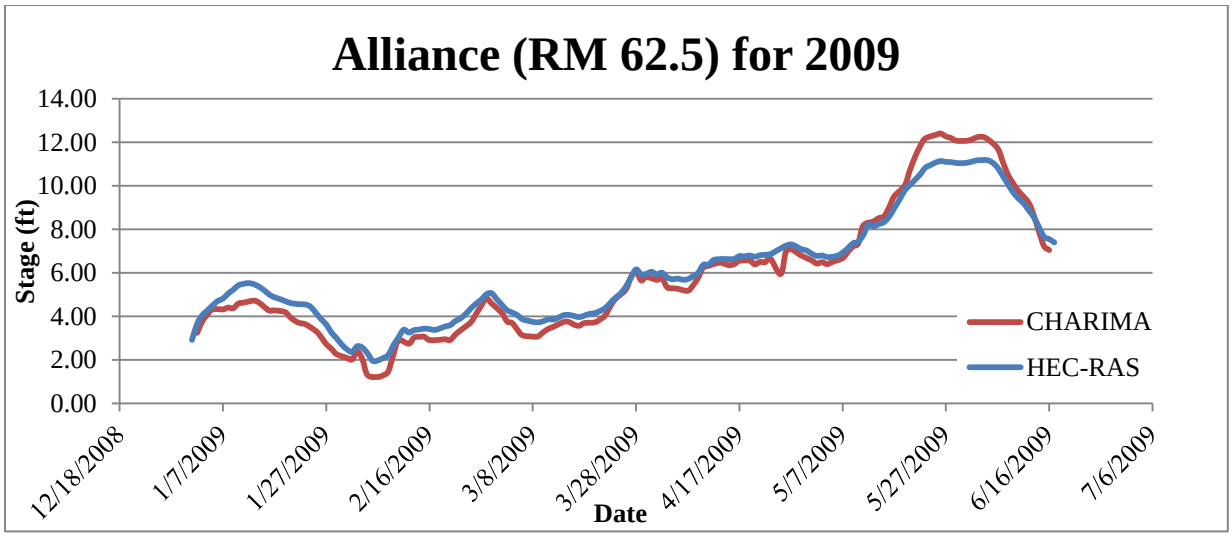

Figure 6-8: Alliance stage comparison for 2009

Visually, there is an agreement with the stage plots for above listed stations. The stages are following the trend of the observed data.

To determine the accuracy of the model, the root mean square error (RMSE), the coefficient of efficiency and the bias error between the model and observed data was measured. Table 6.3 shows the error analysis for calibration period 2009. These results have a good agreement between the simulations and the observed data obtained from HEC-RAS model.

Table 6.3: Error Analysis CHARIMA stage and flow Calibration – 2009

Mississippi River Location	**RMSE (ft)**	**Efficiency**	**Bias Error (ft)**
Alliance (62.4)	0.59	0.94	-0.20
Mississippi River Location	**RMSE (CFS)**	**Efficiency**	**Bias Error (CFS)**
Bohemia	7388.72	0.86	5009.56
Fort St. Philip	9476.27	0.82	8748.52
Mississippi River Location	**RMSE (CFS) % of TL flow on 5/31/2009**		**Bias Error (CFS) % of TL flow on 5/31/2009**
Bohemia	0.57		0.39
Fort St. Philip	0.74		0.68

Table 6.4: Peak flows for Bohemia and Fort St. Philip in CHARIMA for Calibration – 2009

Mississippi River Location	Peak Flow (CFS)	
	Observed (HEC-RAS)	Model (CHARIMA)
Bohemia	71356.00	85369.57
Fort St. Philip	95941.13	93648.30

Figure 6-9 and 6-10 show the comparison between the model flows and the flows calibrated HEC-RAS model for the period of 2009. The Bohemia and Fort St. Philip outflows have been listed. Other outflows comparison can be found in Appendix B. Through error analysis in Table 6.3, it can be considered that the model is calibrated for flow.

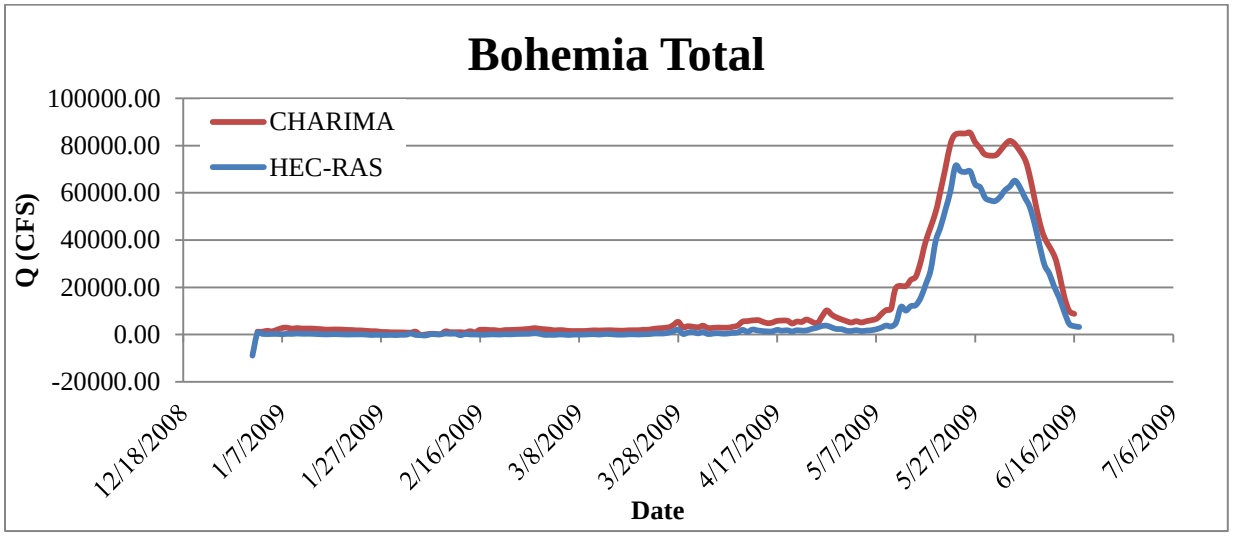

Figure 6-9: Bohemia outflow comparison for 2009

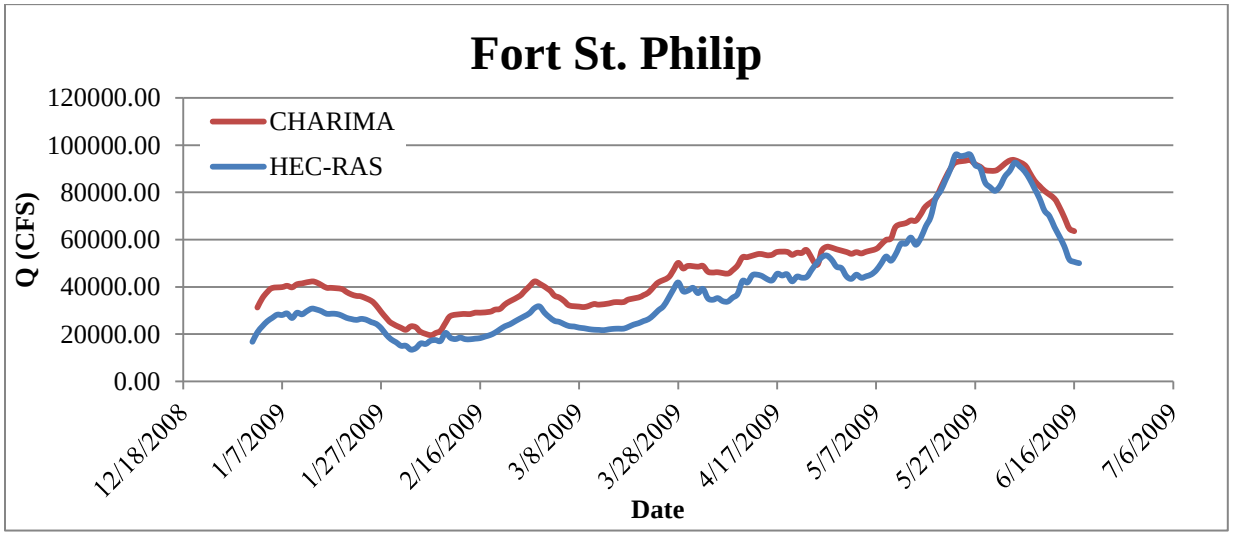

Figure 6-10: Fort St. Philip outflow comparison for 2009

Dr. Mead Allison conducted several field surveys from 2008 through 2011. Data were collected at Myrtle Grove and Magnolia sites in 2009-2011. The bed and suspended load (Tons/day) can be found the report "Water and Sediment Surveys of the Mississippi River Channel conducted at Myrtle Grove and Magnolia in Support of Numerical modeling (October 2008 - May 2011)". The concentrations at the locations were computed based on the flows of those sites published in the report.

Table 6.5: Ratio of model to observed values for sand concentration for Calibration – 2009

Date:	Station	Allison survey field data			CHARIMA model data		
		Total Sand Load Conc. (mg/L)	**Bed Load Conc. (mg/L)**	**Suspended Sand Load Conc. (mg/L)**	**Total Sand Load Conc. (mg/L)**	**Bed Load Conc. (mg/L)**	**Suspended Sand Load Conc. (mg/L)**
4/4/2009	Magnolia	62.80	61.14	1.66	36.47	33.55	2.92
4/7/2009	Myrtle Grove	59.10	56.30	2.80	35.38	38.25	43.01
5/2/2009	Myrtle Grove	17.87	14.30	3.56	36.42	54.81	22.69
Ratios:		**Total Sand Load Conc.**		**Bed Load Conc.**		**Suspended Sand Load Conc.**	
4/4/2009	Magnolia	0.58		0.55		1.76	
4/7/2009	Myrtle Grove	0.60		0.68		15.36	
5/2/2009	Myrtle Grove	2.04		3.83		6.37	
Average Ratios:		1.07		1.69		7.83	

Figure 6-11 shows the sediment concentration from the model compared to the measured data provided by Dr. Allison.

There seems to be very good agreement with the bed load concentration. However, the suspended load concentration seems to deviate from observed value which ultimately is added up to total concentration being off compared to the measured data. The rule for sediment transport is the model should predict the observed values within a factor of plus ½ to 2 (White *et al.* 1978). With this rule, the model was still considered calibrated and used from prediction of suspended sand for other duration and cases.

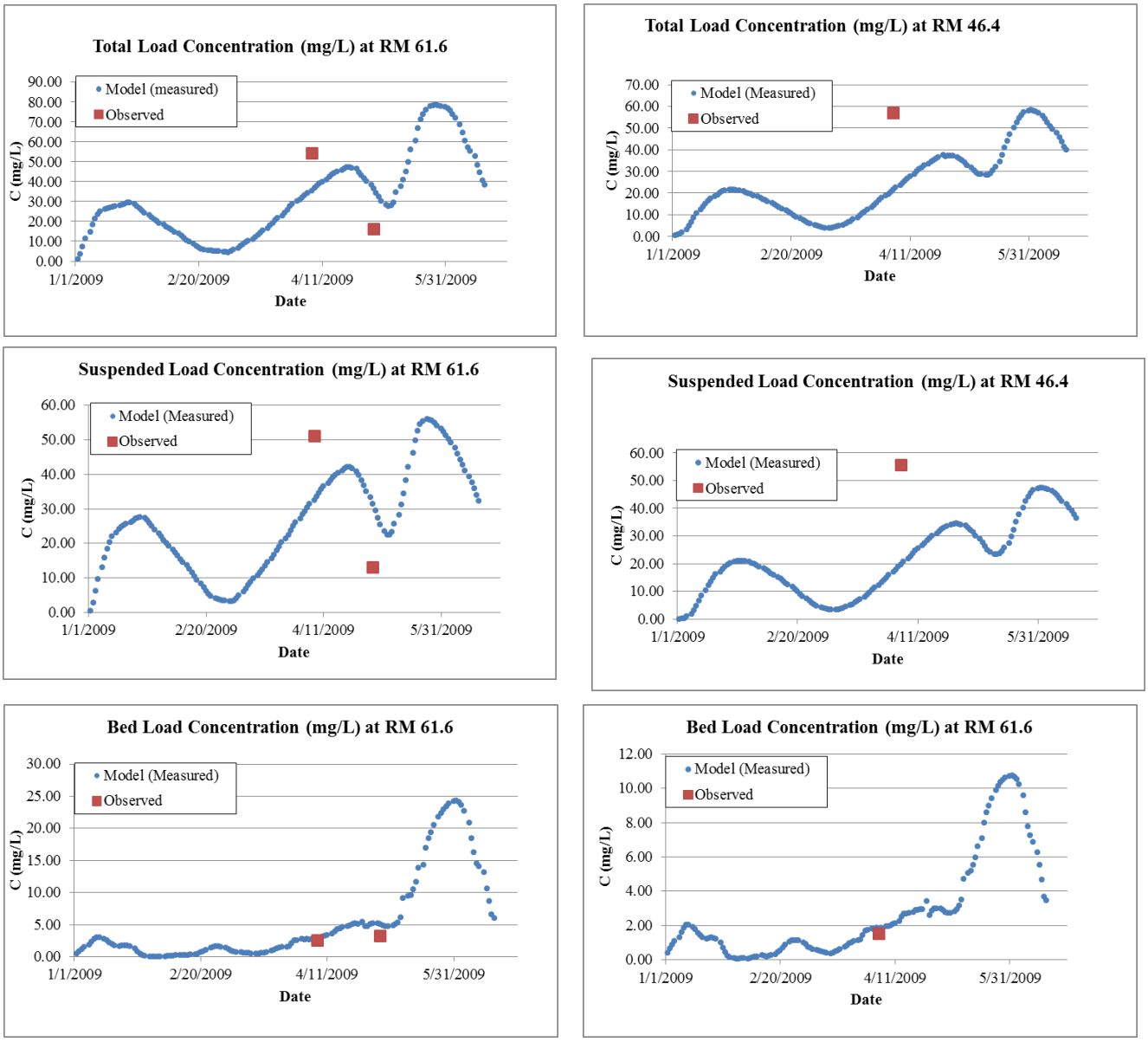

Figure 6-11: Sediment Concentration and Load comparison for 2009 at Myrtle Grove and Magnolia.

6.4 CHARIMA Model Validation

For the validation process, the model was given boundary conditions of the calendar year of 2008. The rest of the model parameters were kept same as the calibrated model. The validation results for 2008 are listed in Figure 6-12.

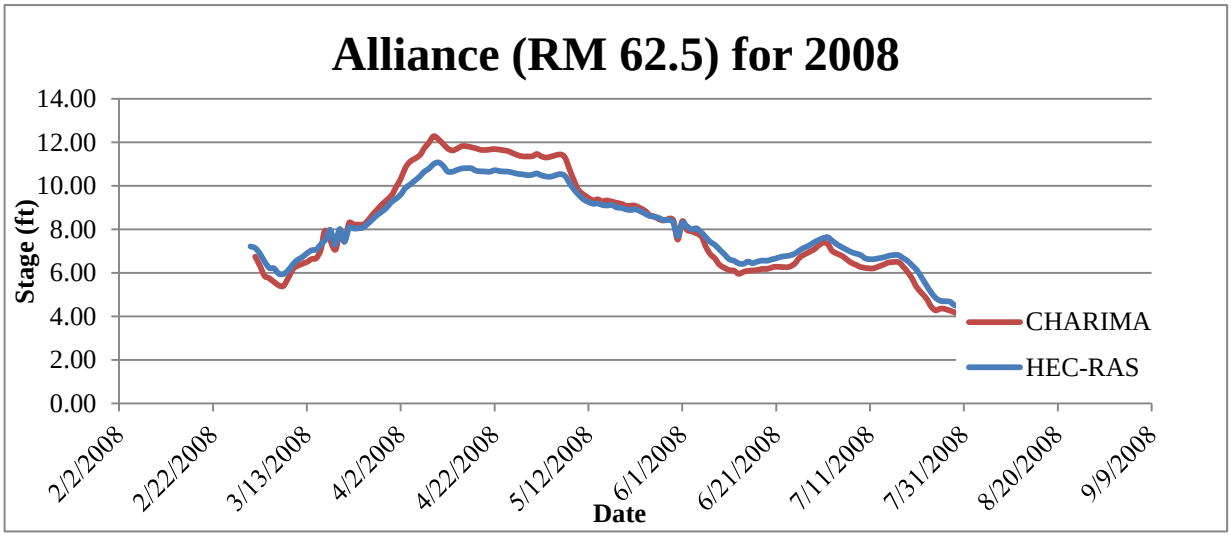

Figure 6-12: Alliance stage comparison for 2008.

Visually, there is an agreement with the stage plots for above listed stations. The stages are following the trend of the observed data.

To determine the accuracy of the model, the root mean square error (RMSE), the coefficient of efficiency and the bias error between the model and observed data was measured. Table 6.6 shows the error analysis for validation period 2008. These results have a good agreement between the simulations and the observed data obtained from USACE.

Table 6.6: Error Analysis CHARIMA stage validation - 2008

Mississippi River Location	RMSE (ft)	Efficiency	Bias Error (ft)
Alliance (62.4)	0.57	0.93	0.01

Figures 6-13 and 6-14 show the comparison between the model flows and the flow estimated by HEC-RAS model for the validation period of 2008. Bohemia and Fort St. Philip outflows for the validation period have been listed. Other outflow plots can be found in Appendix B. Table 6.7 shows the error analysis for the 2008.

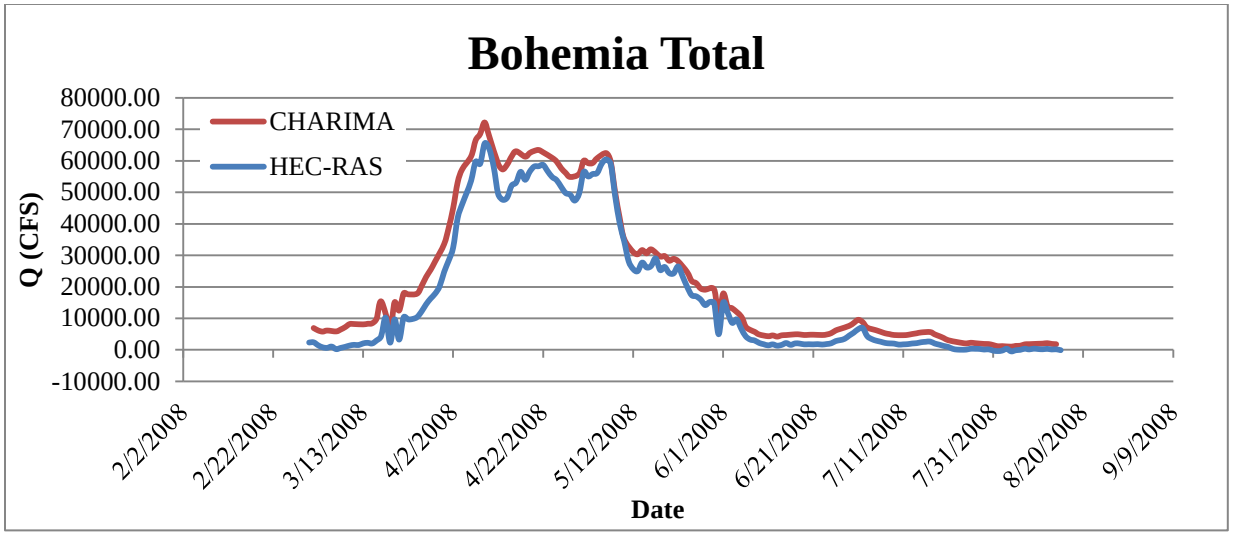

Figure 6-13: Bohemia outflow comparison for 2008.

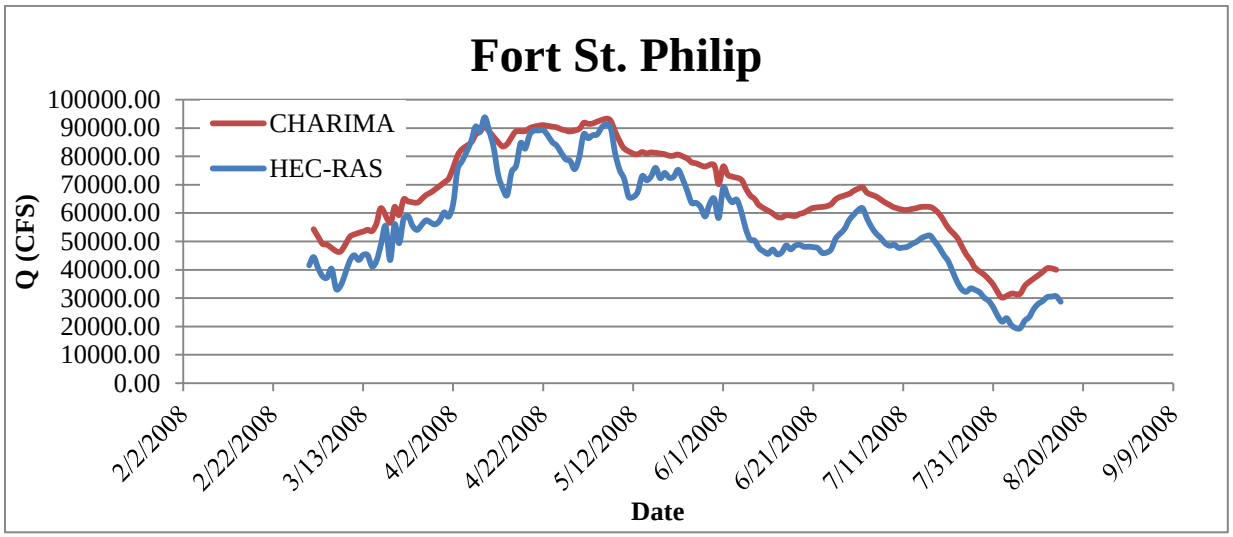

Figure 6-14: Fort St. Philip outflow comparison for 2008.

Table 6.7: Error Analysis CHARIMA Flow validation – 2008

Mississippi River Location	RMSE (CFS)	Efficiency	Bias Error (CFS)
Bohemia	5314.91	0.94	4302.56
Fort St. Philip	10708.76	0.68	9842.54
	RMSE (CFS) % of TL flow on 5/25/2008		**Bias Error (CFS) % of TL flow on 5/25/2008**
Bohemia	0.36		0.29
Fort St. Philip	0.73		0.67

Table 6.8: Peak Flow for Bohemia and Fort St. Philip in CHARIMA for validation - 2008

Mississippi River Location	Peak Flow (CFS)	
	Estimated (HEC-RAS)	Model (CHARIMA)
Bohemia	65536.20	72197.07
Fort St. Philip	93800.55	93264.70

Chapter 7: Applications

7.1 Hurricane Surge Calculation

The effects of hurricanes are numerous and include damage to properties and loss of life. One of the most devastating effects of a hurricane is storm surge which leads to flooding. Storm surge is the rising wall of water that comes ashore when a hurricane makes landfall. Storm surge is responsible for most of the damages of all hurricanes.

During hurricanes, typically some of the gauges along the Lower Mississippi River get damaged. Since storm surge waves move rapidly upstream, it is necessary to collect data at least hourly in the different river stations. The development of a model for hurricane storm surge would be useful to complement the data for the main channel of the Mississippi River. Storm surges can travel hundreds of miles upstream in the river, so it is also important to assess the impact they have on the river system.

The HEC-RAS model with the existing geometry was calibrated and validated for hurricane periods corresponding to Isaac and Gustav in order to assess the impact of the storm surge on the Lower Mississippi River. Hurricane Gustav was used as calibration and Hurricane Isaac was used for validation. Then the model was also used to for surge calculation for Hurricane Katrina.

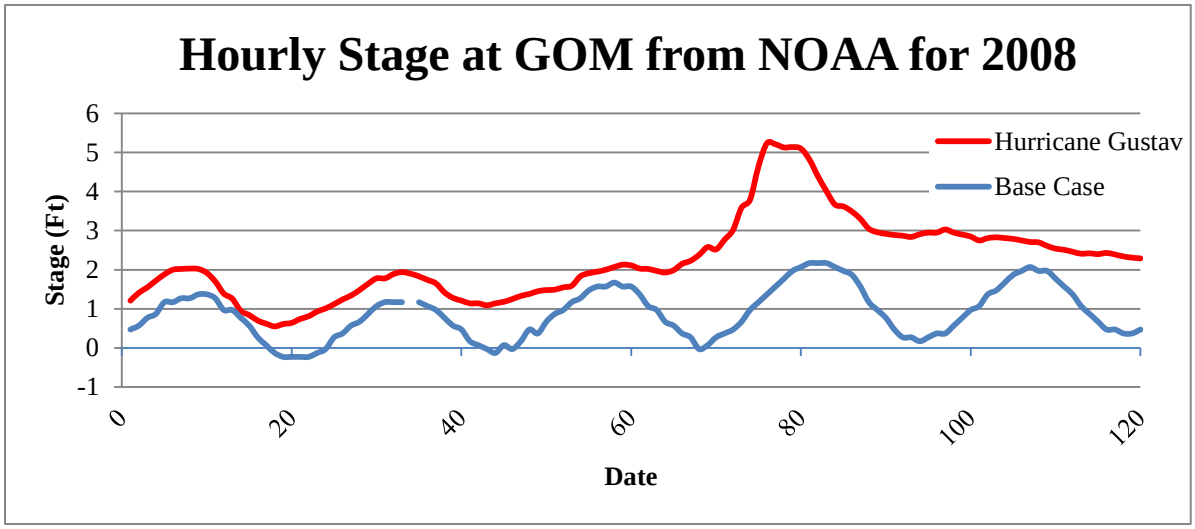

Figure 7-1: HEC-RAS downstream boundary condition for hurricane Gustav (2008).

For Gustav simulation, the Tarbert Landing flow was used as upstream boundary and stage of GOM obtained from NOAA was used at stage boundary. The stage boundaries for other outlets to the open water were provided by the LSU from the ADCIRC model of the Gulf. Figure 7-1 shows the downstream boundary and Figure 7-2 show the upstream boundary used for the hurricane simulation. The hurricane Gustav was simulated from 8/29/2008 to 9/2/2008.

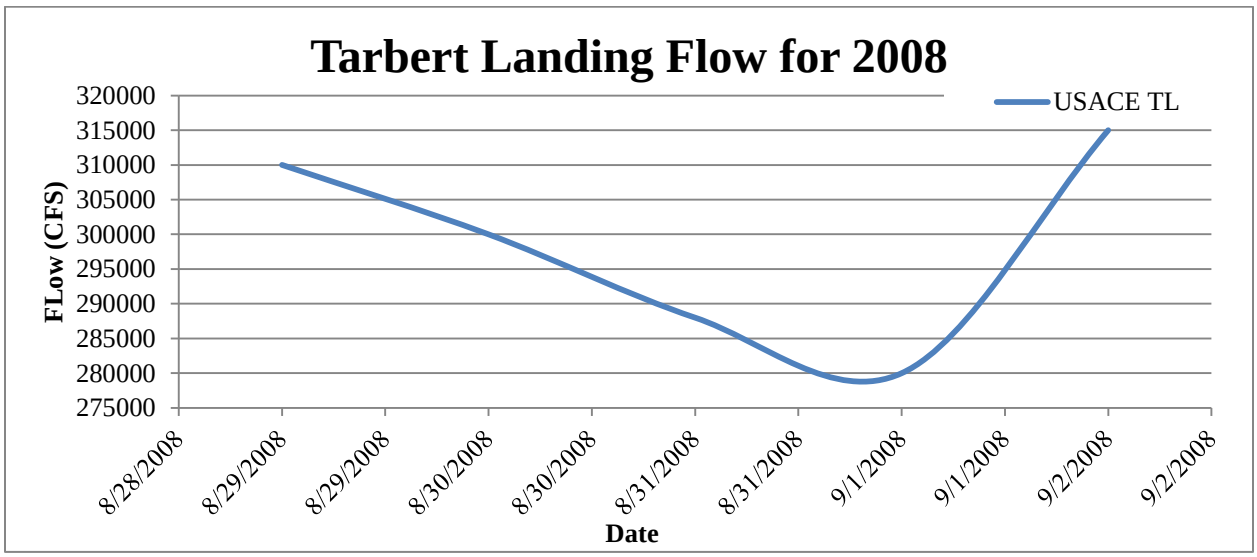

Figure 7-2: HEC-RAS upstream boundary condition for hurricane Gustav (2008).

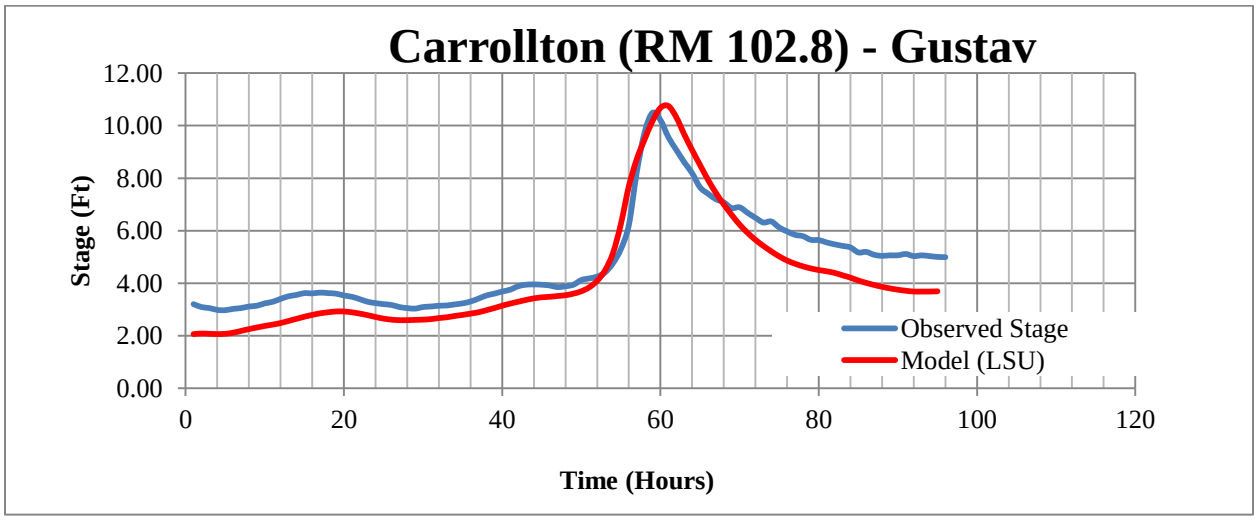

Figure 7-3: Carrollton stage comparison for hurricane Gustav (2008).

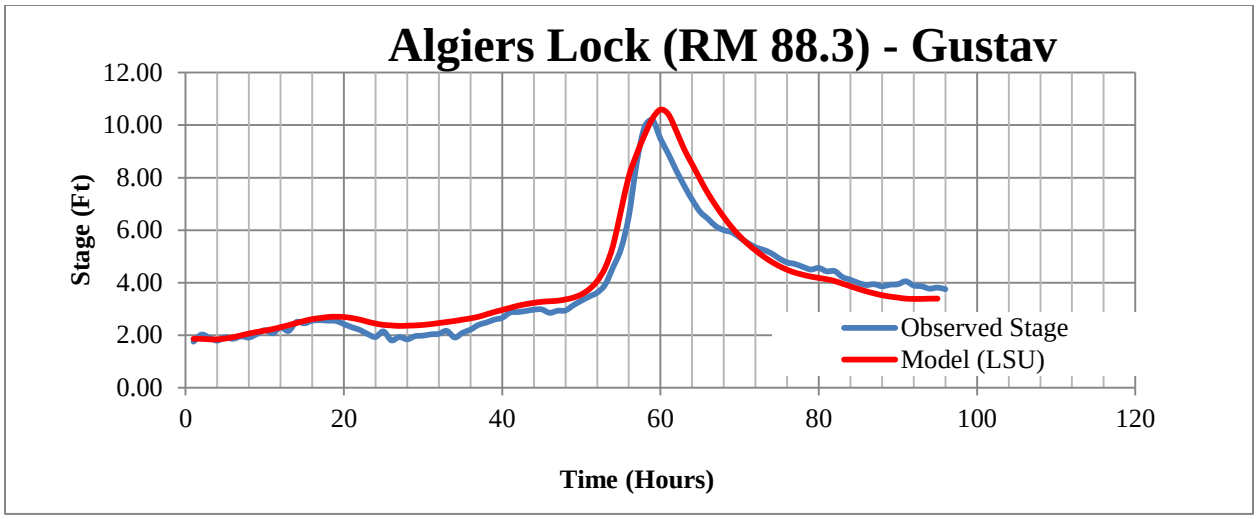

Figure 7-4: Algiers Lock stage comparison for hurricane Gustav (2008).

Figures 7-3 and 7-4 show the model stage compared to the observed stage for Carrollton and Algiers's Lock for the calibration period. Stage comparison for other plots can be found in Appendix B. Visually, the model seems to follow the signal of observed data and there seems to be a very good agreement. Table 7.1 shows the error analysis for the Hurricane Gustav calibration. The model is in good agreement as the model as has 79% efficiency in Carrollton and 93% efficiency at Algiers' Lock. The model under predicts at Carrollton by 0.56 feet and over predicts at Algiers' Lock by 0.21 feet which is acceptable.

Table 7.1: Error Analysis HEC-RAS Hurricane Gustav calibration - 2008

Mississippi River Location	RMSE (ft)	Efficiency	Bias Error (ft)
Carrollton (RM 102.8)	0.84	0.79	-0.56
Algiers' Lock (RM 88.3)	0.53	0.93	0.21

For the validation of the model, Hurricane Isaac (2012) was simulated with the calibrated model parameters. The Isaac model was simulated from 8/27/2012 to 9/1/2012. The upstream boundary conditions for the model simulations consist of daily water flows at Tarbert Landing for the corresponding period provided by USACE New Orleans District. Hourly stages are given as downstream boundary conditions for the base case (no hurricane or storm in the system). The downstream boundary conditions as the 3 passes for the impact case were set with hourly stage values obtained from the stages measured by Pilot Station gage (NOAA). Stages from Pilot Station gage were also used as boundary condition for Tiger Pass, West Bay, Main Pass and Grand Pass. For Bohemia, hourly stage from Shell Beach (NOAA station) was used as the stage boundary. Hourly Stages from West Pointe – A-La-Hache gage (RM 48.7) from USACE was used as boundary for Baptiste Collette (RM 12), Caernarvon Diver (RM 82) and Fort St. Philip (RM 20).

Figure 7-5 shows the downstream boundary condition used for Hurricane Isaac simulation for the base and hurricane case. Figure 7-6 shows the upstream boundary condition used for Hurricane Isaac simulation. Figure 7-7 shows the stage boundary used in Bohemia reach obtained from Shell Beach gage.

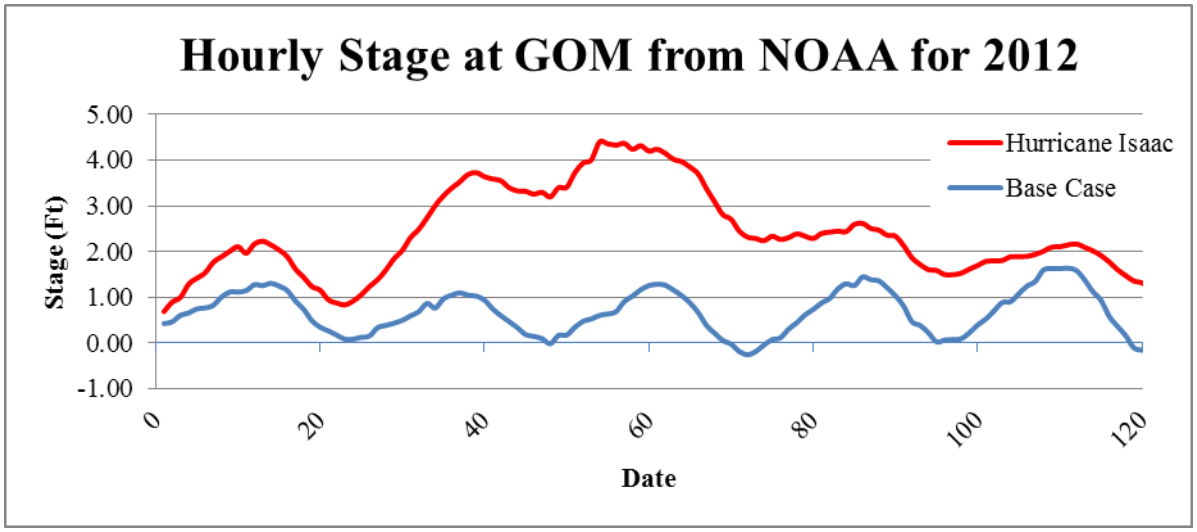

Figure 7-5: Downstream stage boundary for Hurricane Isaac (2012).

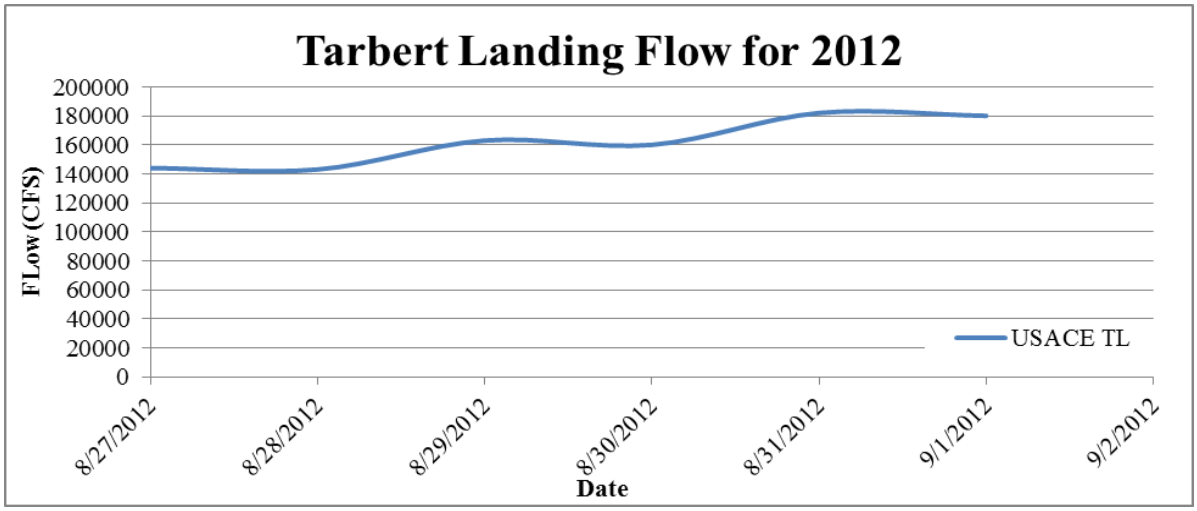

Figure 7-6: Upstream flow boundary for Hurricane Isaac (2012).

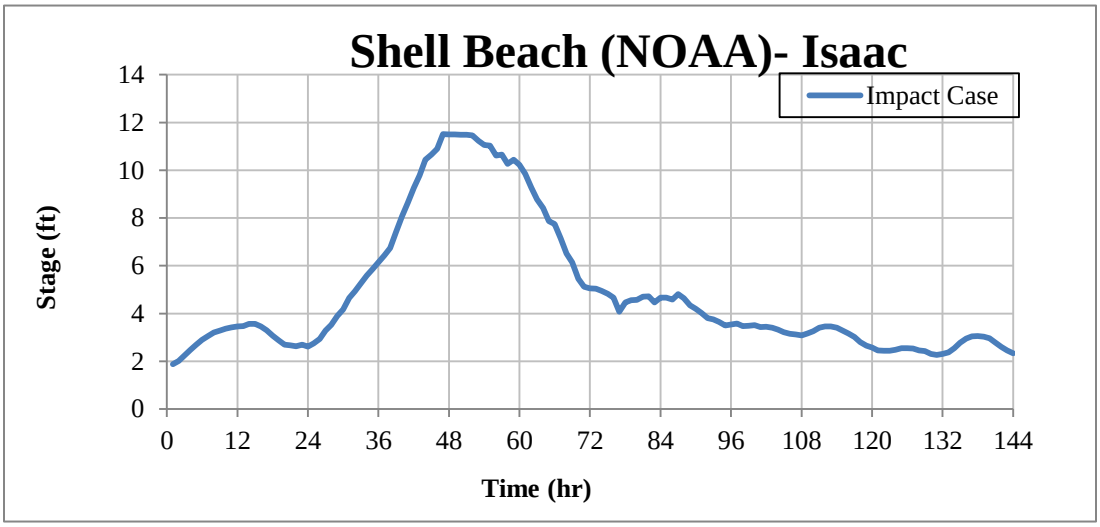

Figure 7-7: Bohemia stage boundary-Observed stages at Shell Beach-Impact Case- Isaac (2012).

Figures 7-8 and 7-9 show the model stage compared to the observed stage for Bonnet Carré and Carrollton for the validation period. Stage comparison for other plots can be found in Appendix B. Visually, the model seems to follow the signal of observed data and there seems to be a very good agreement. Table 7.2 shows the error analysis for the Hurricane Isaac validation. The model is in good agreement as the model as 89% agreement in Carrollton and Bonnet Carré. The model under predicts at Bonnet Carré by 0.30 feet and Carrollton by 0.23 feet which is acceptable.

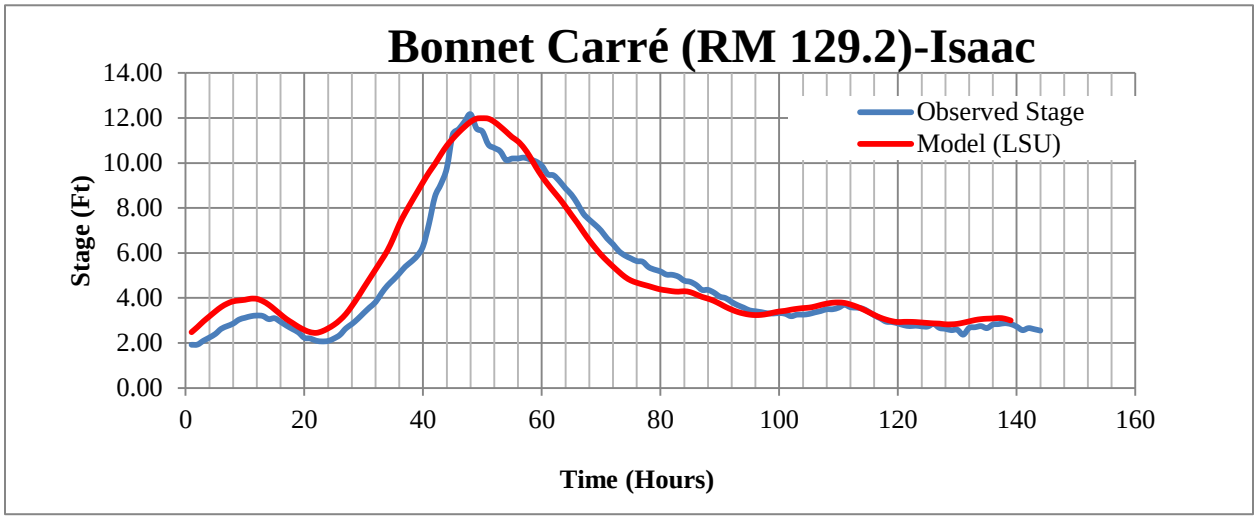

Figure 7-8: Bonnet Carré stage comparison for Hurricane Isaac (2012).

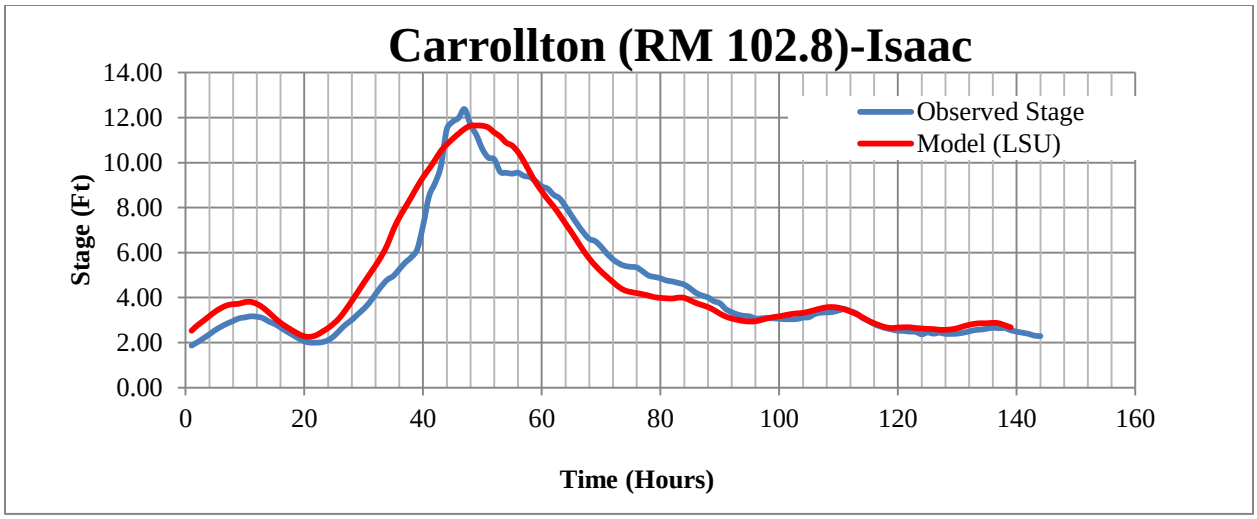

Figure 7-9: Carrollton stage comparison for Hurricane Isaac (2012).

Mississippi River Location	RMSE (ft)	Efficiency	Bias Error (ft)
Baton Rouge (RM 228.4)	1.21	0.83	+0.76
Donaldsonville (RM 173.7)	1.14	0.87	+0.41
Bonnet Carré North of Spillway (RM 129.2)	1.01	0.89	+0.30
New Orleans (RM 102.8)	0.98	0.89	+0.23

Table 7.2: Error Analysis HEC-RAS Hurricane Isaac validation - 2012

7.1.1 Surge Calculation

The model simulated a base case where there are no effects of hurricane for the same flow period. Next, the model simulated for the hurricane and the highest difference in the stage between the hurricane and the base was calculated. The surge plot for Gustav, Isaac and Katrina can be seen in Figure 7-10.

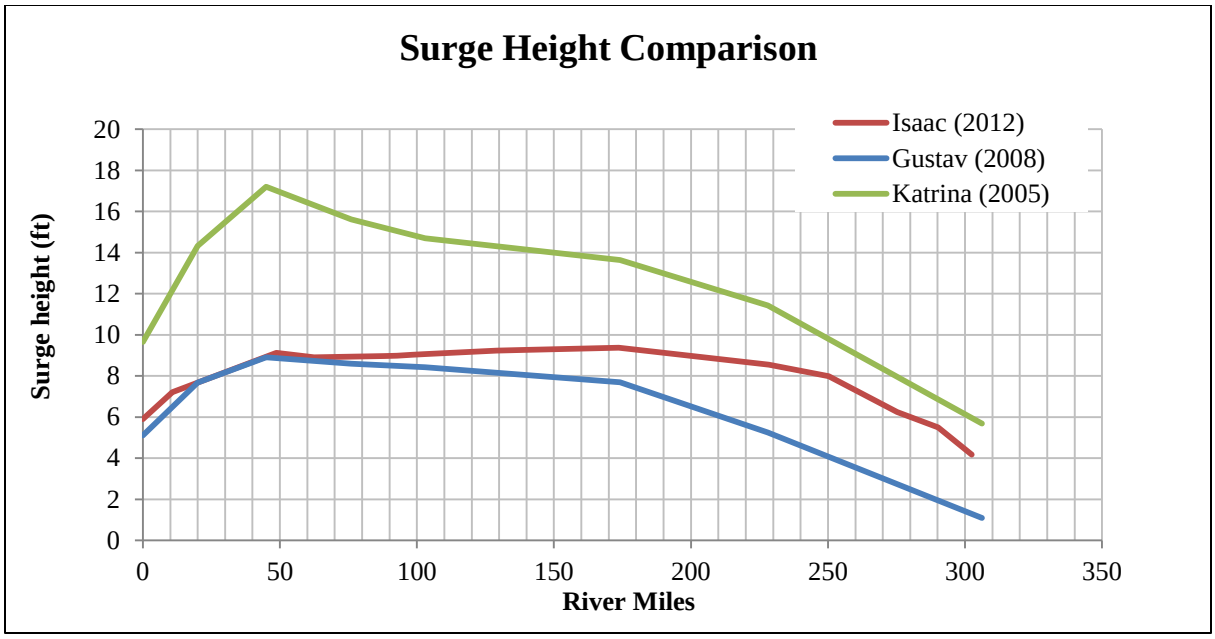

Figure 7-10: Surge height comparison for Hurricanes Isaac, Gustav and Katrina.

From Figure 7-10, the surge for a particular location can be estimated from Tarbert Landing to HOP in MR. This would provide data on the surge at the locations that might have a measurement gage damaged or not installed. The model also shows how each hurricane produced a different intensities surge. Hurricane Katrina produced the highest surge compared to other two hurricanes. The surge propagates as far as the upstream boundary, Tarbert lading (RM 306). All three hurricanes seem to produce the maximum surge at around RM 50 which is the area around West Pointe A-La-Hache (RM 49). During Hurricanes Katrina, Gustav and Isaac, the Tarbert Landing flow was around 150,000, 300,000 and 150,000 CFS respectively. So, all the above hurricanes occurred during the low flow period. However, if similar hurricanes occurred during a higher flow period where MR as a potential to reach 1.2 million CFS, the maximum river state produced would be higher leading to potentially devastating floods.

7.2 Surge for different flow scenarios

The hurricane model was also used to simulate the surge heights and total maximum stage for a range of inflows at Tarbert Landing. This was done to test the impact with the changes in Tarbert landing flows. For example, the 2011 Mississippi River flood extended in the June and thus overlapped with the beginning of the hurricane season. Consequently it is feasible for a high flow in the Mississippi River to be coincident with a hurricane in the gulf.

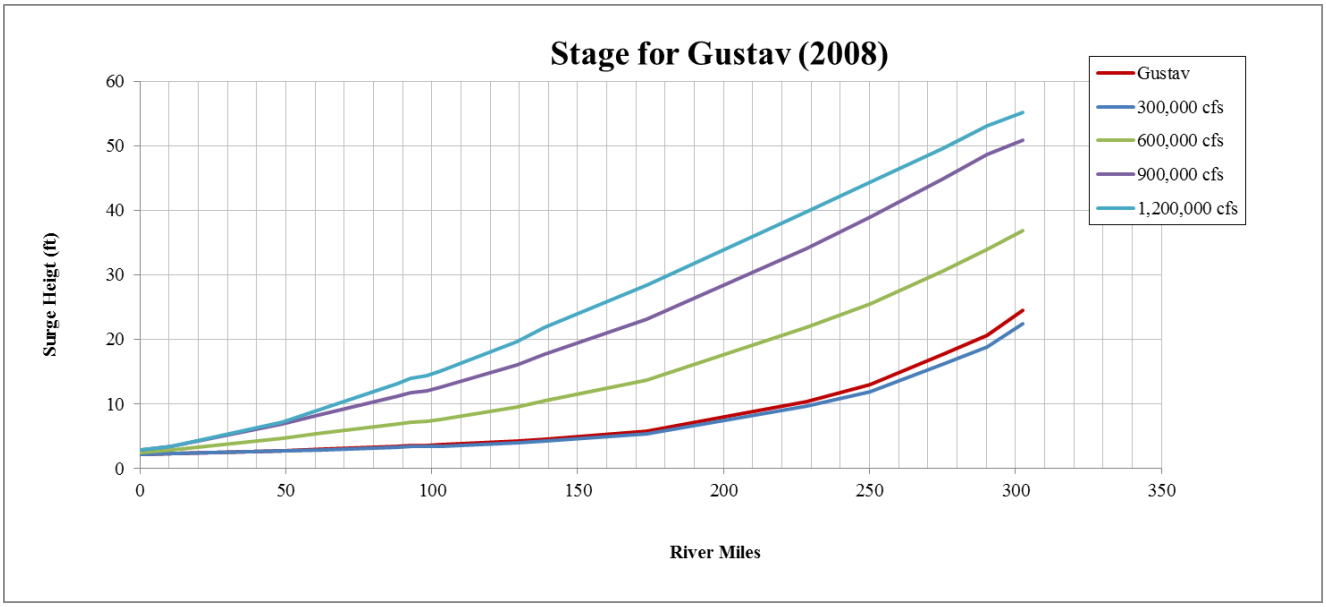

Figure 7-11: Comparison of River stage with surge comparison from Hurricane Gustav for different flow scenarios.

Figures 7-11 and 7-12 show the how the surges would add to the local river stage in MR if hurricanes Gustav and Isaac occurred in different flow conditions. The flow varies from 300,000 CFS to 1.2 million CFS considering the peak flow values for the flood period of 2008 and 2011. Figures 7-11 and 7-12 show the model predicted surge height for different locations from HOP to Tarbert Landing which is the model domain of HEC-RAS. For reference, at New Orleans (RM 102.8) has a levee elevation around 20 to 25 ft (7.5m). Hurricane Gustav would have produced a maximum surge of around 17 feet in New Orleans even if the same hurricane occurred in the peak flood season. However, Hurricane Isaac would have produced a surge of around 24 feet in New Orleans if it had occurred in peak flood period. A surge of such magnitude could easily overtop the levees in New Orleans and cause extensive flooding. This model could be used to redesign the levees for the surge predicted by such model simulation based on the frequency of type of a hurricane category and the flood period conditions.

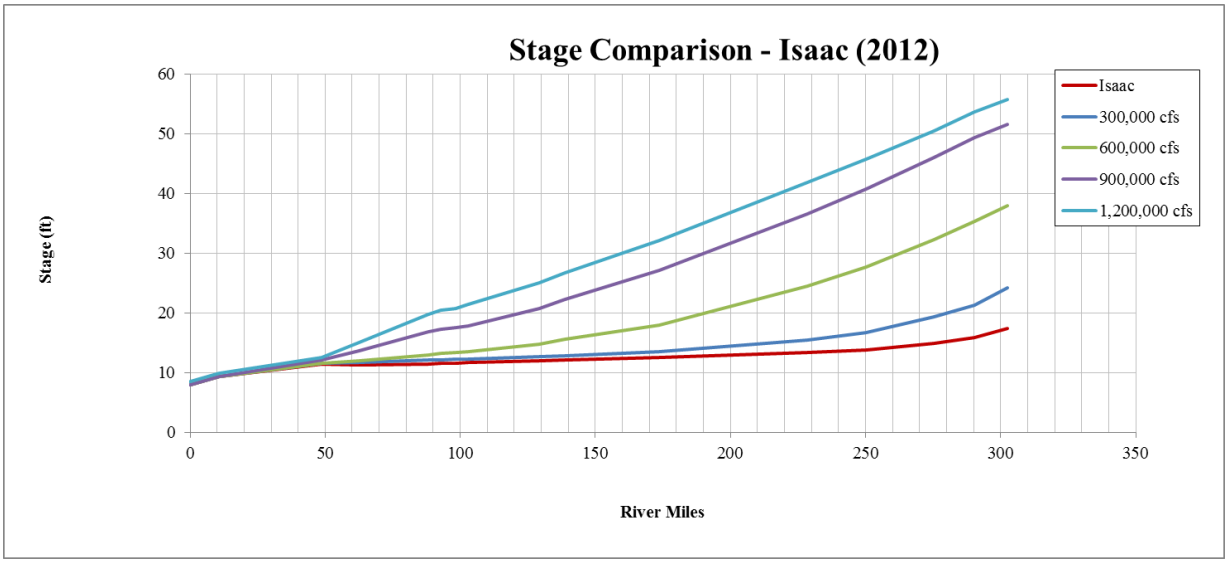

Figure 7-12: Comparison of River stage with surge comparison from Hurricane Isaac for different flow scenarios.

7.3 Simulations with addition of MLODS diversions and Pass Closure

The model was used to simulate for future MLODS diversions, dredging of Pass-A-Loutre for navigation and pass closure. HEC-RAS model simulations were used to observe the flow distribution in outlets and diversions with the introduction of the dredged Pass-A-Loutre and pass closure. CHARIMA model simulations were used to observe the sand load, concentration and flow distribution in the MR as well as the outlets and diversions. The CHARIMA model was also simulated for addition of MLODS diversions, dredging of Pass-A-Loutre and pass closure.

7.3.1 Existing and future MLODS diversions with Pass Closure (HEC-RAS)

Figure 7-13 shows the outflows on 4/25/2008 from HEC-RAS model for the various scenario runs from Morganza Spillway to West Pointe-A-La-Hache. Morganza Spillway was closed during 2008. Bohemia Spillway, Lagan, Johnson, ICCW at Harvey, ICCW at Chalmette, Violet, Jesuit, Belair, White Ditch, Naomi, Myrtle Grove, Deer Range and West Pointe-A-La-Hache were all inserted as flow extraction in the model. So, they show constant values in the outflows. Belair is a significant outflow with a peak discharge above 200,000 CFS which seems to impact all other outflows considerably.

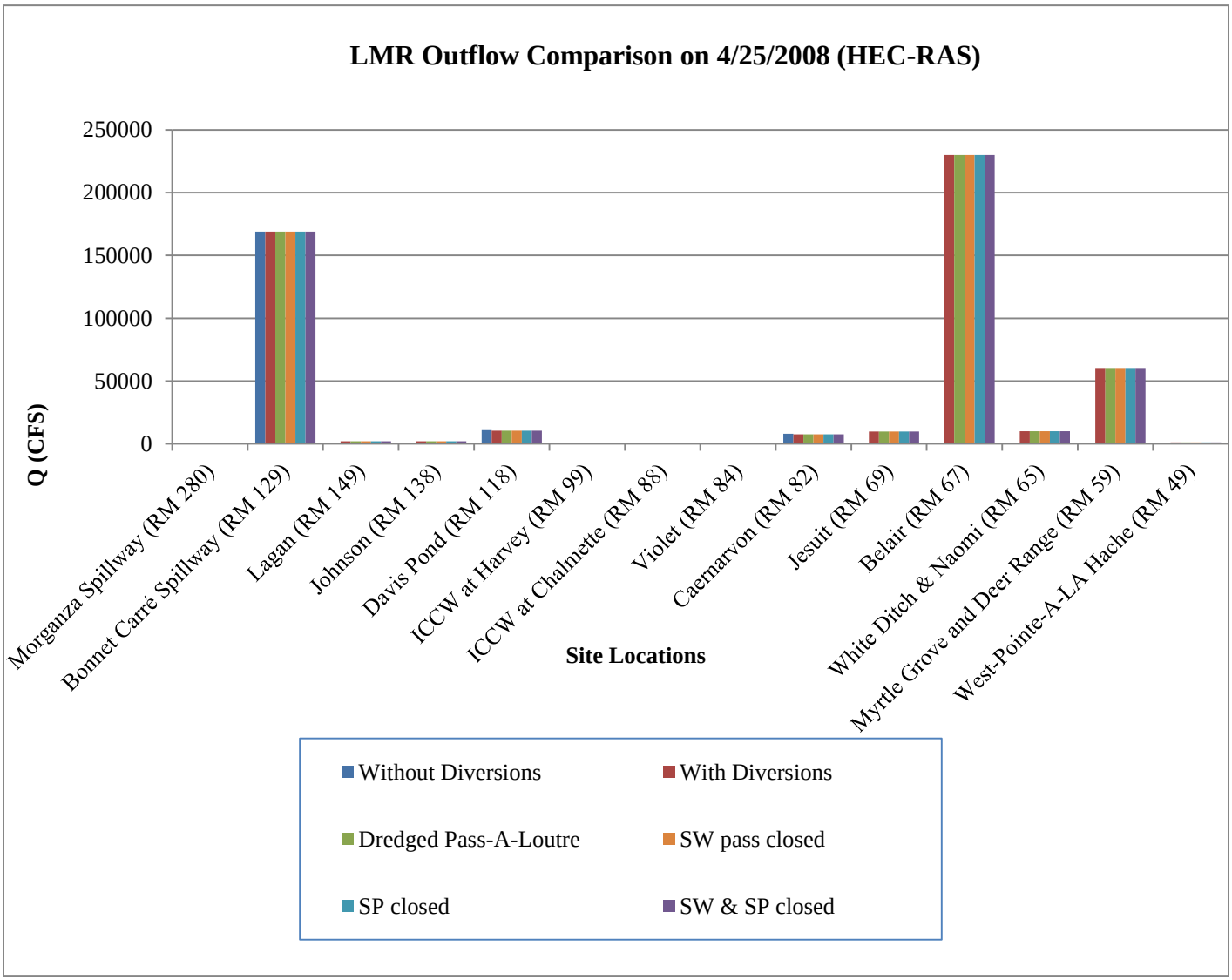

Figure 7-13: Outflows comparison for HEC-RAS on 4/25/2008

Figure 7-14 shows the outflows on 4/25/2008 from HEC-RAS model for the various scenario runs from Bohemia to the passes. There is a drastic decrease in the flows in Bohemia reach due to Belair (RM 67.1) extracting huge amount of lows. Another significant diversion introduced is the Buras (RM 23.1) which has a peak flow extraction around 150,000 CFS. Due to the Buras diversion, the outflow downstream such has Fort St. Philip, Baptiste Collette and the passes in general have drops in their peak flows. The impact of dredged Pass-A-Loutre to the dimension of a navigational channel (Minimum 600 feet wide and 45 feet deep) and pass closure to the outflows can also be seen though the Figure 7-14. The impact of dredged Pass A-Loutre is can be seen upstream as well as the passes. The discharge in the outflows has been reduced more significantly in the passes compared to other outflows. With closure of both South and

Southwest pass, flow as high as 250,000 CFS pushed through Pass-A-Loutre compared to 80,000 CFS for existing conditions.

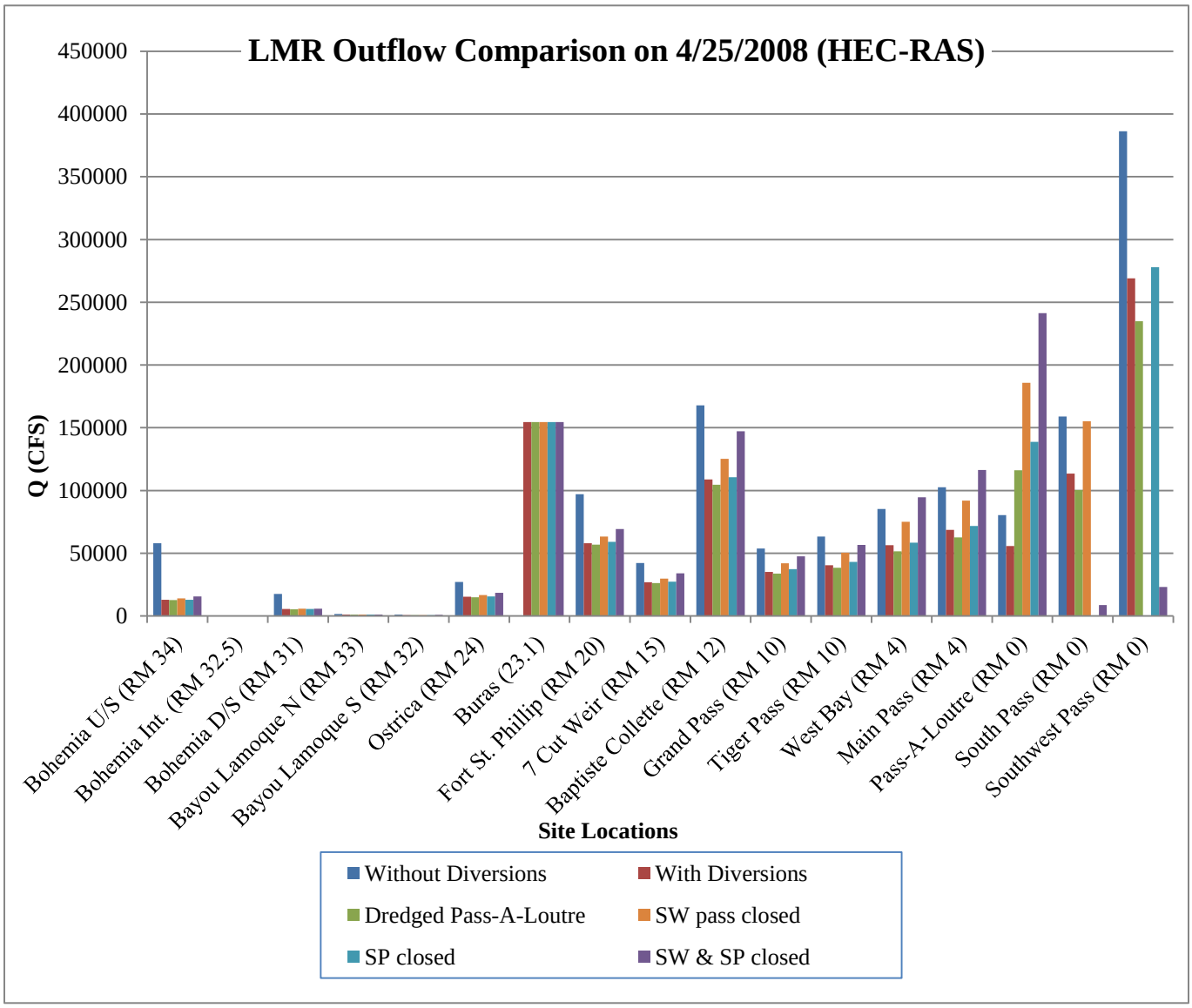

Figure 7-14: Outflows comparison for HEC-RAS on 4/25/2008

7.3.2 Existing and future MLODS diversions with Pass Closure (CHARIMA)

Figure 7-15 shows the outflows on 4/25/2008 from CHARIMA model for the various scenario runs from Jesuit to West Pointe-A-La-Hache. The flows are constant as they have been modeled as later flow extraction. Belair (RM 67.1) extracting significant amount of flow close to 20 percent of the peak Tarbert Landing flow has a substantial effect in the other outflows.

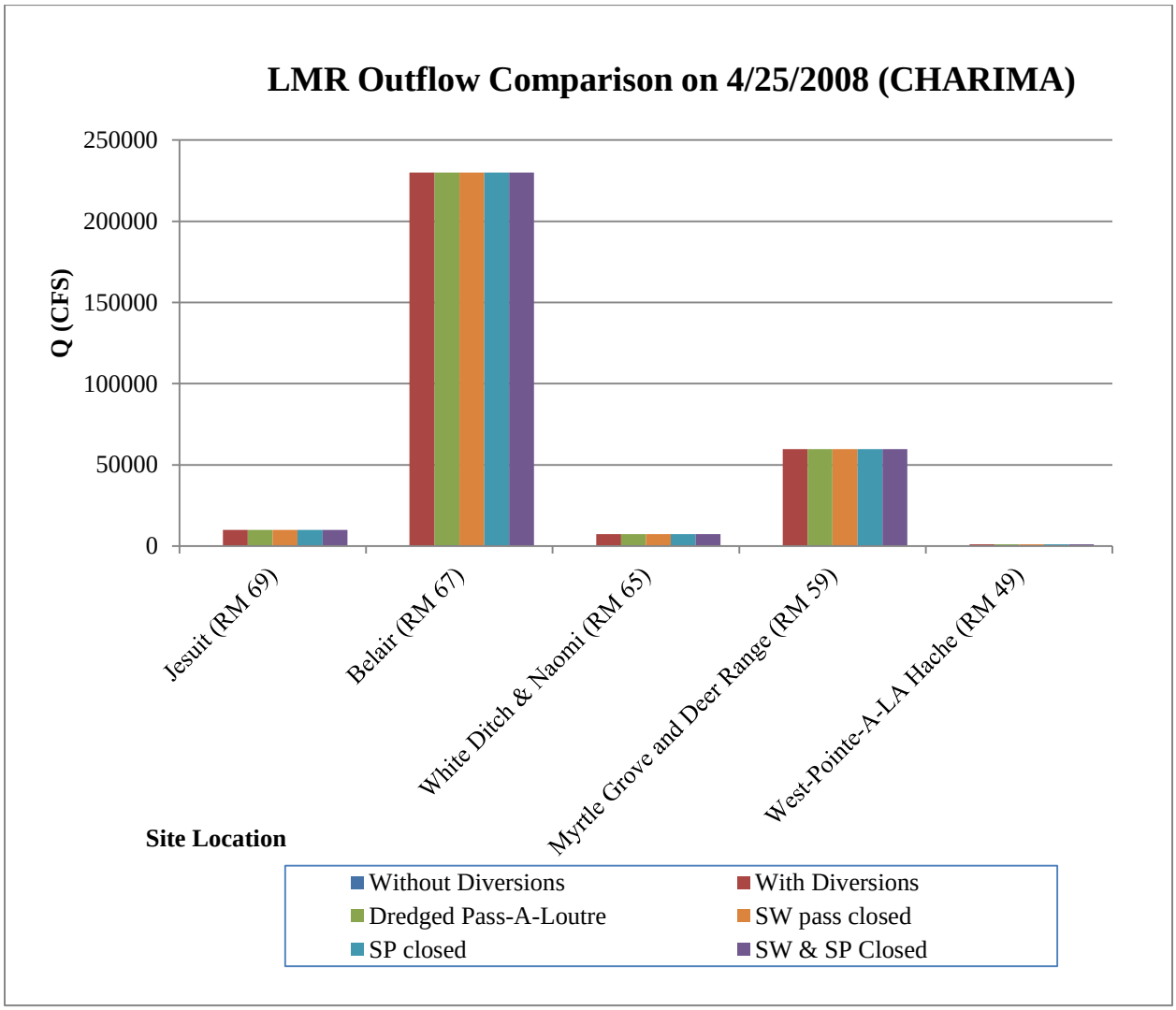

Figure 7-15: Outflows comparison for CHARIMA on 4/25/2008

Figure 7-16 shows the outflows on 4/25/2008 from CHARIMA model for the various scenario runs from Bohemia to the Passes. Similar effects observed in the HEC-RAS model can also be scene for the outflows from CHARIMA model. With the introduction of diversions, Belair and Buras being significant diversions, the outflows have a drop in their peak flows comparatively. The impact can be seen more on the outflows located downstream of these large diversions. Other outflows also have drop in their peak flow all the way to the passes but they are comparatively lower than those downstream outflows.

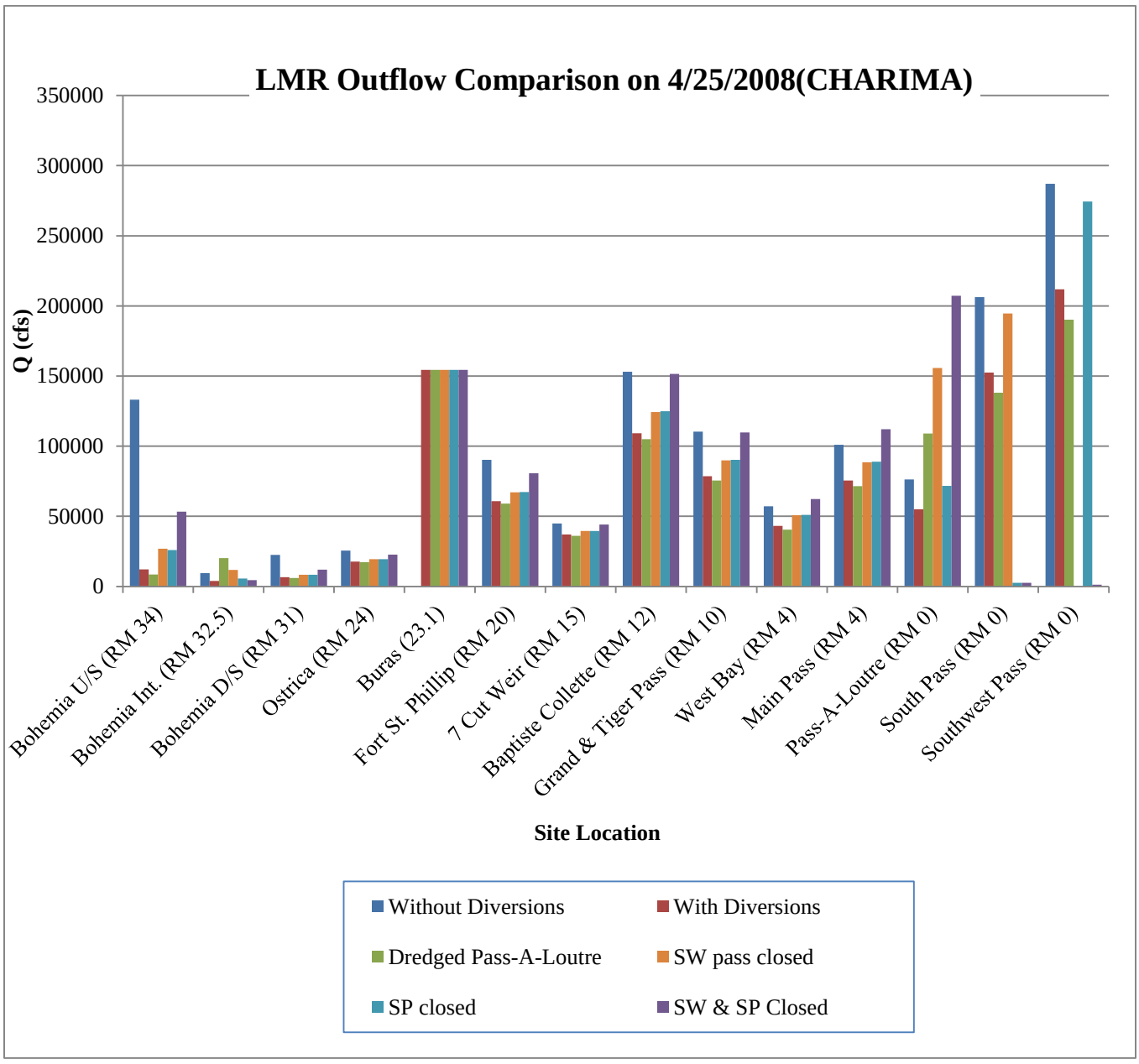

Figure 7-16: Outflows comparison for CHARIMA on 4/25/2008

Figure 7-17 shows the outflows on 4/25/2008 from CHARIMA model from Bohemia to the Passes for existing diversions, future MLODS and with future MLODS, dredged Pass-A-Loutre and both South & Southwest Pass closed. With the introduction of the diversions, there is a significant drop in Bohemia reach flows which lies downstream of Belair diversion. All outflows downstream of Buras also have drop in the flows measured on 4/25/2008. However with the closure of both South and Southwest pass, the outflows seem to pick up the excessive flow in the MR. The effect can be seen up to the upstream outflows such as Bohemia. Flow in the Pass A-Loutre increases significantly from 80,000 CFS for existing conditions to 200,000 CFS with other two passes closed.

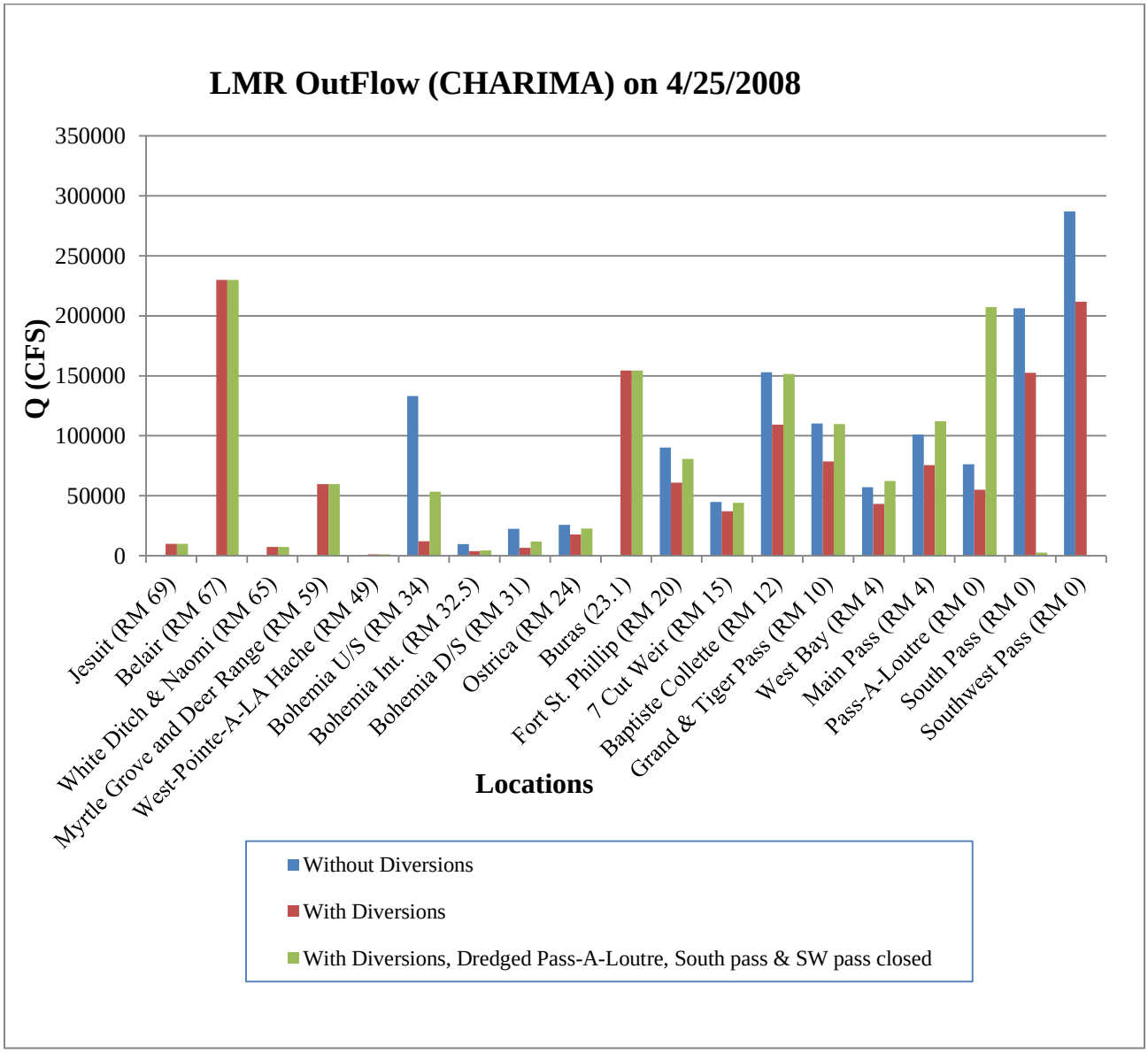

Figure 7-17: Outflows comparison for CHARIMA on 4/25/2008

Figure 7-18 shows the total sand load in the outflows on 4/25/2008. For the existing conditions, all outflows seem to take higher sand load compared to with the introduction of the diversions. However, with the closure of the South and Southwest pass, sediment load increases in the outflows corresponding to the increase in discharge in the channels. Pass A-Loutre increase its capacity from 5000 Tons per day to 10000 Tons per day with the dredging and closure of the passes. The high sand load at the 7-Cut Weir may be an outlier due to a possible bug in the model that sometimes incorrectly computes the suspended sand load.

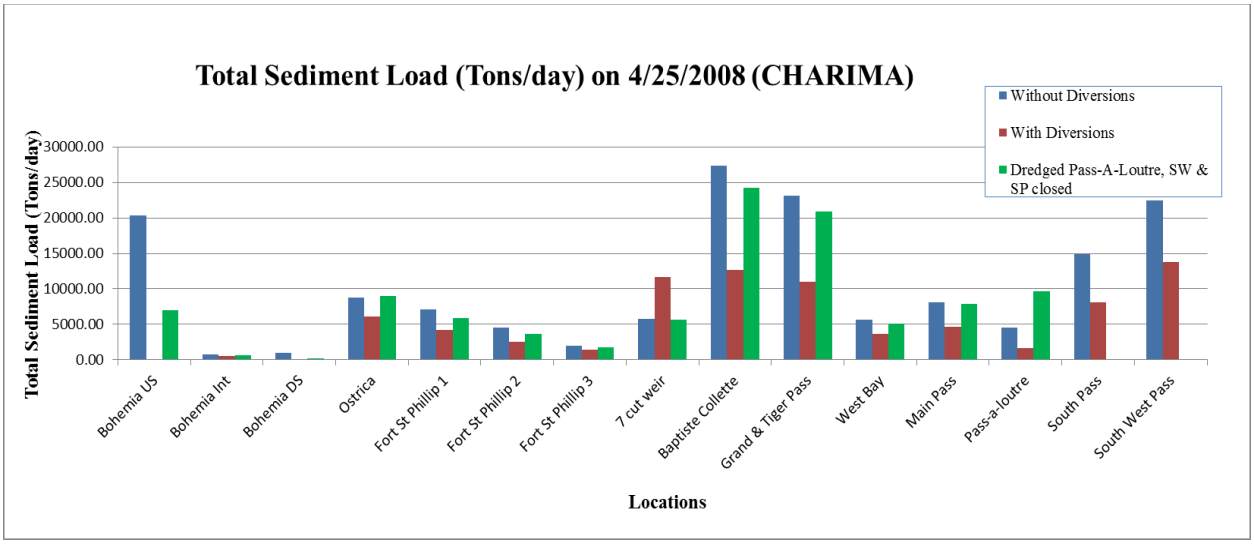

Figure 7-18: Total Sand Load for outlets from CHARIMA model on 4/25/2008

Sediment to Water Ration (SWR) is the ratio of total sand concentration in the outlet to the total sand concentration in the MR. SWR values can represent the erosional and shoaling effects in the main stem river. For a flow of around 1 percent of Tarbert Landing, the shoaling and erosional effect is minor. However, for a flow around 10 percent of Tarbet Landing or more, the shoaling and erosional effects are siginificant. Figure 7-19 shows the SWR for the outlets for all cases simulated for the study. Figure 7-20 shows the SWR for the outlets for existing diversions, addition of future MLODS diversions and closing of both South and Southwest passes with dredged Pass-A-Loutre including the future MLODS diversions. The SWR for Bohemia reach seems to be below 1 for all three cases suggesting shoaling in the downstream of Bohemia reach. The Bohemia outlets are taking flows with less sand concentration compared with the main stem river. So, higher sediment concentration in the MR leads to a possibility of shoaling in the main stem. SWR for Ostrica is higher than 1 for all three cases indicating erosional activities in the Ostrica Reach in the MR. The outflow extracts flows with higher sand concentration than the MR. However, for outlets taking smaller discharge, higher SWR might not necessarily mean erosional activity in the main stem. Even though the concentration of sand

might be high in the outlet, due to its smaller discharge, the effect in the sediment load in the MR is very small. The SWR in the Pass A-Loutre increases for the pass closure compared to existing condition but it is still lower than 1. It indicates that the Pass A-Loutre has increased in its sand carrying capacity compared to existing conditions however its concentration is still lower than the corresponding main stem river.

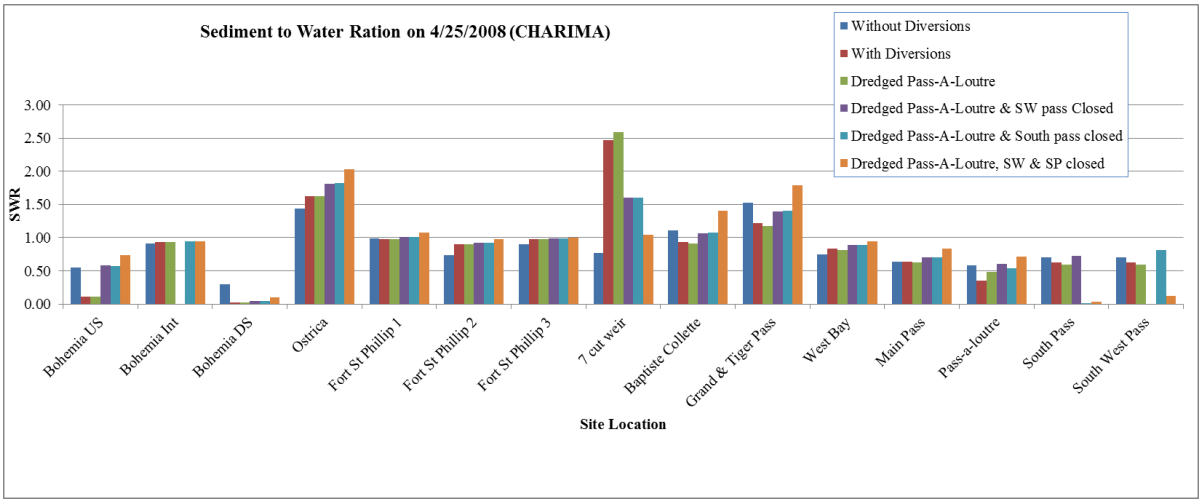

Figure 7-19: Sediment to water ratio for outlets from CHARIMA model on 4/25/2008

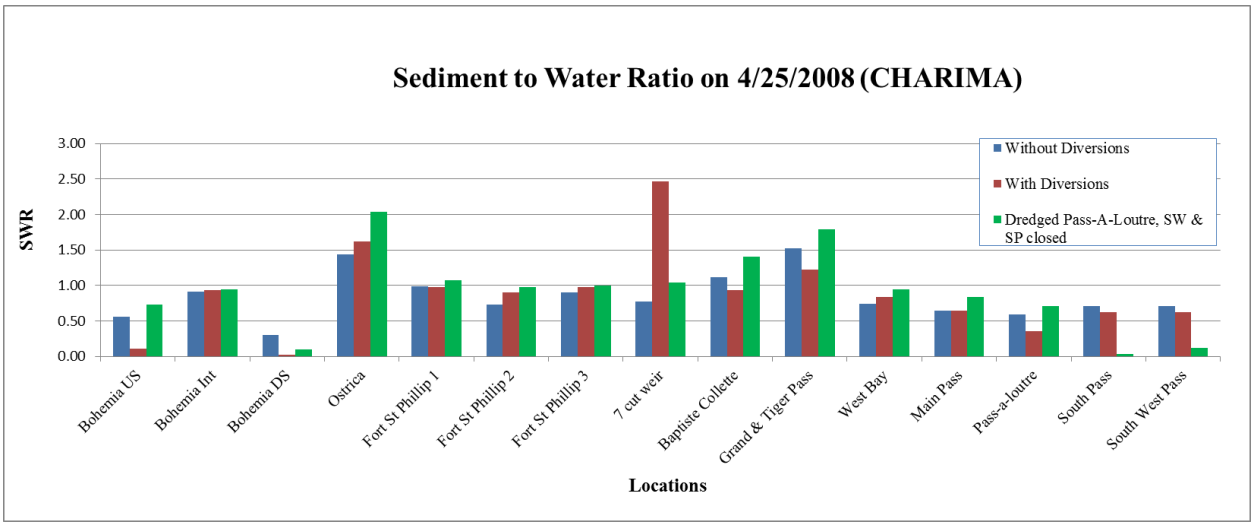

Figure 7-20: Sediment to water ratio for outlets from CHARIMA model on 4/25/2008

Figure 7-21 shows the total sand concentration in the MR on 4/25/2008 for existing conditions, future MLODS diversions and for the closure of South and Southwest pass with a dredged Pass-A-Loutre including MLODS diversions. There is drop in the sand concentration overall with the introduction of the future MLODS diversions. The concentration in the MR seems to drop further with the Pass A-Loutre being dredged and closure of both South and Southwest Pass.

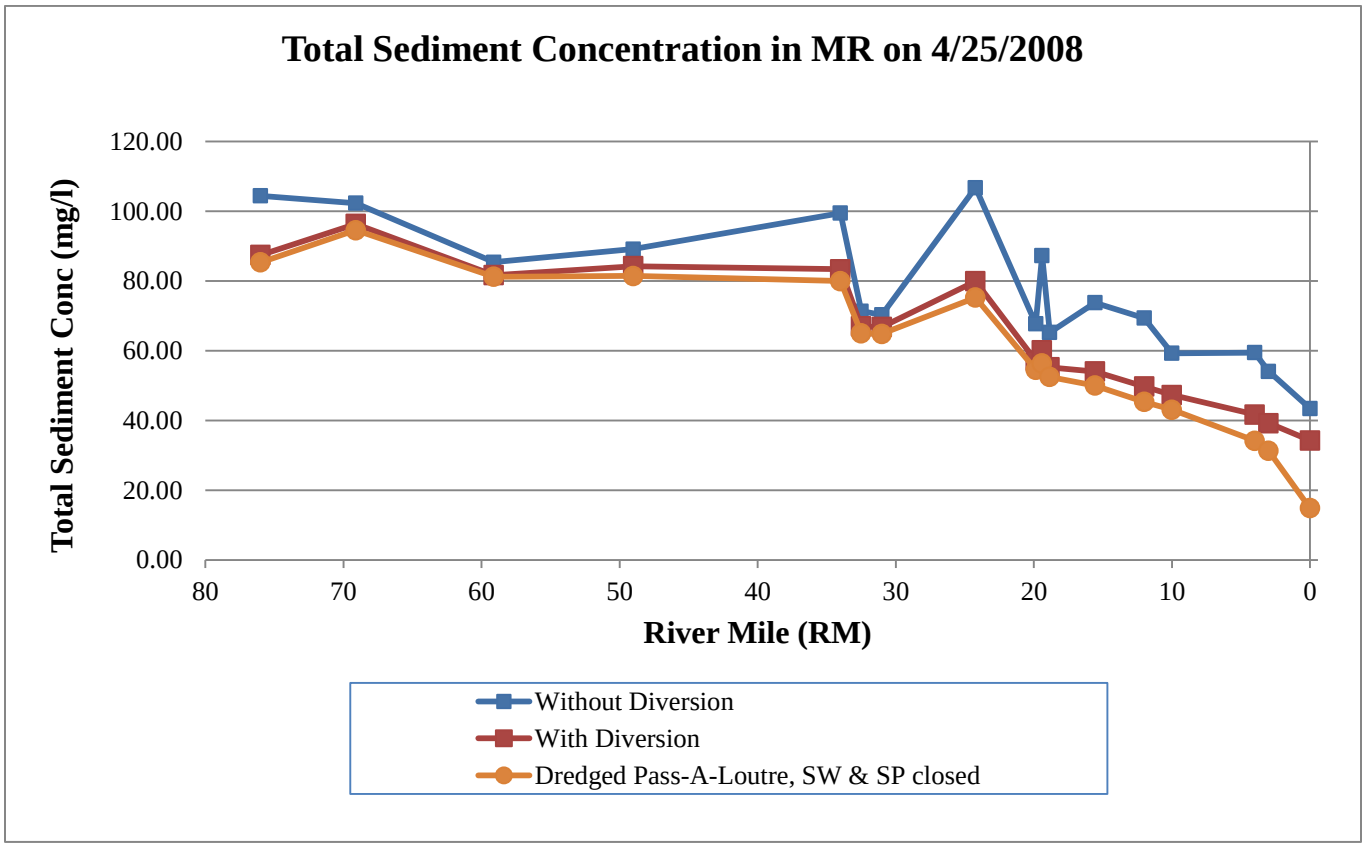

Figure 7-21: Total Sand concentration in the MR from CHARIMA model on 4/25/2008

Figure 7-22 shows the peak discharge in the MR from HEC-RAS model for existing conditions, future MLODS diversions and for the closure of South and Southwest pass with a dredged Pass-A-Loutre including MLODS diversions. There is drop in the discharge overall with the introduction of the future MLODS diversions. With the closure of the South and Southwest passes, the drop in discharge is higher. The HOP receives around 200,000 CFS for pass closure which is the flow pushed through Pass-A-Loutre. Also, with the closure of two passes, more flows are pushed through upstream outflows up to Fort St. Philip reach. So, there is a sharp drop in the peak discharge around RM 20 compared to previous conditions.

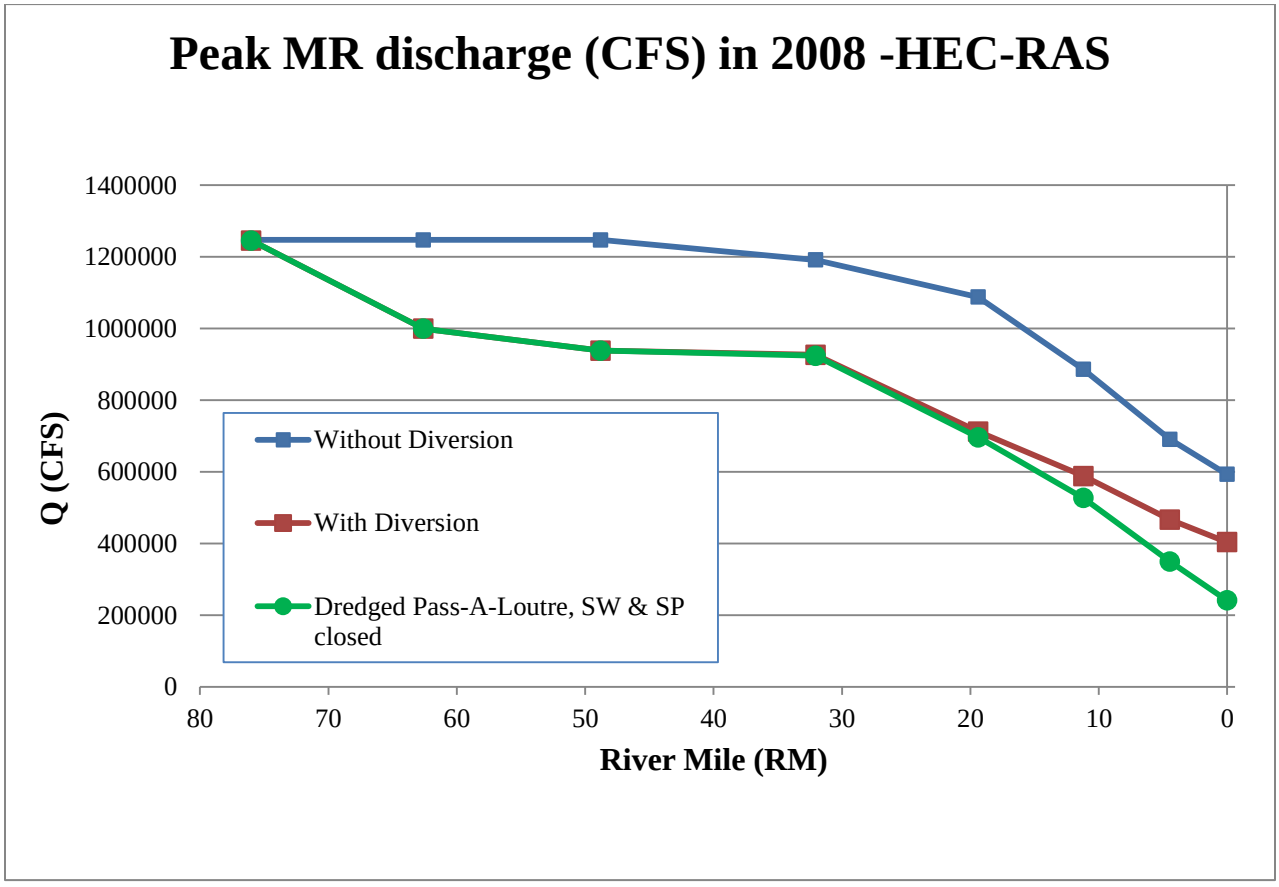

Figure 7-22: Total Discharge in the MR from CHARIMA model on 4/25/2008

Figure 7-23 shows the total sand load in the MR on 4/25/2008 for existing conditions, future MLODS diversions and for the closure of South and Southwest pass with a dredged Pass-A-Loutre including MLODS diversions. There is drop in the total sand load overall with the introduction of the future MLODS diversions.

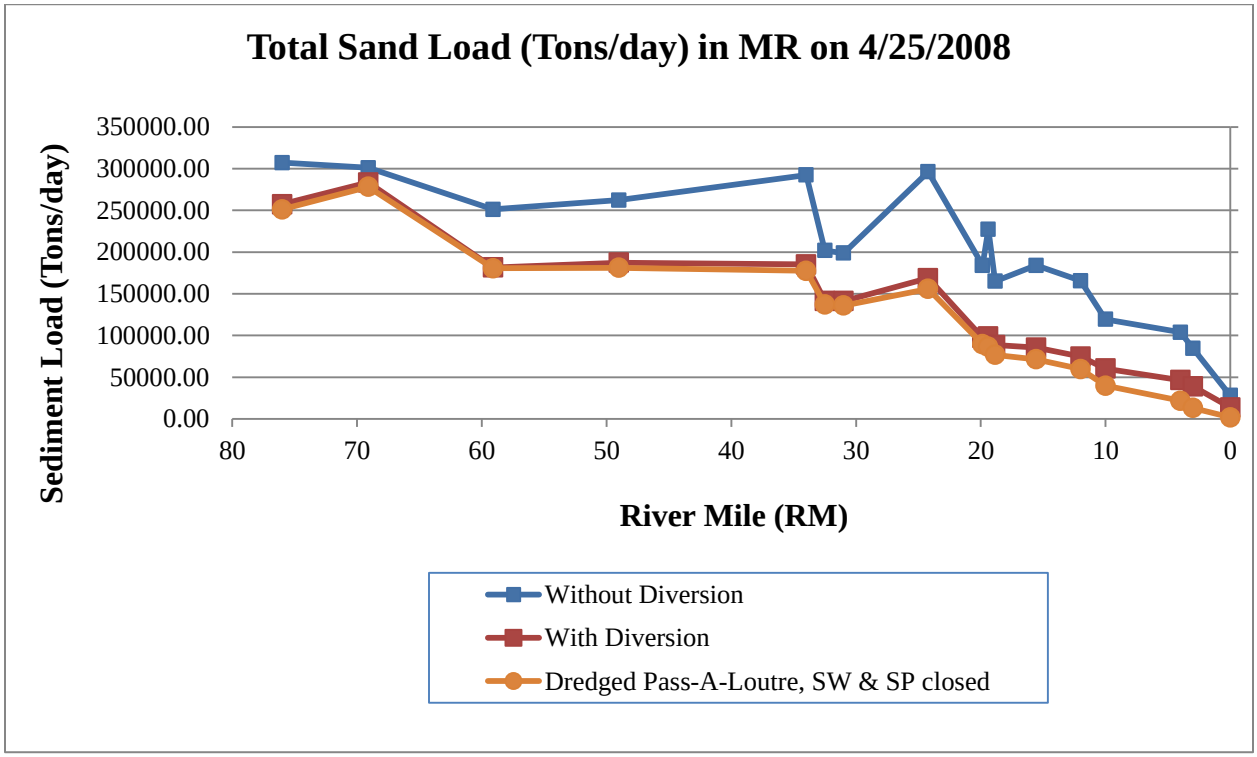

Figure 7-23: Total Sand Load in the MR from CHARIMA model on 4/25/2008

7.4 Mardi Gras Pass Simulations

Mardi Gras Pass is a new channel being formed in Bohemia reach (RM 44). It was made a channelized connections with the Mississippi River during the spring flood of 2011and the LPBF has been studying its change and growth since then. Currently, the outlet has a capacity of approximately 5000 CFS and thus has been included in the HEC-RAS and the CHARIMA model to study the sand load and discharge capacity. With the channel included in both the models, data for flow and sediment was obtained.

Figure 7-24 shows the Mardi Gras pass on Google Earth Image. The first part of channel geometry was based on the survey conducted by LPBF. The second part of channel geometry was obtained based on Google Earth. The flow estimate for the Mardi Gras pass by LPBF was also used to obtain the velocity in the channel.

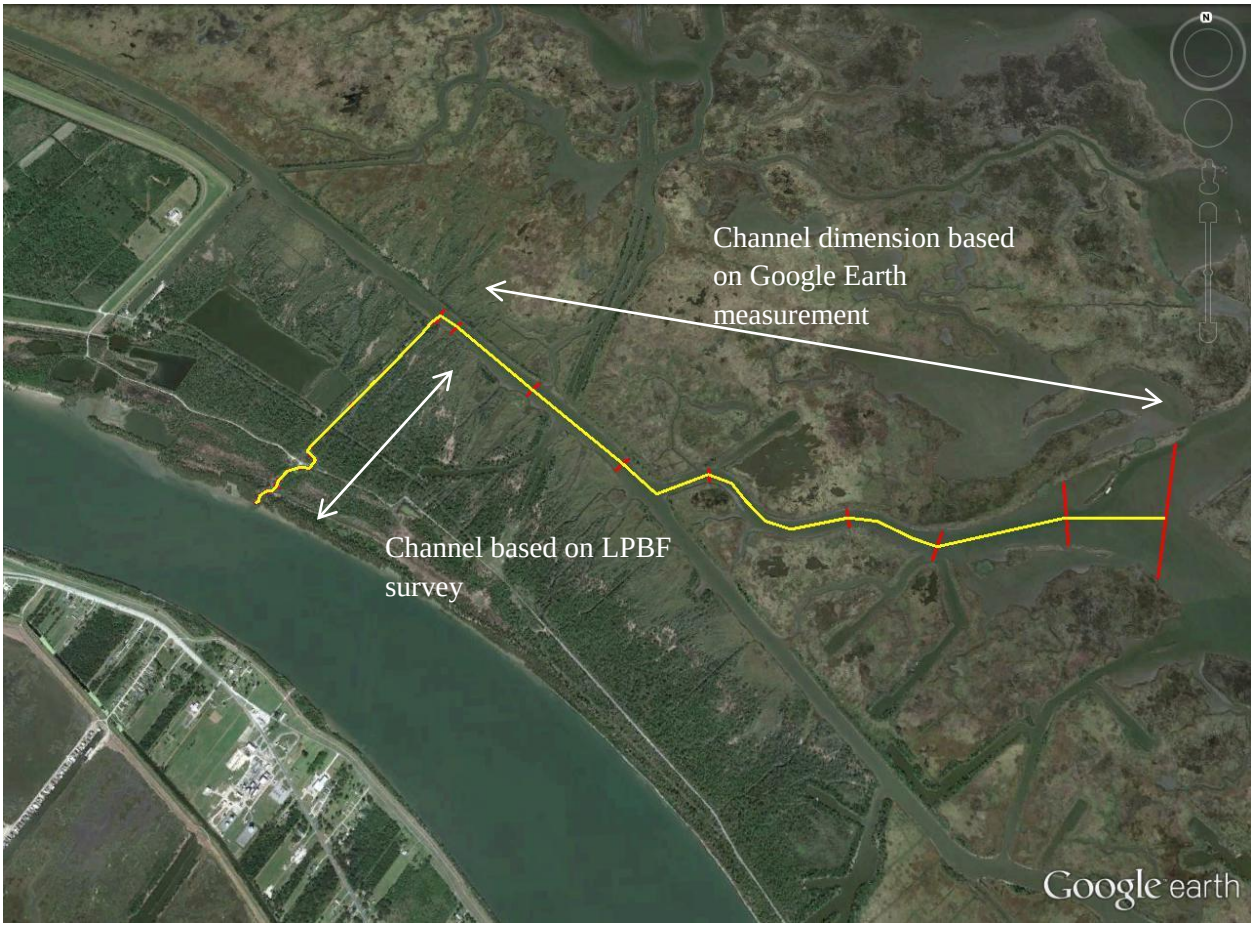

Figure 7-24: Mardi Gras Pass in Google Earth image.

With the geometry available, the channel was included in both HEC-RAS and CHARIMA model. The model was simulated for the year 2007-2008 with the current channel dimensions for Mardi Gras Pass. Figure 7-25 shows the rating curve for the Mardi Gras flow based on Belle Chasse (RM 76) flow. It can be seen the channel with current dimensions reach a peak flow around 6000 CFS when the Belle Chasse has flow around 1.3 million CFS.

Figure 7-26 show the flow in the Mardi Gras Pass from HEC-RAS and CHARIMA model. Both model produces similar flow in the channel for the same period.

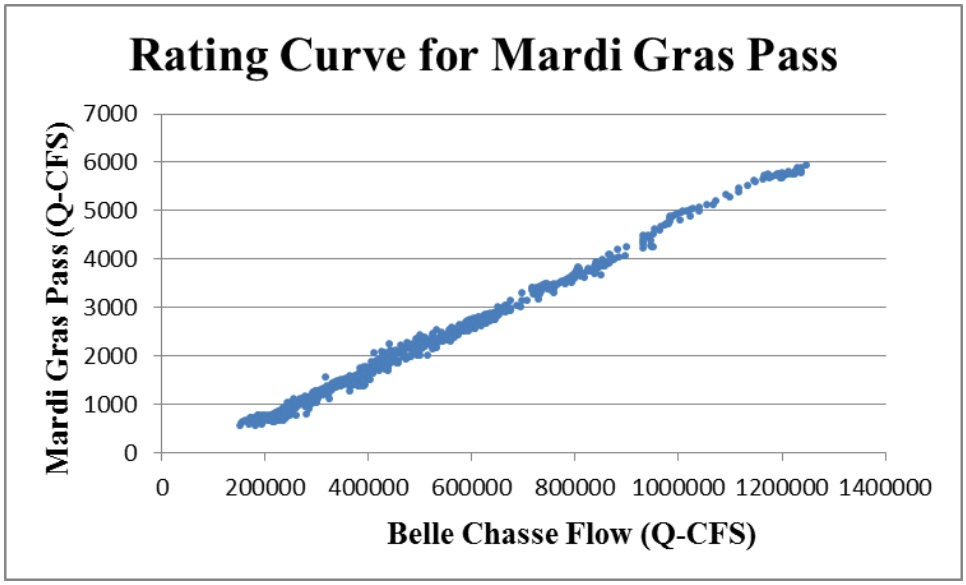

Figure 7-25: Rating Curve for the Mardi Gras Channel based on 2013 Survey.

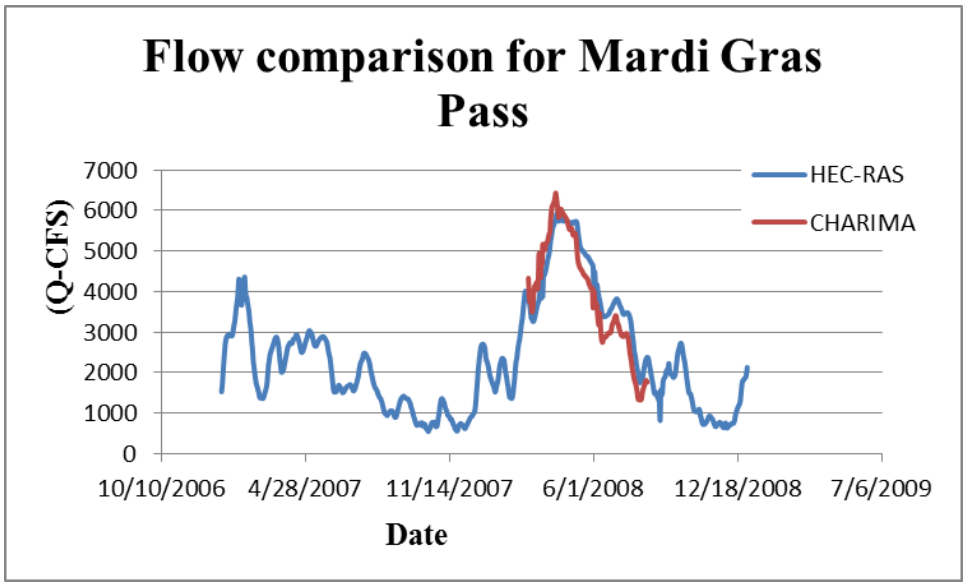

Figure 7-26: Flow Comparison for Mardi Gras Channel based on 2013 Survey.

Figure 7-27 shows the SWR in Mardi Gras Pass for 2008 using the 2013 channel dimensions. The SWR is above 1 overall. This indicates that the sand concentration in the channel is higher than the MR. The cause of higher concentration might be extraction of sediment from the MR as well as erosional activity in the channel. Figure 7-28 shows the total sand load in the Mardi Gras Pass. The highest sand load reaches around 1100 Tons per day.

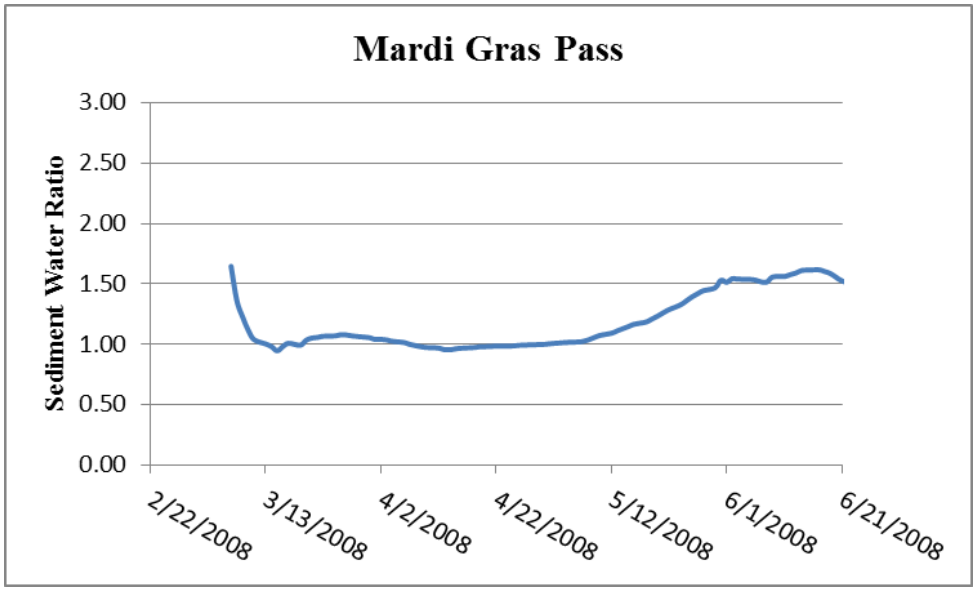

Figure 7-27: SWR in Mardi Gras Channel based on 2013 Survey.

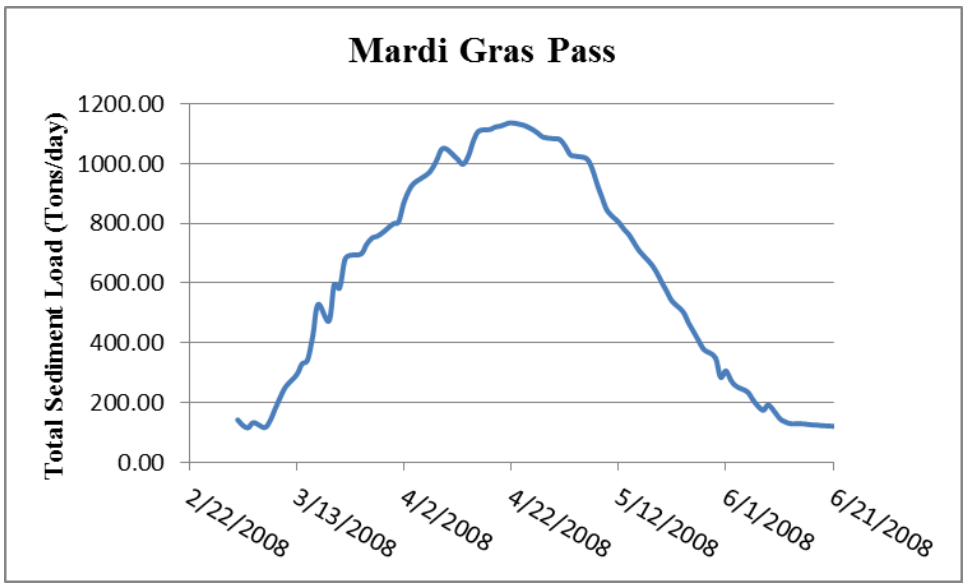

Figure 7-28: Total Sediment Load in Mardi Gras Channel based on 2013 Survey.

Chapter 8: Summary of Findings and Discussion

The HEC-RAS model was selected for the hydrodynamic simulation of the Lower Mississippi River for its large spatial domain and long-term time predictions. The model was successfully calibrated and validated for the model domain from Tarbert Landing to the GOM. The calibrated model had 97% efficiency for stage at Carrollton compared to the observed data. The model slightly over predicts stage by 0.1 feet at Carrollton for 2011. The validated model had 98% efficiency with observed stage at Carrollton. The model over predicts the stage by 0.25 feet. The model was used for other applications such as introducing future diversions, pass closure scenarios, hurricane simulations and as source of data for other complex models.

The model was used to run simulations where future MLODS diversions were included. The model was used to estimate the discharge in the outflows with the additional diversions. The model results showed drop in the flows of the outlets due to the introduction of future MLODS diversions as Belair and Buras were significantly large. Outlets located downstream of such large diversions seem to have higher impact compared to other outlets. Pass A-Loutre was also dredged according to the navigational channel requirements and thus simulated further for closure of South and Southwest pass. The closure of the pass pushes significant amount of flow into the Pass-A-Loutre as high as 200,000 CFS compared to 80,000 for existing conditions. The impact of the pass closure can be seen upstream up to Bohemia reach. The flow in outlets increased with the pass closures.

Model was also simulated for Hurricane Katrina (2005), Gustav (2008) and Isaac (2012). Surge heights were calculated based on the model data. These surge heights indicate stages of MR during hurricane conditions. One can observe the locations where the water might overtop the levee system in the MR and probable flooding areas. Hurricane Gustav and Isaac were also simulated for a range of flows from 300,000 CFS to 1.2 million CFS. These hurricanes occurred when the flow at the Tarbert landing was low around 300,000 CFS. However, these hurricanes can occur during the high flows in MR when the hurricane season overlaps with the flood period such as 2011. From the model simulation, it is observed that higher inflows at Tarbert Landing lead to higher surge in the river. So, the levees can be redesigned based on the new surge heights obtained based on the most frequent hurricanes and peak flows in the MR. This can avoid future potential flooding devastation due to levees failures.

HEC-RAS model was a source of data for other complex 2-D and 3-D models. Stage and flow data from the model in the MR and outlets from 2007 to 2013 were supplied to 3-d

modeling of Lower Mississippi River by Teran (2014). Stage and flow data from the calibrated model was also supplied for 3-d flow and salinity modeling of the passes by Pavlyukova (2014). Hurricane stage and flow data in the MR produced by HEC-RAS model was supplied to Khadka and Kazi who are research scientist working on 3-D modeling of the Lower Mississippi River at the Water Institute of the Gulf. HEC-RAS flow results were also provided to Dr. Georgiou who is working on a Lake Pontchartrain model using FV-COM.

The CHARIMA mode was selected over HEC-RAS to be used in the sand transport simulation of the Lower Mississippi River because it has the capacity to modeling the split of both flows and sediment at distributaries and is an unsteady-flow model. The CHARIMA model had the domain from Belle Chasse to the GOM. Belle Chasse was chosen as the upstream boundary because of the availability of sediment boundary from USGS. The model was calibrated for 2009 with 94% agreement on stage at Alliance and 86% flow efficiency at Bohemia reach. The sand transport model was calibrated with average factor of 1.07 for total sand load and 1.69 for bed load. The suspended sand load had an average factor of 7.83 which is beyond the acceptable calibration range. However, the model was considered acceptable because the study focused on total sand load.

During the simulations, it was found that in CHARIMA model, the suspended load results are time-step dependent which contradicts the theory. A smaller time-step tends to give a lower suspended load concentration. The use of a larger time step (14.4 hours) in the sediment simulations was a way of obtaining a good suspended-load calibration with realistic sediment-size and roughness coefficients. However, the model should be used with caution for flows outside of the calibration range. Future research is needed to improve the time step independence of CHARIMA with respect to the suspended sediment load.

The calibrated sand transport model was used to compute the total sand load and sand concentrations in the MR as well as the outlets. The model was also simulated with the addition of future MLODS diversions, dredging of Pass A-Loutre and closure of South and Southwest passes. The model produced results indicating the decrease in sediment concentration and total sand load over all with the inclusion of diversions and pass closure compared to existing conditions. However, the total sand load double from 5000 to 10,000 tons per day with the diversions and pass closure. The discharge in Pass A-Loutre also increased from 80,000 CFS to 200,000 CFS.

Chapter 9: Conclusions

The following conclusions can be made based on this study:

1) Two dynamic 1-D models (HEC-RAS and CHARIMA) have been calibrated and validated for the Lower Mississippi River.
2) The current models were improved by the height of land survey data supplied by LPBF.
3) The application of HEC-RAS to hurricane surge propagation indicated that a 1-D model is capable of an accurate and rapid simulation of hurricane propagation in the Mississippi River. The model and the observation data indicated that the hurricane surges can move more than 300 miles upriver. The model showed that there is a risk of levee overtopping if the hurricane surge is combined with the high River discharges.
4) The introductions of the MLODS diversions lead to overall drop in flows in the outlets. The outlets such as Bohemia and Fort St. Philip located downstream of large diversions like Belair and Buras have the most significant drops in discharge.
5) The introduction of the MLODS diversions also lead to drop in the sand load in all outlets compared to existing conditions.
6) With the closure of both South and Southwest Pass, the outlets located upstream up to Bohemia were affected. The discharge in the outlets increased compared to the addition of MLODS diversions. Pass-A-Loutre Discharge increased from 80,000 CFS to 200,000 CFS.
7) The closure of both South and Southwest Pass lead to increase in the sand load in the outlets. Pass-A-Loutre had a total sand load of 10,000 tons per day compared to 5,000 tons per day for existing conditions.
8) Mardi Gras Pass developed in 2011 has a peak flow of around 6000 CFS and total sand load capacity of 1200 tons per day based on cross-sectional survey data of 2013 provided by LPBF.

References

Copeland, R.R., & Thomas, W.A. (1992). "Lower Mississippi River Tarbert Landing to East Jetty Sedimentation Study". *Technical Report HL-92-6*, U.S. Army Corps of Engineers, New Orleans District.

Davis, M.A. *Numerical Simulation of Unsteady Hydrodynamics in the Lower Mississippi River*. MS thesis. University of New Orleans, 2010. Web. <http://scholarworks.uno.edu/td/1126/>.

Meselhe, E.A., Pereira, J.F, Georgiou, I.Y., Allison, M.A., McCorquodale, J.A., & Davis, M.A. (2010). Numerical Modeling of Mobile-Bed Hydrodynamics in the Lower Mississippi River, *Proc. of World Environmental & Water Resources Congress (EWRI) 2010,* A.S.C.E., Providence, RI.

Lake Pontchartrain Basin Foundation (LPBF). (2008). "Comprehensive Recommendations Supporting the Use of the Multiple Lines of Defense Strategy to Sustain Coastal Louisiana 2008 Report (Version 1)", Lake Pontchartrain Basin Foundation. Metairie, LA.

Papanicolaou, A.N., Elhakeem, M., Krallis, G., Prakash, S., & Edinger, J. (2008). Sediment Transport Modeling Review – Current and Future Developments. *Journal of Hydraulic Engineering*. ASCE. January 2008.

Parker, G., Sequeiros, O., & River Morphodynamics Class of Spring 2006. (2006). Large Scale River Morphodynamics: Application to the Mississippi Delta. *Proceedings, River Flow 2006 Conference*. September 6 – 8, 2006.

Pereira, J.F., McCorquodale, J.A., Meselhe, E.A., Georgiou, I.Y. & Allison, M.A. (2009). Numerical Simulation of Bed Material Transport in the Lower Mississippi River. *Journal of Coastal Research, Proceedings of the 10th International Coastal Symposium* (SI 56), 1449-1453. Lisbon, Portugal.

Pereira, J.F. *Numerical Modeling of River Diversions in the Lower Mississippi River*. Diss. University of New Orleans, 2011. Web. <http://scholarworks.uno.edu/cgi/viewcontent.cgi?article=2293&context=td>.

Nittrouer, J.A.; Allison, M.A. and Campanella, R., 2008. Bedform transport rates for the lowermost Mississippi River, *Journal of Geophysical Research Earth Surface*, 113 (F03004)

U.S. Army Corps of Engineers, New Orleans District (USACE NOD). (2007). "Mississippi River Hydrographic Survey: 2003 – 2004; Black Hawk, LA to Gulf of Mexico." Mississippi River Commission, Vicksburg, MS.

Waldron, R. (2008). "Physical Modeling of Flow and Sediment Transport Using Distorted Scale Modeling." Thesis, Louisiana State University and Agricultural and Mechanical College, Baton Rouge, LA

White, W.R., Milli, H. and Crabbe, A.D. (1978). Sediment Transport: An Appraisal of Available Methods, Report No. IT 119, Second Ed. Hydraulic Research Station, Wallingford, UK.

Appendix A:

Boundary Condition:

Daily Stage Boundary:

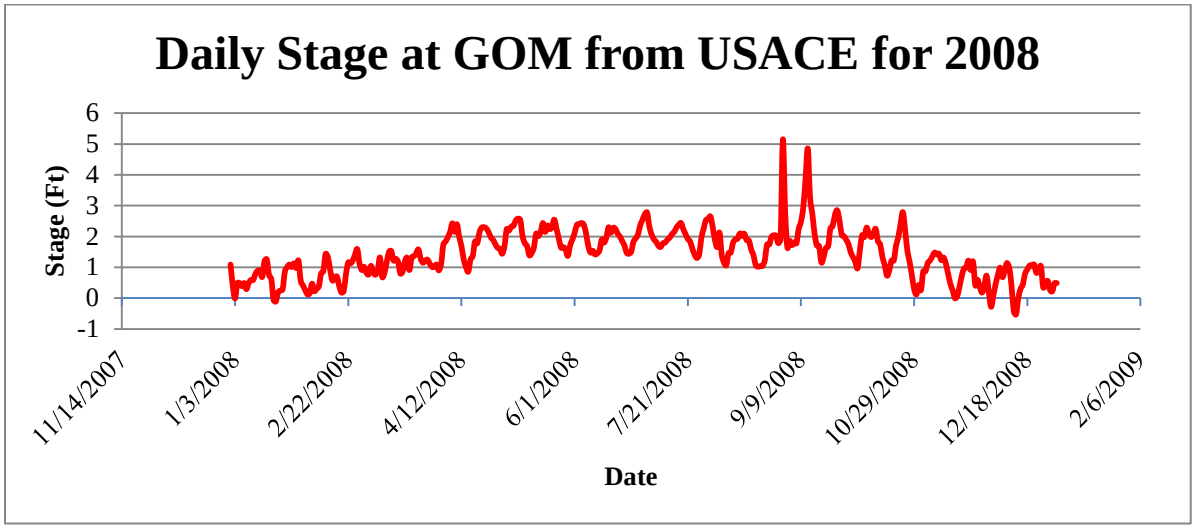

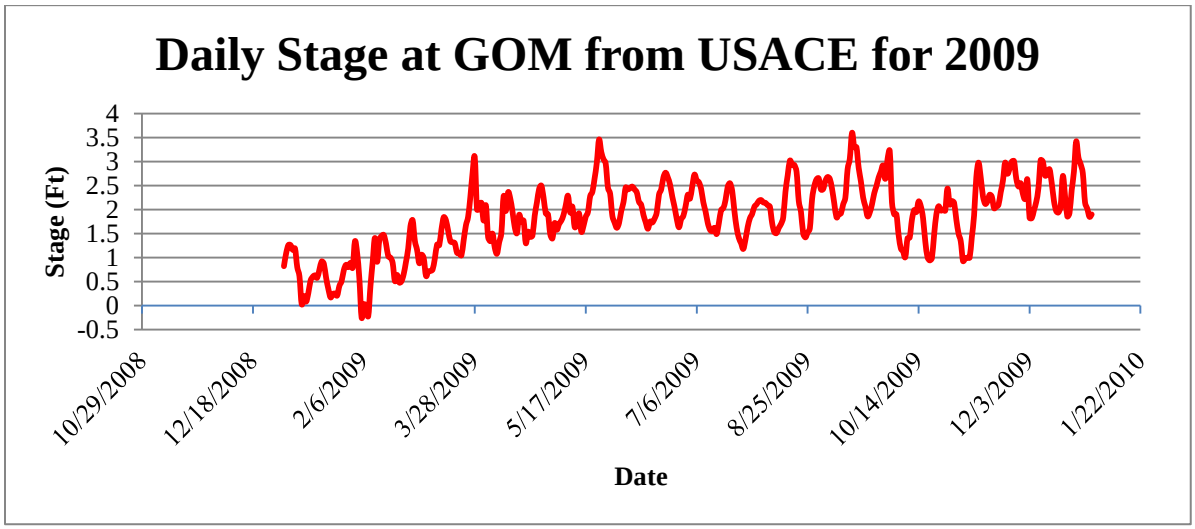

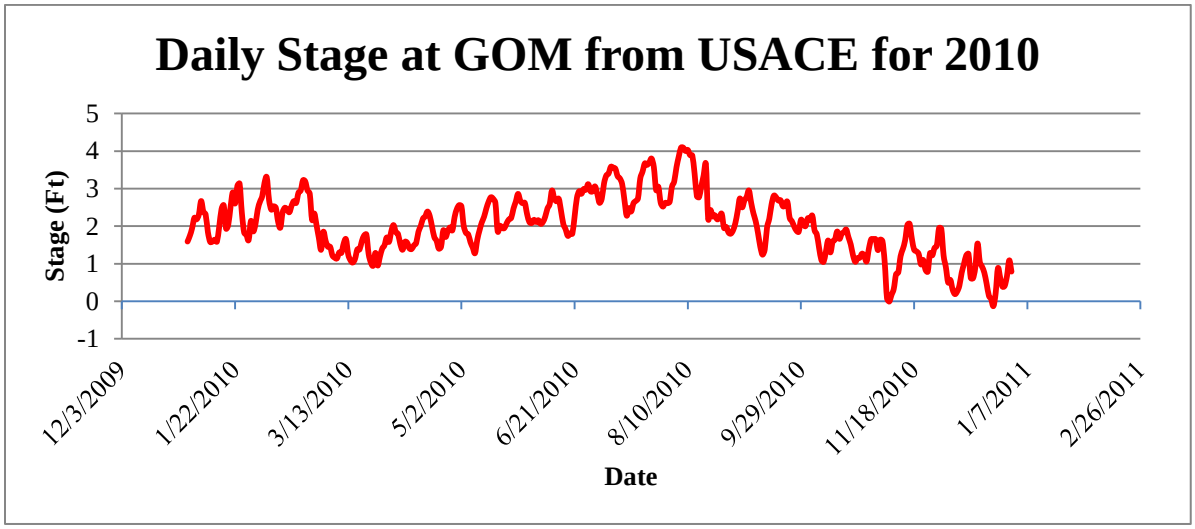

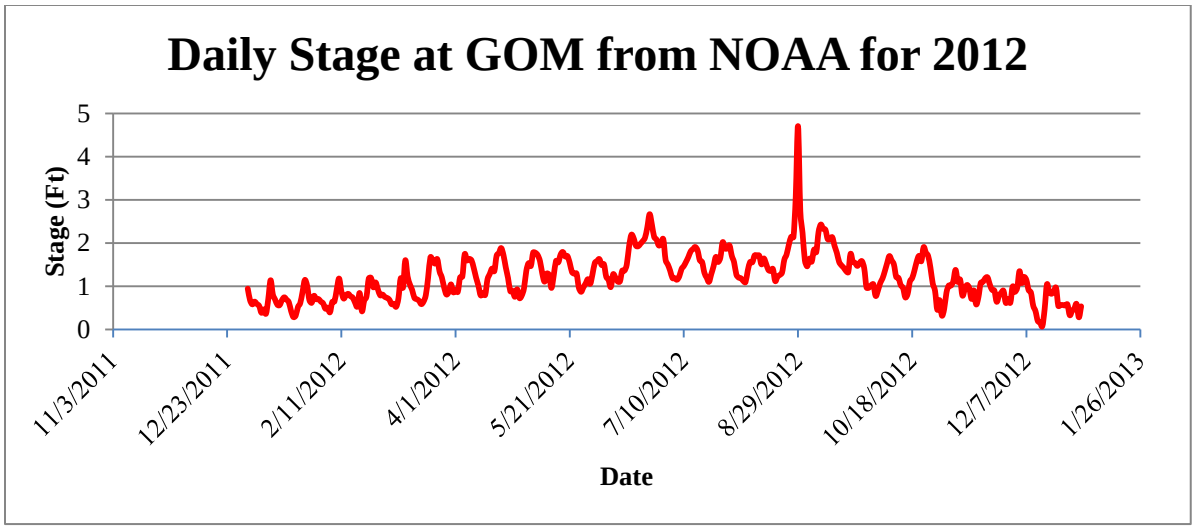

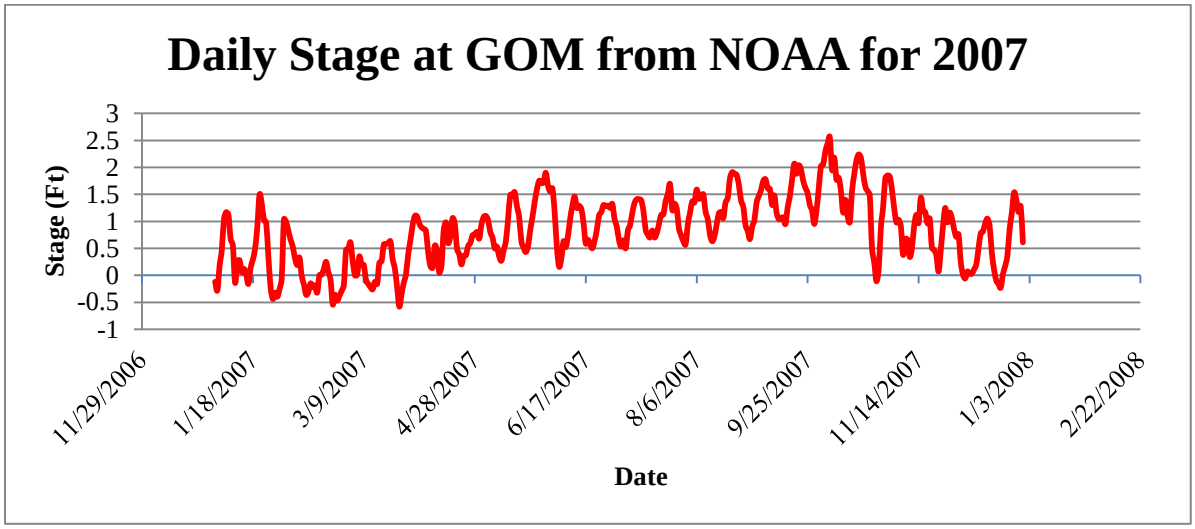

Hourly Stage Boundary:

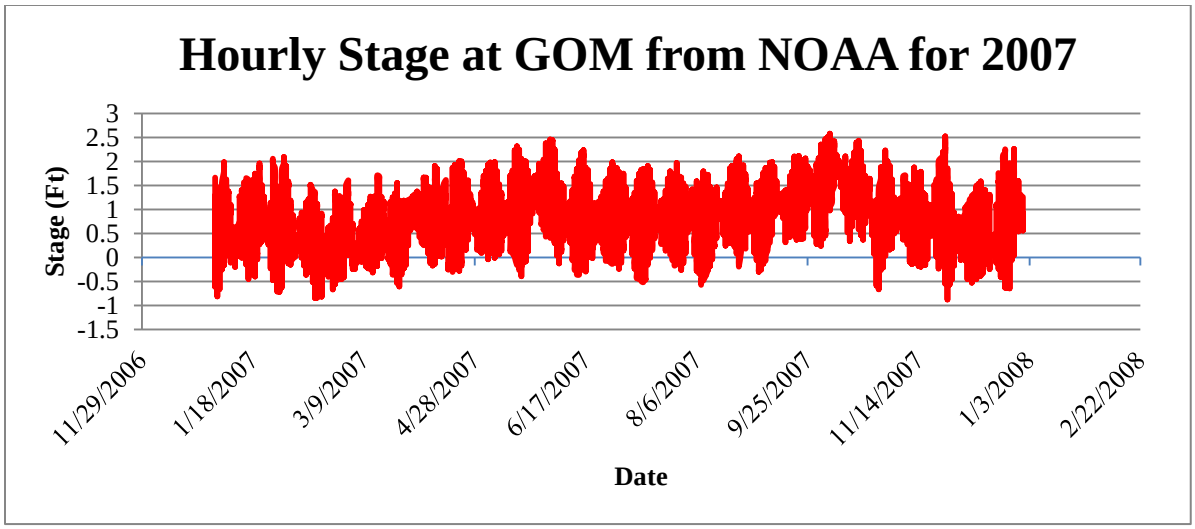
Hourly Stage at GOM from NOAA for 2007
Stage (Ft)
3
2.5
2
1.5
1
0.5
0
-0.5
-1
-1.5
11/29/2006
1/18/2007
3/9/2007
4/28/2007
6/17/2007
8/6/2007
9/25/2007
11/14/2007
1/3/2008
2/22/2008
Date

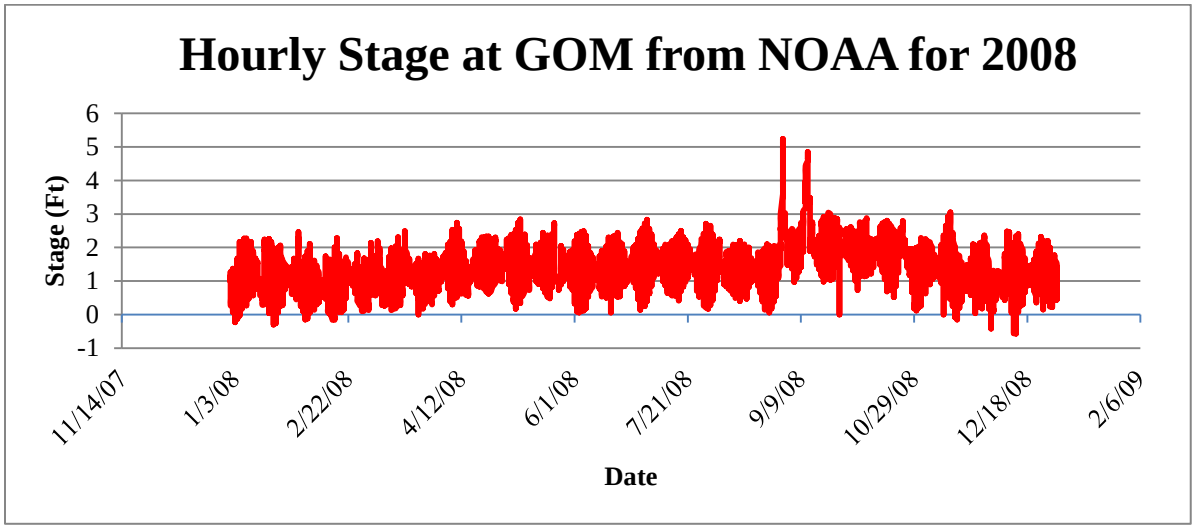
Hourly Stage at GOM from NOAA for 2008
Stage (Ft)
6
5
4
3
2
1
0
-1
11/14/07
1/3/08
2/22/08
4/12/08
6/1/08
7/21/08
9/9/08
10/29/08
12/18/08
2/6/09
Date

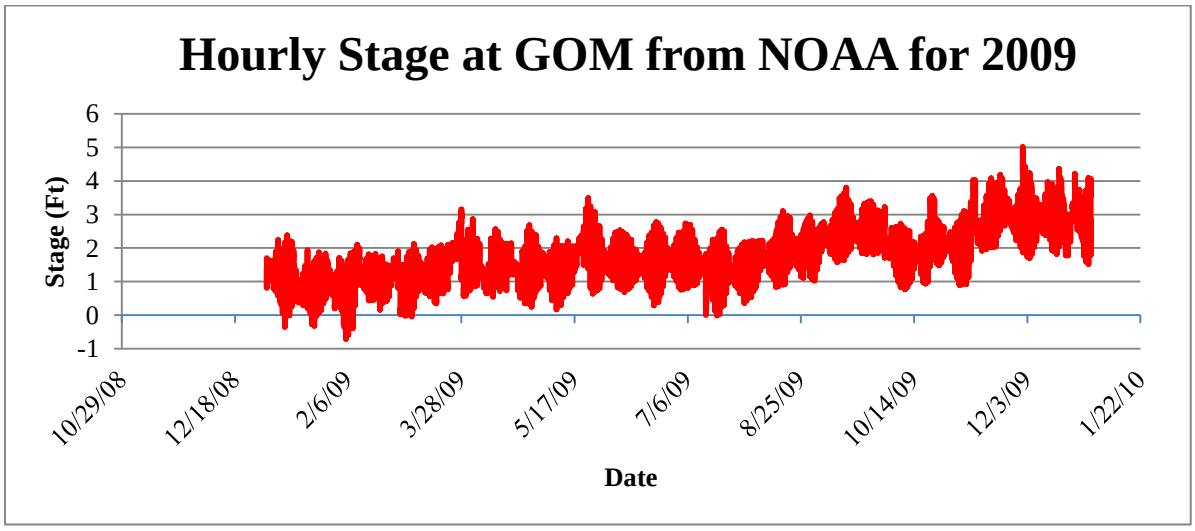
Hourly Stage at GOM from NOAA for 2009
Stage (Ft)
6
5
4
3
2
1
0
-1
10/29/08
12/18/08
2/6/09
3/28/09
5/17/09
7/6/09
8/25/09
10/14/09
12/3/09
1/22/10
Date

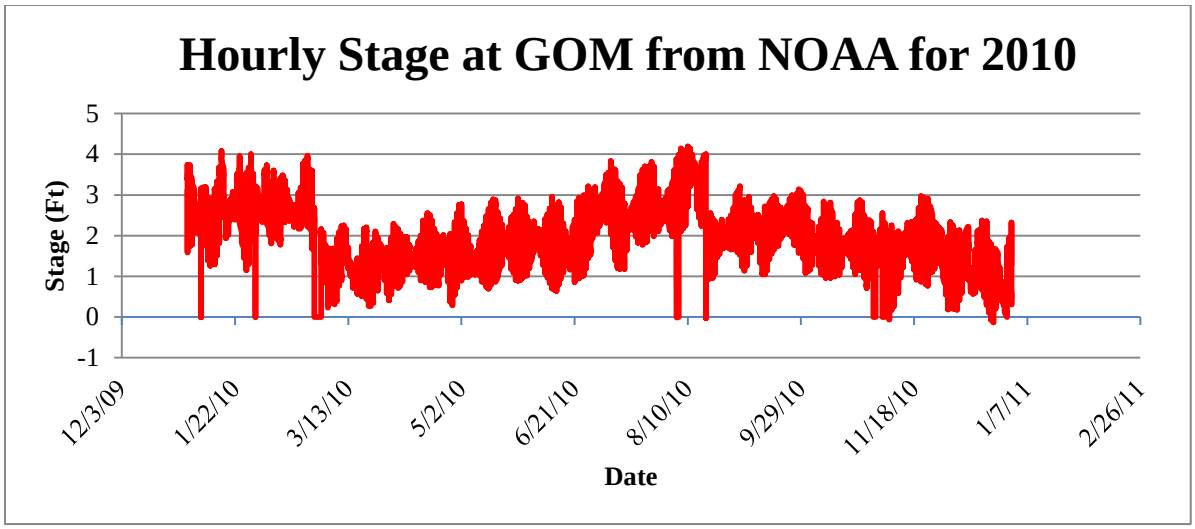
Hourly Stage at GOM from NOAA for 2010
Stage (Ft)
5
4
3
2
1
0
-1
12/3/09
1/22/10
3/13/10
5/2/10
6/21/10
8/10/10
9/29/10
11/18/10
1/7/11
2/26/11
Date

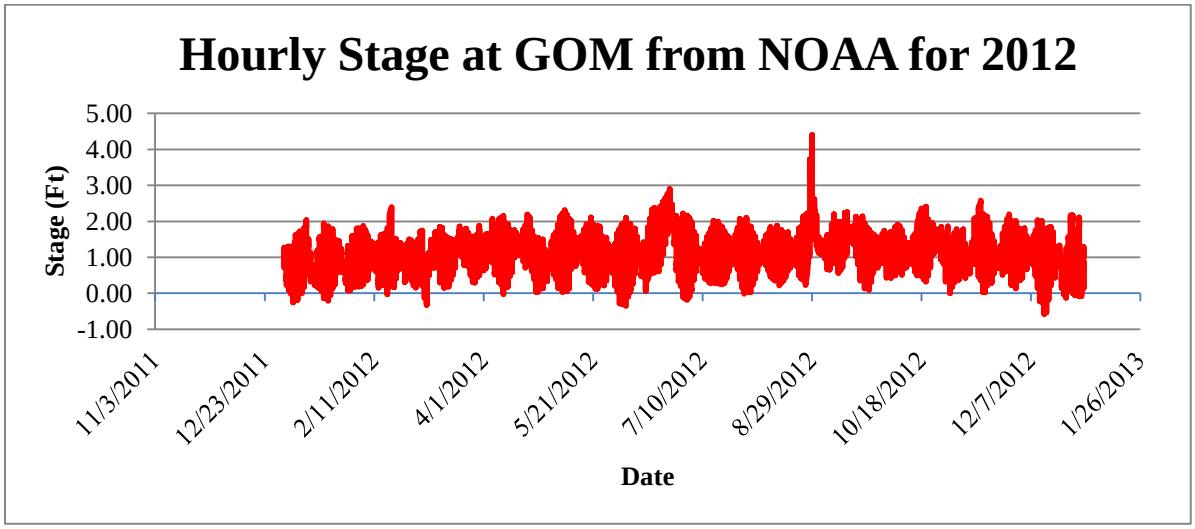
Hourly Stage at GOM from NOAA for 2012
Stage (Ft)
5.00
4.00
3.00
2.00
1.00
0.00
-1.00
11/3/2011
12/23/2011
2/11/2012
4/1/2012
5/21/2012
7/10/2012
8/29/2012
10/18/2012
12/7/2012
1/26/2013
Date

Flow Boundary:

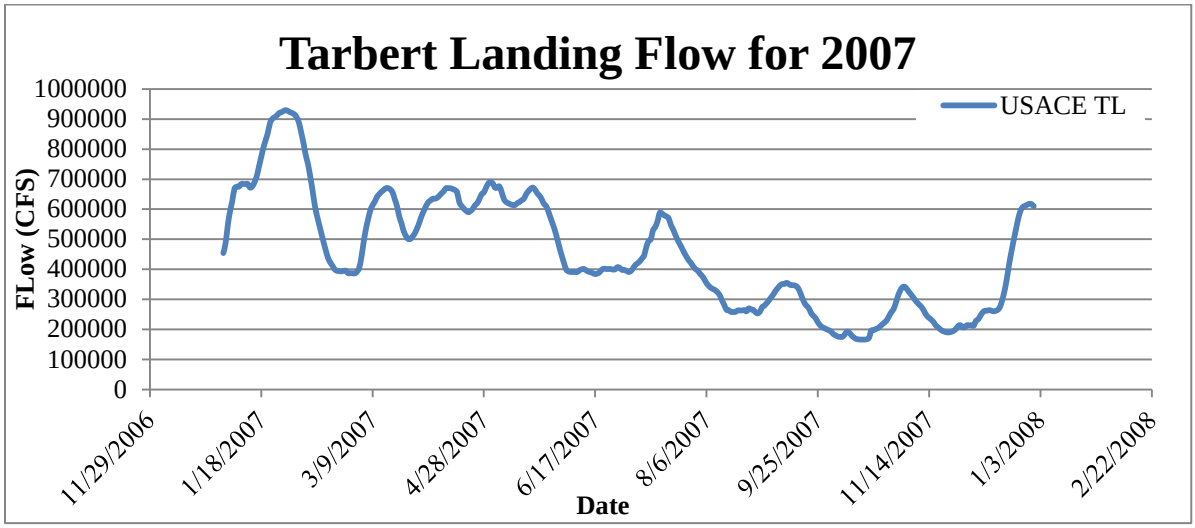

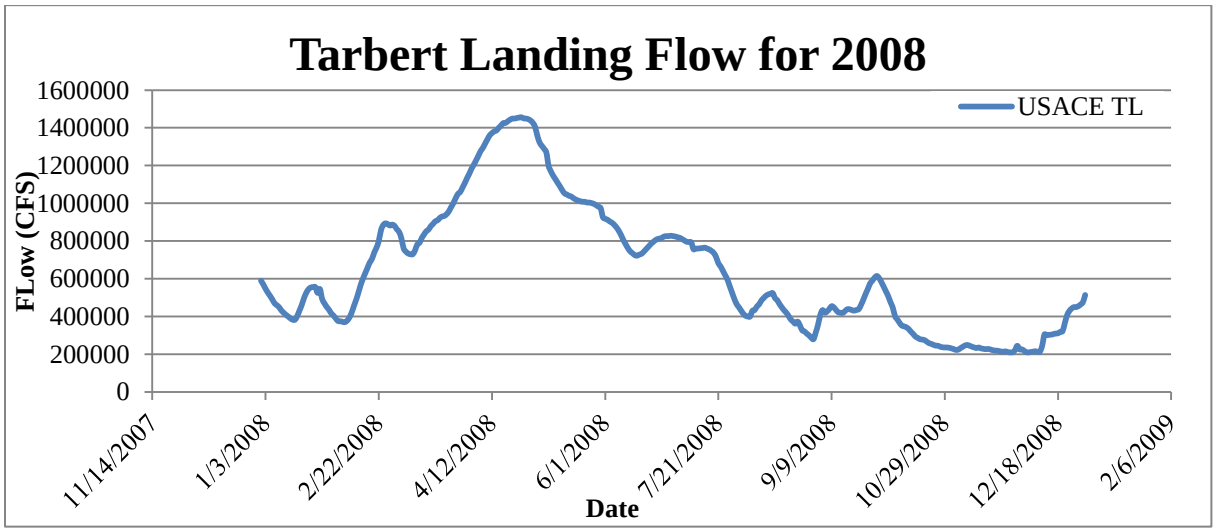

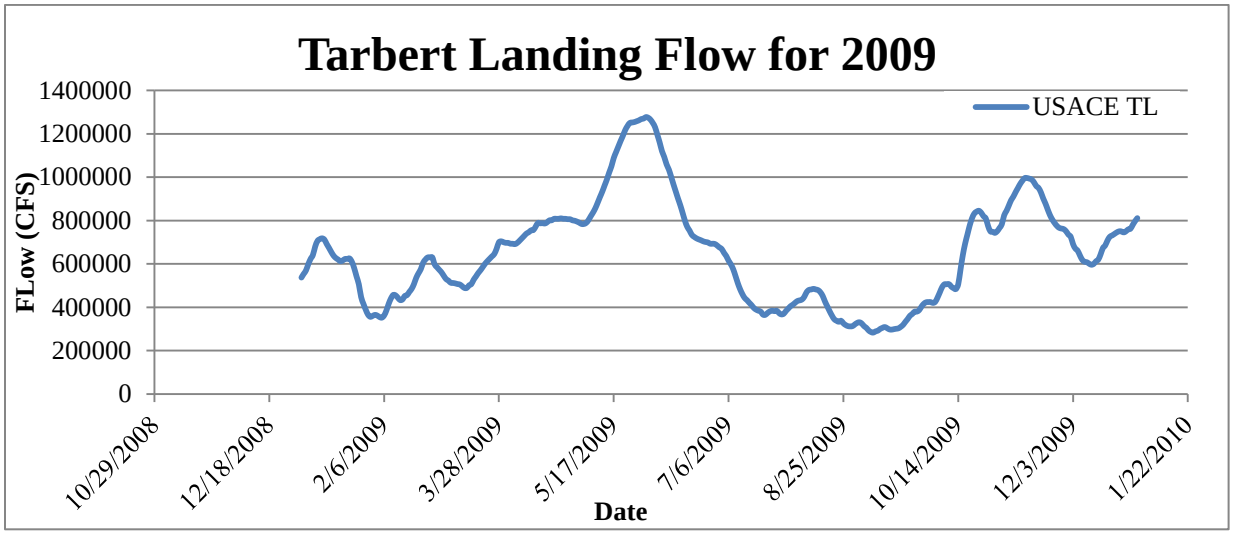

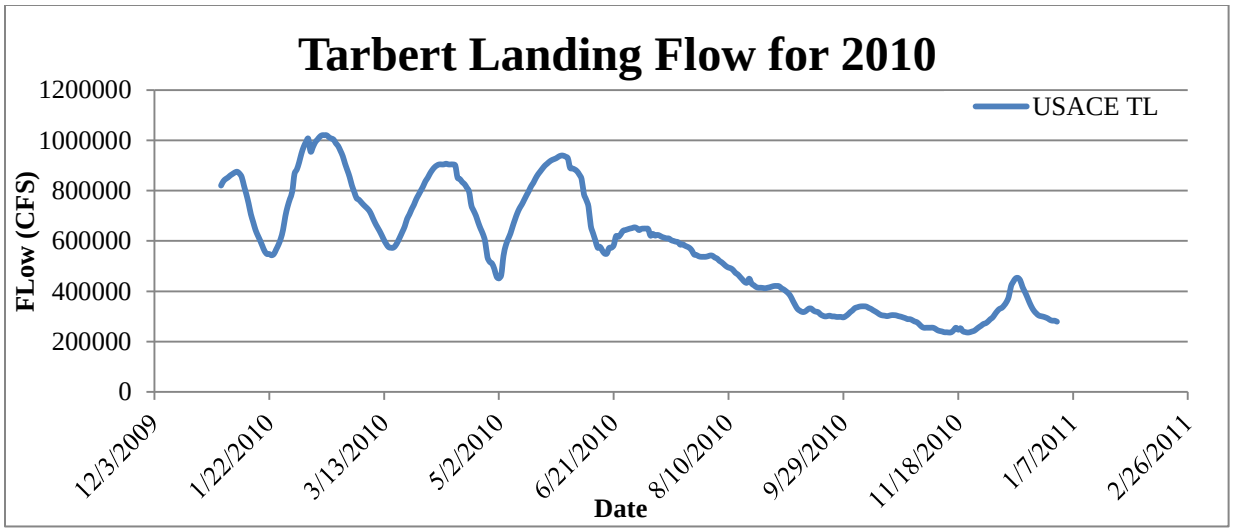
Tarbert Landing Flow for 2010
1200000
1000000
800000
600000
400000
200000
0
FLow (CFS)
USACE TL
12/3/2009
1/22/2010
3/13/2010
5/2/2010
6/21/2010
8/10/2010
9/29/2010
11/18/2010
1/7/2011
2/26/2011
Date

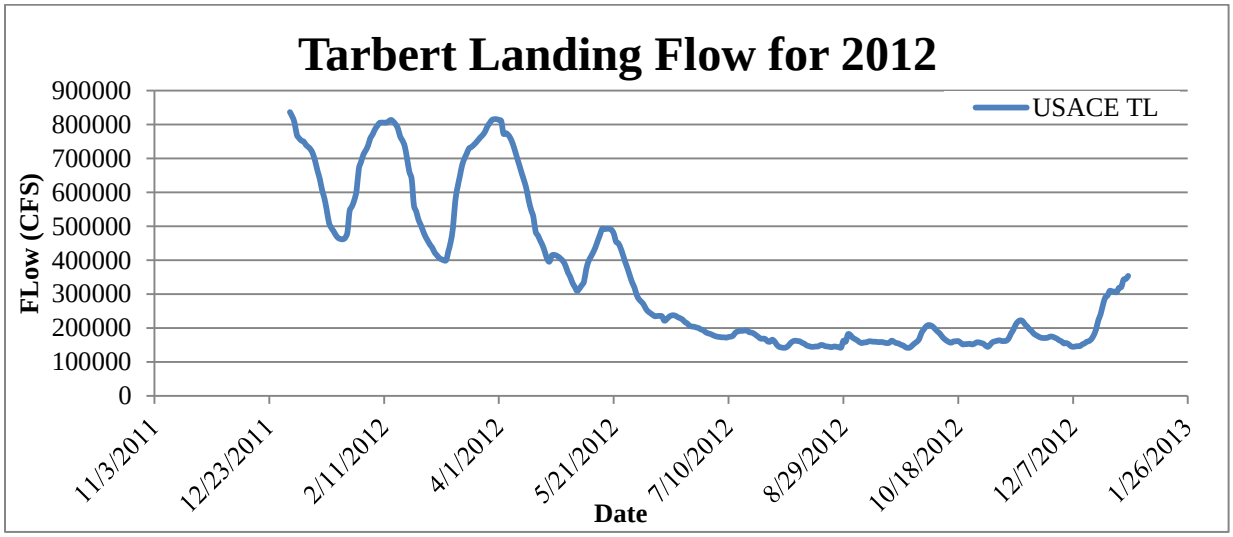
Tarbert Landing Flow for 2012
900000
800000
700000
600000
500000
400000
300000
200000
100000
0
FLow (CFS)
USACE TL
11/3/2011
12/23/2011
2/11/2012
4/1/2012
5/21/2012
7/10/2012
8/29/2012
10/18/2012
12/7/2012
1/26/2013
Date

Appendix B:

Calibration and Validation Results

HEC-RAS Calibration Results (2011):

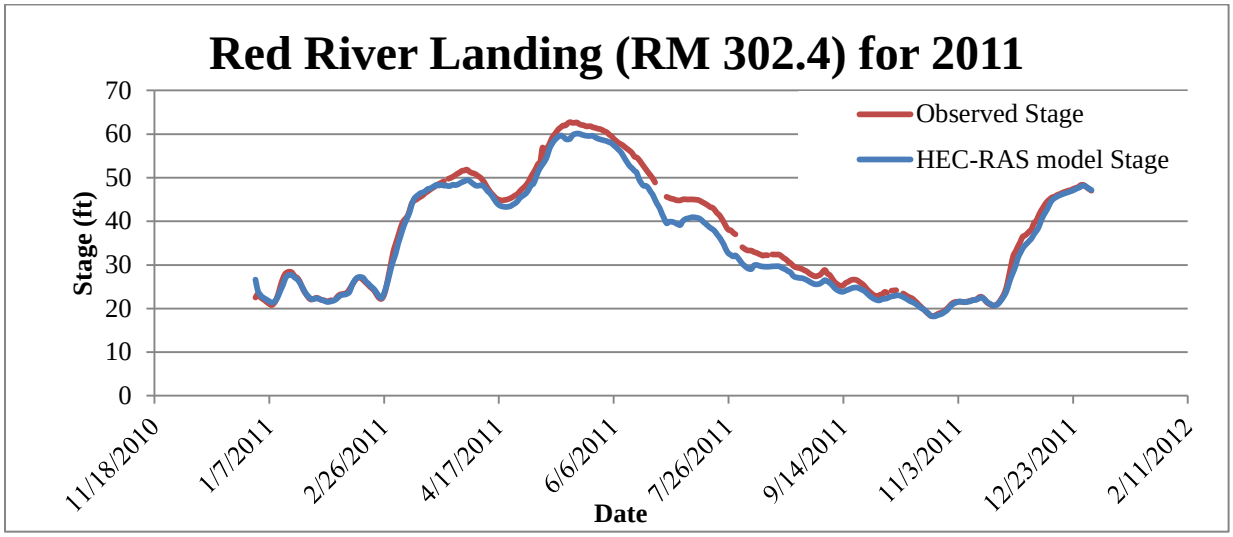

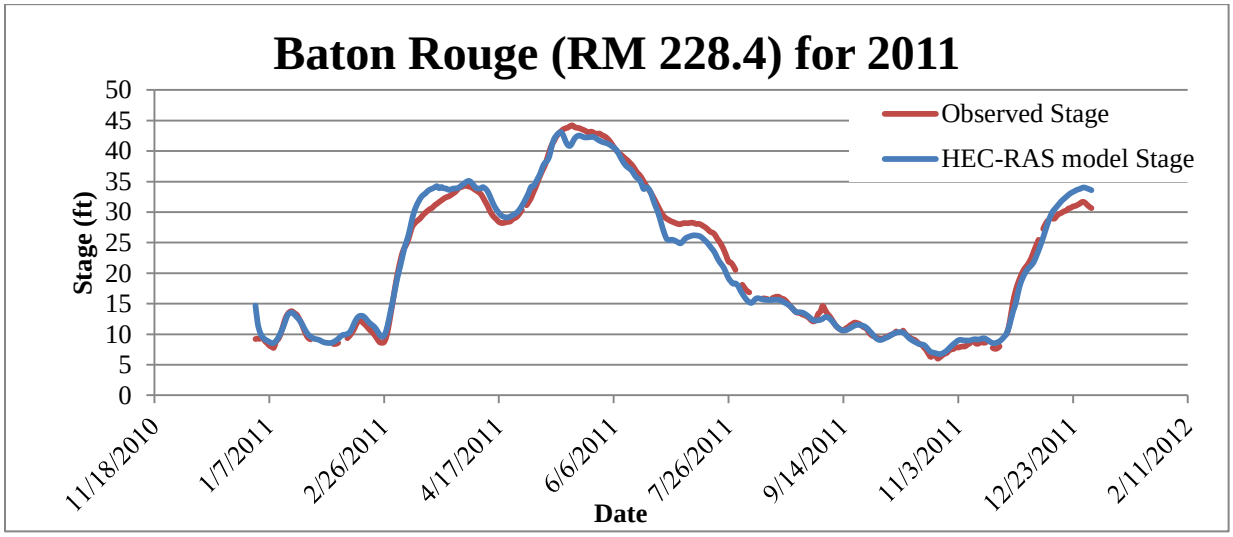

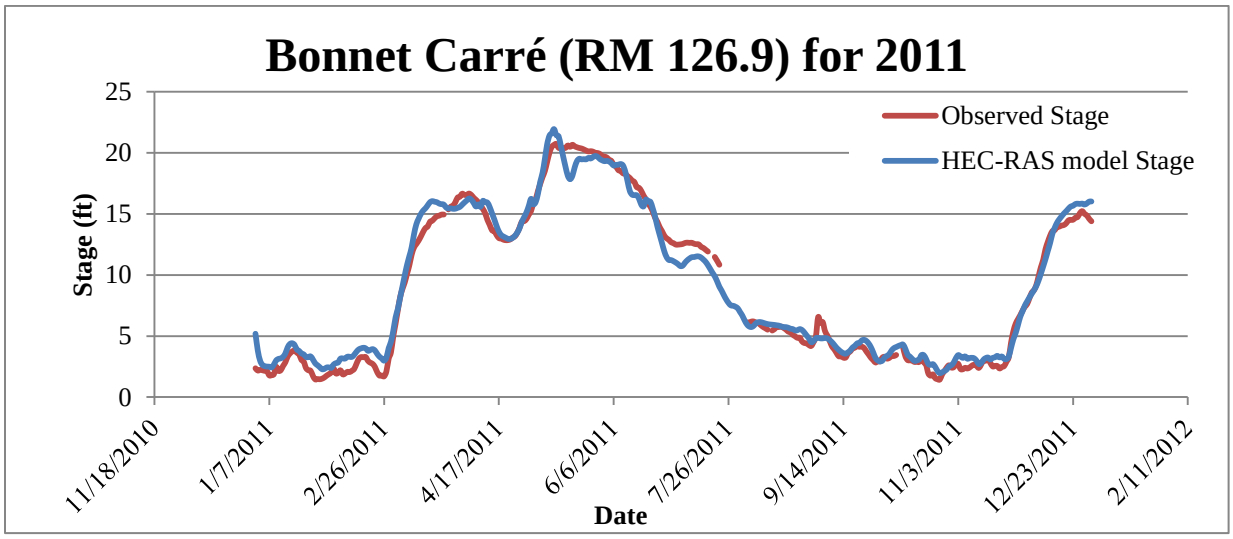

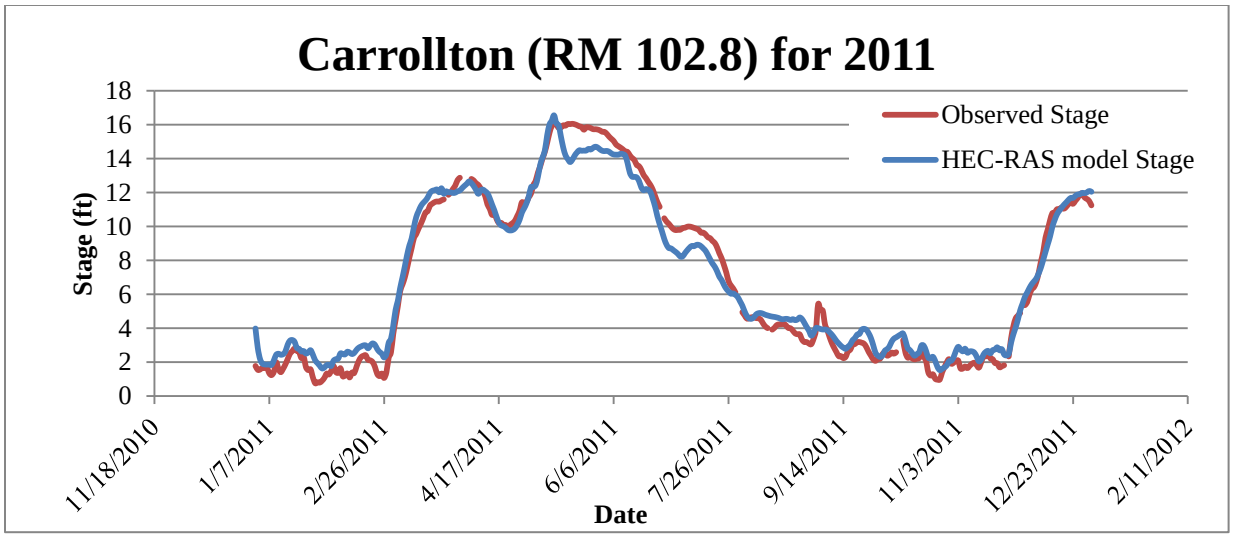
Carrollton (RM 102.8) for 2011
Observed Stage
HEC-RAS model Stage
Stage (ft)
Date
18
16
14
12
10
8
6
4
2
0
11/18/2010
1/7/2011
2/26/2011
4/17/2011
6/6/2011
7/26/2011
9/14/2011
11/3/2011
12/23/2011
2/11/2012

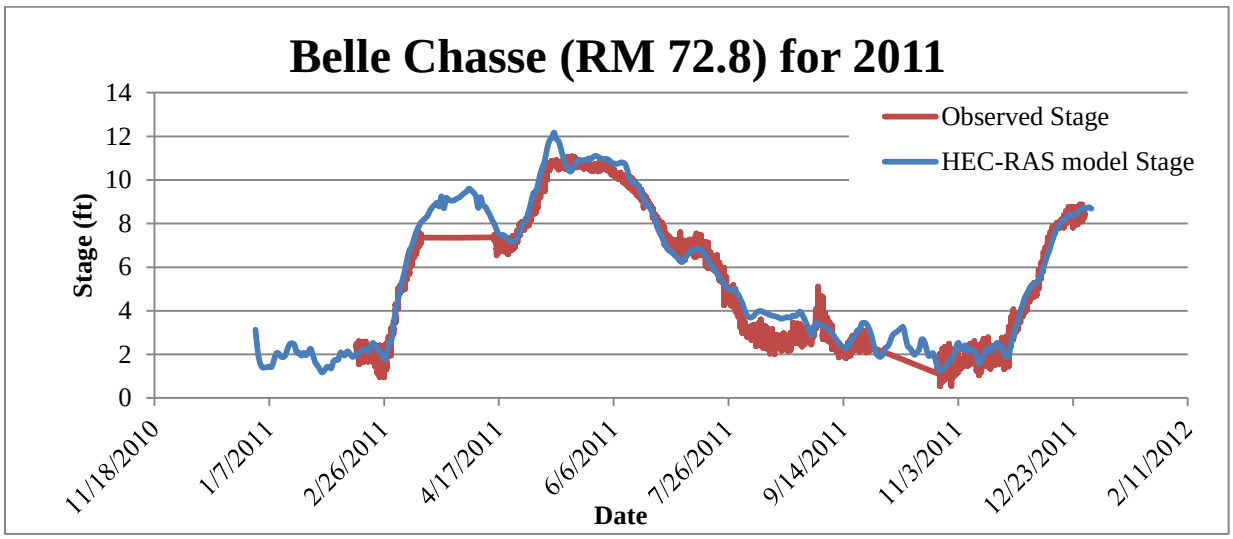
Belle Chasse (RM 72.8) for 2011
Observed Stage
HEC-RAS model Stage
Stage (ft)
Date
14
12
10
8
6
4
2
0
11/18/2010
1/7/2011
2/26/2011
4/17/2011
6/6/2011
7/26/2011
9/14/2011
11/3/2011
12/23/2011
2/11/2012

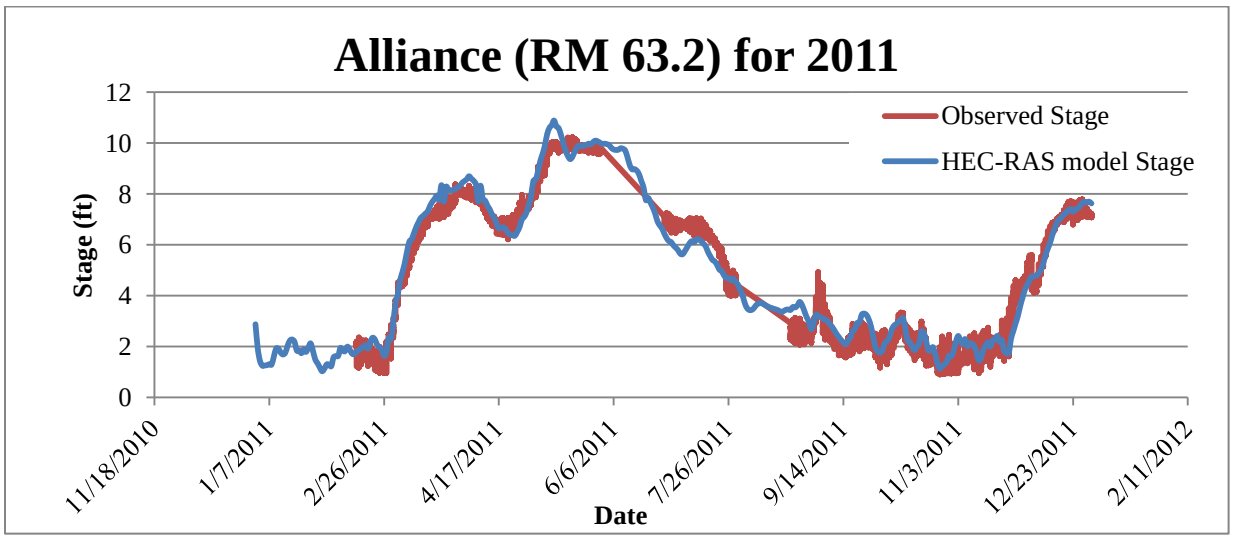
Alliance (RM 63.2) for 2011
Observed Stage
HEC-RAS model Stage
Stage (ft)
Date
12
10
8
6
4
2
0
11/18/2010
1/7/2011
2/26/2011
4/17/2011
6/6/2011
7/26/2011
9/14/2011
11/3/2011
12/23/2011
2/11/2012

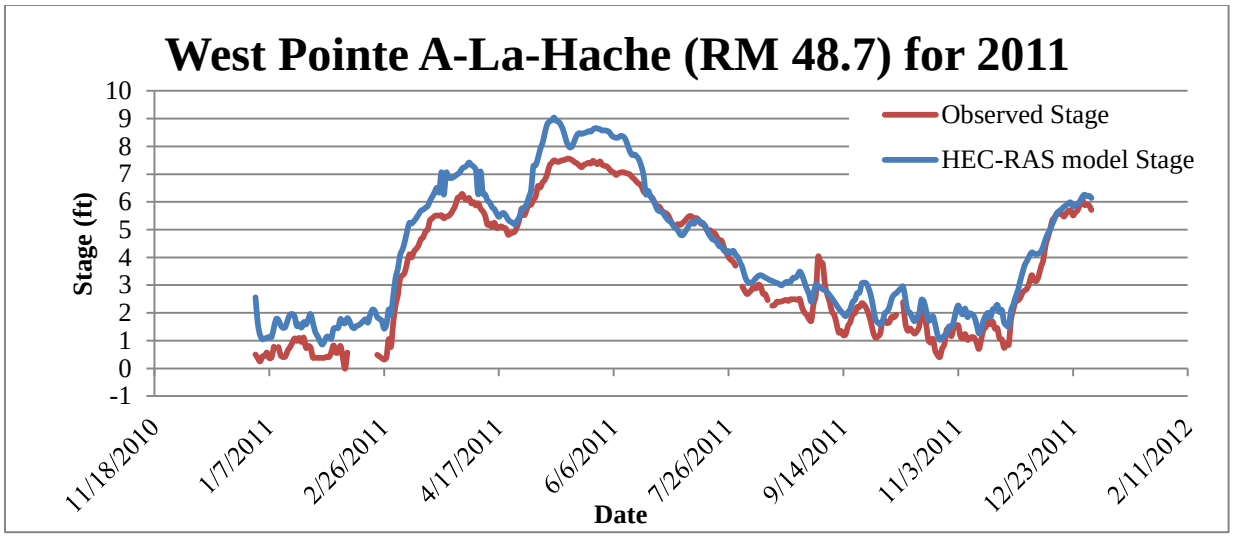
West Pointe A-La-Hache (RM 48.7) for 2011
Observed Stage
HEC-RAS model Stage
Stage (ft)
10
9
8
7
6
5
4
3
2
1
0
-1
11/18/2010
1/7/2011
2/26/2011
4/17/2011
6/6/2011
7/26/2011
9/14/2011
11/3/2011
12/23/2011
2/11/2012
Date

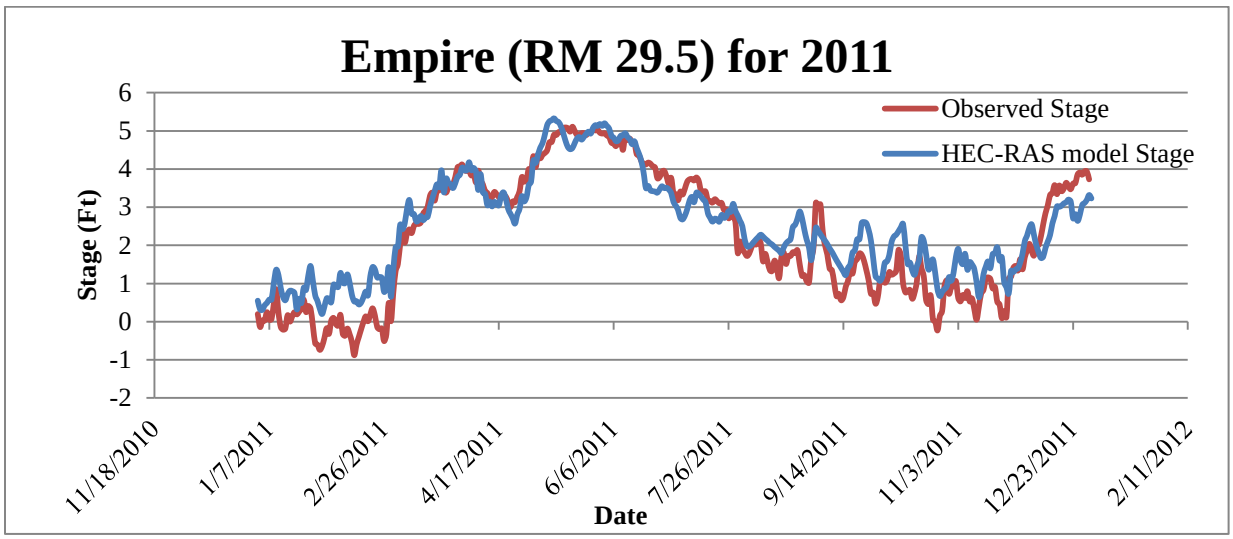
Empire (RM 29.5) for 2011
Observed Stage
HEC-RAS model Stage
Stage (Ft)
6
5
4
3
2
1
0
-1
-2
11/18/2010
1/7/2011
2/26/2011
4/17/2011
6/6/2011
7/26/2011
9/14/2011
11/3/2011
12/23/2011
2/11/2012
Date

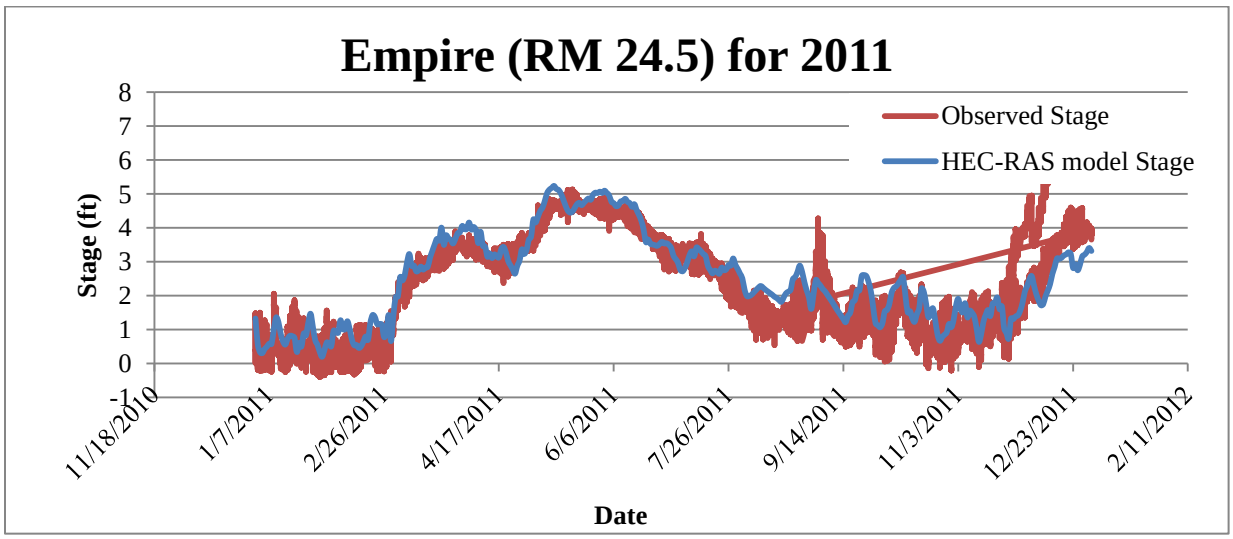
Empire (RM 24.5) for 2011
Observed Stage
HEC-RAS model Stage
Stage (ft)
8
7
6
5
4
3
2
1
0
-1
11/18/2010
1/7/2011
2/26/2011
4/17/2011
6/6/2011
7/26/2011
9/14/2011
11/3/2011
12/23/2011
2/11/2012
Date

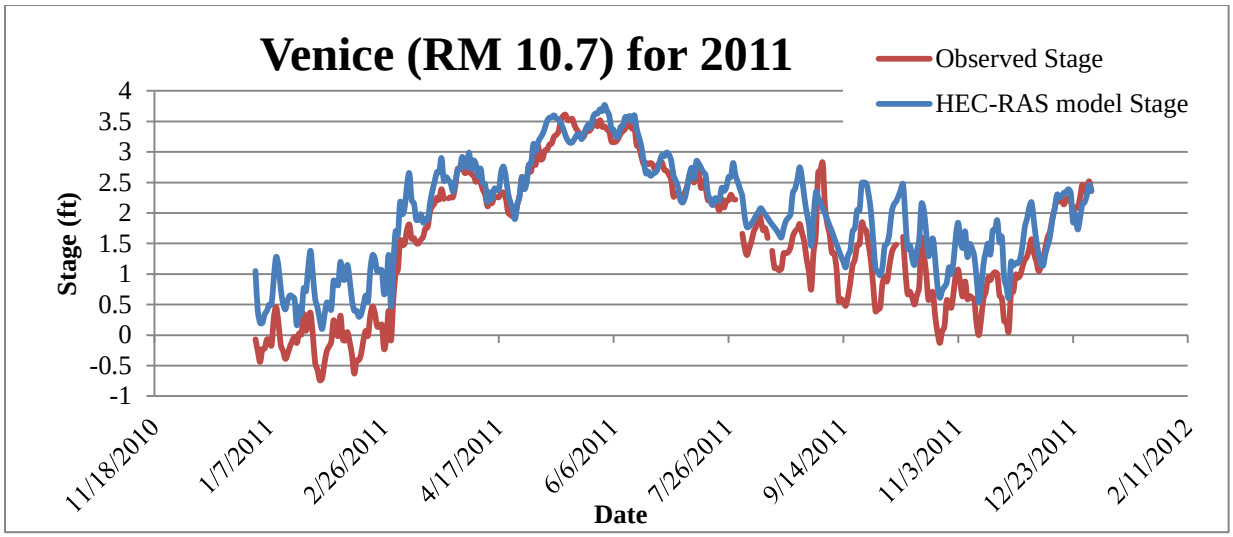
Venice (RM 10.7) for 2011
Observed Stage
HEC-RAS model Stage
Stage (ft)
4
3.5
3
2.5
2
1.5
1
0.5
0
-0.5
-1
11/18/2010
1/7/2011
2/26/2011
4/17/2011
6/6/2011
7/26/2011
9/14/2011
11/3/2011
12/23/2011
2/11/2012
Date

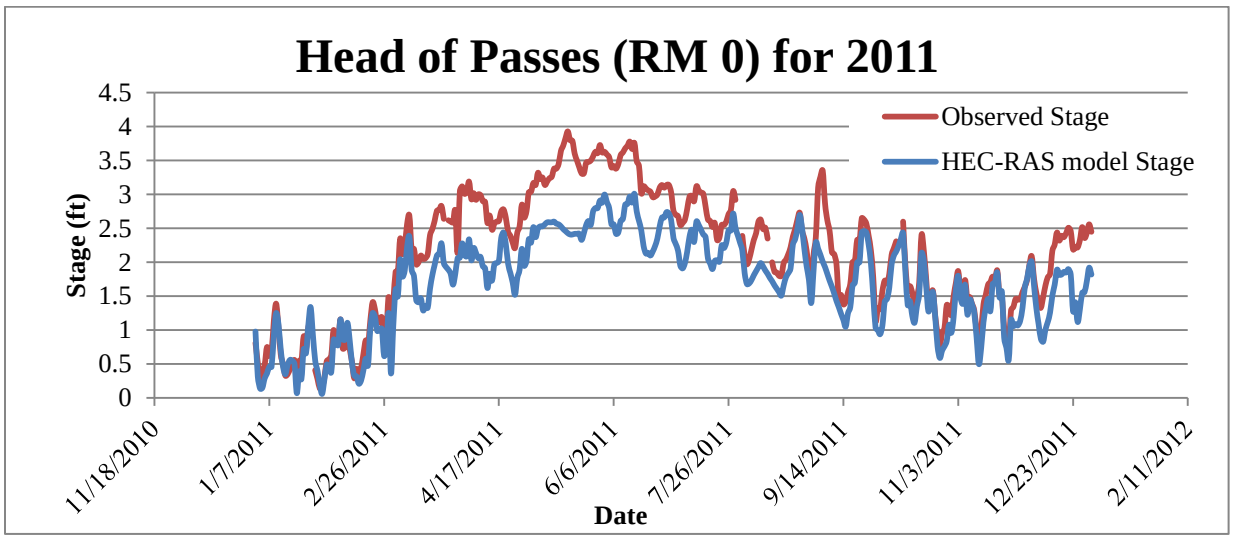
Head of Passes (RM 0) for 2011
Observed Stage
HEC-RAS model Stage
Stage (ft)
4.5
4
3.5
3
2.5
2
1.5
1
0.5
0
11/18/2010
1/7/2011
2/26/2011
4/17/2011
6/6/2011
7/26/2011
9/14/2011
11/3/2011
12/23/2011
2/11/2012
Date

HEC-RAS Validation Results (2008):

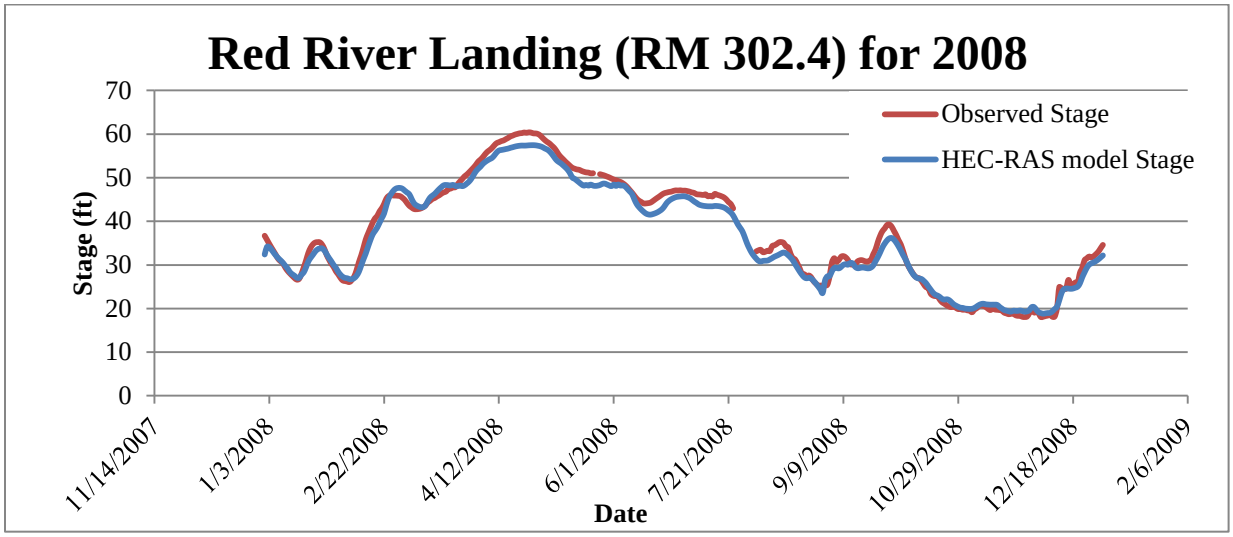

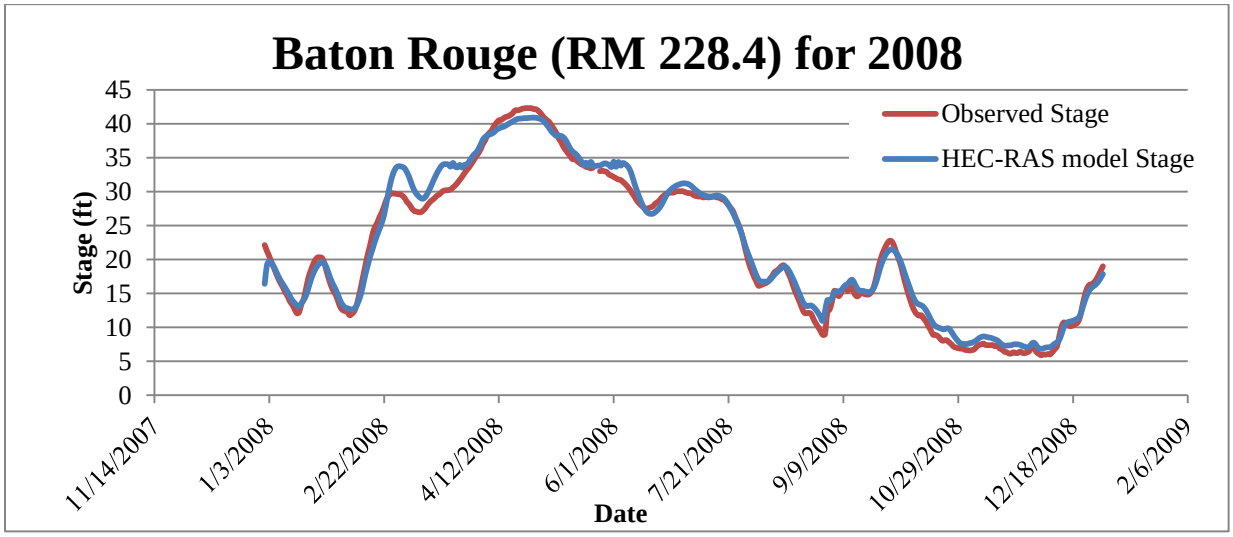

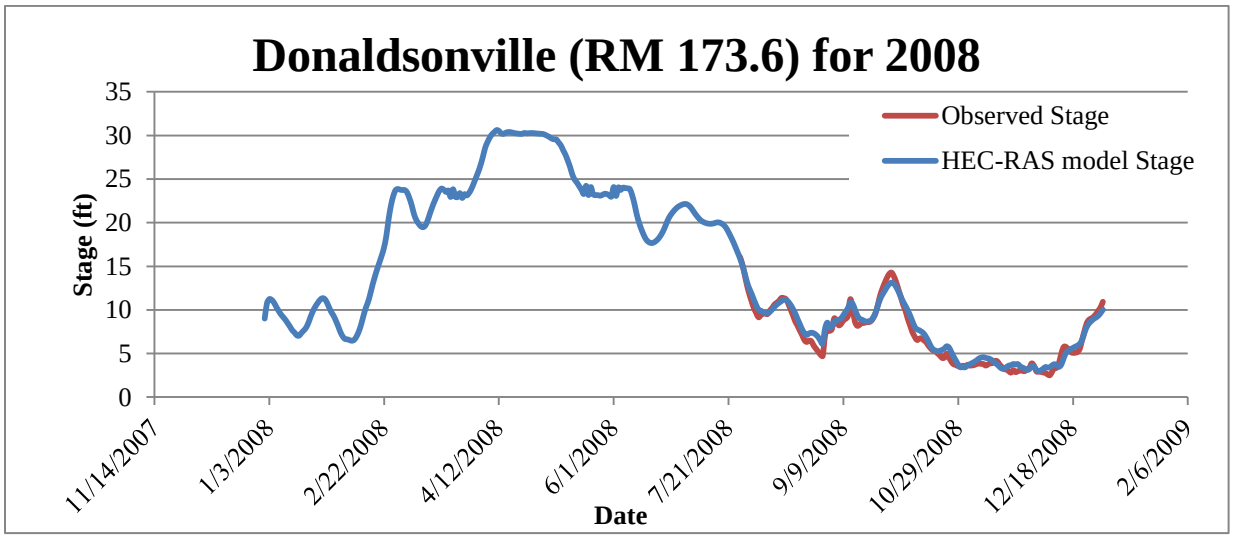

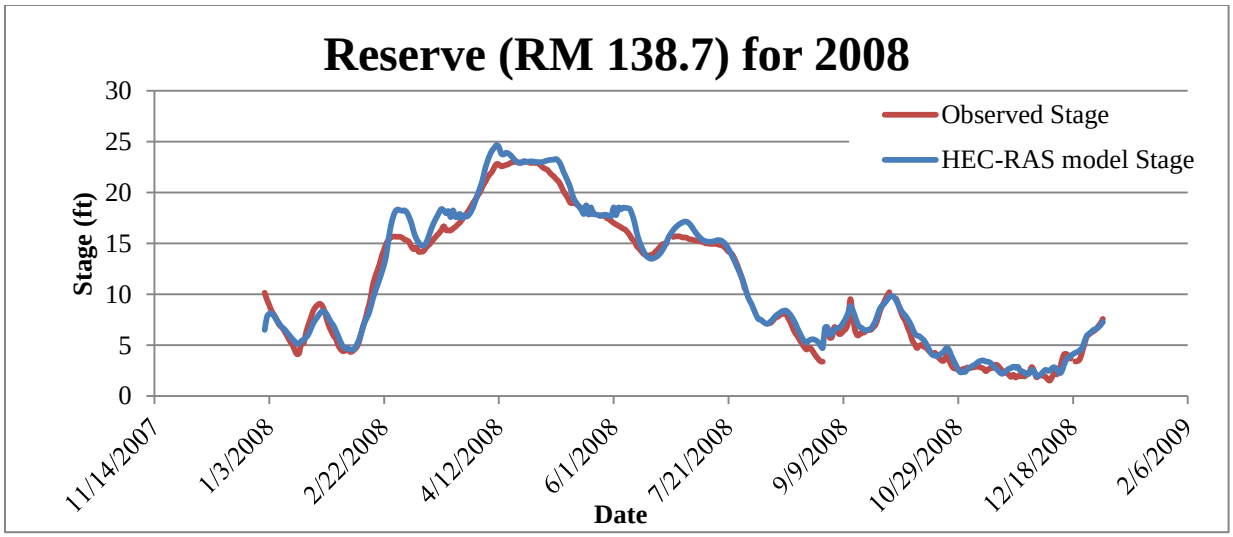
Reserve (RM 138.7) for 2008
Observed Stage
HEC-RAS model Stage
Stage (ft)
30
25
20
15
10
5
0
11/14/2007
1/3/2008
2/22/2008
4/12/2008
6/1/2008
7/21/2008
9/9/2008
10/29/2008
12/18/2008
2/6/2009
Date

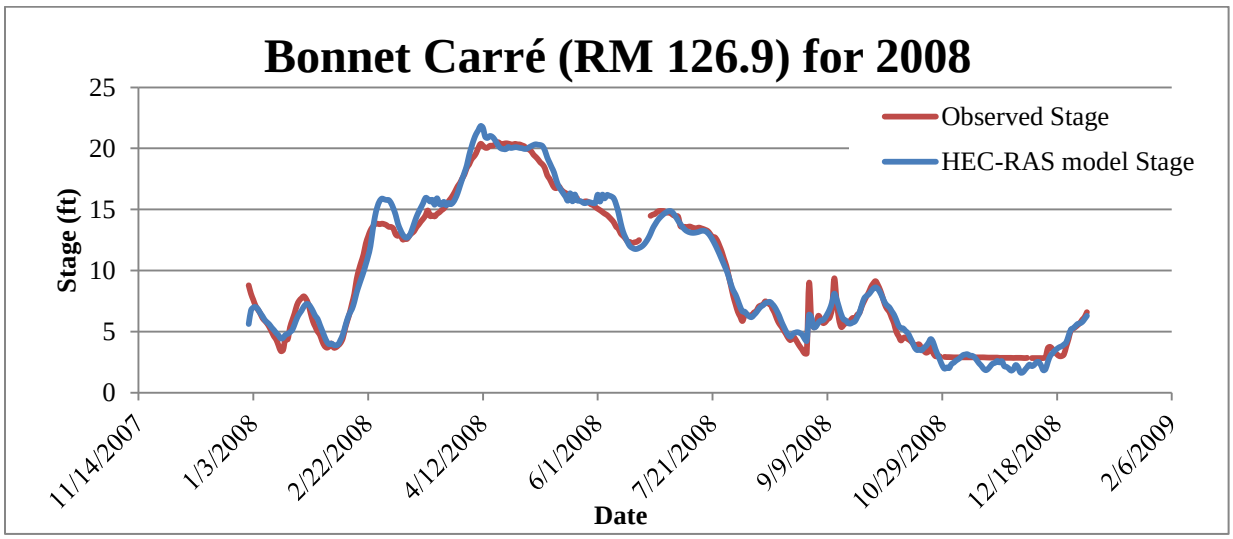
Bonnet Carré (RM 126.9) for 2008
Observed Stage
HEC-RAS model Stage
Stage (ft)
25
20
15
10
5
0
11/14/2007
1/3/2008
2/22/2008
4/12/2008
6/1/2008
7/21/2008
9/9/2008
10/29/2008
12/18/2008
2/6/2009
Date

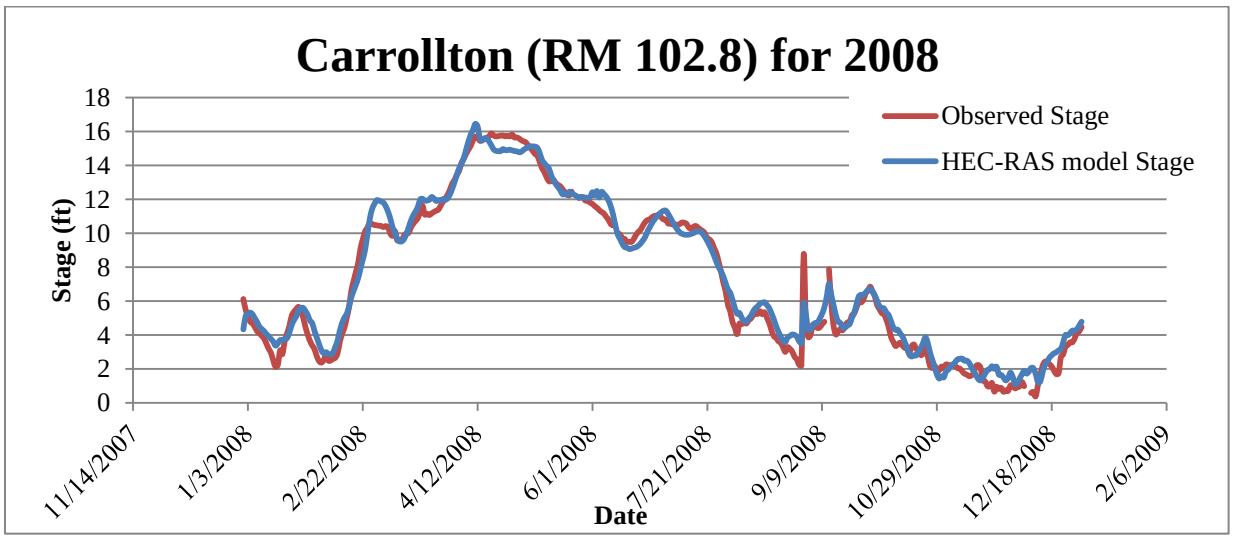
Carrollton (RM 102.8) for 2008
Observed Stage
HEC-RAS model Stage
Stage (ft)
18
16
14
12
10
8
6
4
2
0
11/14/2007
1/3/2008
2/22/2008
4/12/2008
6/1/2008
7/21/2008
9/9/2008
10/29/2008
12/18/2008
2/6/2009
Date

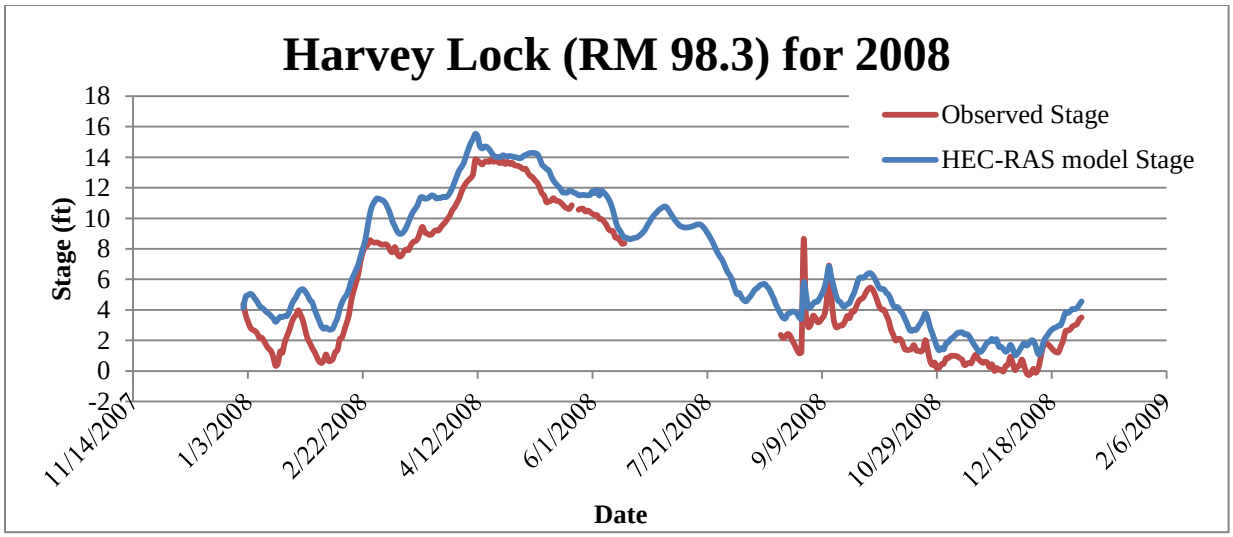
Harvey Lock (RM 98.3) for 2008
Observed Stage
HEC-RAS model Stage
Stage (ft)
18
16
14
12
10
8
6
4
2
0
-2
11/14/2007
1/3/2008
2/22/2008
4/12/2008
6/1/2008
7/21/2008
9/9/2008
10/29/2008
12/18/2008
2/6/2009
Date

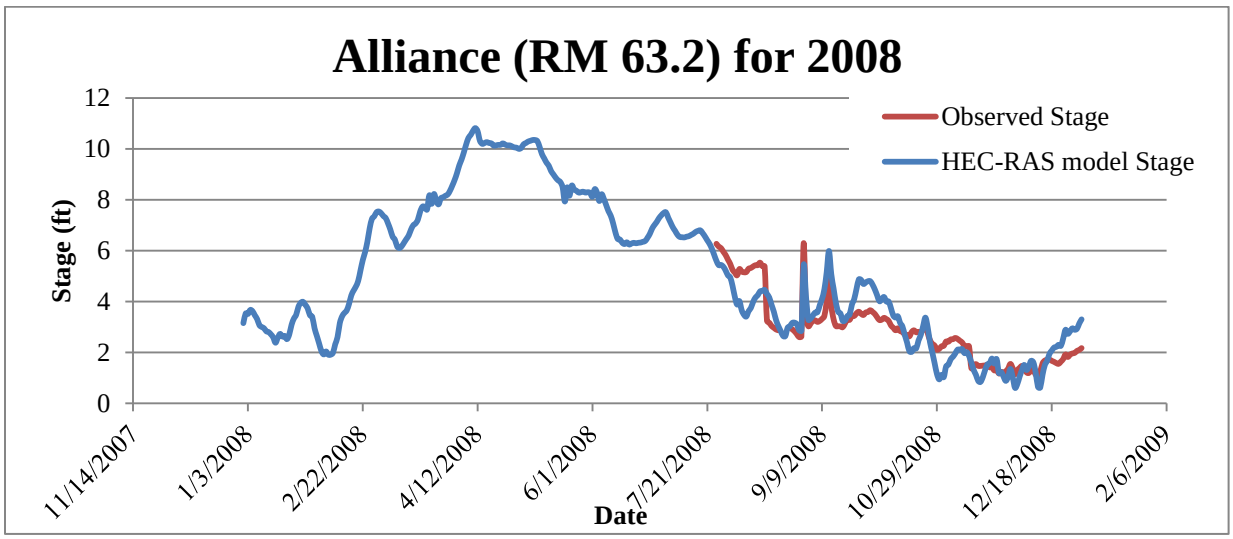
Alliance (RM 63.2) for 2008
Observed Stage
HEC-RAS model Stage
Stage (ft)
12
10
8
6
4
2
0
11/14/2007
1/3/2008
2/22/2008
4/12/2008
6/1/2008
7/21/2008
9/9/2008
10/29/2008
12/18/2008
2/6/2009
Date

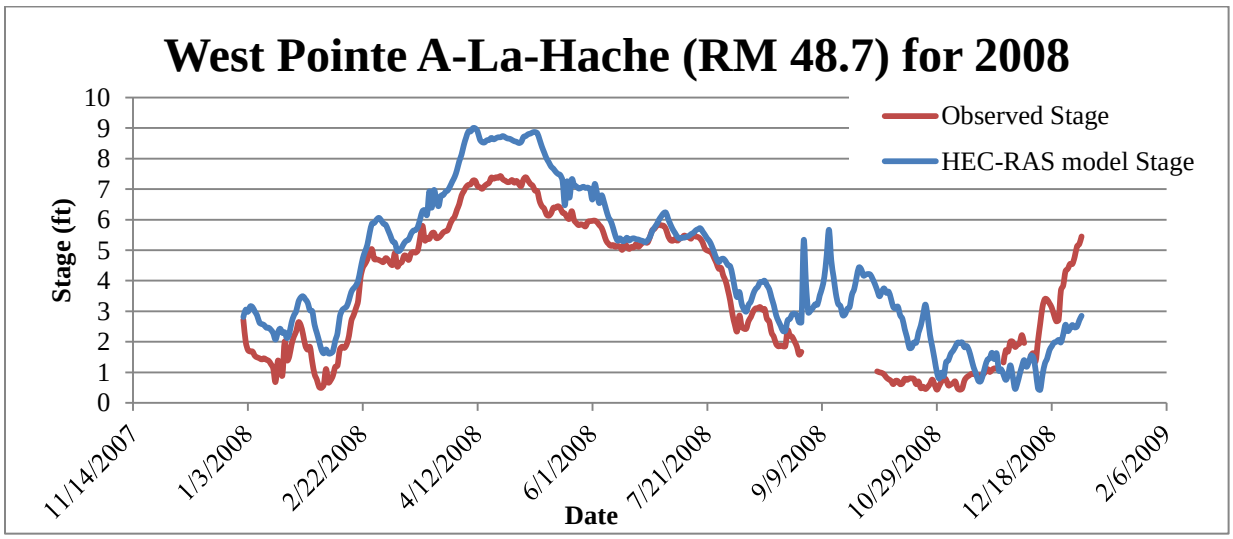
West Pointe A-La-Hache (RM 48.7) for 2008
Observed Stage
HEC-RAS model Stage
Stage (ft)
10
9
8
7
6
5
4
3
2
1
0
11/14/2007
1/3/2008
2/22/2008
4/12/2008
6/1/2008
7/21/2008
9/9/2008
10/29/2008
12/18/2008
2/6/2009
Date

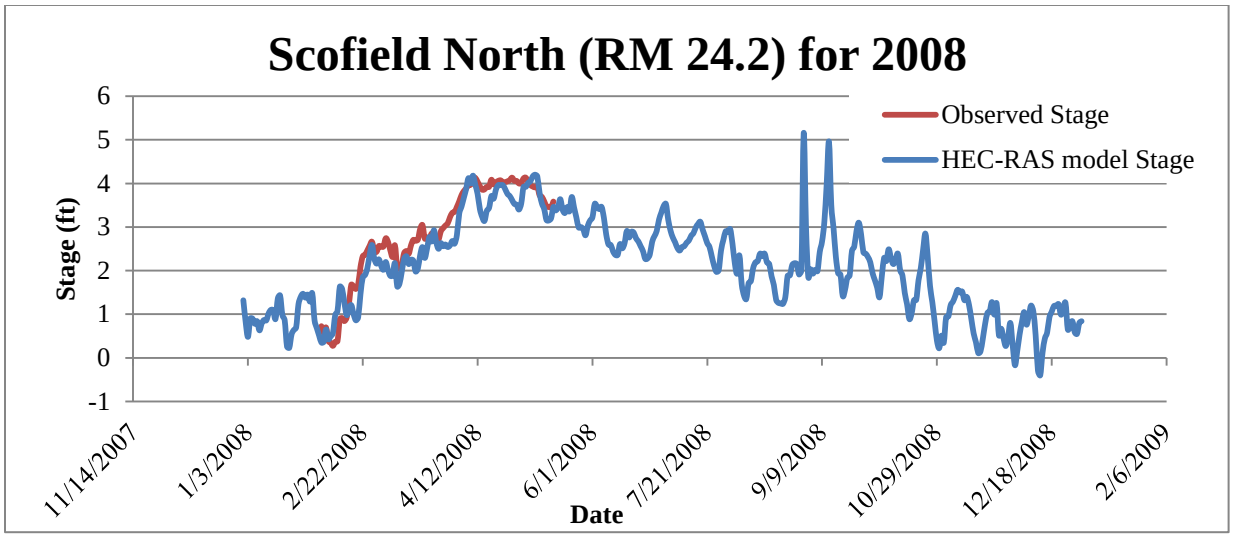
Scofield North (RM 24.2) for 2008
Observed Stage
HEC-RAS model Stage
Stage (ft)
6
5
4
3
2
1
0
-1
11/14/2007
1/3/2008
2/22/2008
4/12/2008
6/1/2008
7/21/2008
9/9/2008
10/29/2008
12/18/2008
2/6/2009
Date

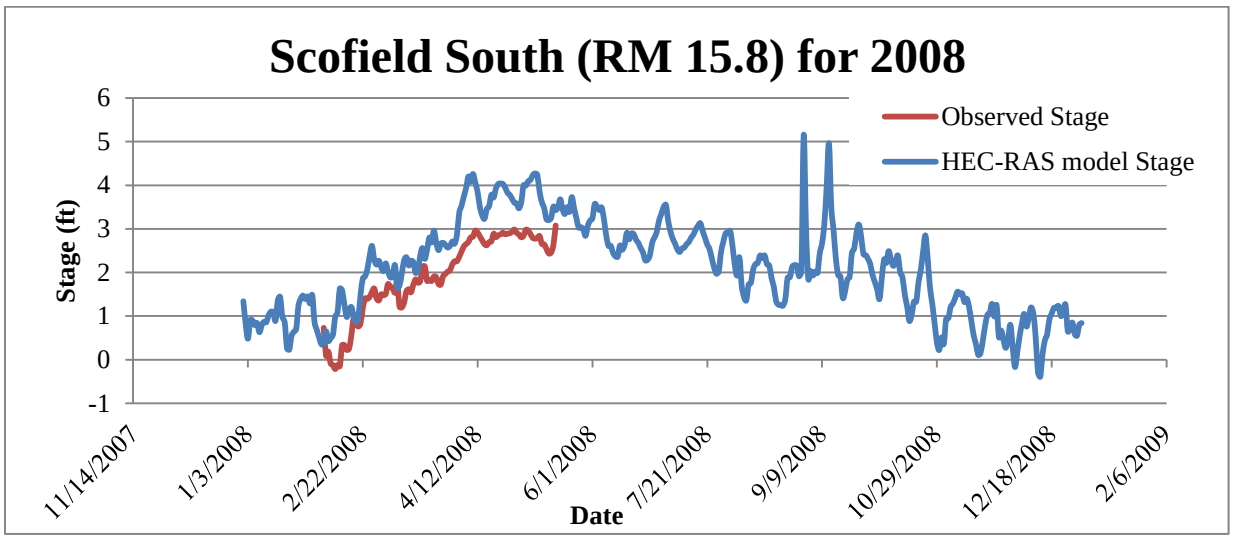
Scofield South (RM 15.8) for 2008
Observed Stage
HEC-RAS model Stage
Stage (ft)
6
5
4
3
2
1
0
-1
11/14/2007
1/3/2008
2/22/2008
4/12/2008
6/1/2008
7/21/2008
9/9/2008
10/29/2008
12/18/2008
2/6/2009
Date

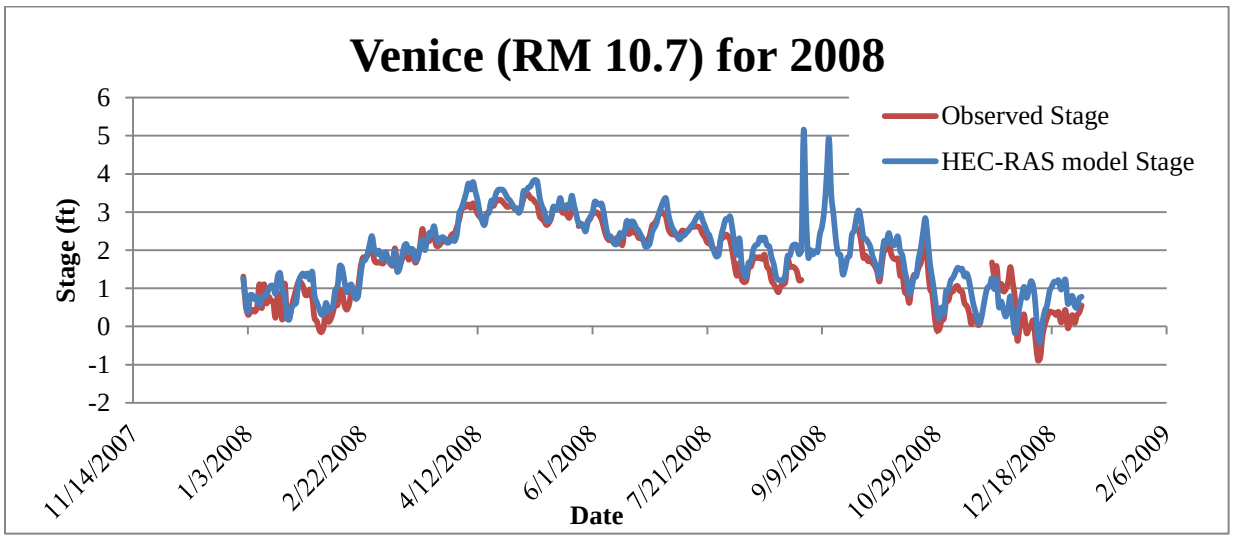
Venice (RM 10.7) for 2008
Observed Stage
HEC-RAS model Stage
Stage (ft)
6
5
4
3
2
1
0
-1
-2
11/14/2007
1/3/2008
2/22/2008
4/12/2008
6/1/2008
7/21/2008
9/9/2008
10/29/2008
12/18/2008
2/6/2009
Date

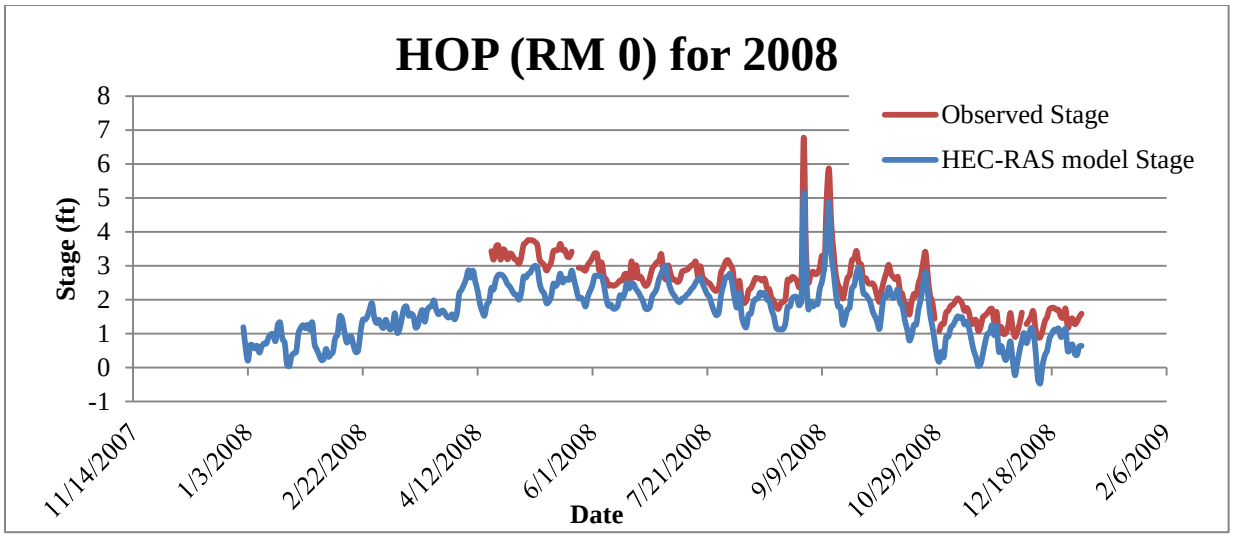
HOP (RM 0) for 2008
Observed Stage
HEC-RAS model Stage
Stage (ft)
8
7
6
5
4
3
2
1
0
-1
11/14/2007
1/3/2008
2/22/2008
4/12/2008
6/1/2008
7/21/2008
9/9/2008
10/29/2008
12/18/2008
2/6/2009
Date

Validation Results (2009):

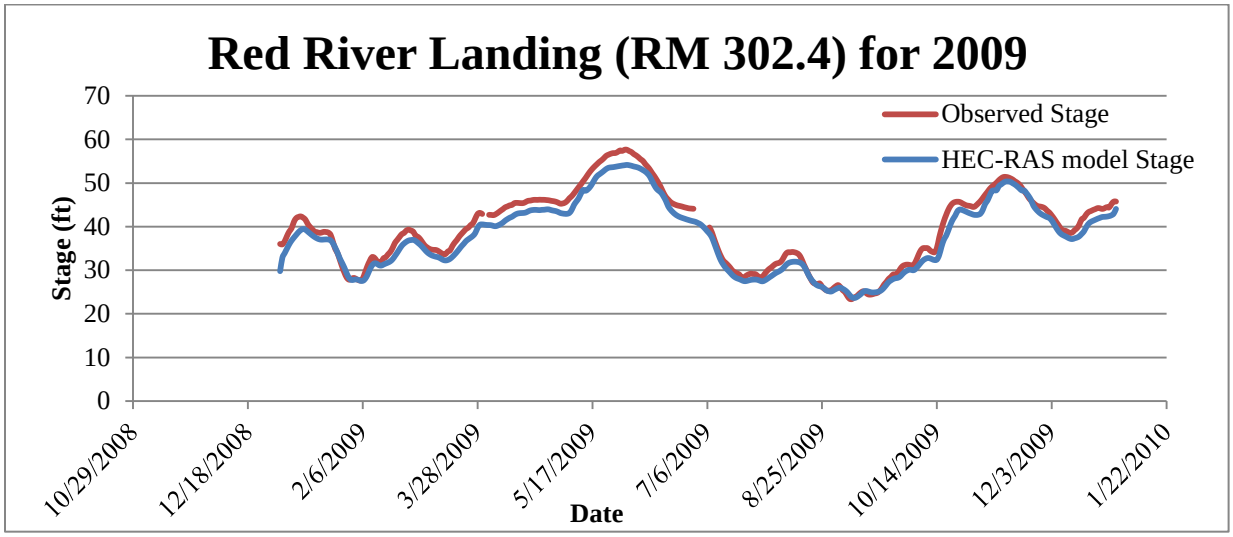

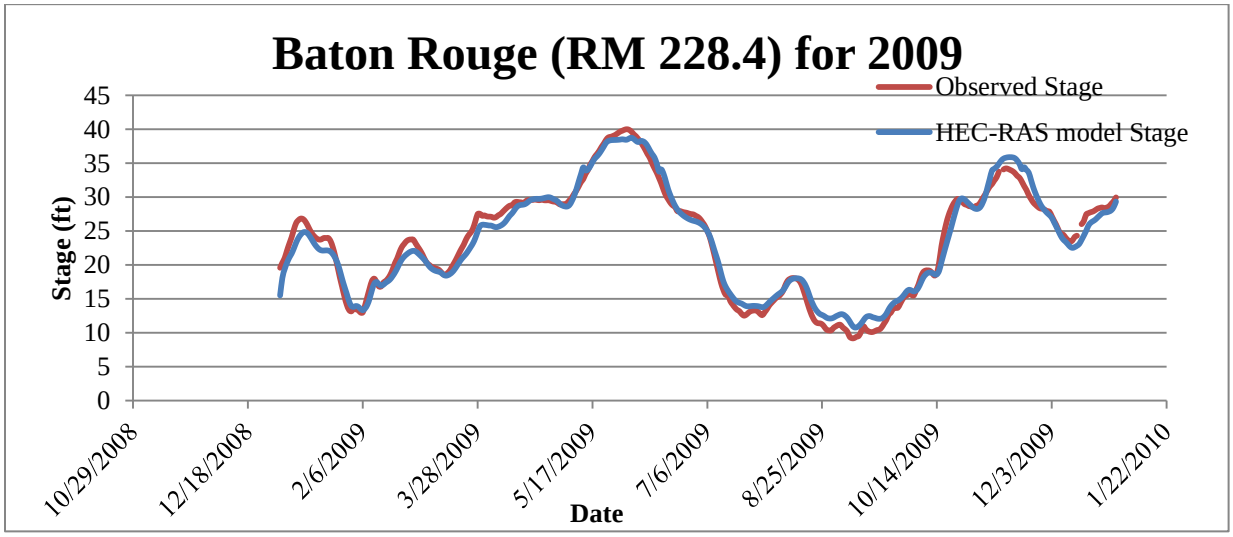

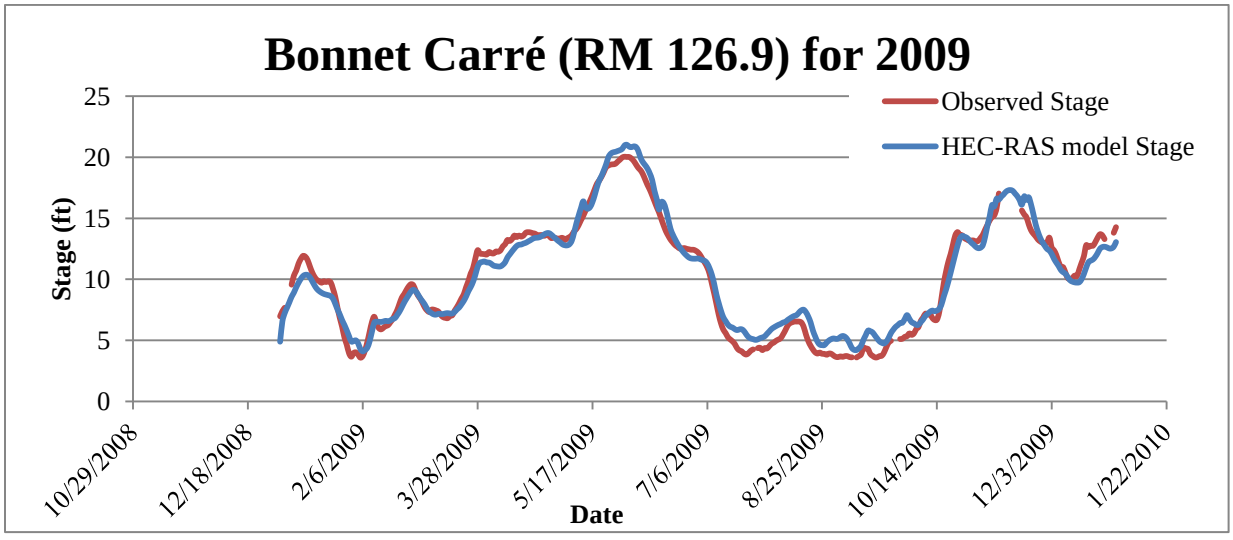

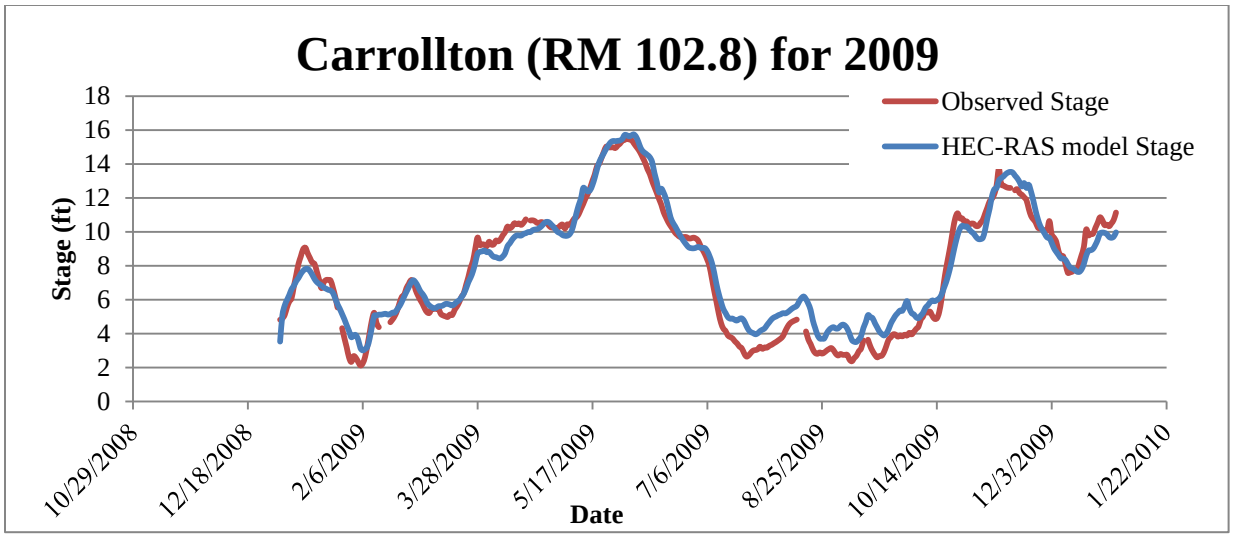
Carrollton (RM 102.8) for 2009
Observed Stage
HEC-RAS model Stage
Stage (ft)
0
2
4
6
8
10
12
14
16
18
10/29/2008
12/18/2008
2/6/2009
3/28/2009
5/17/2009
7/6/2009
8/25/2009
10/14/2009
12/3/2009
1/22/2010
Date

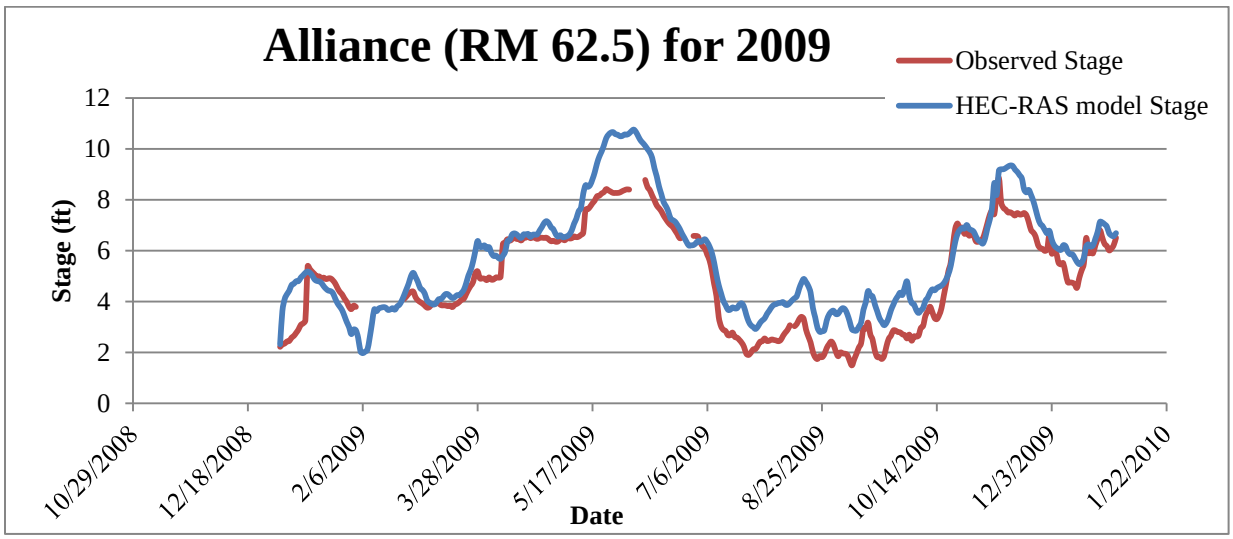
Alliance (RM 62.5) for 2009
Observed Stage
HEC-RAS model Stage
Stage (ft)
0
2
4
6
8
10
12
10/29/2008
12/18/2008
2/6/2009
3/28/2009
5/17/2009
7/6/2009
8/25/2009
10/14/2009
12/3/2009
1/22/2010
Date

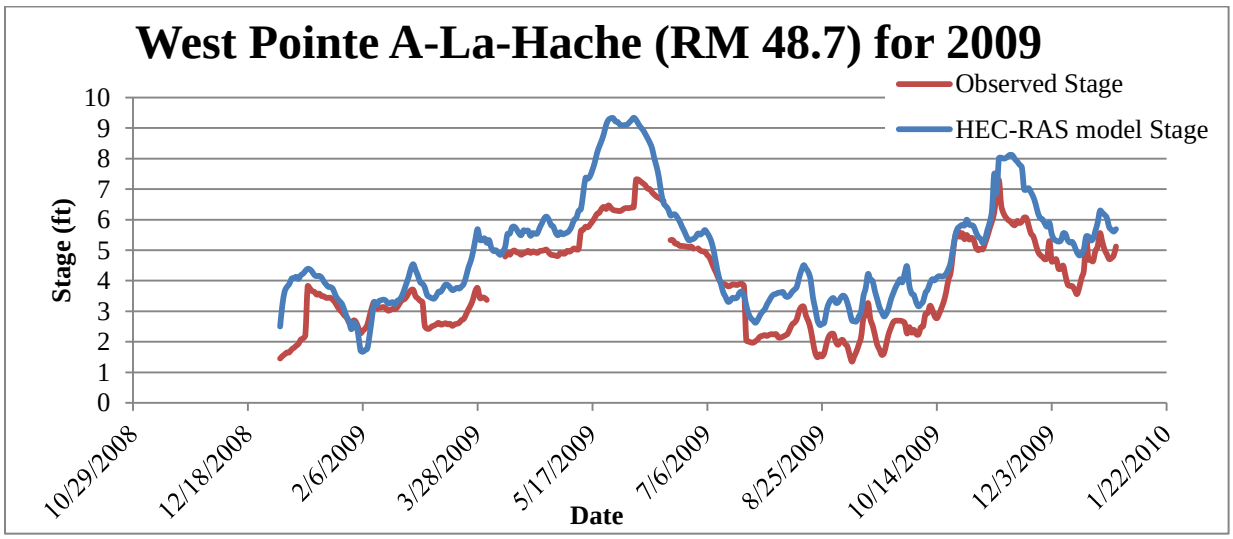
West Pointe A-La-Hache (RM 48.7) for 2009
Observed Stage
HEC-RAS model Stage
Stage (ft)
0
1
2
3
4
5
6
7
8
9
10
10/29/2008
12/18/2008
2/6/2009
3/28/2009
5/17/2009
7/6/2009
8/25/2009
10/14/2009
12/3/2009
1/22/2010
Date

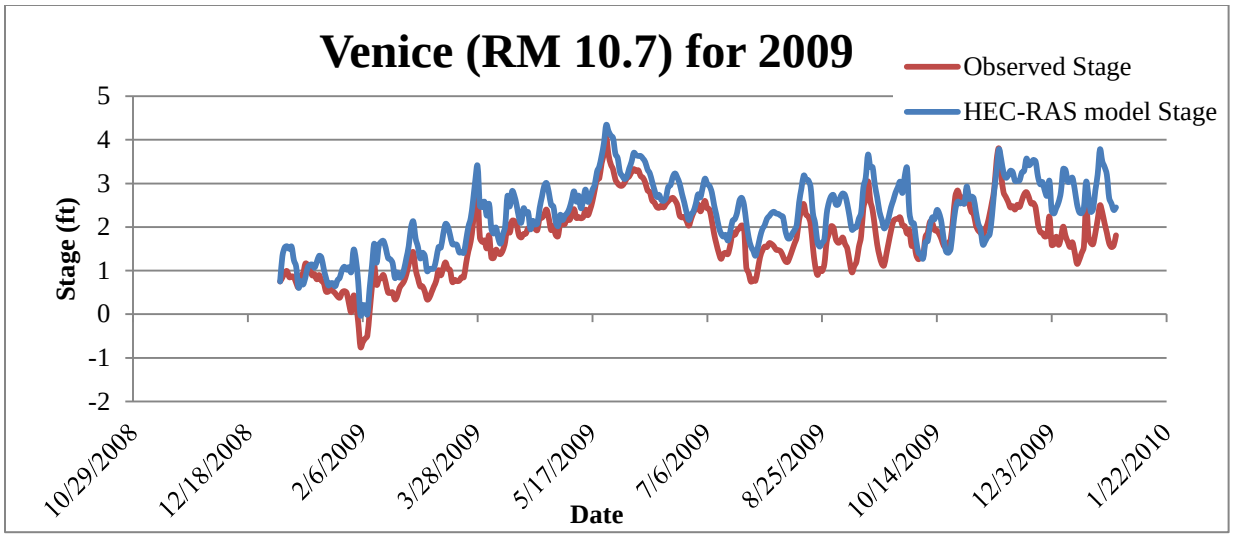
Venice (RM 10.7) for 2009
Observed Stage
HEC-RAS model Stage
Stage (ft)
5
4
3
2
1
0
-1
-2
10/29/2008
12/18/2008
2/6/2009
3/28/2009
5/17/2009
7/6/2009
8/25/2009
10/14/2009
12/3/2009
1/22/2010
Date

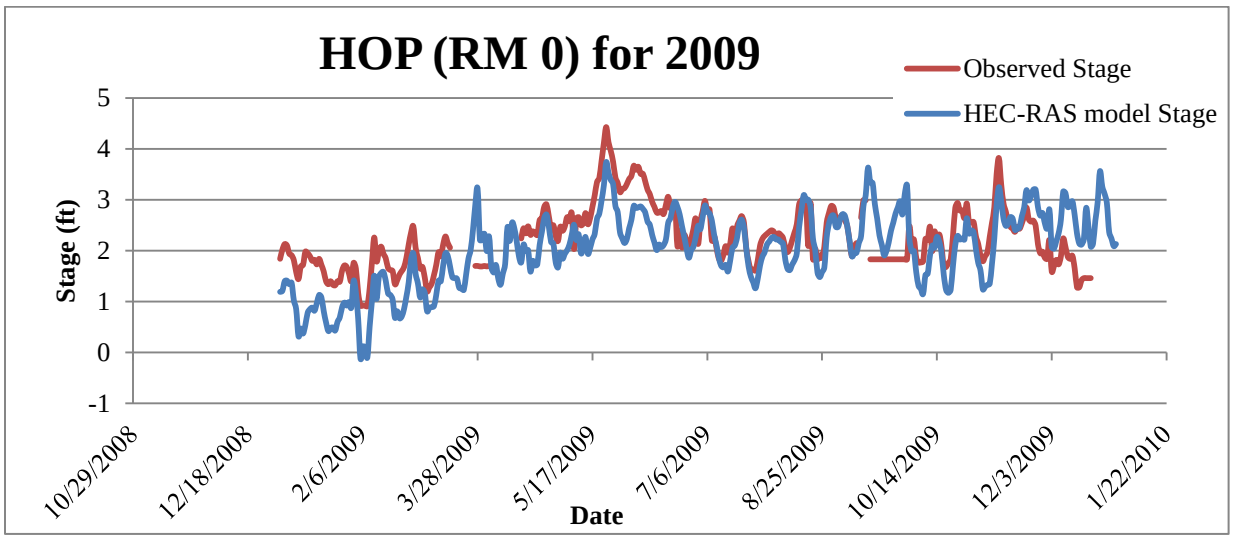
HOP (RM 0) for 2009
Observed Stage
HEC-RAS model Stage
Stage (ft)
5
4
3
2
1
0
-1
10/29/2008
12/18/2008
2/6/2009
3/28/2009
5/17/2009
7/6/2009
8/25/2009
10/14/2009
12/3/2009
1/22/2010
Date

Validation Results (2010):

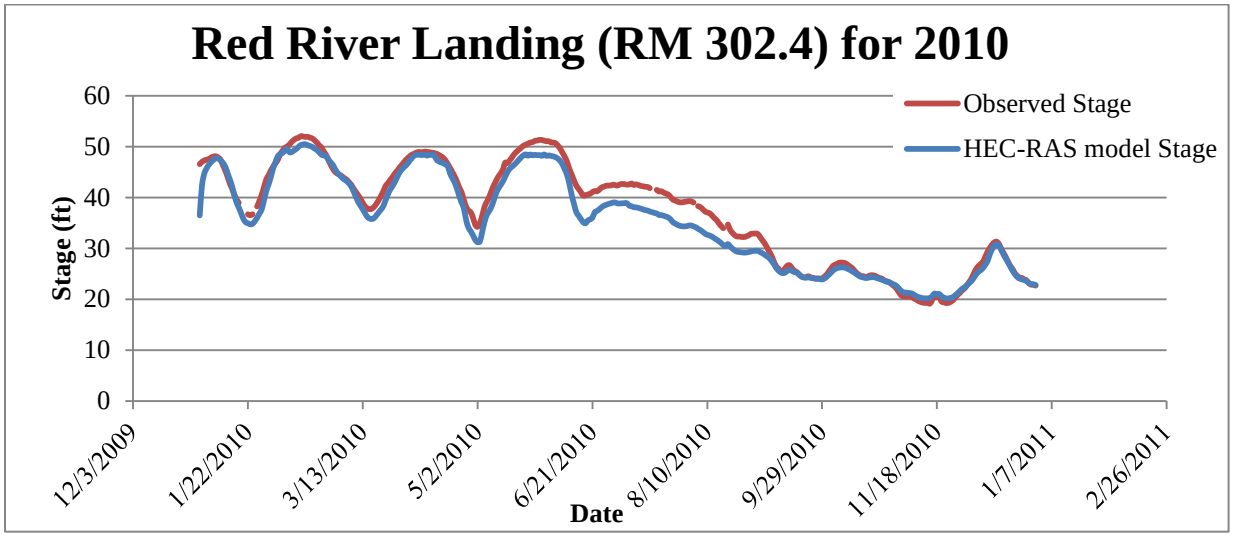

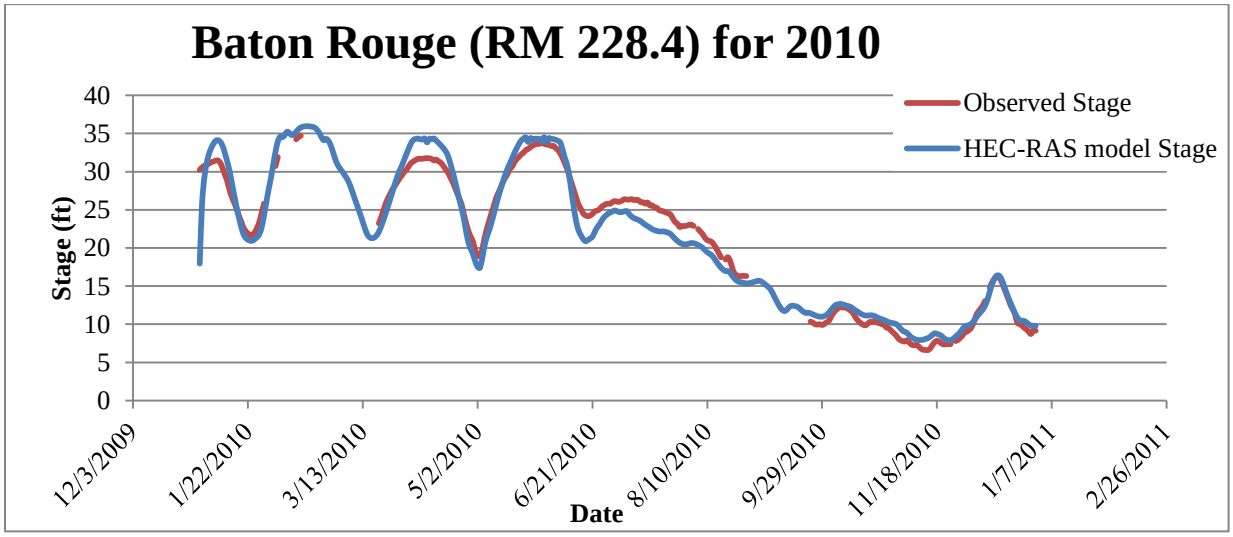

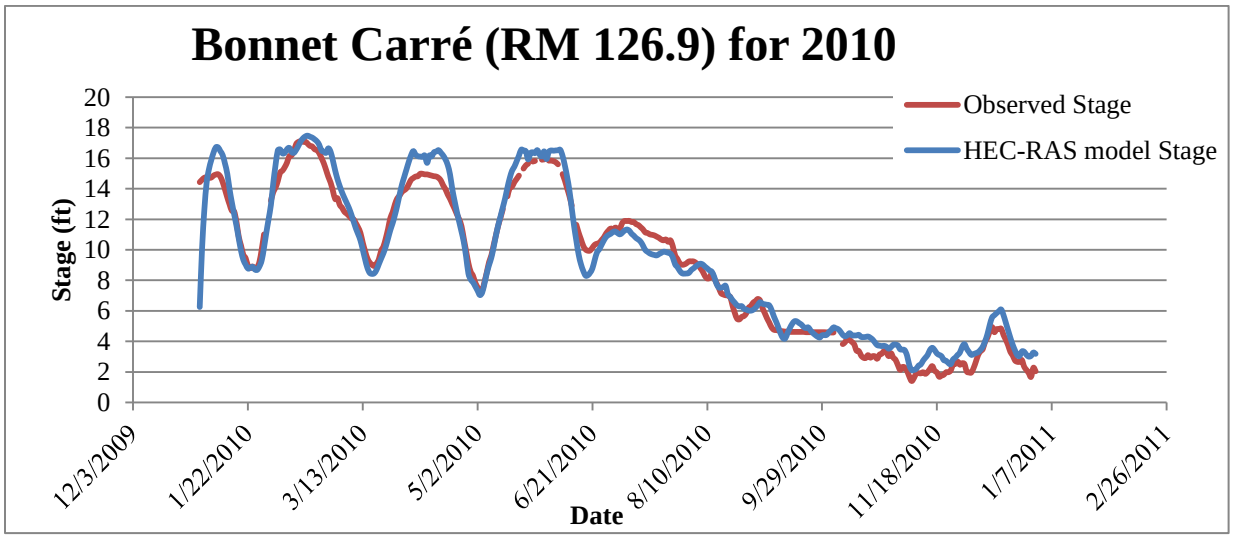

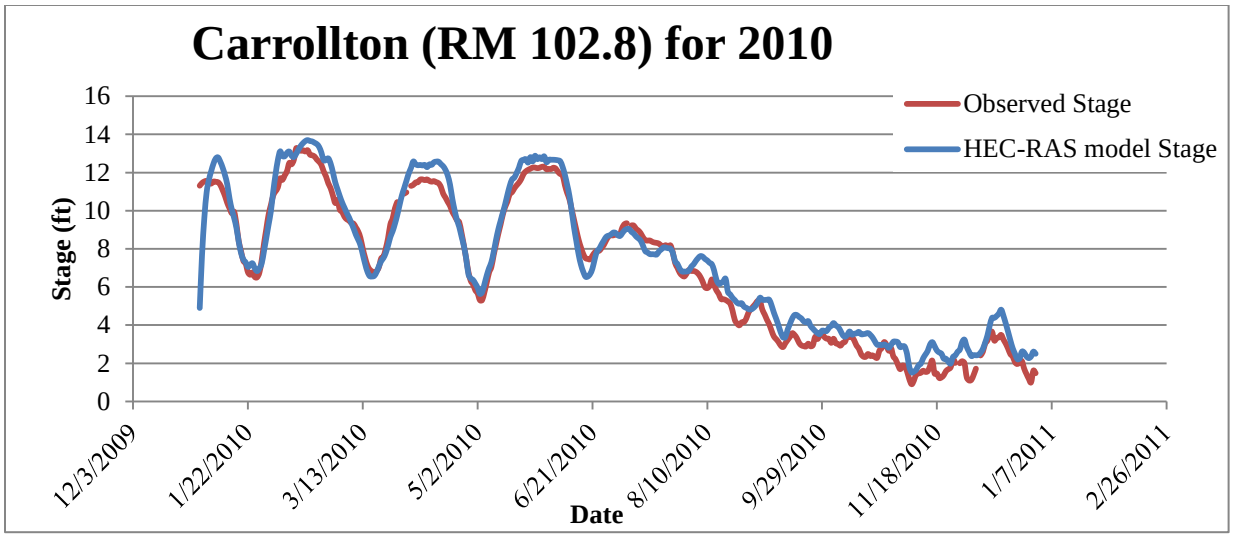
Carrollton (RM 102.8) for 2010
Observed Stage
HEC-RAS model Stage
Stage (ft)
0
2
4
6
8
10
12
14
16
12/3/2009
1/22/2010
3/13/2010
5/2/2010
6/21/2010
8/10/2010
9/29/2010
11/18/2010
1/7/2011
2/26/2011
Date

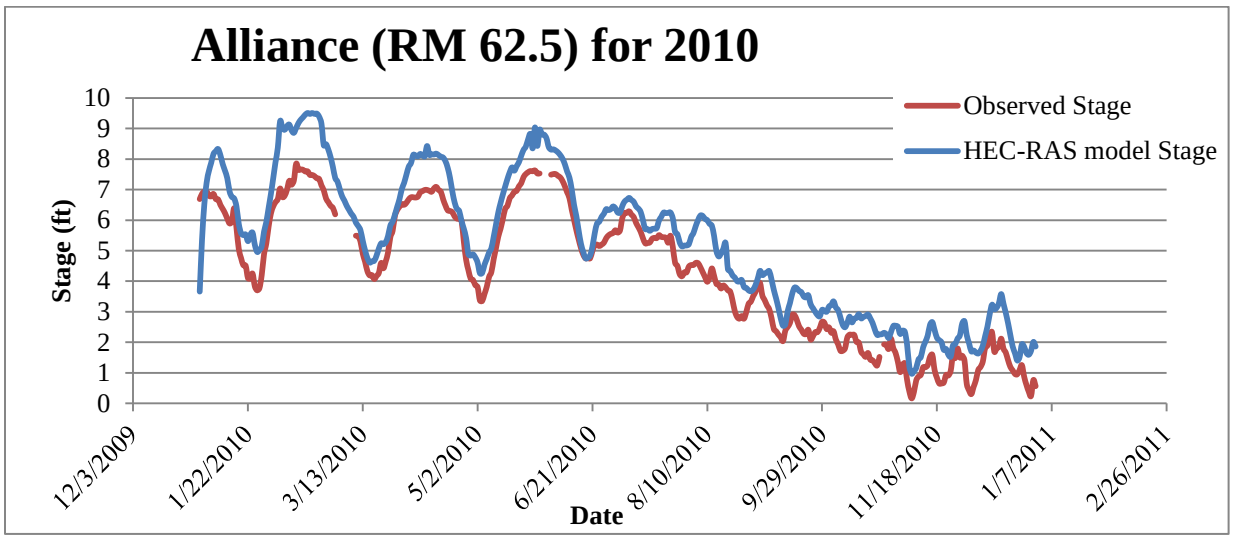
Alliance (RM 62.5) for 2010
Observed Stage
HEC-RAS model Stage
Stage (ft)
0
1
2
3
4
5
6
7
8
9
10
12/3/2009
1/22/2010
3/13/2010
5/2/2010
6/21/2010
8/10/2010
9/29/2010
11/18/2010
1/7/2011
2/26/2011
Date

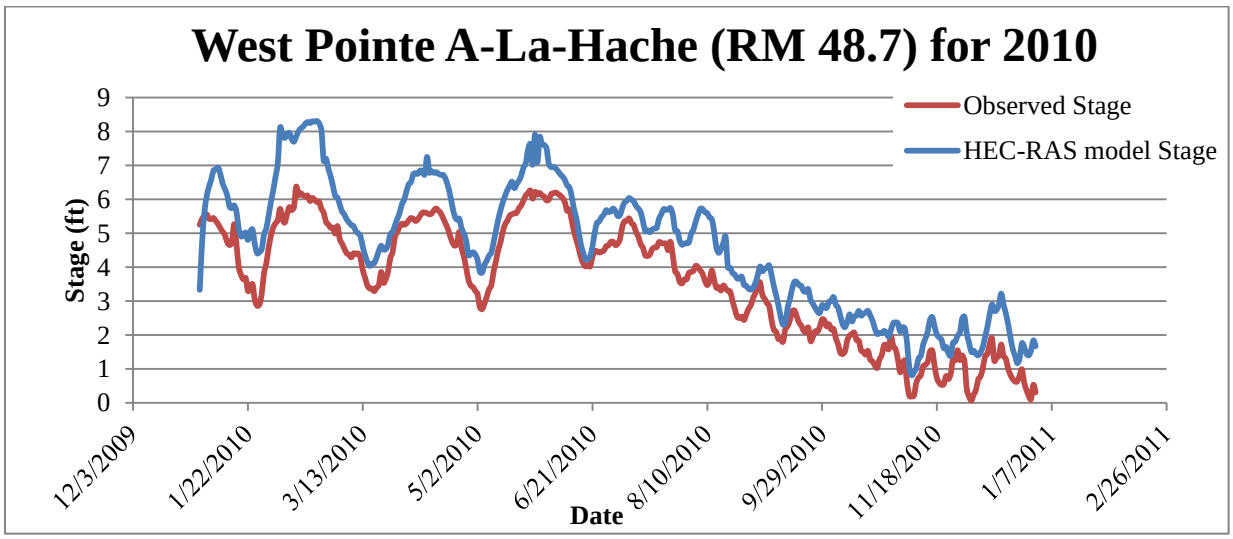
West Pointe A-La-Hache (RM 48.7) for 2010
Observed Stage
HEC-RAS model Stage
Stage (ft)
0
1
2
3
4
5
6
7
8
9
12/3/2009
1/22/2010
3/13/2010
5/2/2010
6/21/2010
8/10/2010
9/29/2010
11/18/2010
1/7/2011
2/26/2011
Date

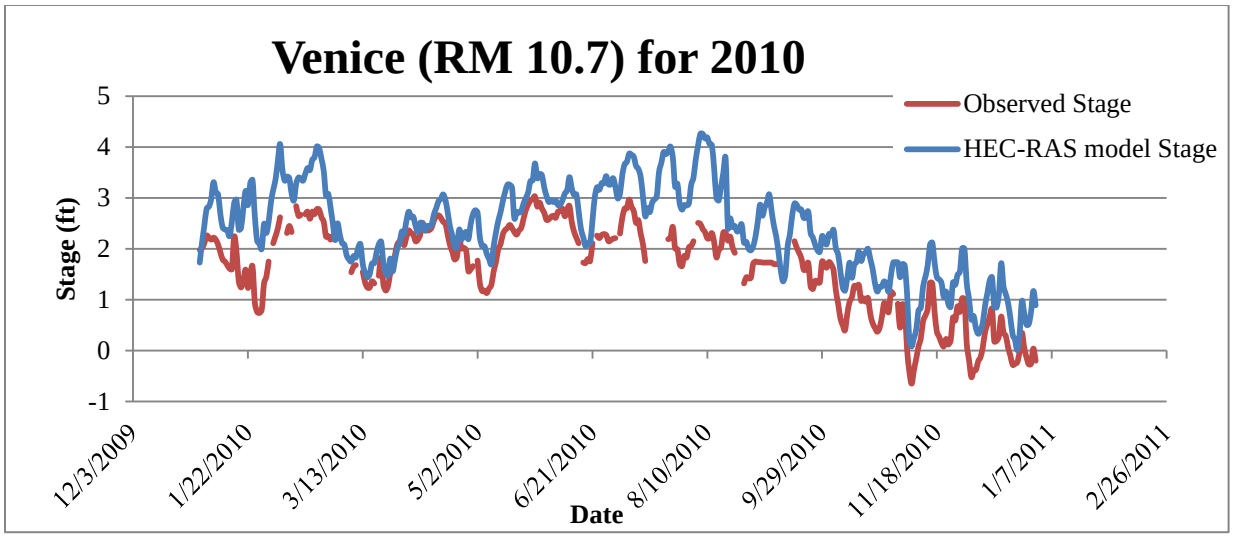
Venice (RM 10.7) for 2010
Observed Stage
HEC-RAS model Stage
Stage (ft)
5
4
3
2
1
0
-1
12/3/2009
1/22/2010
3/13/2010
5/2/2010
6/21/2010
8/10/2010
9/29/2010
11/18/2010
1/7/2011
2/26/2011
Date

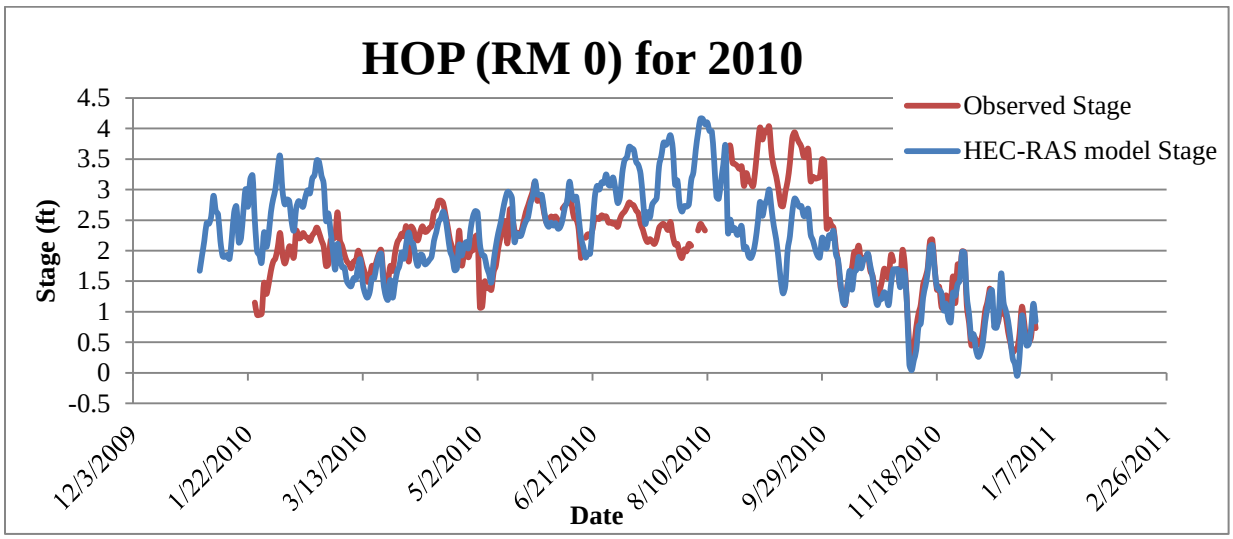
HOP (RM 0) for 2010
Observed Stage
HEC-RAS model Stage
Stage (ft)
4.5
4
3.5
3
2.5
2
1.5
1
0.5
0
-0.5
12/3/2009
1/22/2010
3/13/2010
5/2/2010
6/21/2010
8/10/2010
9/29/2010
11/18/2010
1/7/2011
2/26/2011
Date

Validation Results (2012):

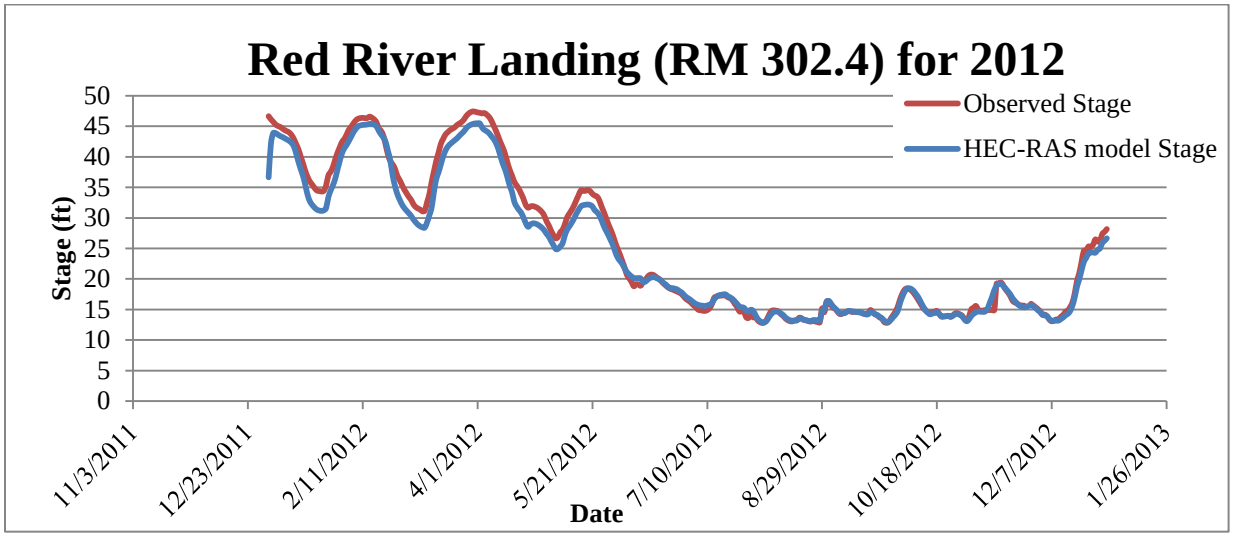

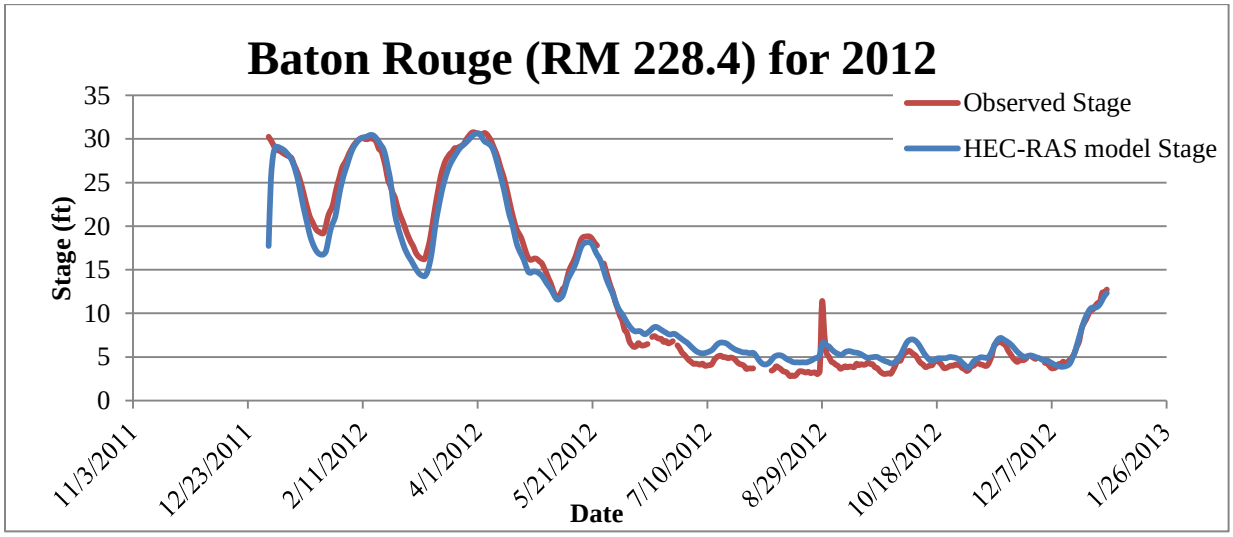

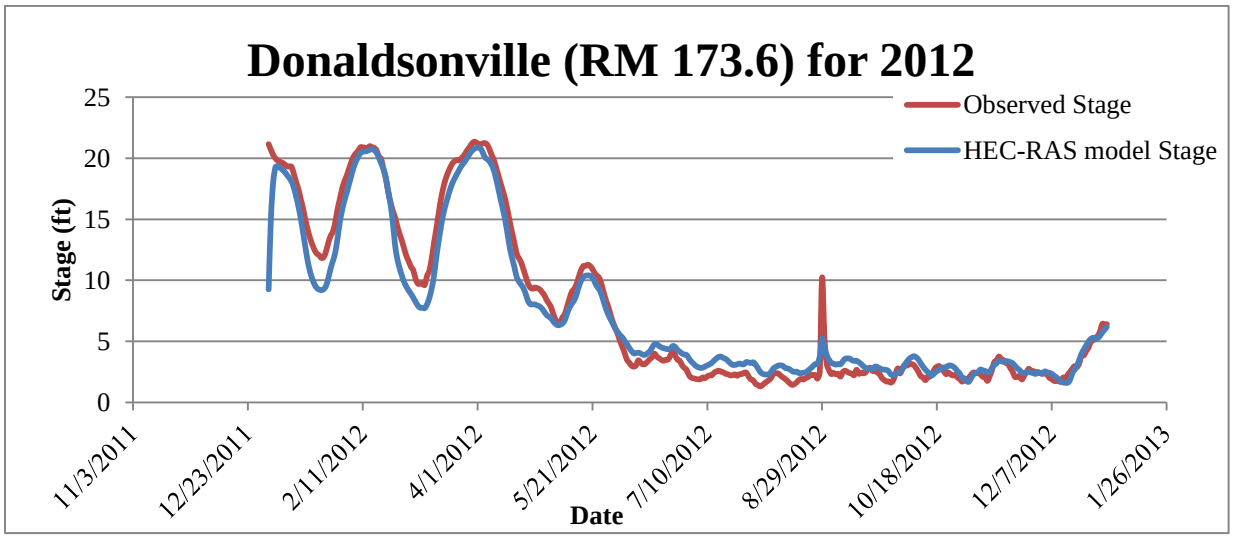

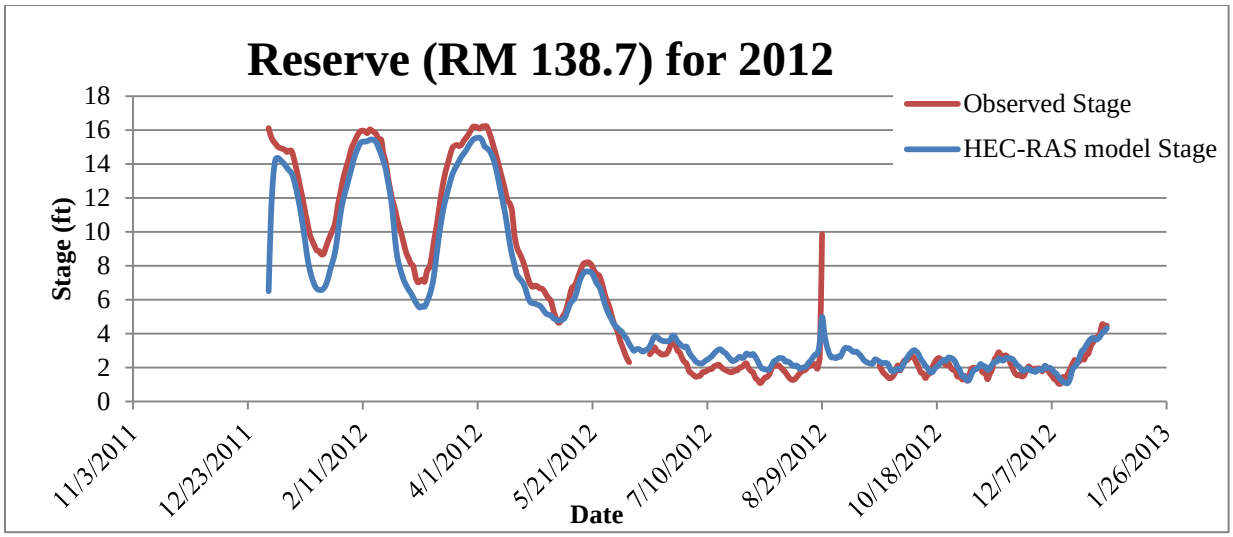
Reserve (RM 138.7) for 2012
Observed Stage
HEC-RAS model Stage
Stage (ft)
0
2
4
6
8
10
12
14
16
18
11/3/2011
12/23/2011
2/11/2012
4/1/2012
5/21/2012
7/10/2012
8/29/2012
10/18/2012
12/7/2012
1/26/2013
Date

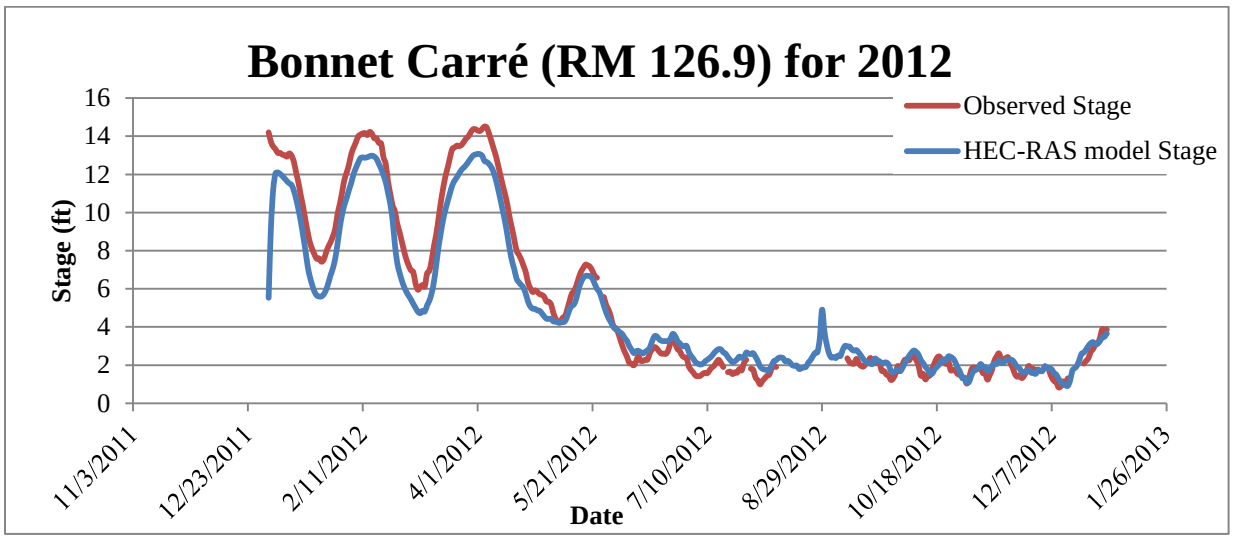
Bonnet Carré (RM 126.9) for 2012
Observed Stage
HEC-RAS model Stage
Stage (ft)
0
2
4
6
8
10
12
14
16
11/3/2011
12/23/2011
2/11/2012
4/1/2012
5/21/2012
7/10/2012
8/29/2012
10/18/2012
12/7/2012
1/26/2013
Date

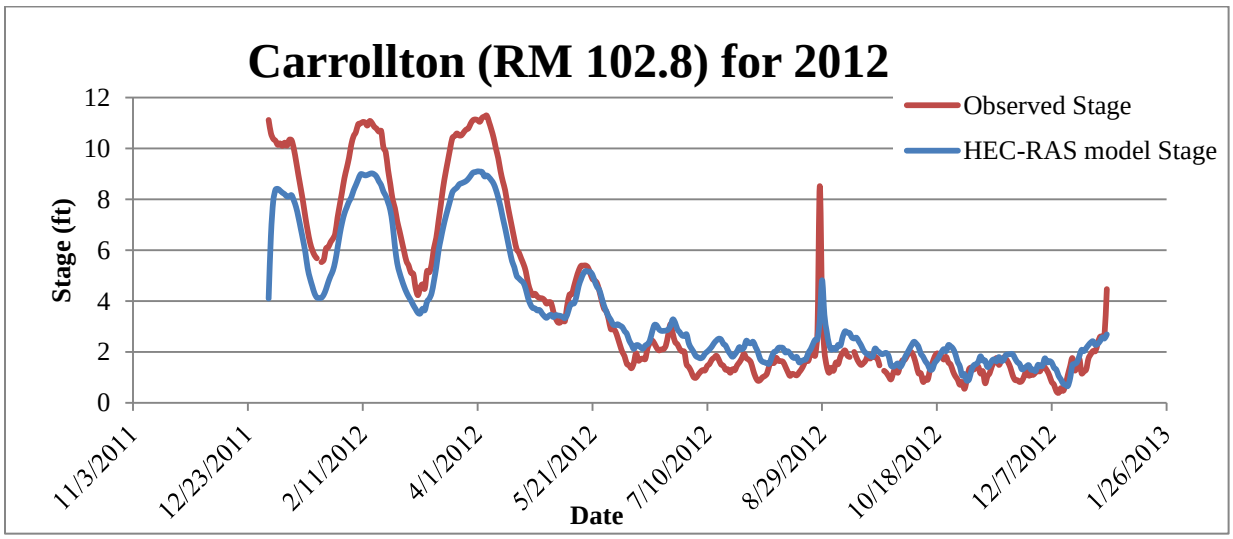
Carrollton (RM 102.8) for 2012
Observed Stage
HEC-RAS model Stage
Stage (ft)
0
2
4
6
8
10
12
11/3/2011
12/23/2011
2/11/2012
4/1/2012
5/21/2012
7/10/2012
8/29/2012
10/18/2012
12/7/2012
1/26/2013
Date

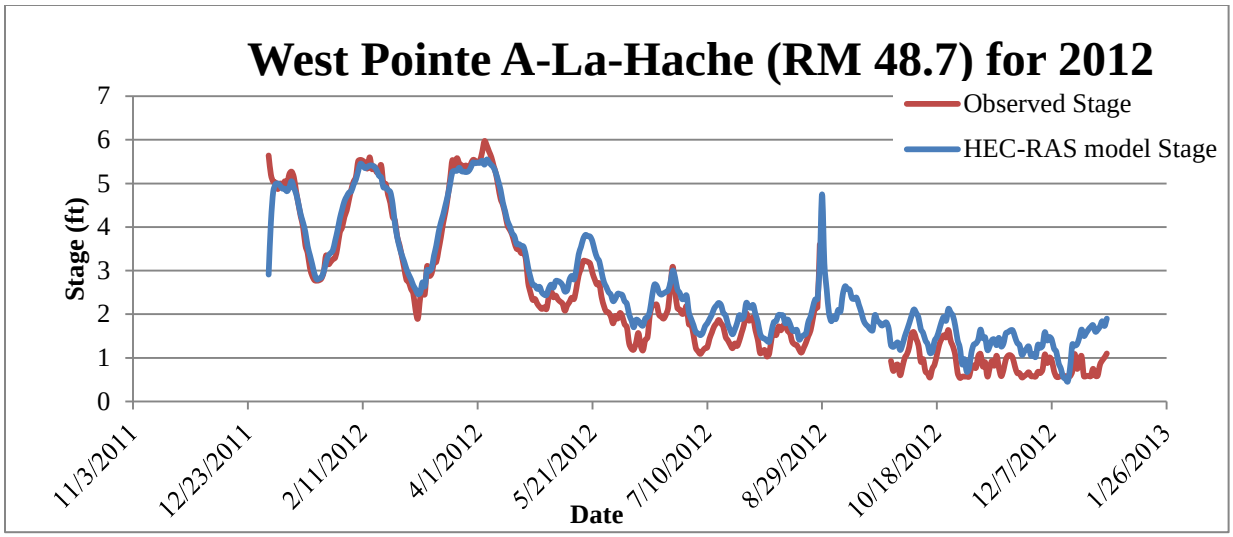
West Pointe A-La-Hache (RM 48.7) for 2012
Observed Stage
HEC-RAS model Stage
Stage (ft)
0
1
2
3
4
5
6
7
11/3/2011
12/23/2011
2/11/2012
4/1/2012
5/21/2012
7/10/2012
8/29/2012
10/18/2012
12/7/2012
1/26/2013
Date

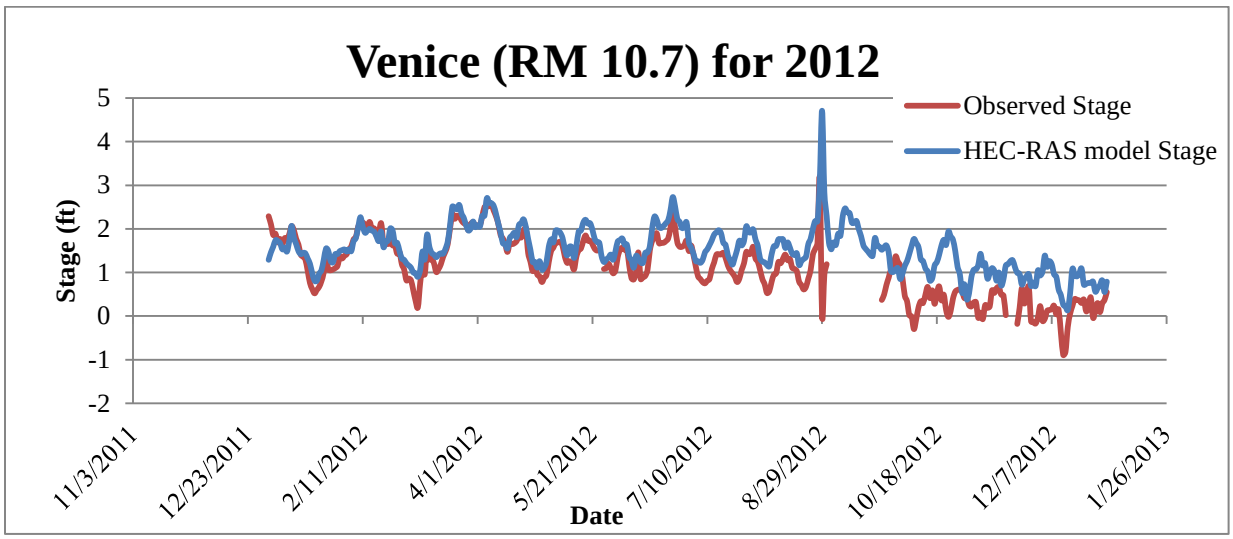
Venice (RM 10.7) for 2012
Observed Stage
HEC-RAS model Stage
Stage (ft)
-2
-1
0
1
2
3
4
5
11/3/2011
12/23/2011
2/11/2012
4/1/2012
5/21/2012
7/10/2012
8/29/2012
10/18/2012
12/7/2012
1/26/2013
Date

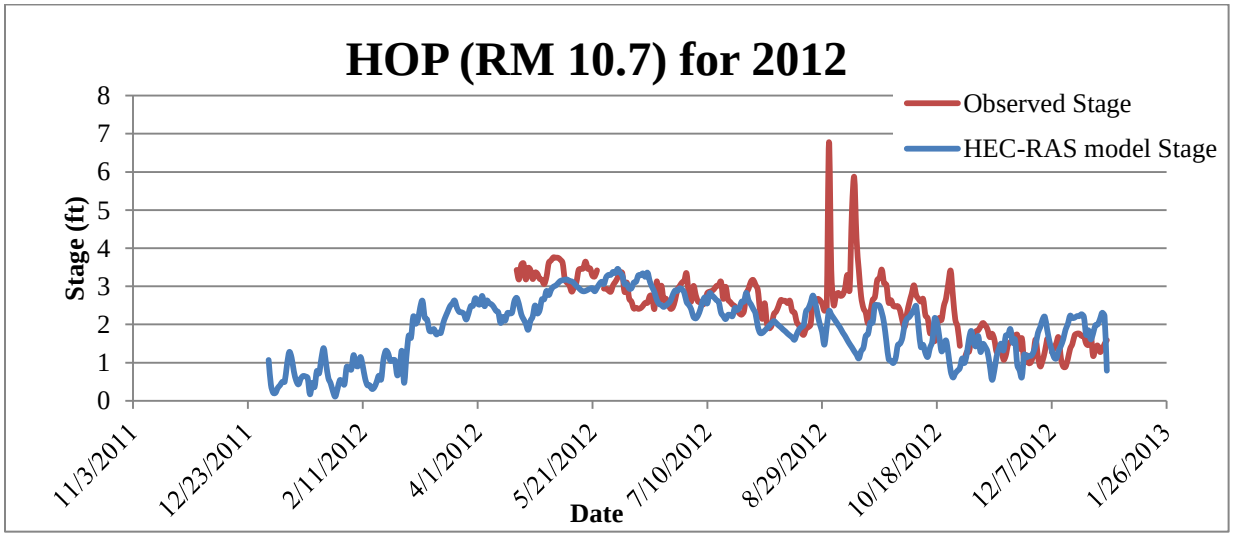
HOP (RM 10.7) for 2012
Observed Stage
HEC-RAS model Stage
Stage (ft)
0
1
2
3
4
5
6
7
8
11/3/2011
12/23/2011
2/11/2012
4/1/2012
5/21/2012
7/10/2012
8/29/2012
10/18/2012
12/7/2012
1/26/2013
Date

Hourly Validation 2008:

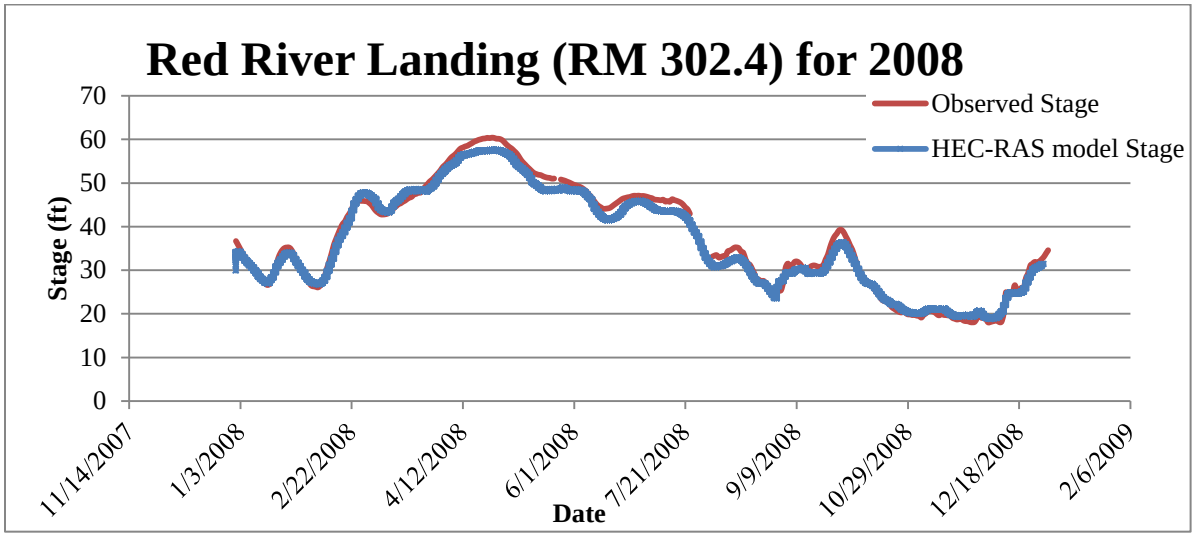

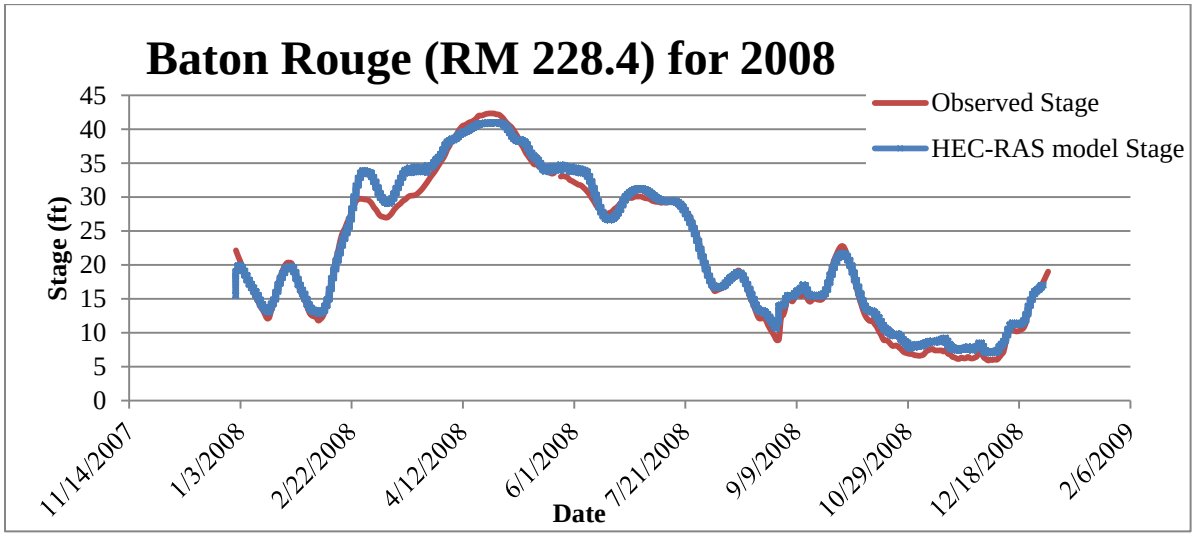

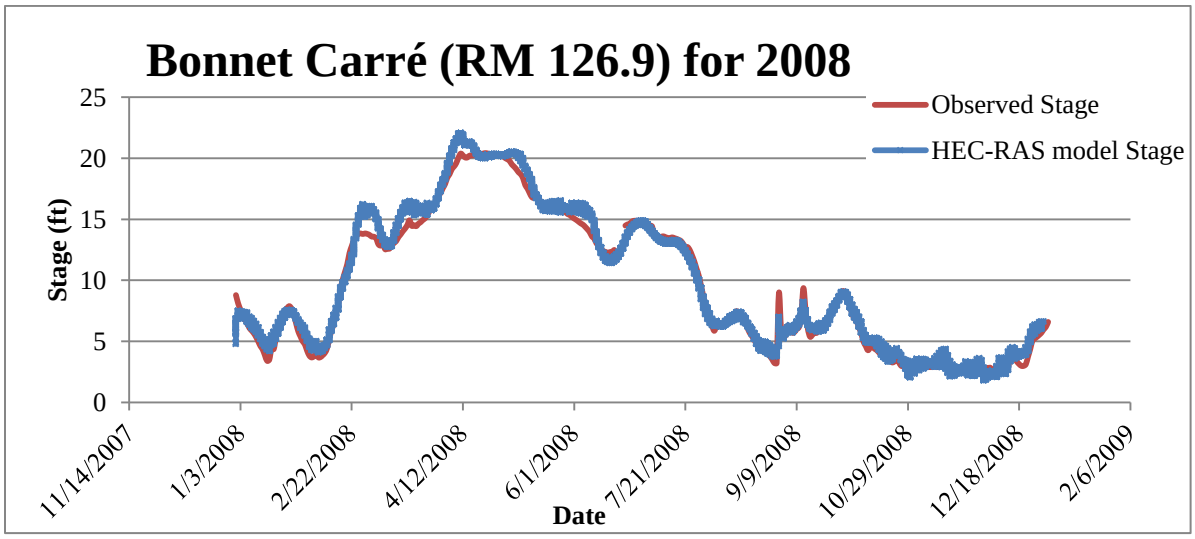

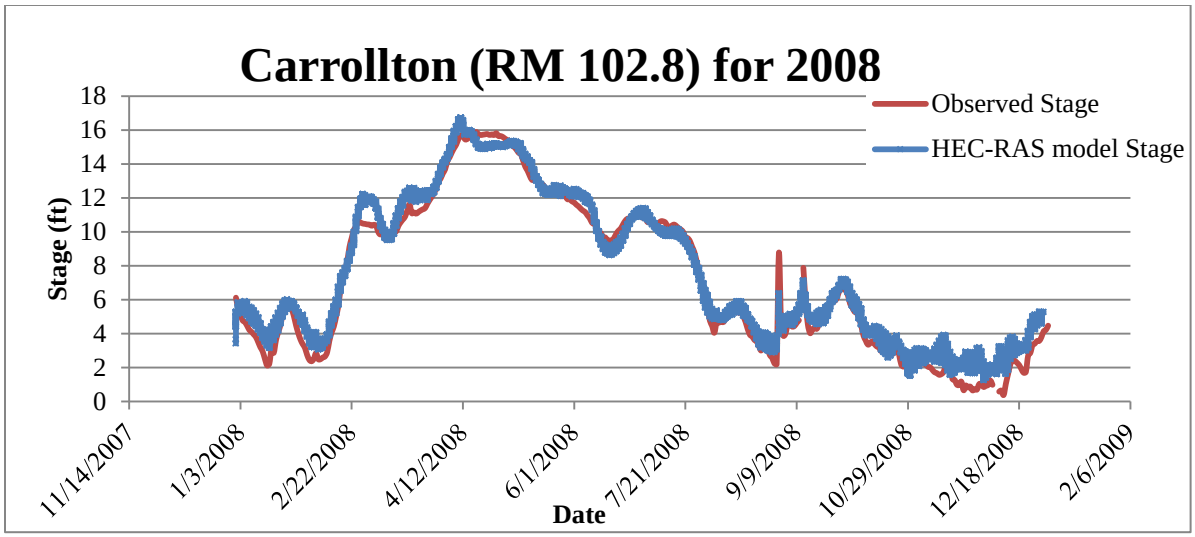
Carrollton (RM 102.8) for 2008
Observed Stage
HEC-RAS model Stage
Stage (ft)
18
16
14
12
10
8
6
4
2
0
11/14/2007
1/3/2008
2/22/2008
4/12/2008
6/1/2008
7/21/2008
9/9/2008
10/29/2008
12/18/2008
2/6/2009
Date

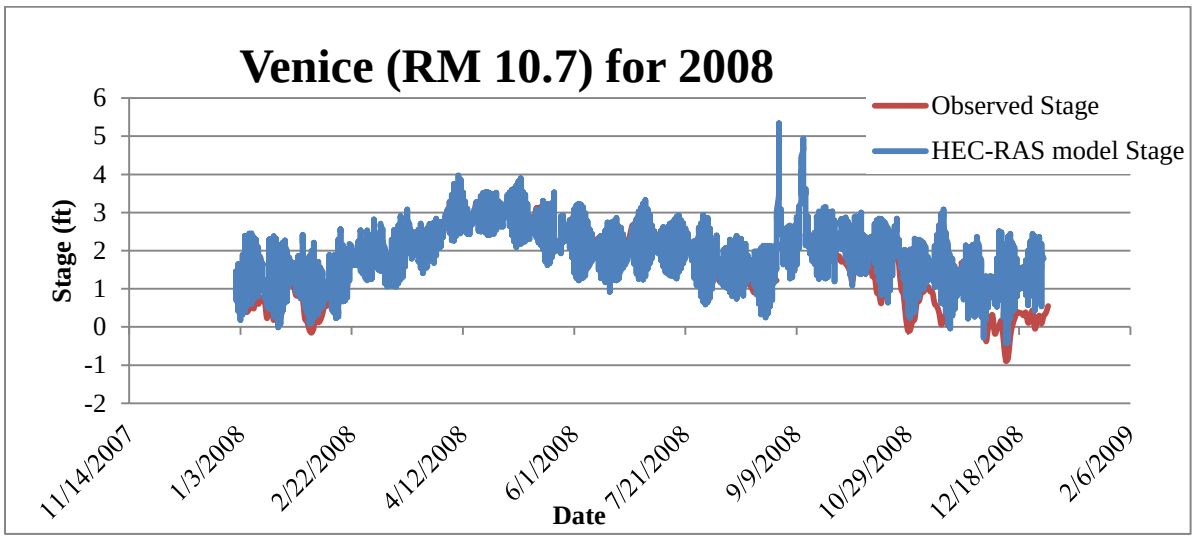
Venice (RM 10.7) for 2008
Observed Stage
HEC-RAS model Stage
Stage (ft)
6
5
4
3
2
1
0
-1
-2
11/14/2007
1/3/2008
2/22/2008
4/12/2008
6/1/2008
7/21/2008
9/9/2008
10/29/2008
12/18/2008
2/6/2009
Date

Hourly Validation 2011:

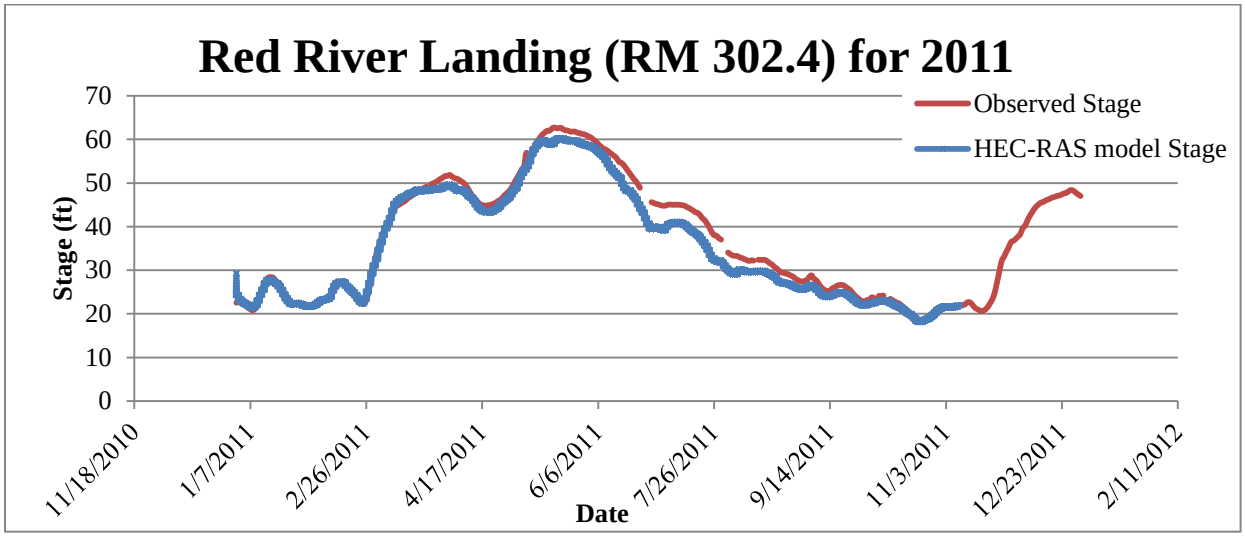

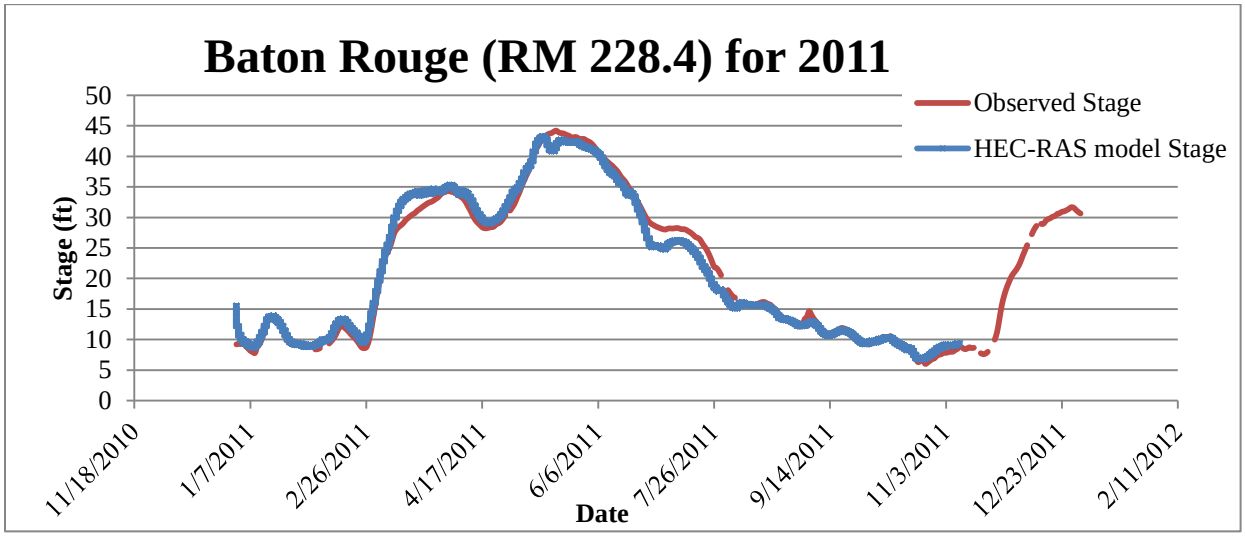

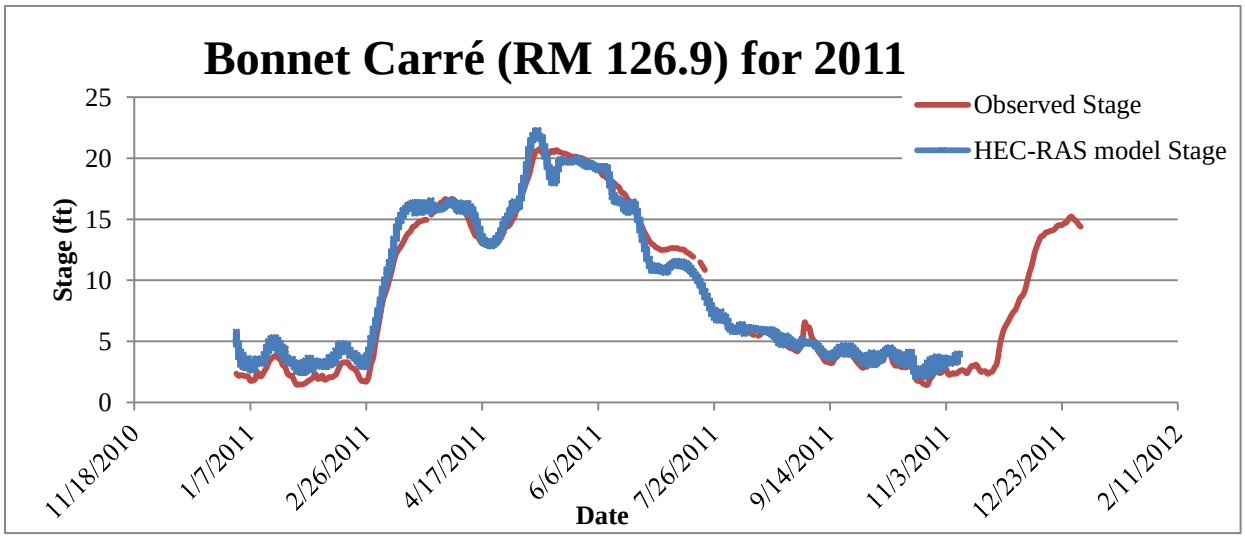

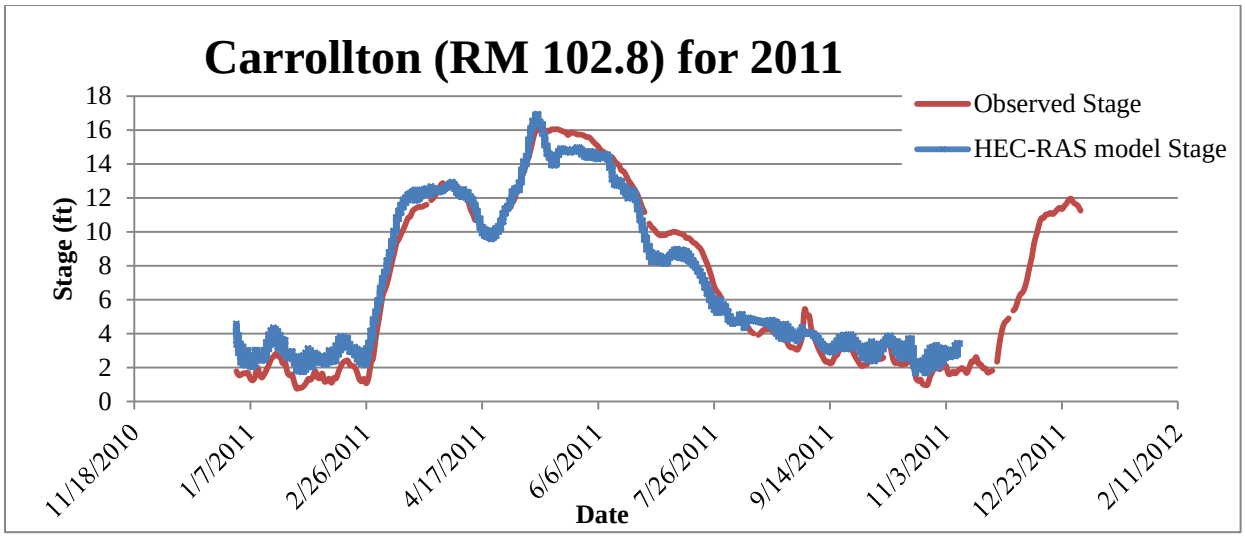
Carrollton (RM 102.8) for 2011
Observed Stage
HEC-RAS model Stage
Stage (ft)
18
16
14
12
10
8
6
4
2
0
11/18/2010
1/7/2011
2/26/2011
4/17/2011
6/6/2011
7/26/2011
9/14/2011
11/3/2011
12/23/2011
2/11/2012
Date

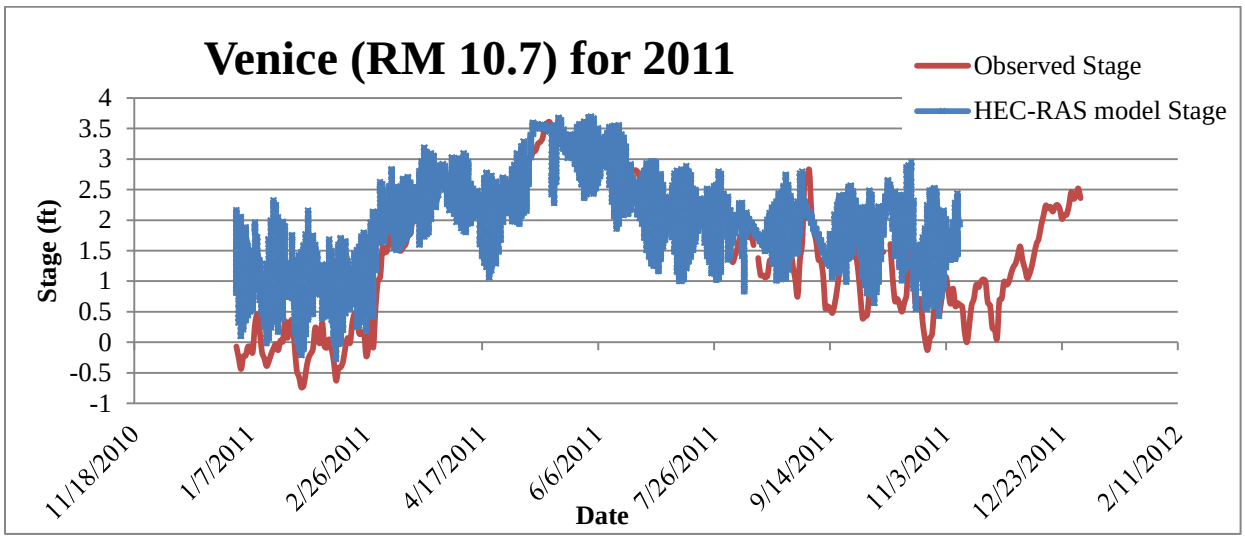
Venice (RM 10.7) for 2011
Observed Stage
HEC-RAS model Stage
Stage (ft)
4
3.5
3
2.5
2
1.5
1
0.5
0
-0.5
-1
11/18/2010
1/7/2011
2/26/2011
4/17/2011
6/6/2011
7/26/2011
9/14/2011
11/3/2011
12/23/2011
2/11/2012
Date

CHARIMA Calibration Results (2009):

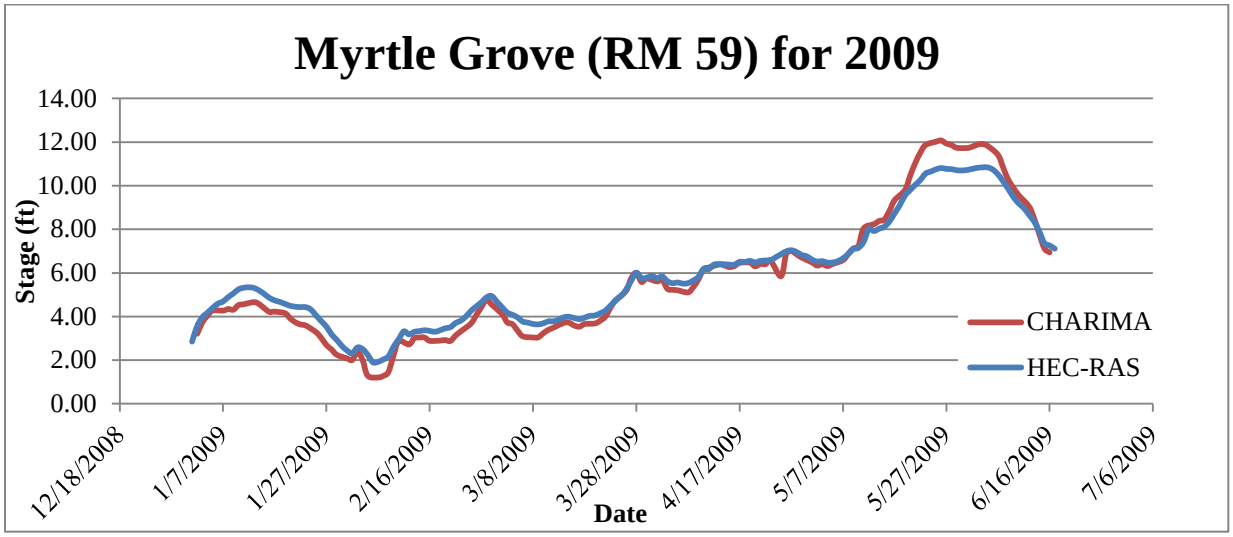

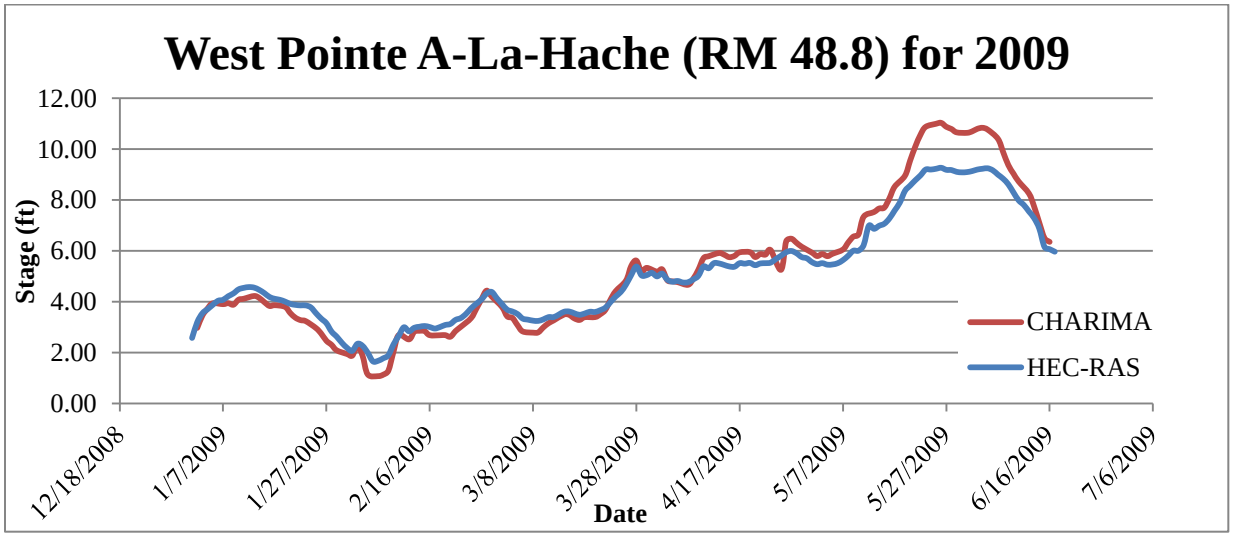

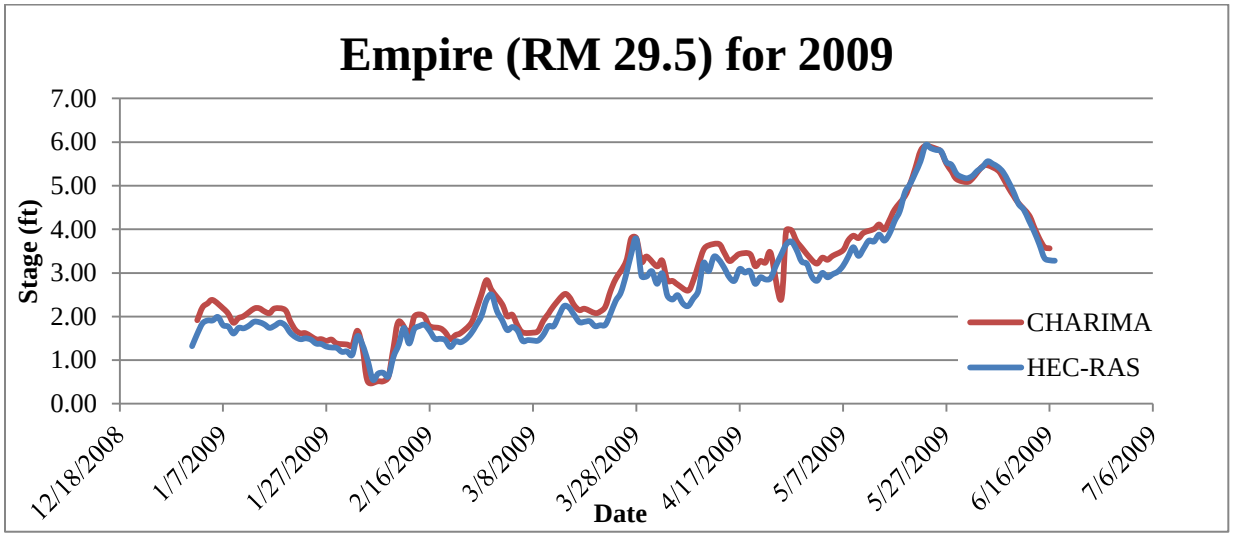

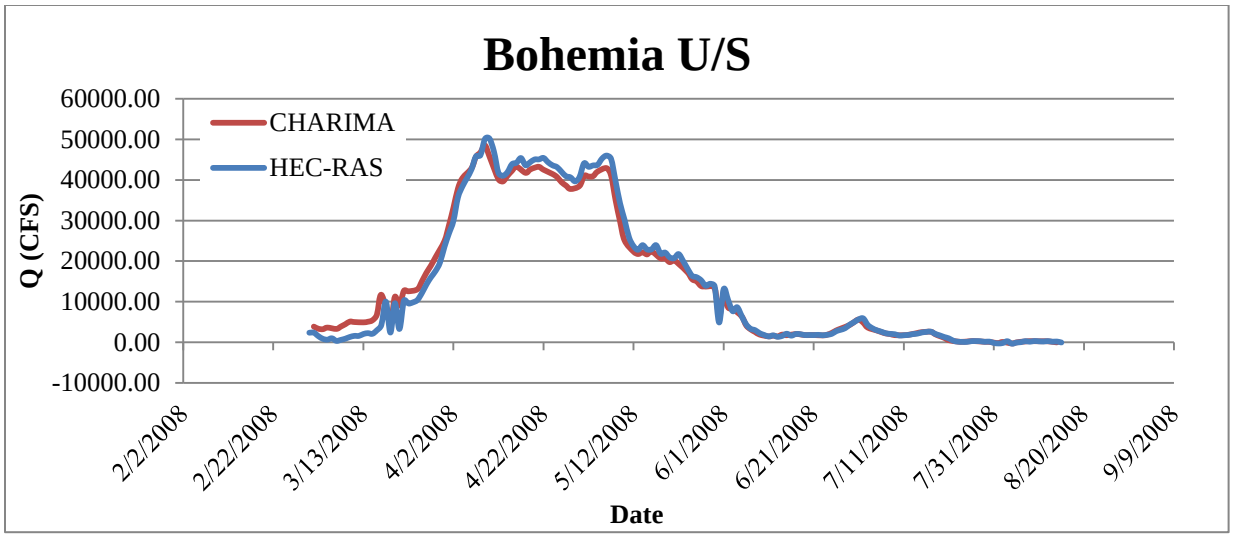
Bohemia U/S
60000.00
50000.00
40000.00
30000.00
20000.00
10000.00
0.00
-10000.00
CHARIMA
HEC-RAS
Q (CFS)
2/2/2008
2/22/2008
3/13/2008
4/2/2008
4/22/2008
5/12/2008
6/1/2008
6/21/2008
7/11/2008
7/31/2008
8/20/2008
9/9/2008
Date

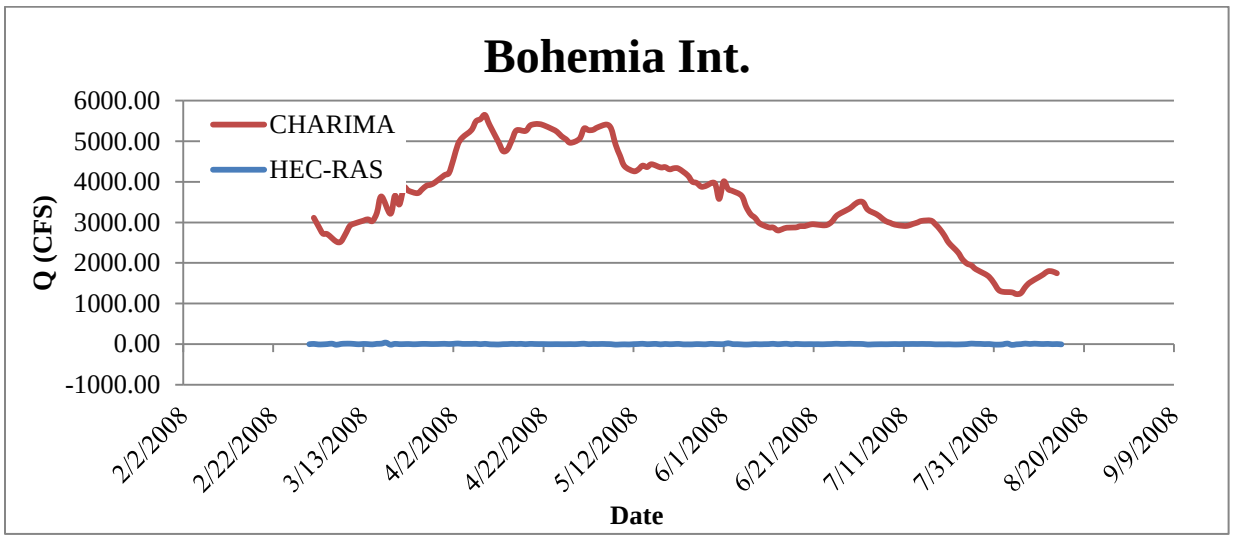
Bohemia Int.
6000.00
5000.00
4000.00
3000.00
2000.00
1000.00
0.00
-1000.00
CHARIMA
HEC-RAS
Q (CFS)
2/2/2008
2/22/2008
3/13/2008
4/2/2008
4/22/2008
5/12/2008
6/1/2008
6/21/2008
7/11/2008
7/31/2008
8/20/2008
9/9/2008
Date

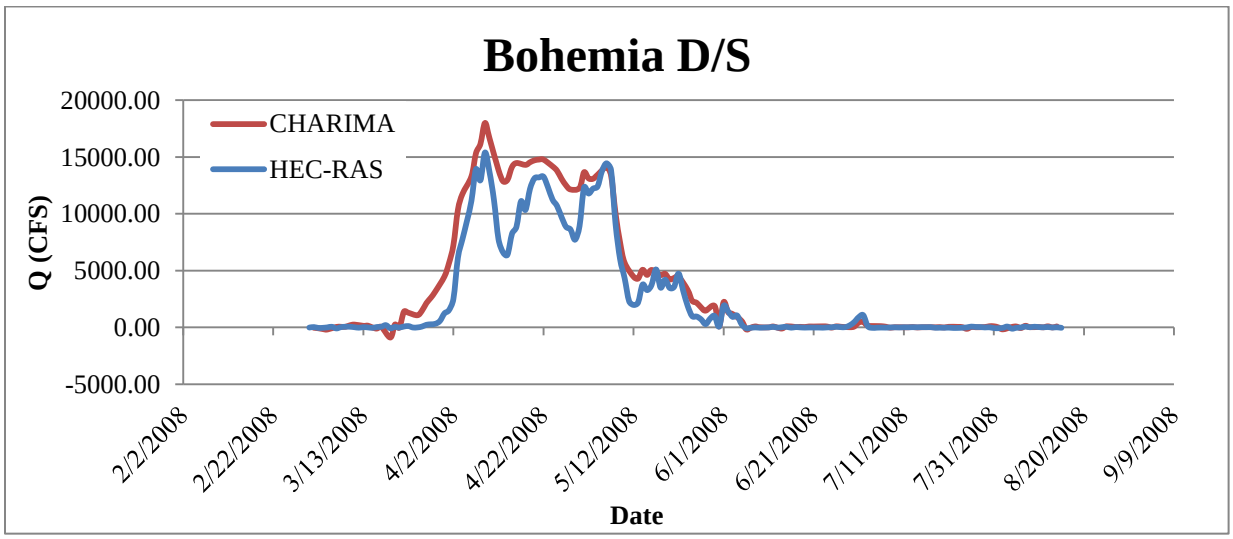
Bohemia D/S
20000.00
15000.00
10000.00
5000.00
0.00
-5000.00
CHARIMA
HEC-RAS
Q (CFS)
2/2/2008
2/22/2008
3/13/2008
4/2/2008
4/22/2008
5/12/2008
6/1/2008
6/21/2008
7/11/2008
7/31/2008
8/20/2008
9/9/2008
Date

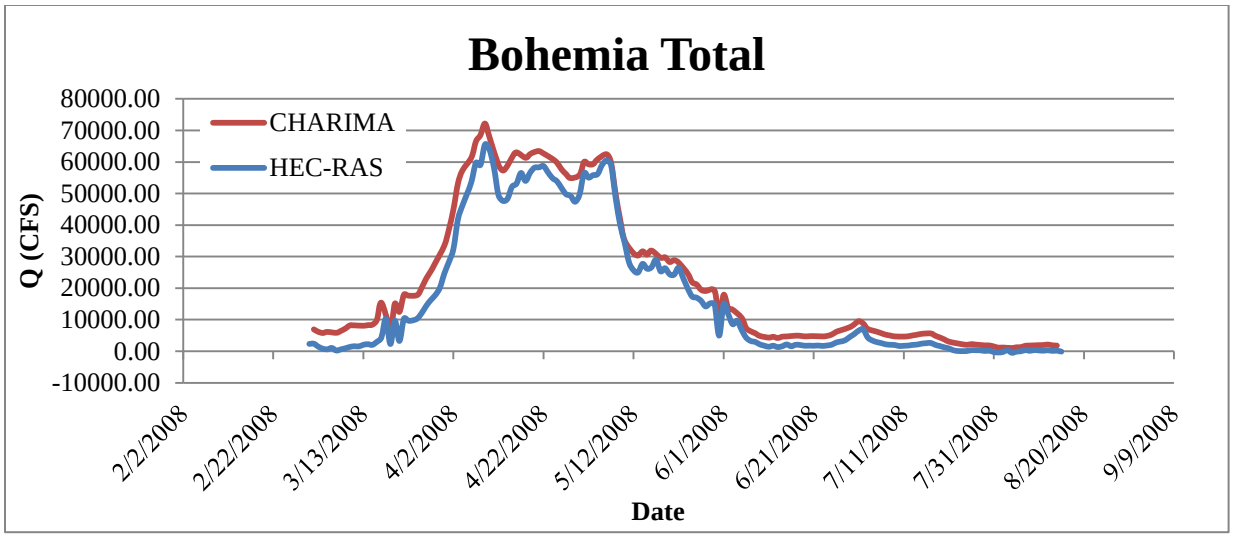
Bohemia Total
80000.00
70000.00
60000.00
50000.00
40000.00
30000.00
20000.00
10000.00
0.00
-10000.00
Q (CFS)
CHARIMA
HEC-RAS
2/2/2008
2/22/2008
3/13/2008
4/2/2008
4/22/2008
5/12/2008
6/1/2008
6/21/2008
7/11/2008
7/31/2008
8/20/2008
9/9/2008
Date

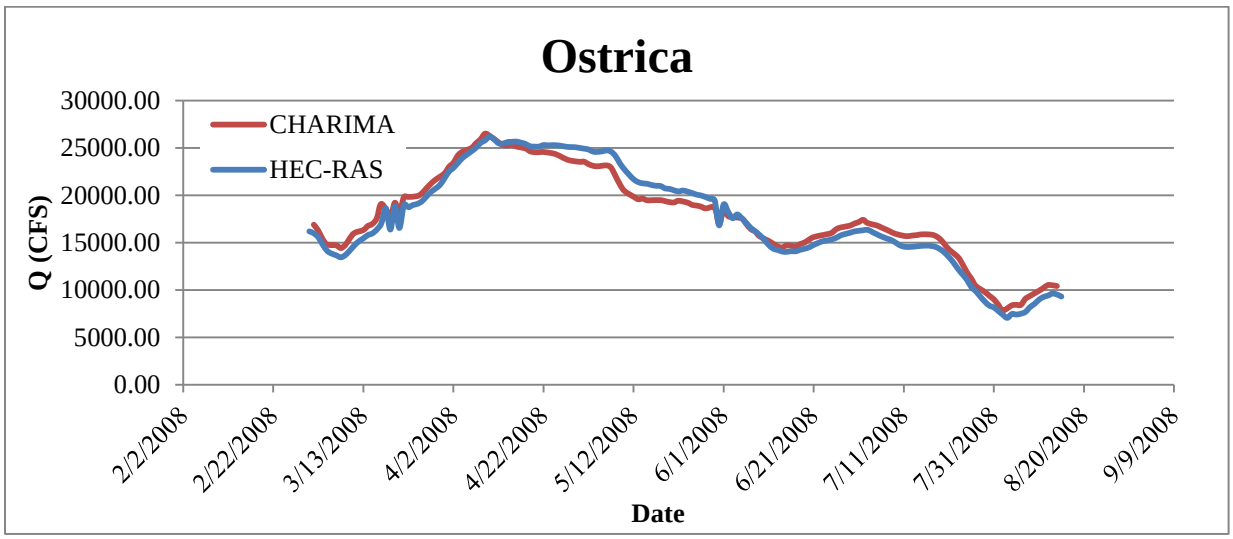
Ostrica
30000.00
25000.00
20000.00
15000.00
10000.00
5000.00
0.00
Q (CFS)
CHARIMA
HEC-RAS
2/2/2008
2/22/2008
3/13/2008
4/2/2008
4/22/2008
5/12/2008
6/1/2008
6/21/2008
7/11/2008
7/31/2008
8/20/2008
9/9/2008
Date

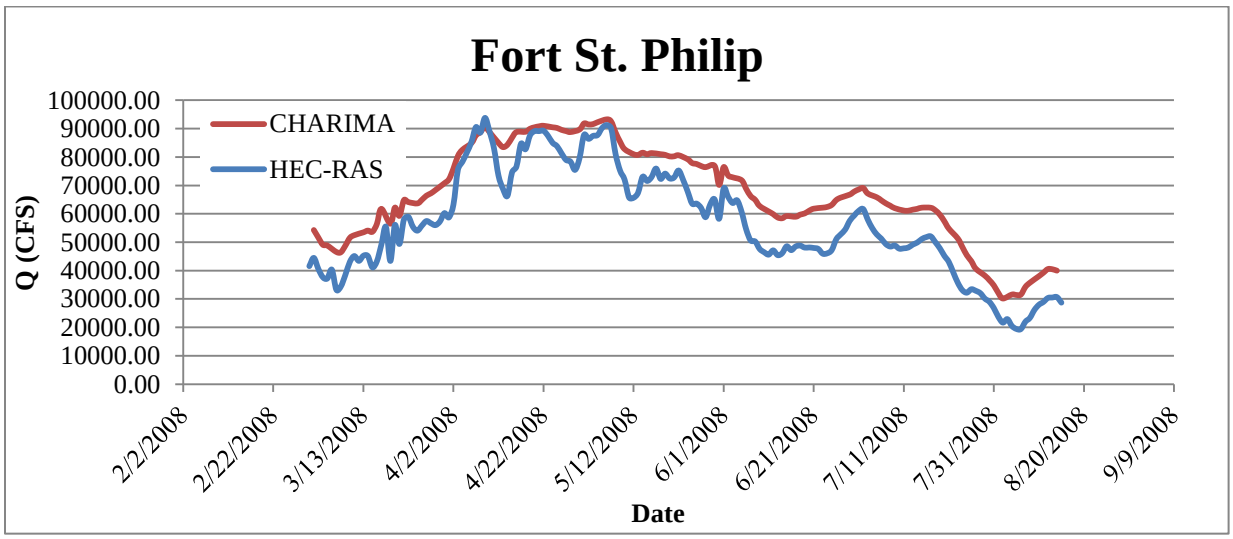
Fort St. Philip
100000.00
90000.00
80000.00
70000.00
60000.00
50000.00
40000.00
30000.00
20000.00
10000.00
0.00
Q (CFS)
CHARIMA
HEC-RAS
2/2/2008
2/22/2008
3/13/2008
4/2/2008
4/22/2008
5/12/2008
6/1/2008
6/21/2008
7/11/2008
7/31/2008
8/20/2008
9/9/2008
Date

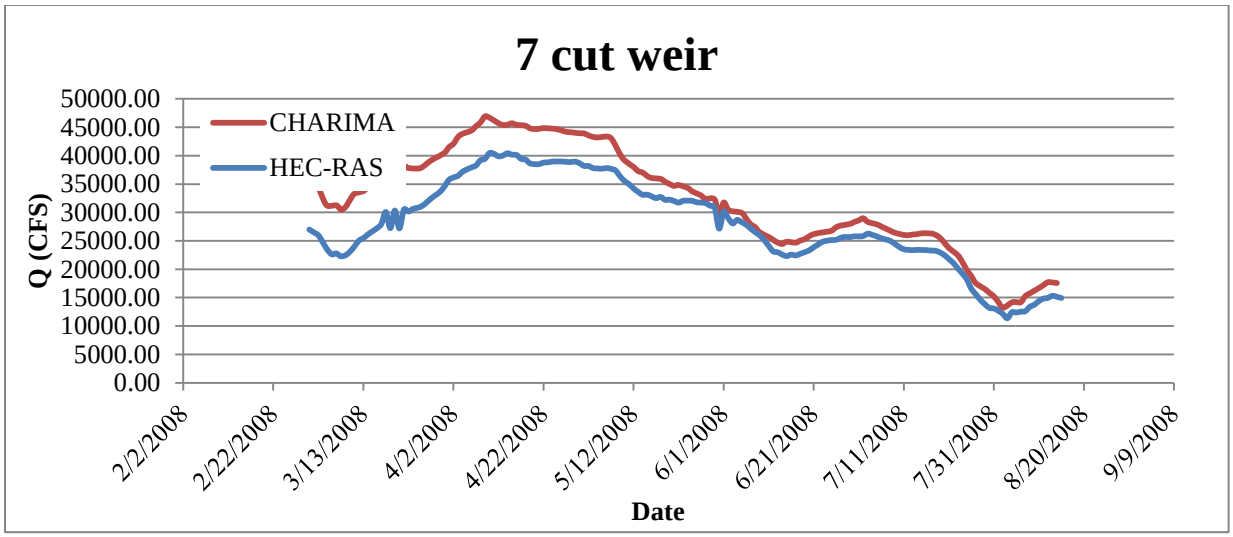
7 cut weir
CHARIMA
HEC-RAS
Q (CFS)
50000.00
45000.00
40000.00
35000.00
30000.00
25000.00
20000.00
15000.00
10000.00
5000.00
0.00
2/2/2008
2/22/2008
3/13/2008
4/2/2008
4/22/2008
5/12/2008
6/1/2008
6/21/2008
7/11/2008
7/31/2008
8/20/2008
9/9/2008
Date

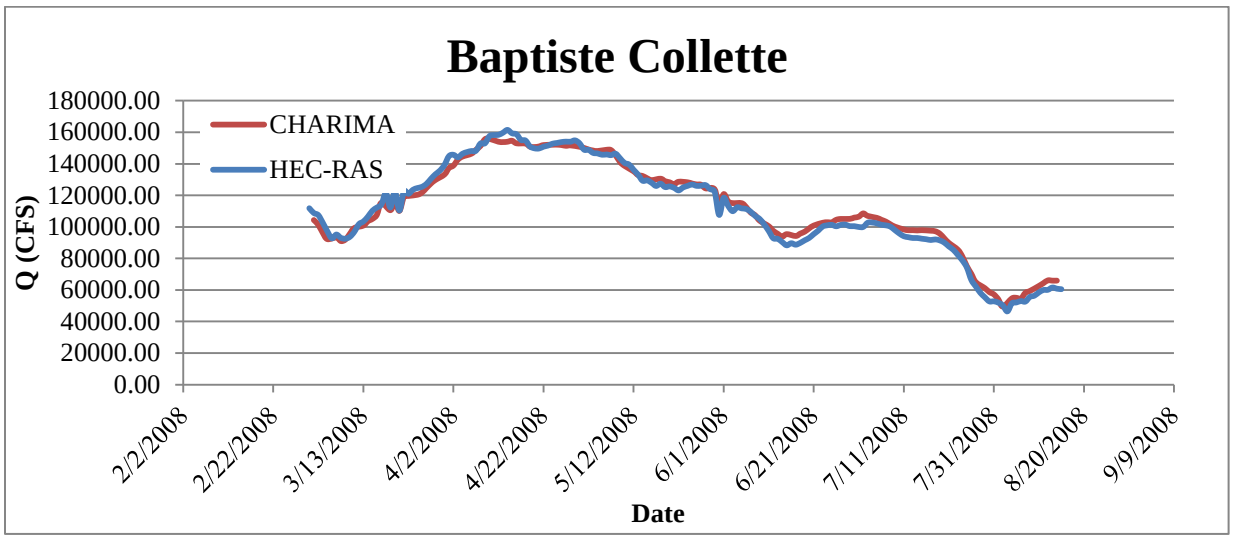
Baptiste Collette
CHARIMA
HEC-RAS
Q (CFS)
180000.00
160000.00
140000.00
120000.00
100000.00
80000.00
60000.00
40000.00
20000.00
0.00
2/2/2008
2/22/2008
3/13/2008
4/2/2008
4/22/2008
5/12/2008
6/1/2008
6/21/2008
7/11/2008
7/31/2008
8/20/2008
9/9/2008
Date

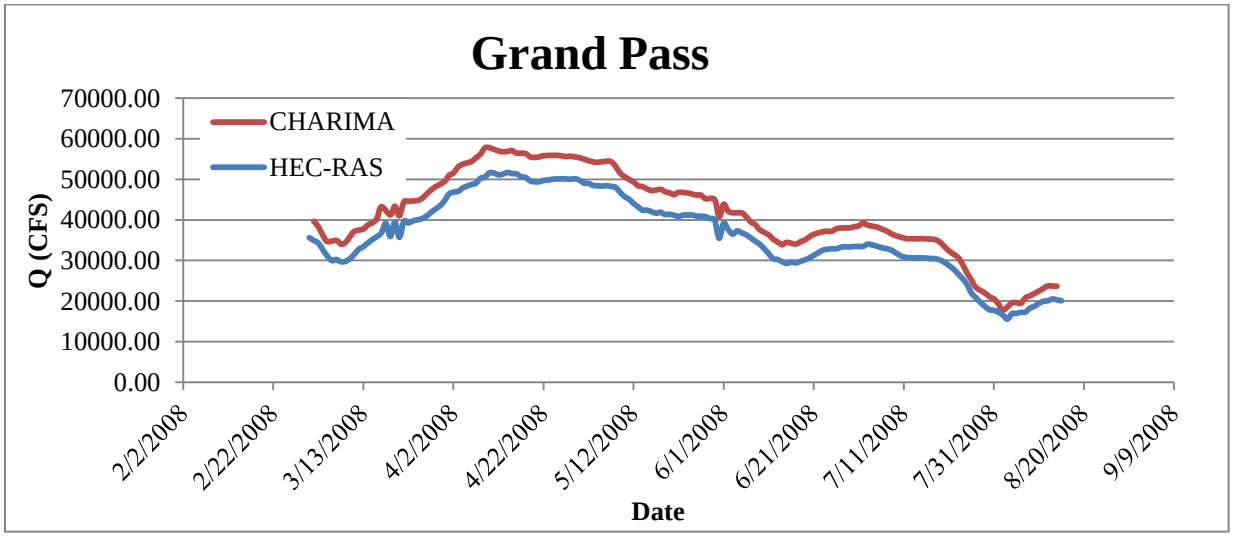
Grand Pass
CHARIMA
HEC-RAS
Q (CFS)
70000.00
60000.00
50000.00
40000.00
30000.00
20000.00
10000.00
0.00
2/2/2008
2/22/2008
3/13/2008
4/2/2008
4/22/2008
5/12/2008
6/1/2008
6/21/2008
7/11/2008
7/31/2008
8/20/2008
9/9/2008
Date

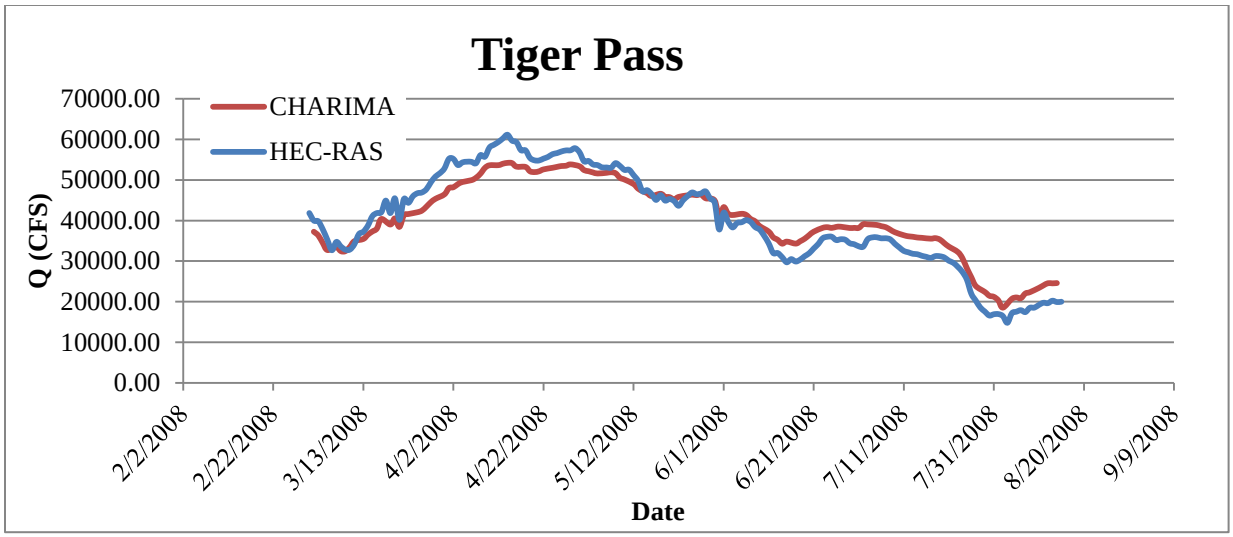
Tiger Pass
70000.00
60000.00
50000.00
40000.00
30000.00
20000.00
10000.00
0.00
Q (CFS)
CHARIMA
HEC-RAS
2/2/2008
2/22/2008
3/13/2008
4/2/2008
4/22/2008
5/12/2008
6/1/2008
6/21/2008
7/11/2008
7/31/2008
8/20/2008
9/9/2008
Date

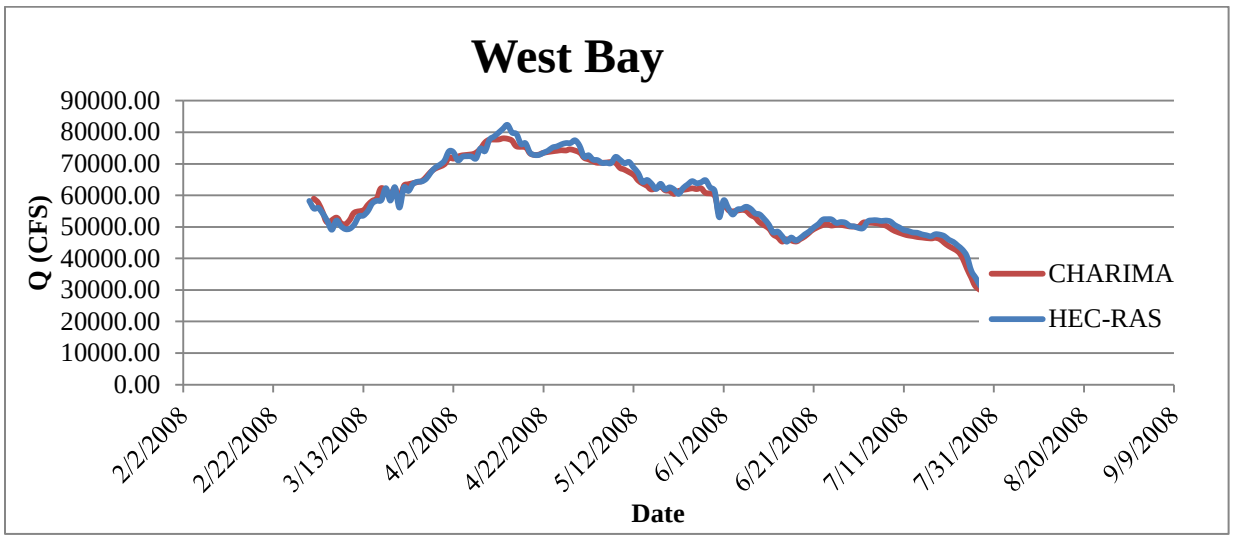
West Bay
90000.00
80000.00
70000.00
60000.00
50000.00
40000.00
30000.00
20000.00
10000.00
0.00
Q (CFS)
CHARIMA
HEC-RAS
2/2/2008
2/22/2008
3/13/2008
4/2/2008
4/22/2008
5/12/2008
6/1/2008
6/21/2008
7/11/2008
7/31/2008
8/20/2008
9/9/2008
Date

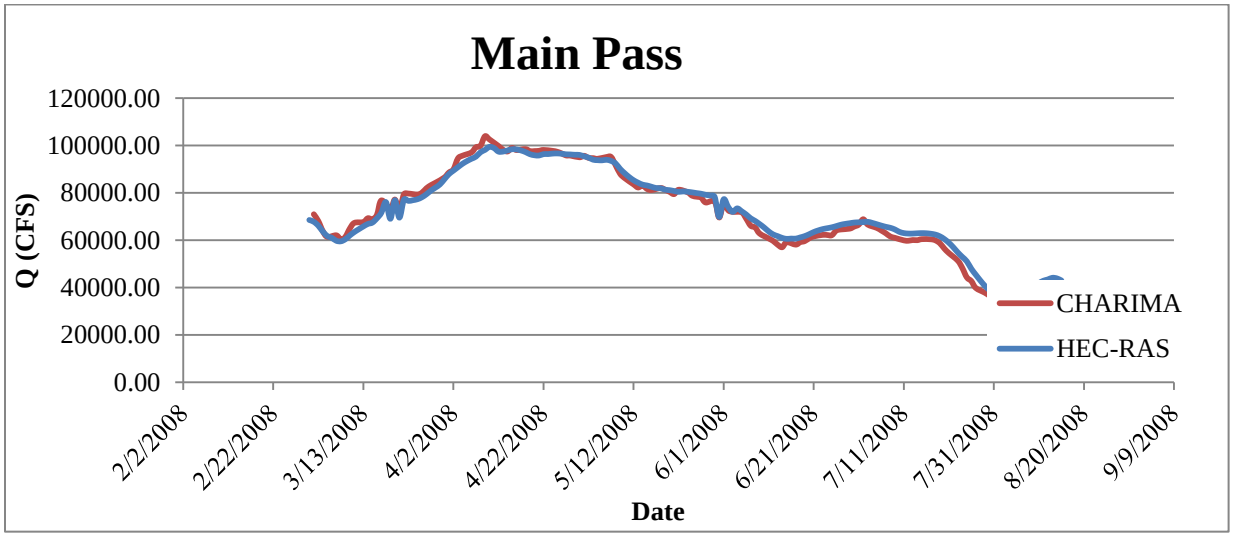
Main Pass
120000.00
100000.00
80000.00
60000.00
40000.00
20000.00
0.00
Q (CFS)
CHARIMA
HEC-RAS
2/2/2008
2/22/2008
3/13/2008
4/2/2008
4/22/2008
5/12/2008
6/1/2008
6/21/2008
7/11/2008
7/31/2008
8/20/2008
9/9/2008
Date

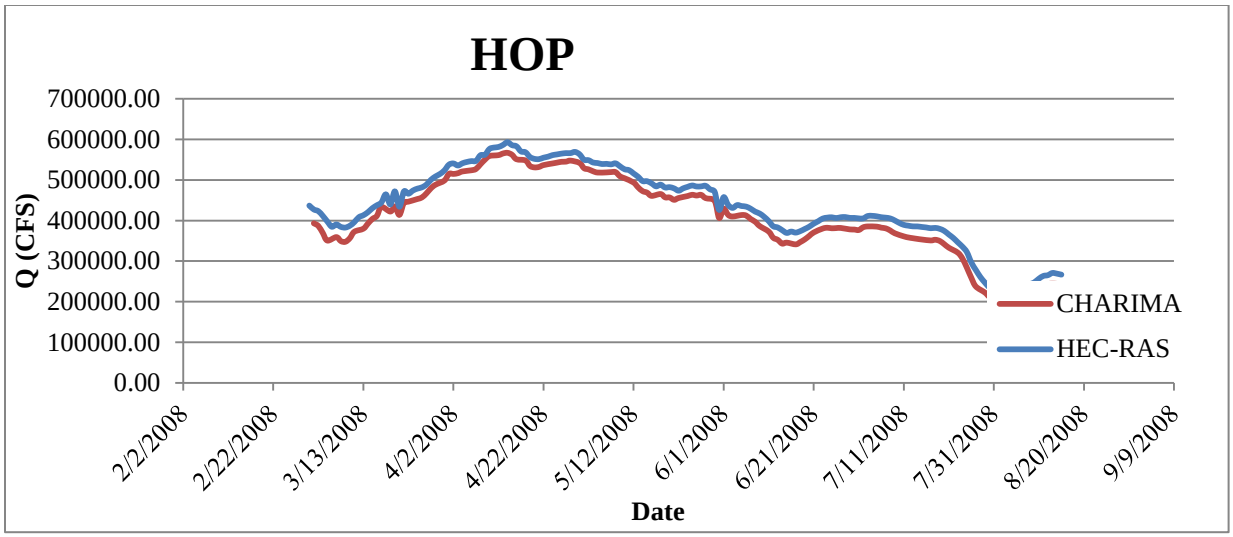
HOP
700000.00
600000.00
500000.00
400000.00
300000.00
200000.00
100000.00
0.00
Q (CFS)
2/2/2008
2/22/2008
3/13/2008
4/2/2008
4/22/2008
5/12/2008
6/1/2008
6/21/2008
7/11/2008
7/31/2008
8/20/2008
9/9/2008
Date
CHARIMA
HEC-RAS

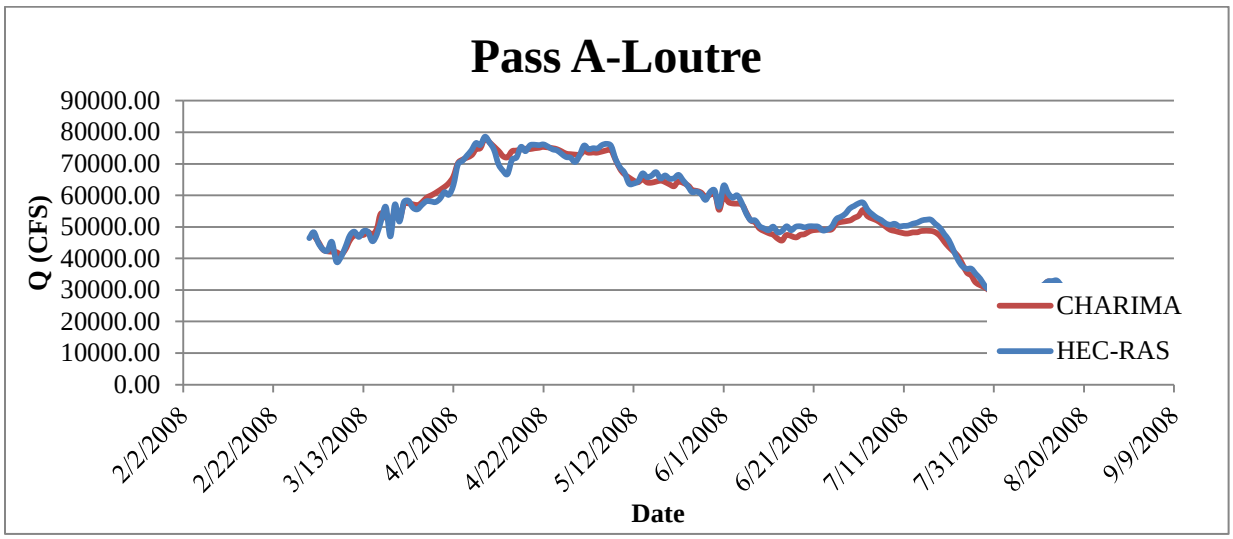
Pass A-Loutre
90000.00
80000.00
70000.00
60000.00
50000.00
40000.00
30000.00
20000.00
10000.00
0.00
Q (CFS)
2/2/2008
2/22/2008
3/13/2008
4/2/2008
4/22/2008
5/12/2008
6/1/2008
6/21/2008
7/11/2008
7/31/2008
8/20/2008
9/9/2008
Date
CHARIMA
HEC-RAS

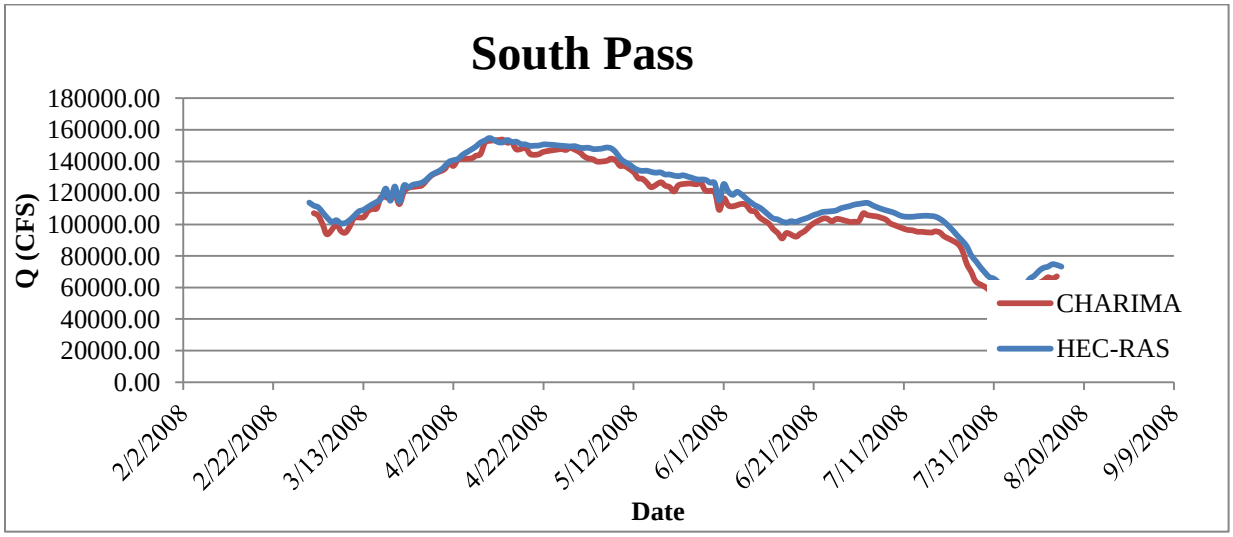
South Pass
180000.00
160000.00
140000.00
120000.00
100000.00
80000.00
60000.00
40000.00
20000.00
0.00
Q (CFS)
2/2/2008
2/22/2008
3/13/2008
4/2/2008
4/22/2008
5/12/2008
6/1/2008
6/21/2008
7/11/2008
7/31/2008
8/20/2008
9/9/2008
Date
CHARIMA
HEC-RAS

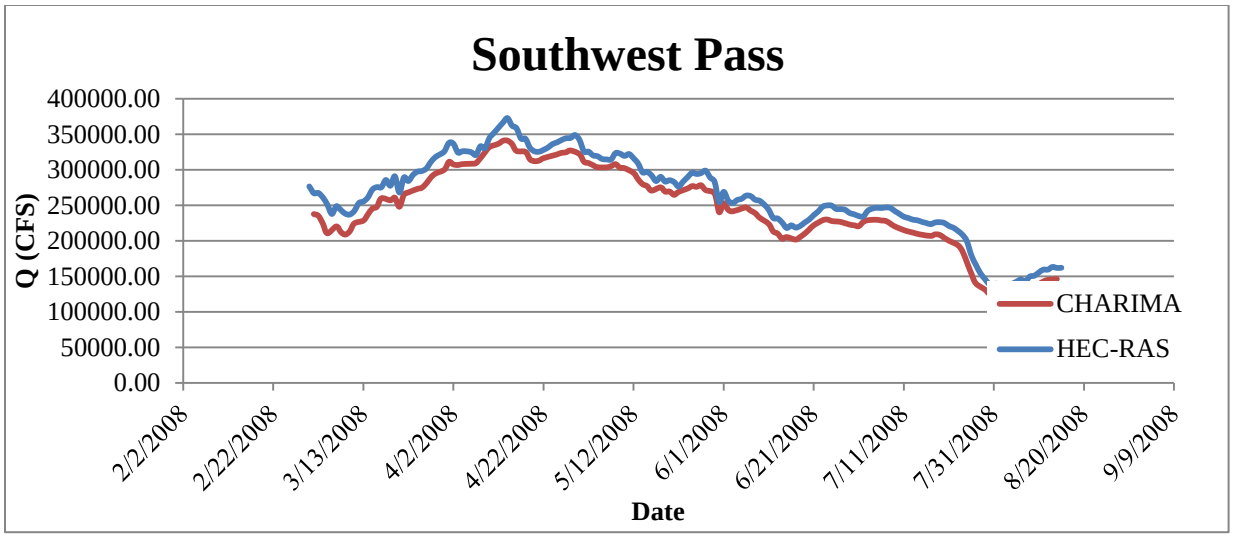

CHARIMA Validation Results (2008):

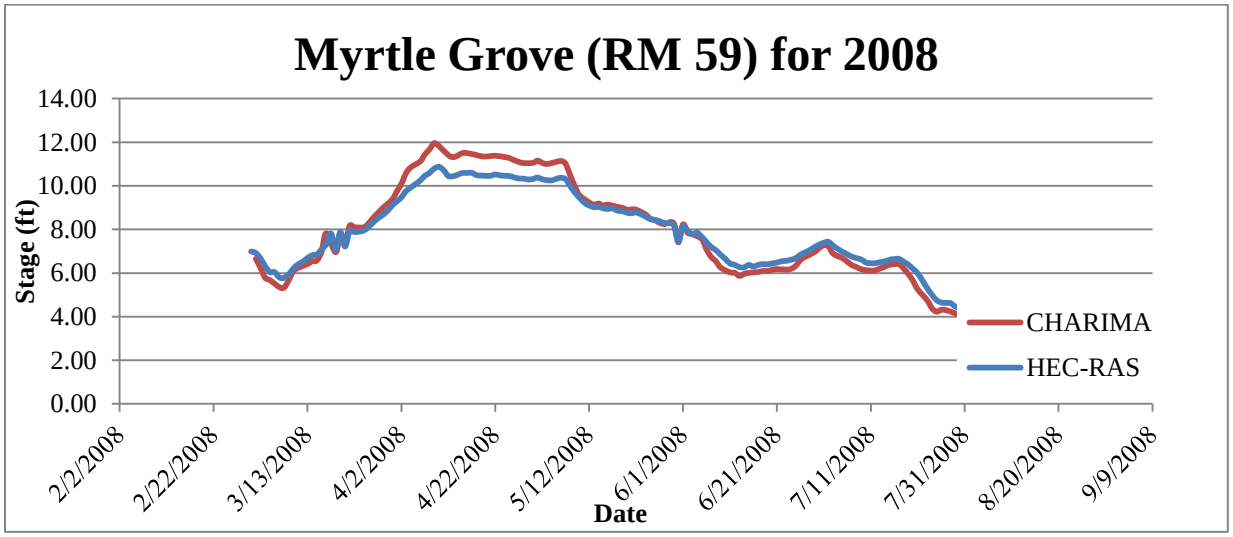

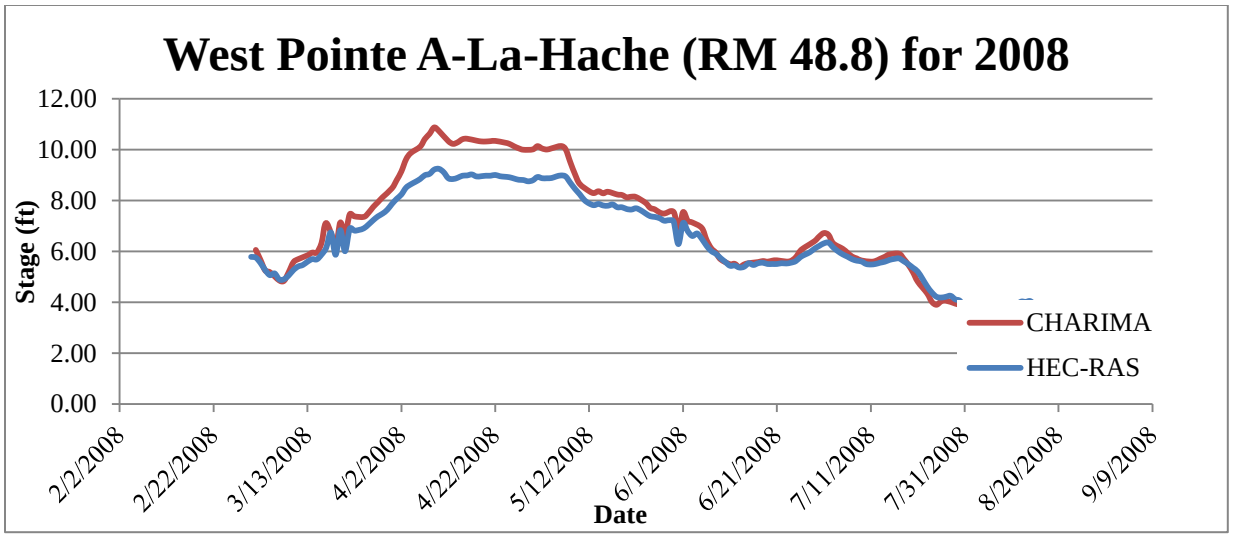
West Pointe A-La-Hache (RM 48.8) for 2008
12.00
10.00
8.00
6.00
4.00
2.00
0.00
Stage (ft)
CHARIMA
HEC-RAS
2/2/2008
2/22/2008
3/13/2008
4/2/2008
4/22/2008
5/12/2008
6/1/2008
6/21/2008
7/11/2008
7/31/2008
8/20/2008
9/9/2008
Date

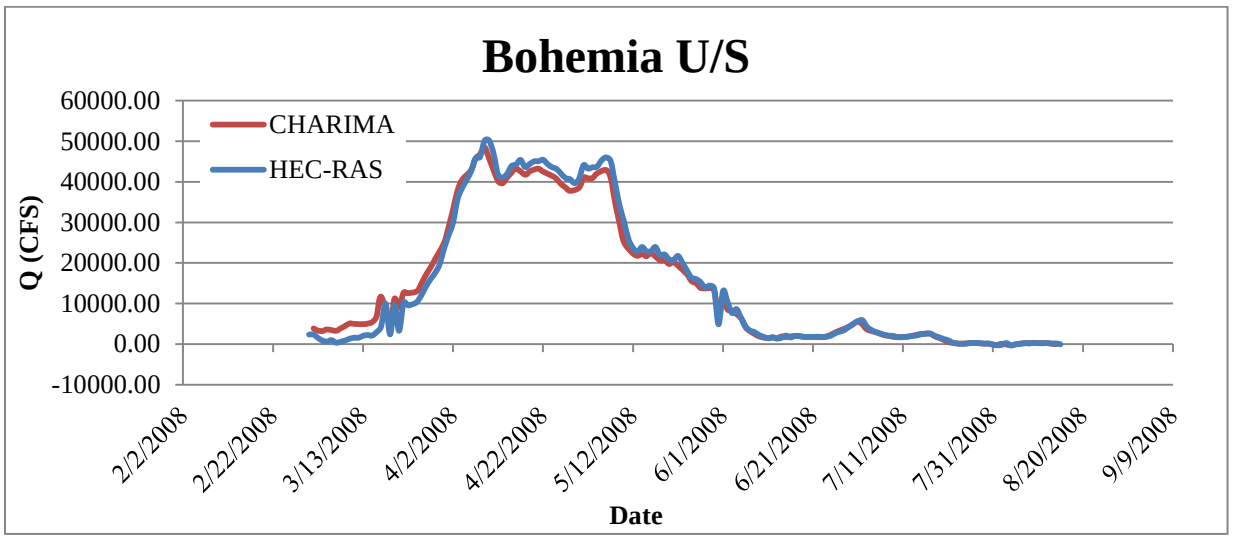
Bohemia U/S
60000.00
50000.00
40000.00
30000.00
20000.00
10000.00
0.00
-10000.00
Q (CFS)
CHARIMA
HEC-RAS
2/2/2008
2/22/2008
3/13/2008
4/2/2008
4/22/2008
5/12/2008
6/1/2008
6/21/2008
7/11/2008
7/31/2008
8/20/2008
9/9/2008
Date

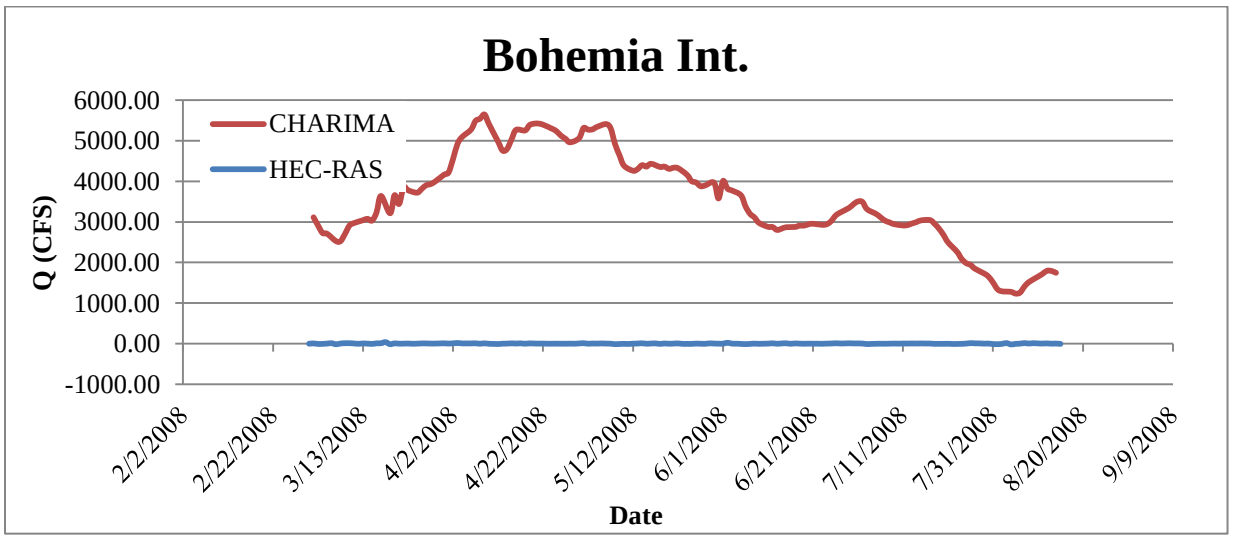
Bohemia Int.
6000.00
5000.00
4000.00
3000.00
2000.00
1000.00
0.00
-1000.00
Q (CFS)
CHARIMA
HEC-RAS
2/2/2008
2/22/2008
3/13/2008
4/2/2008
4/22/2008
5/12/2008
6/1/2008
6/21/2008
7/11/2008
7/31/2008
8/20/2008
9/9/2008
Date

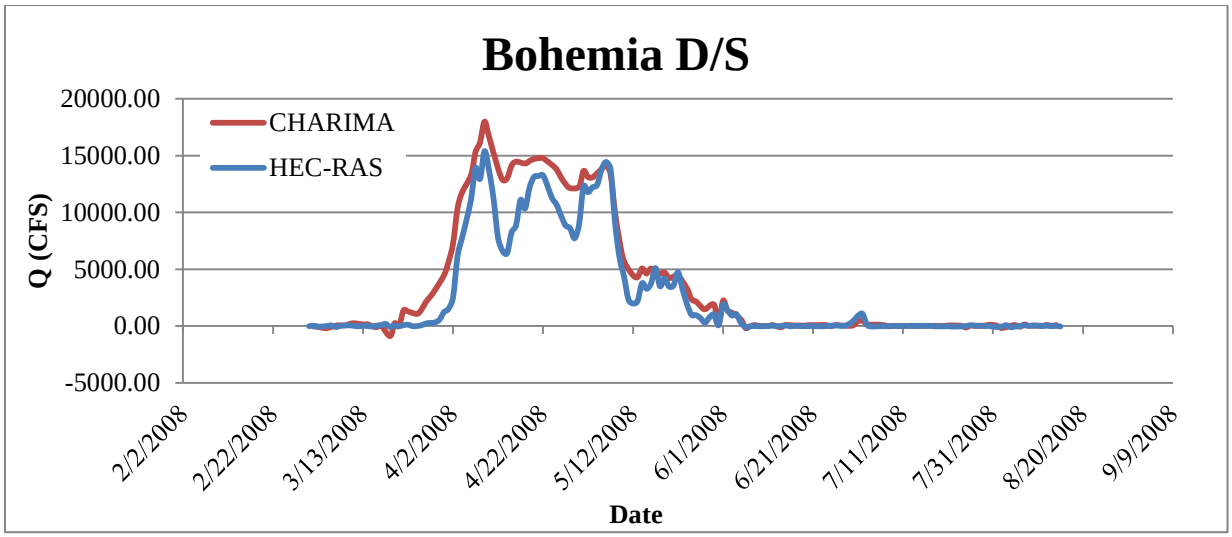
Bohemia D/S
20000.00
15000.00
10000.00
5000.00
0.00
-5000.00
Q (CFS)
CHARIMA
HEC-RAS
2/2/2008
2/22/2008
3/13/2008
4/2/2008
4/22/2008
5/12/2008
6/1/2008
6/21/2008
7/11/2008
7/31/2008
8/20/2008
9/9/2008
Date

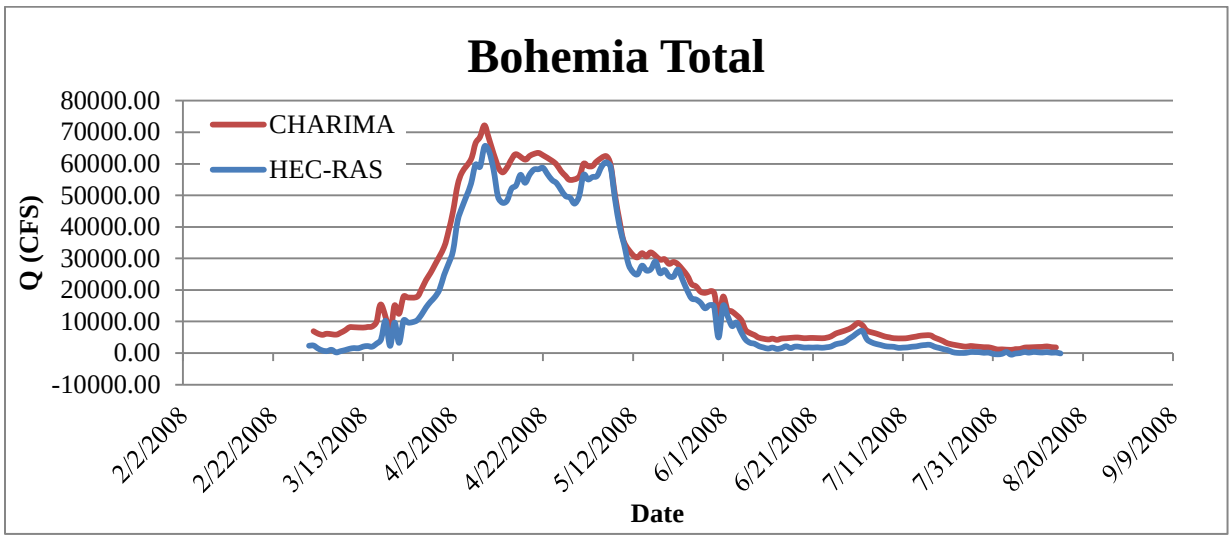
Bohemia Total
80000.00
70000.00
60000.00
50000.00
40000.00
30000.00
20000.00
10000.00
0.00
-10000.00
Q (CFS)
CHARIMA
HEC-RAS
2/2/2008
2/22/2008
3/13/2008
4/2/2008
4/22/2008
5/12/2008
6/1/2008
6/21/2008
7/11/2008
7/31/2008
8/20/2008
9/9/2008
Date

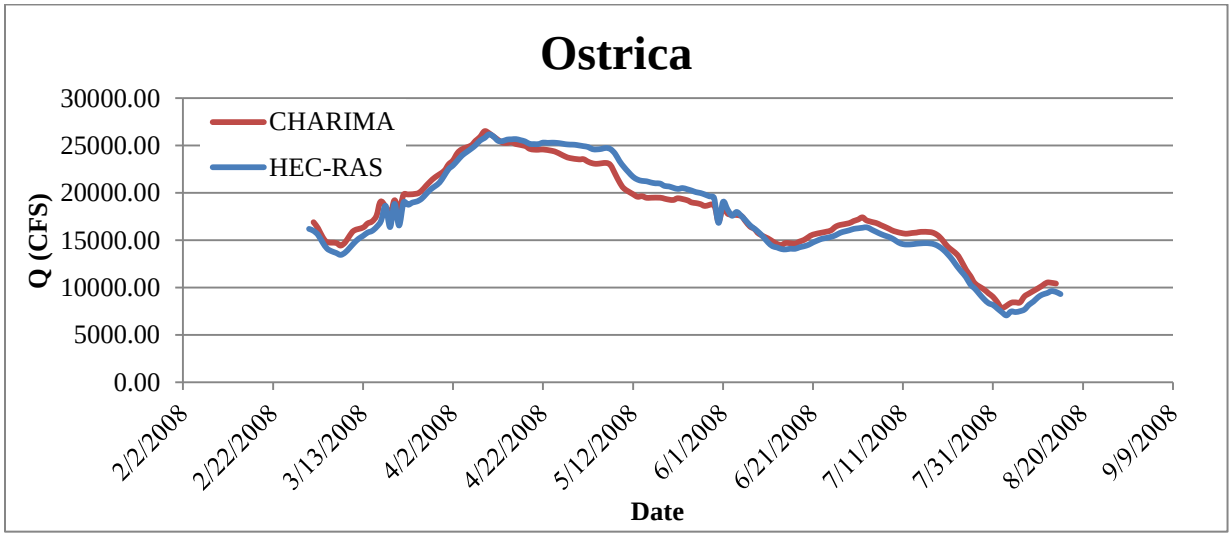
Ostrica
30000.00
25000.00
20000.00
15000.00
10000.00
5000.00
0.00
Q (CFS)
CHARIMA
HEC-RAS
2/2/2008
2/22/2008
3/13/2008
4/2/2008
4/22/2008
5/12/2008
6/1/2008
6/21/2008
7/11/2008
7/31/2008
8/20/2008
9/9/2008
Date

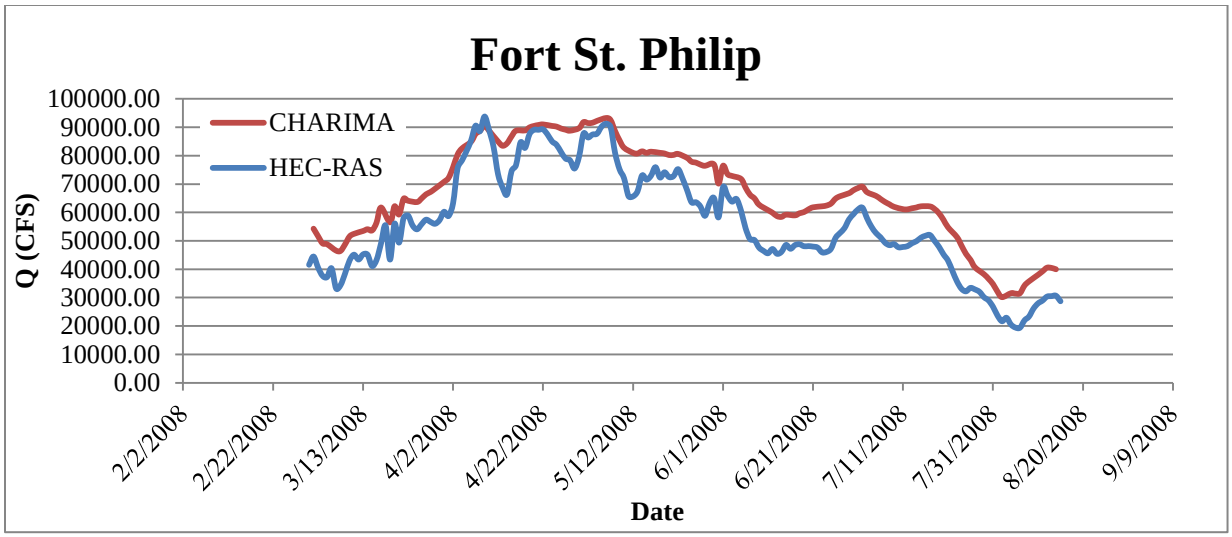
Fort St. Philip
100000.00
90000.00
80000.00
70000.00
60000.00
50000.00
40000.00
30000.00
20000.00
10000.00
0.00
Q (CFS)
CHARIMA
HEC-RAS
2/2/2008
2/22/2008
3/13/2008
4/2/2008
4/22/2008
5/12/2008
6/1/2008
6/21/2008
7/11/2008
7/31/2008
8/20/2008
9/9/2008
Date

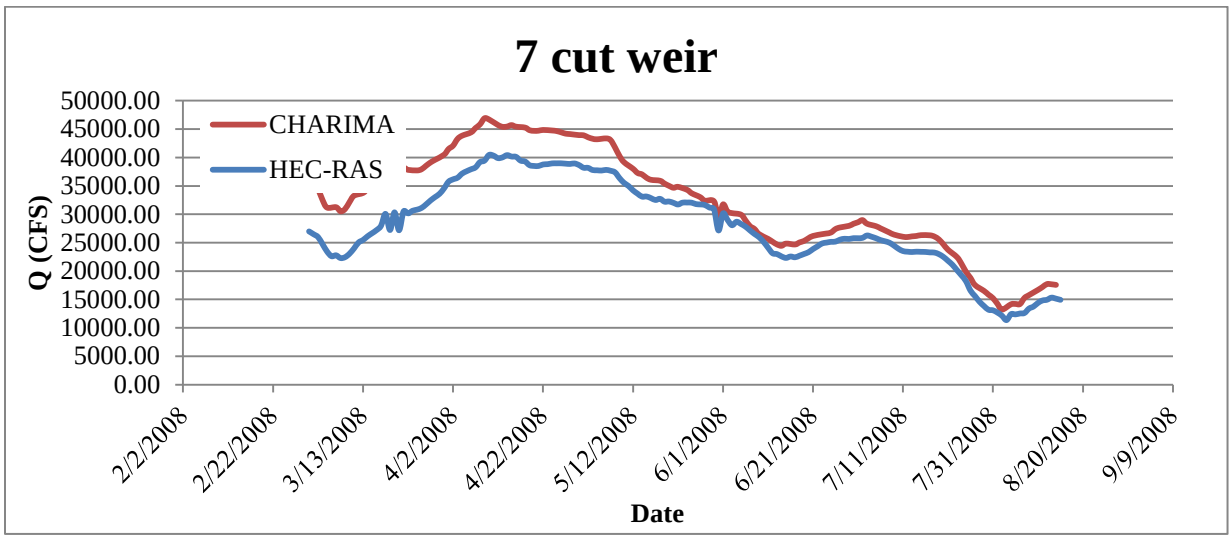
7 cut weir
50000.00
45000.00
40000.00
35000.00
30000.00
25000.00
20000.00
15000.00
10000.00
5000.00
0.00
Q (CFS)
CHARIMA
HEC-RAS
2/2/2008
2/22/2008
3/13/2008
4/2/2008
4/22/2008
5/12/2008
6/1/2008
6/21/2008
7/11/2008
7/31/2008
8/20/2008
9/9/2008
Date

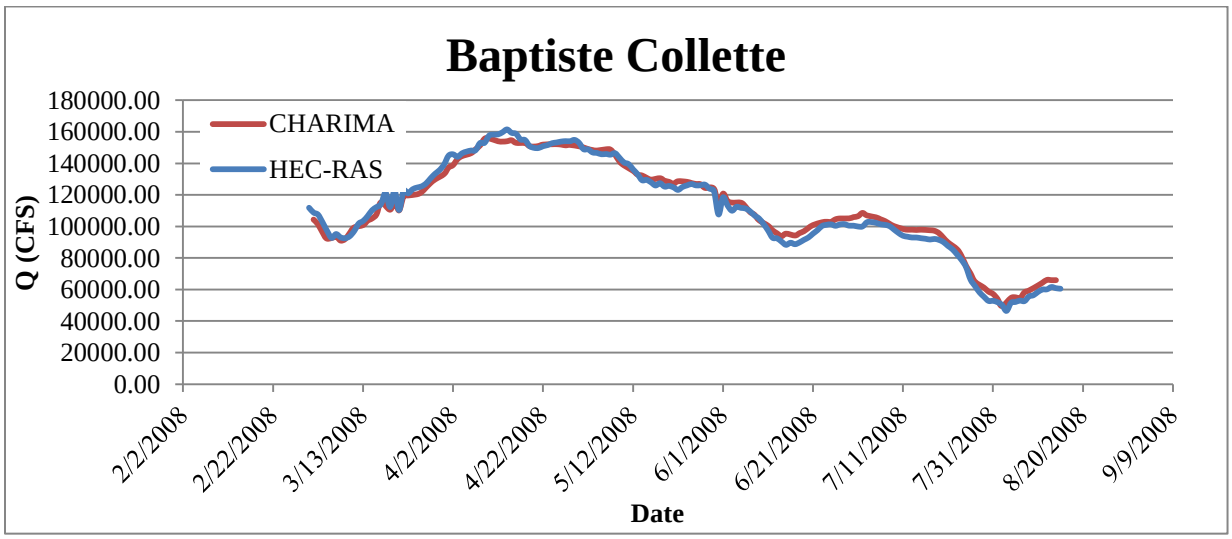
Baptiste Collette
180000.00
160000.00
140000.00
120000.00
100000.00
80000.00
60000.00
40000.00
20000.00
0.00
Q (CFS)
CHARIMA
HEC-RAS
2/2/2008
2/22/2008
3/13/2008
4/2/2008
4/22/2008
5/12/2008
6/1/2008
6/21/2008
7/11/2008
7/31/2008
8/20/2008
9/9/2008
Date

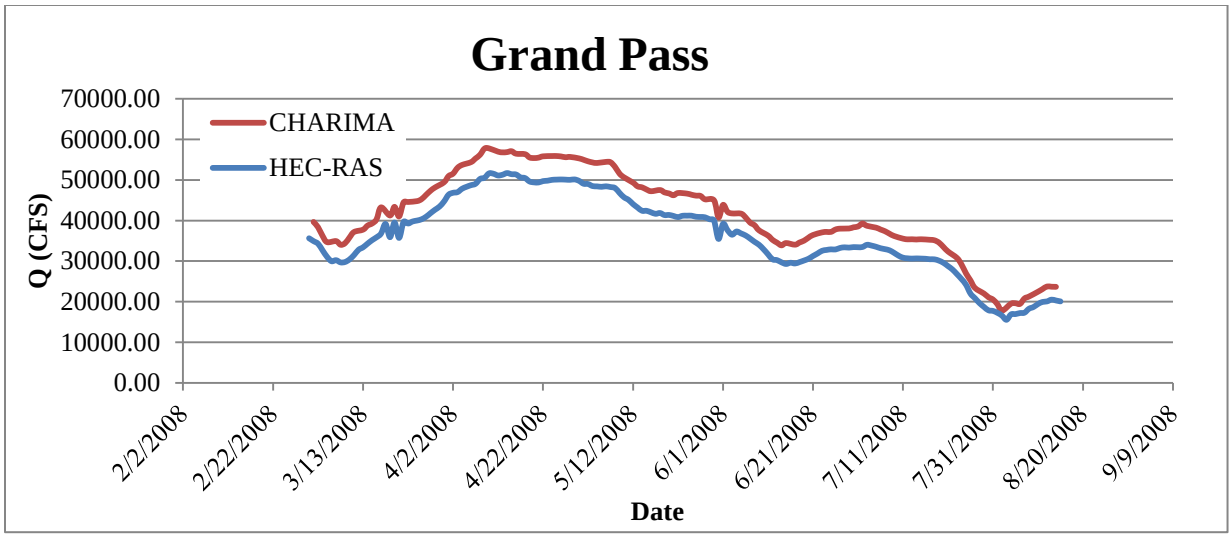
Grand Pass
70000.00
60000.00
50000.00
40000.00
30000.00
20000.00
10000.00
0.00
Q (CFS)
CHARIMA
HEC-RAS
2/2/2008
2/22/2008
3/13/2008
4/2/2008
4/22/2008
5/12/2008
6/1/2008
6/21/2008
7/11/2008
7/31/2008
8/20/2008
9/9/2008
Date

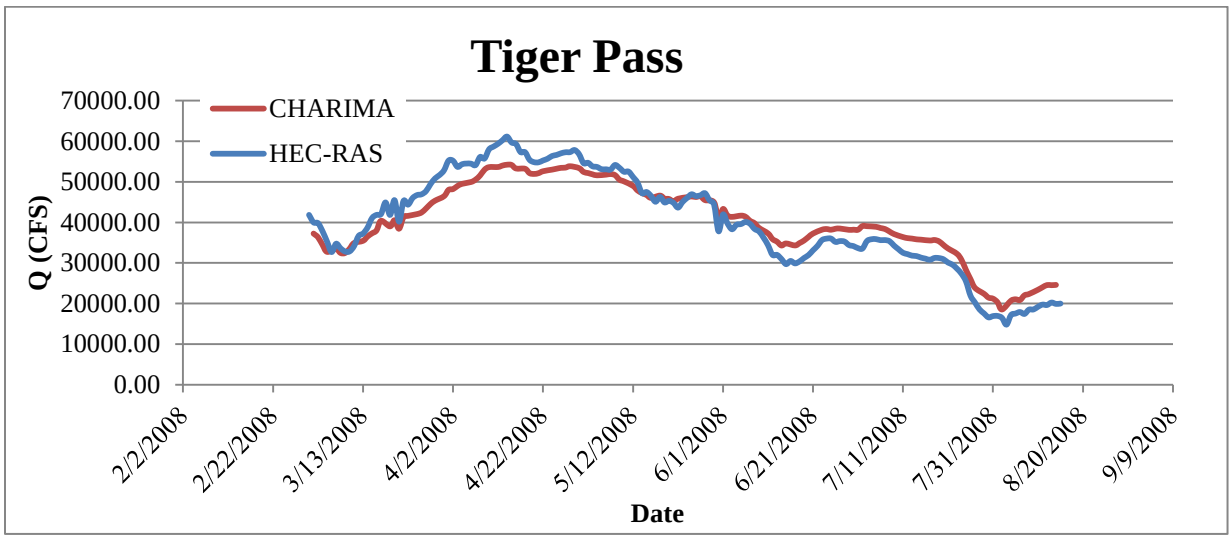
Tiger Pass
70000.00
60000.00
50000.00
40000.00
30000.00
20000.00
10000.00
0.00
Q (CFS)
CHARIMA
HEC-RAS
2/2/2008
2/22/2008
3/13/2008
4/2/2008
4/22/2008
5/12/2008
6/1/2008
6/21/2008
7/11/2008
7/31/2008
8/20/2008
9/9/2008
Date

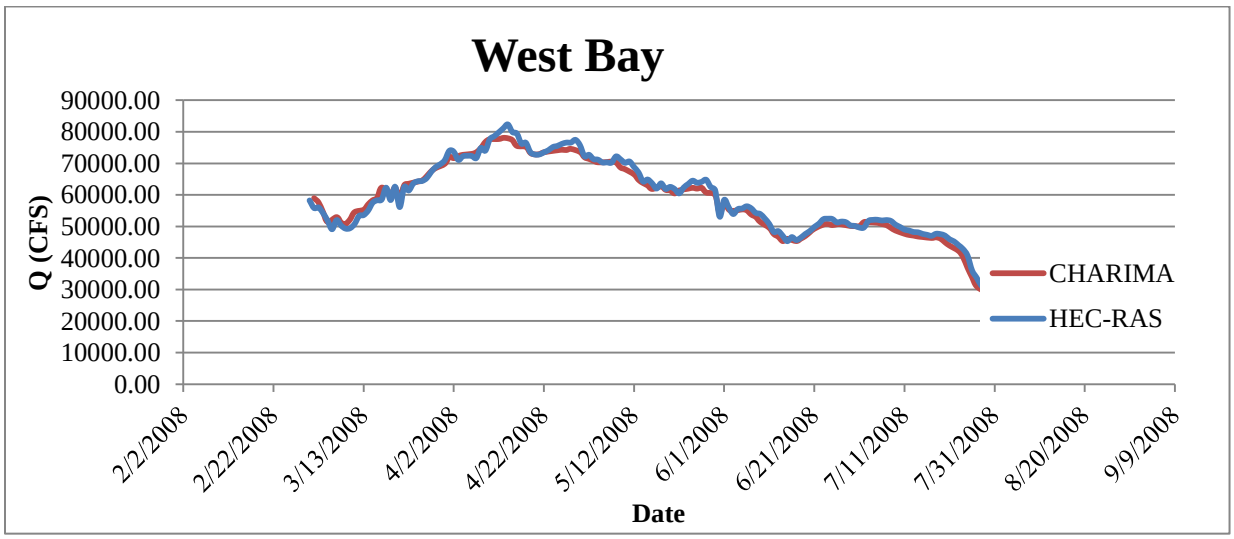
West Bay
90000.00
80000.00
70000.00
60000.00
50000.00
40000.00
30000.00
20000.00
10000.00
0.00
Q (CFS)
CHARIMA
HEC-RAS
2/2/2008
2/22/2008
3/13/2008
4/2/2008
4/22/2008
5/12/2008
6/1/2008
6/21/2008
7/11/2008
7/31/2008
8/20/2008
9/9/2008
Date

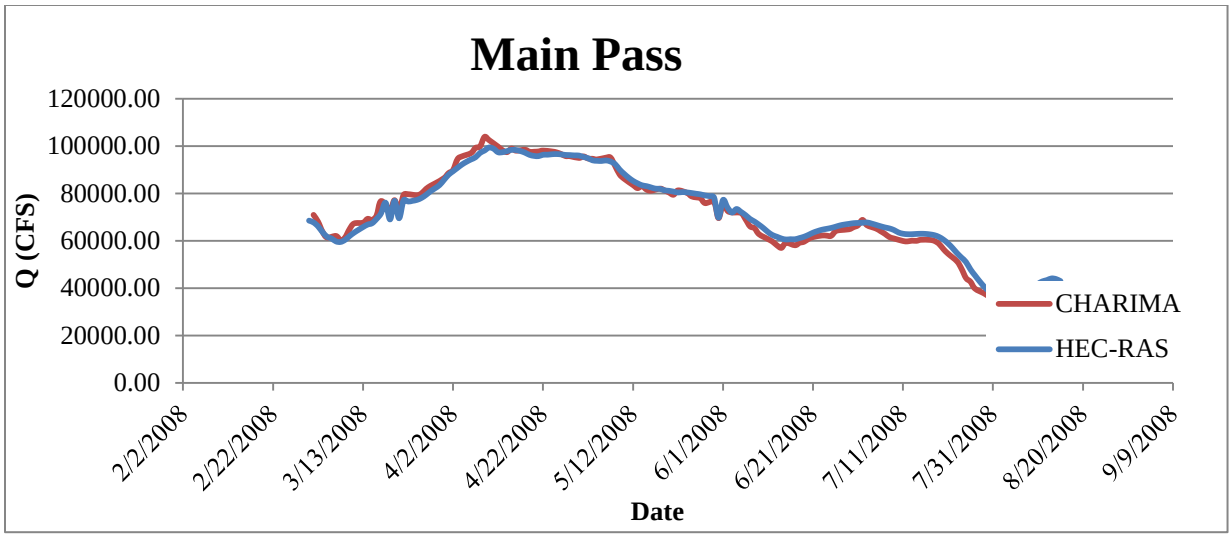
Main Pass
120000.00
100000.00
80000.00
60000.00
40000.00
20000.00
0.00
Q (CFS)
2/2/2008
2/22/2008
3/13/2008
4/2/2008
4/22/2008
5/12/2008
6/1/2008
6/21/2008
7/11/2008
7/31/2008
8/20/2008
9/9/2008
Date
CHARIMA
HEC-RAS

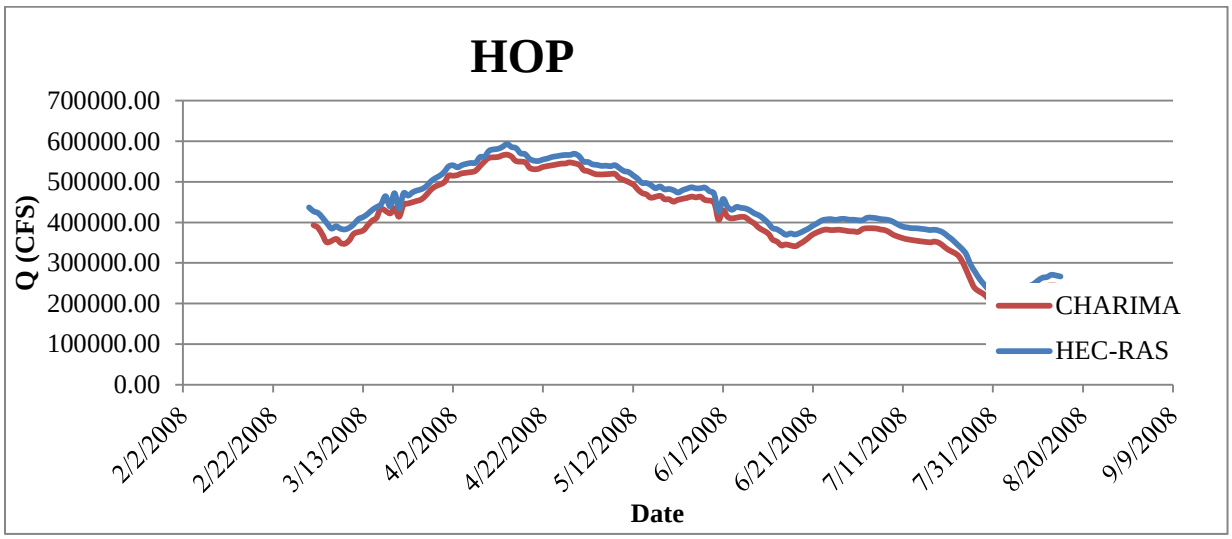
HOP
700000.00
600000.00
500000.00
400000.00
300000.00
200000.00
100000.00
0.00
Q (CFS)
2/2/2008
2/22/2008
3/13/2008
4/2/2008
4/22/2008
5/12/2008
6/1/2008
6/21/2008
7/11/2008
7/31/2008
8/20/2008
9/9/2008
Date
CHARIMA
HEC-RAS

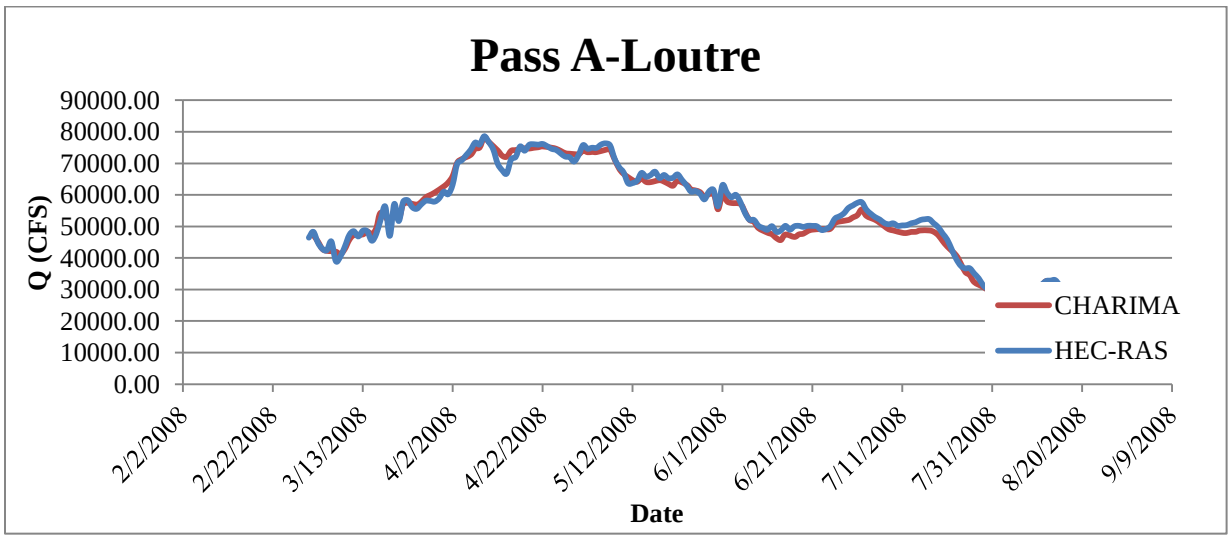
Pass A-Loutre
90000.00
80000.00
70000.00
60000.00
50000.00
40000.00
30000.00
20000.00
10000.00
0.00
Q (CFS)
2/2/2008
2/22/2008
3/13/2008
4/2/2008
4/22/2008
5/12/2008
6/1/2008
6/21/2008
7/11/2008
7/31/2008
8/20/2008
9/9/2008
Date
CHARIMA
HEC-RAS

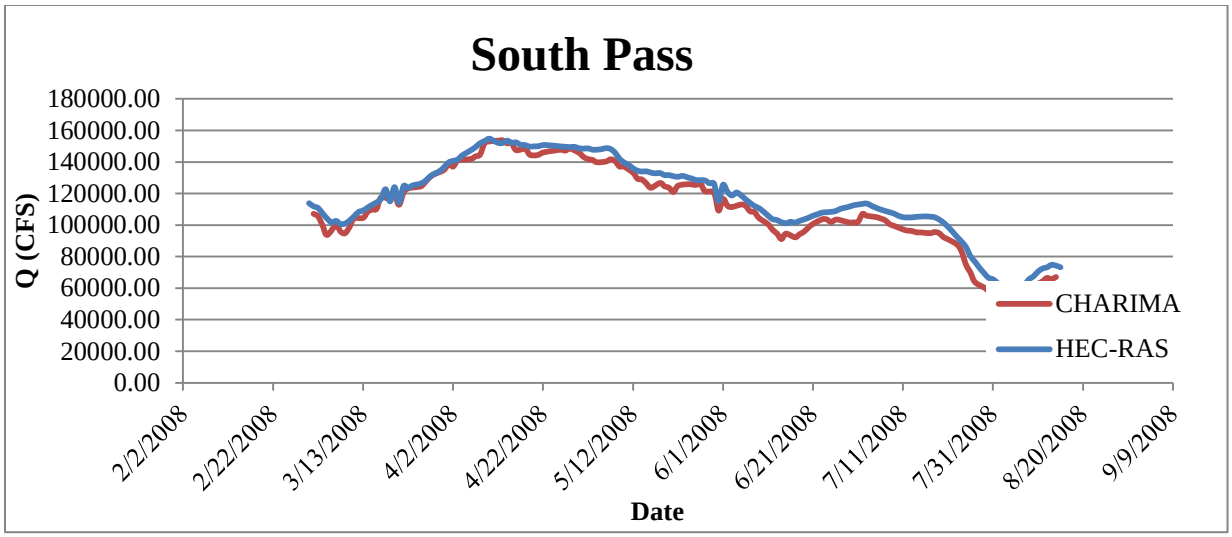
South Pass
180000.00
160000.00
140000.00
120000.00
100000.00
80000.00
60000.00
40000.00
20000.00
0.00
Q (CFS)
2/2/2008
2/22/2008
3/13/2008
4/2/2008
4/22/2008
5/12/2008
6/1/2008
6/21/2008
7/11/2008
7/31/2008
8/20/2008
9/9/2008
Date
CHARIMA
HEC-RAS

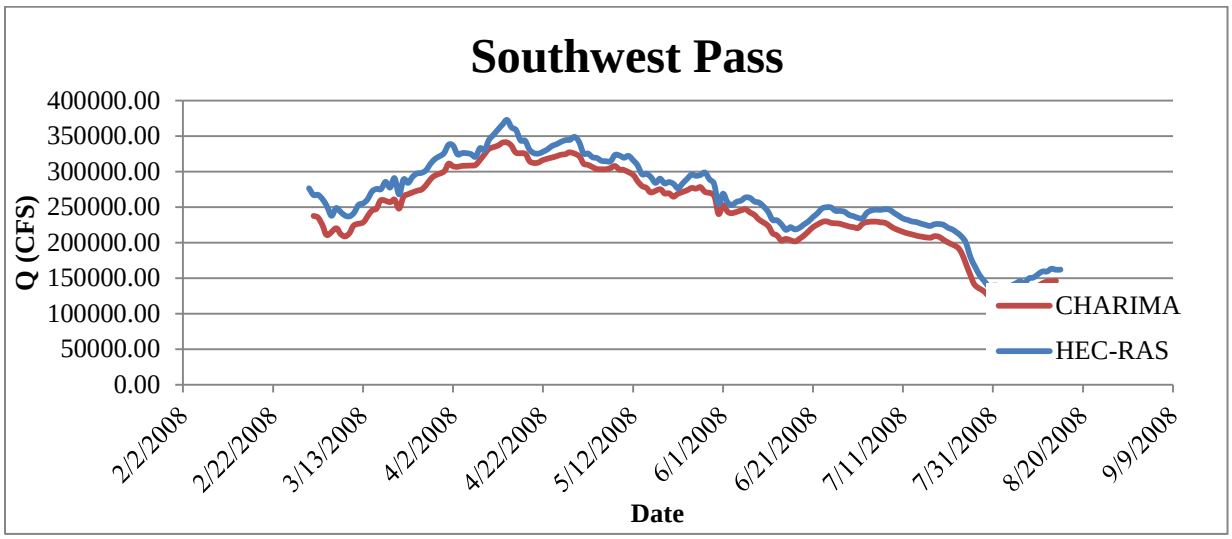
Southwest Pass
400000.00
350000.00
300000.00
250000.00
200000.00
150000.00
100000.00
50000.00
0.00
Q (CFS)
2/2/2008
2/22/2008
3/13/2008
4/2/2008
4/22/2008
5/12/2008
6/1/2008
6/21/2008
7/11/2008
7/31/2008
8/20/2008
9/9/2008
Date
CHARIMA
HEC-RAS

Hurricane Gustav (2008) Calibration:

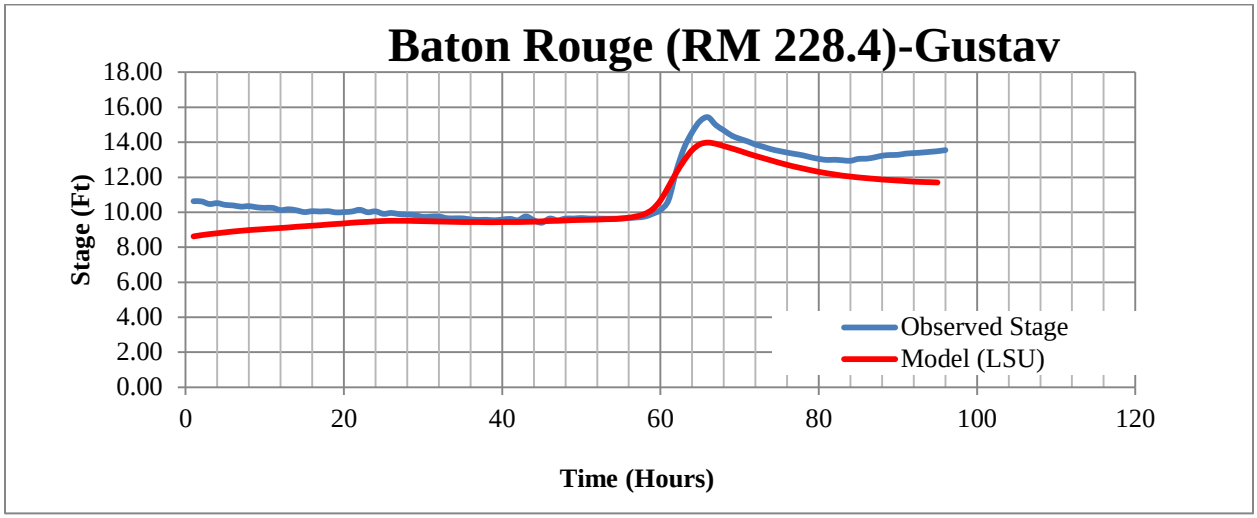

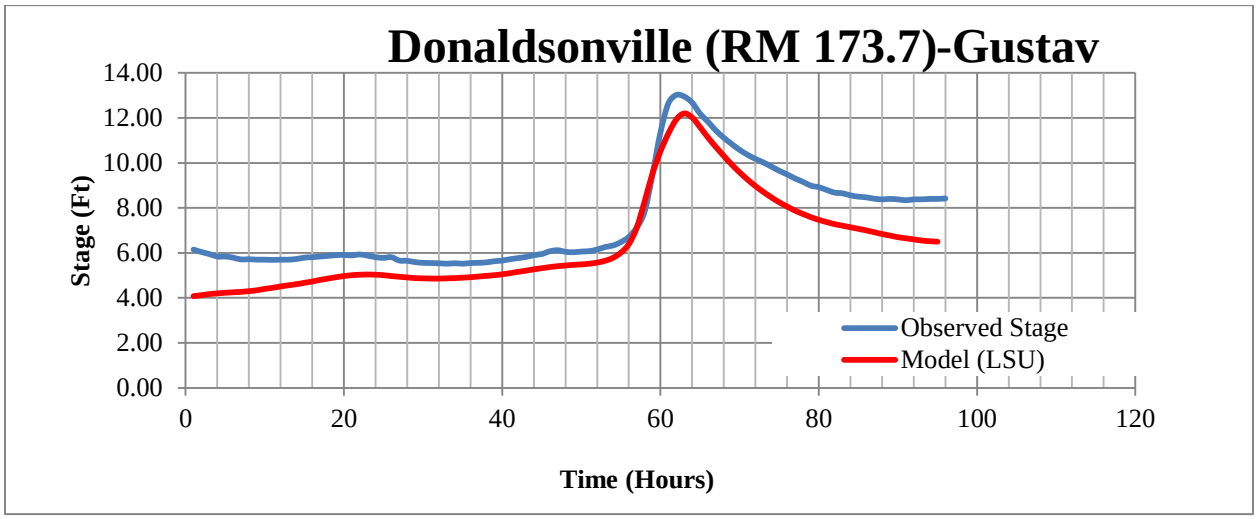

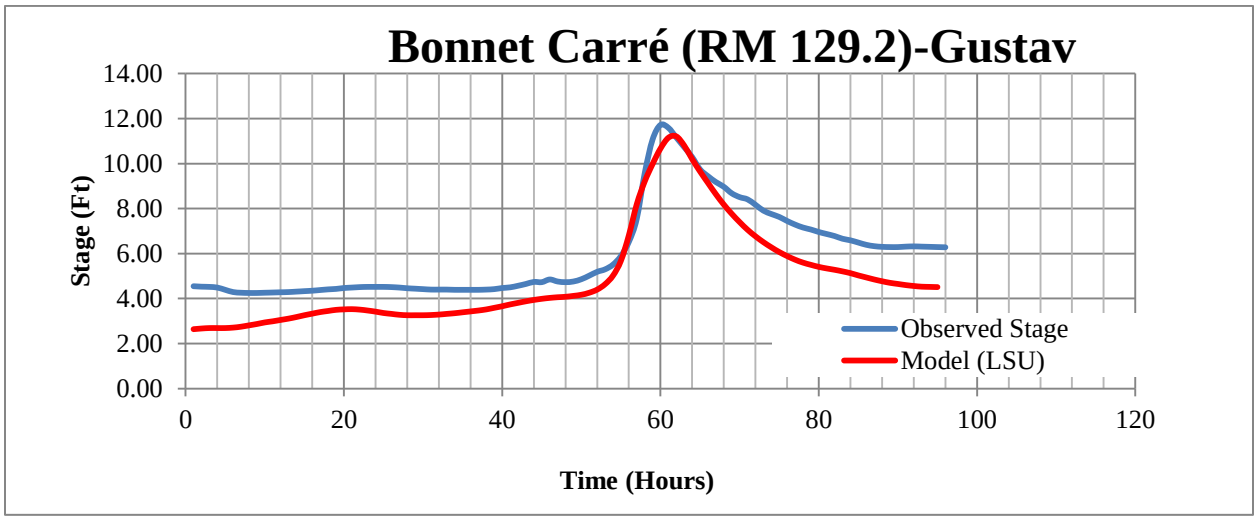

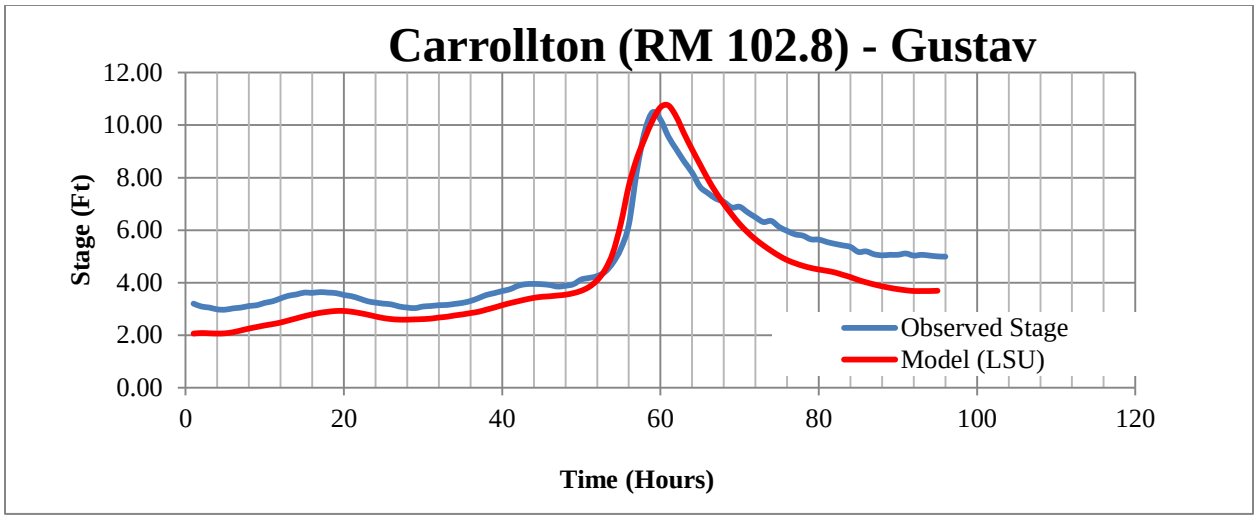
Carrollton (RM 102.8) - Gustav
Stage (Ft)
12.00
10.00
8.00
6.00
4.00
2.00
0.00
0
20
40
60
80
100
120
Time (Hours)
Observed Stage
Model (LSU)

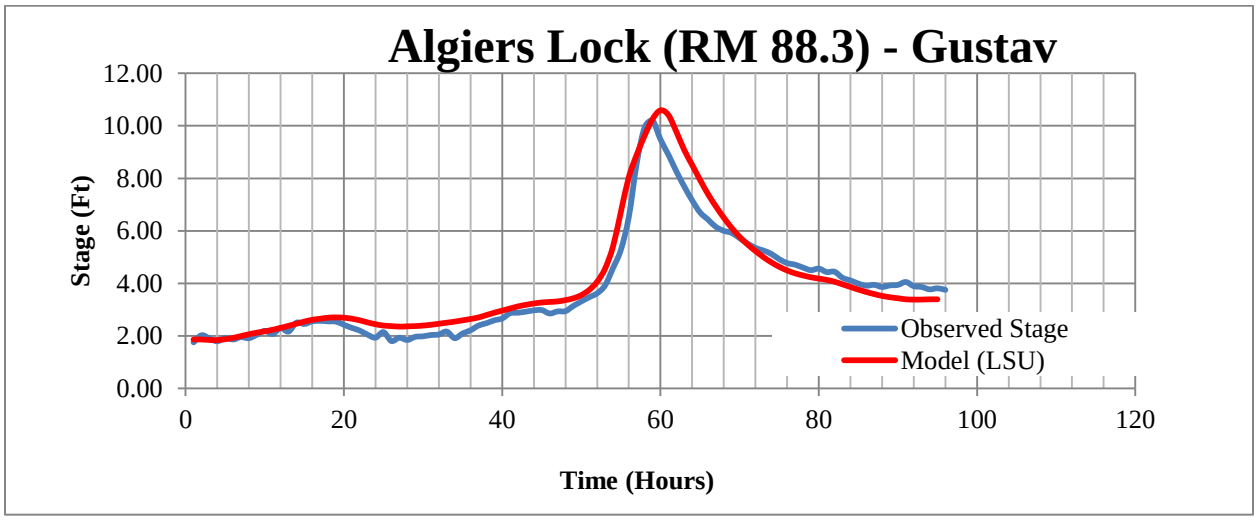
Algiers Lock (RM 88.3) - Gustav
Stage (Ft)
12.00
10.00
8.00
6.00
4.00
2.00
0.00
0
20
40
60
80
100
120
Time (Hours)
Observed Stage
Model (LSU)

Hurricane Isaac (2012) validation:

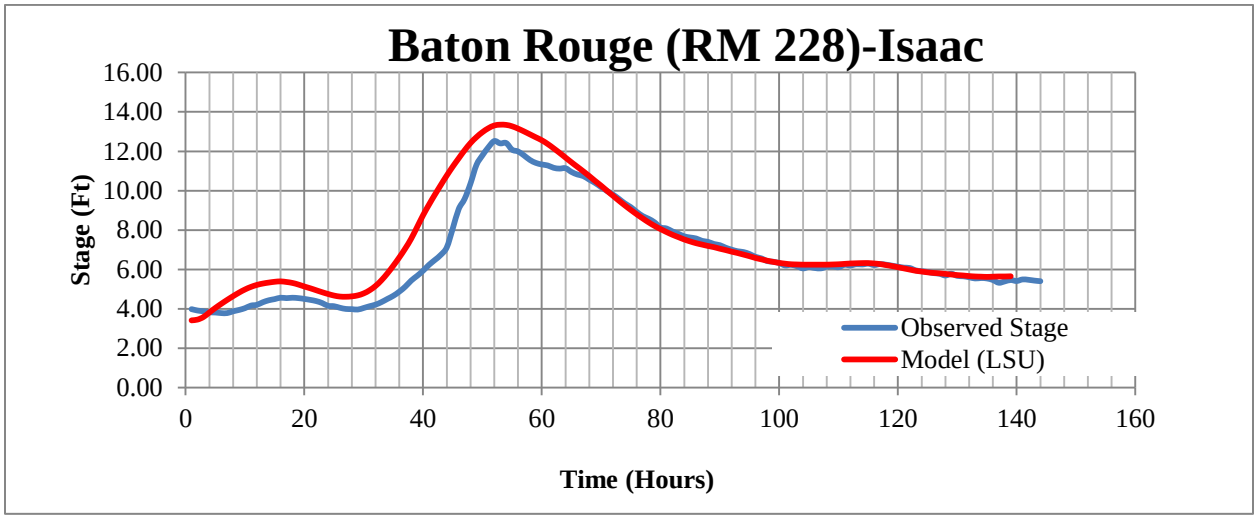

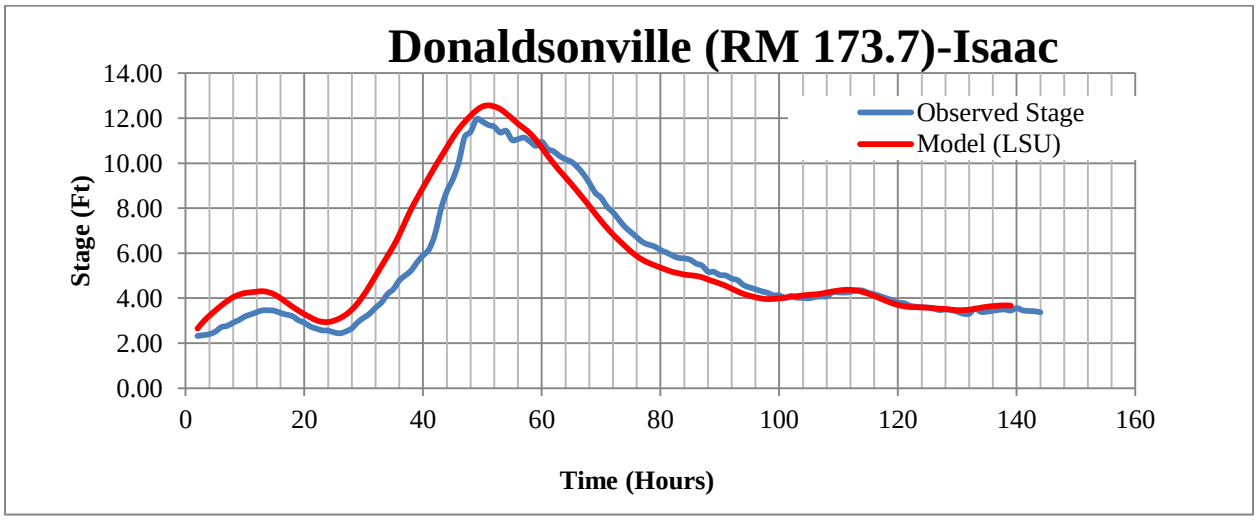

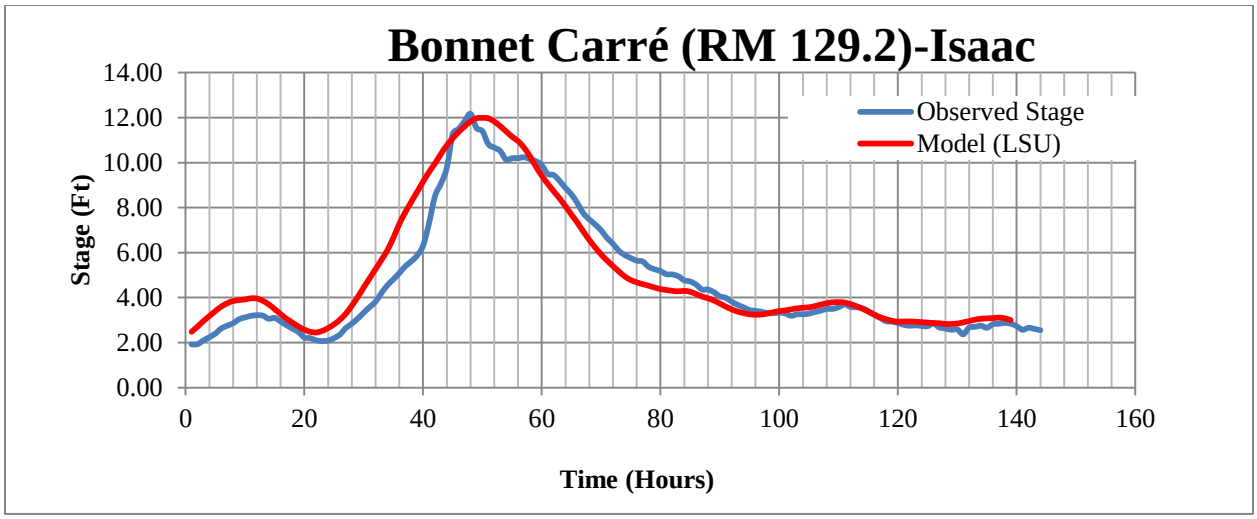
Bonnet Carré (RM 129.2)-Isaac
Observed Stage
Model (LSU)
Stage (Ft)
Time (Hours)
14.00
12.00
10.00
8.00
6.00
4.00
2.00
0.00
0
20
40
60
80
100
120
140
160

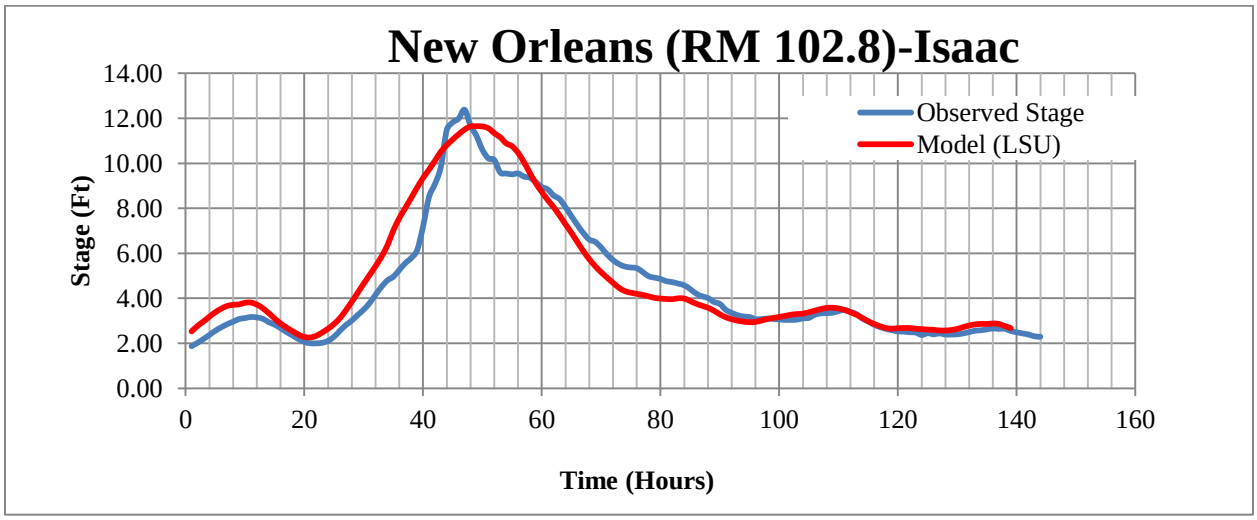
New Orleans (RM 102.8)-Isaac
Observed Stage
Model (LSU)
Stage (Ft)
Time (Hours)
14.00
12.00
10.00
8.00
6.00
4.00
2.00
0.00
0
20
40
60
80
100
120
140
160

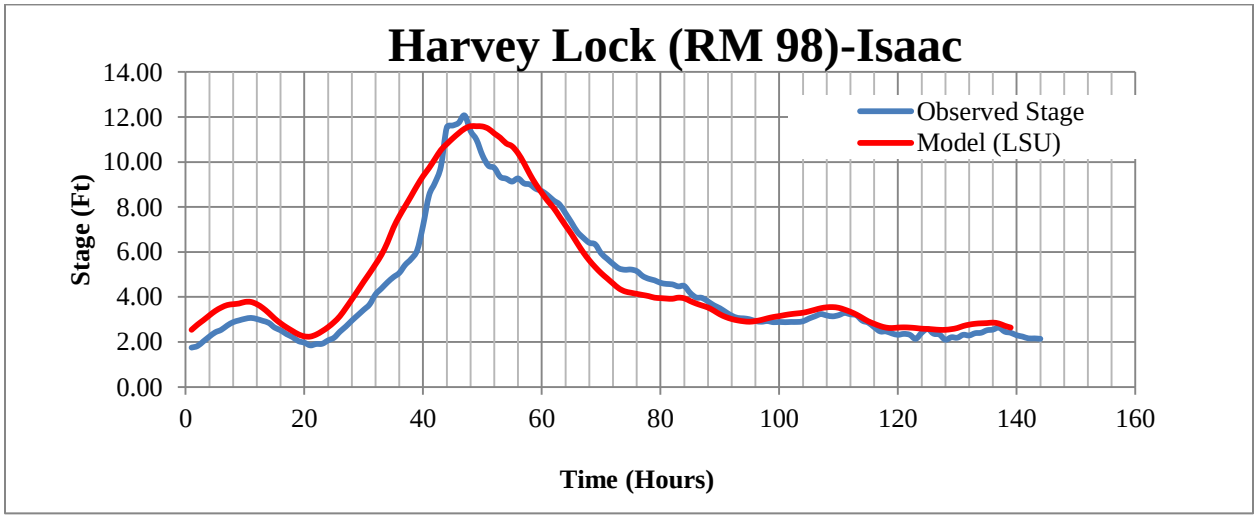
Harvey Lock (RM 98)-Isaac
Observed Stage
Model (LSU)
Stage (Ft)
Time (Hours)
14.00
12.00
10.00
8.00
6.00
4.00
2.00
0.00
0
20
40
60
80
100
120
140
160

Appendix C

Manning's n Values in HEC-RAS model

Manning's n values for Mississippi River main channel						
Number	**Reach**	**River Station**	**Friction (n/K)**	**Left Bank**	**Channel**	**Right Bank**
1	Reach 1	306.0	n	0.024	0.026	
2	Reach 1	305.8	n	0.024	0.026	
3	Reach 1	305.6	n	0.024	0.026	
4	Reach 1	305.4	n	0.026	0.024	0.026
5	Reach 1	305.2	n	0.026	0.024	0.026
6	Reach 1	305.0	n	0.026	0.024	0.026
7	Reach 1	304.8	n	0.026	0.024	0.026
8	Reach 1	304.5	n	0.026	0.024	0.026
9	Reach 1	304.2	n	0.024	0.026	
10	Reach 1	303.7	n	0.024	0.026	
11	Reach 1	303.2	n	0.026	0.024	0.026
12	Reach 1	302.7	n	0.026	0.024	0.026
13	Reach 1	302.3	n	0.026	0.024	0.026
14	Reach 1	302.0	n	0.026	0.024	0.026
15	Reach 1	301.7	n	0.026	0.024	0.026
16	Reach 1	301.2	n	0.024	0.026	
17	Reach 1	300.9	n	0.024	0.026	
18	Reach 1	300.5	n	0.024	0.026	
19	Reach 1	300.1	n	0.024	0.026	
20	Reach 1	299.7	n	0.026	0.024	0.026
21	Reach 1	299.4	n	0.026	0.024	0.026
22	Reach 1	299.0	n	0.026	0.024	0.026
23	Reach 1	298.5	n	0.024	0.026	
24	Reach 1	298.1	n	0.026	0.024	0.026
25	Reach 1	297.6	n	0.026	0.024	0.026
26	Reach 1	297.3	n	0.026	0.024	0.026
27	Reach 1	296.9	n	0.026	0.024	0.026
28	Reach 1	296.6	n	0.026	0.024	0.026
29	Reach 1	296.5	Lateral structure			
30	Reach 1	296.3	n	0.026	0.024	0.026
31	Reach 1	296.0	n	0.026	0.024	0.026
32	Reach 1	295.7	n	0.026	0.024	0.026
33	Reach 1	295.3	n	0.026	0.024	0.026
34	Reach 1	295.0	n	0.024	0.026	
35	Reach 1	294.7	n	0.024	0.026	
36	Reach 1	294.3	n	0.024	0.026	
37	Reach 1	293.9	n	0.026	0.024	0.026
38	Reach 1	293.5	n	0.024	0.026	

39	Reach 1	293.1	n	0.026	0.024	0.026
40	Reach 1	292.7	n	0.024	0.026	
41	Reach 1	292.3	n	0.024	0.026	
42	Reach 1	292.0	n	0.024	0.026	
43	Reach 1	291.7	n	0.024	0.026	
44	Reach 1	291.3	n	0.024	0.026	
45	Reach 1	290.9	n	0.024	0.026	
46	Reach 1	290.6	n	0.026	0.024	0.026
47	Reach 1	290.2	n	0.026	0.024	0.026
48	Reach 1	289.9	n	0.026	0.024	0.026
49	Reach 1	289.5	n	0.026	0.024	0.026
50	Reach 1	289.2	n	0.026	0.024	0.026
51	Reach 1	289.0	n	0.026	0.024	0.026
52	Reach 1	288.7	n	0.026	0.024	0.026
53	Reach 1	288.4	n	0.026	0.024	0.026
54	Reach 1	288.1	n	0.026	0.024	0.026
55	Reach 1	287.8	n	0.026	0.024	0.026
56	Reach 1	287.5	n	0.026	0.024	0.026
57	Reach 1	287.2	n	0.026	0.024	0.026
58	Reach 1	287.0	n	0.026	0.024	0.026
59	Reach 1	286.8	n	0.026	0.024	0.026
60	Reach 1	286.6	n	0.026	0.024	0.026
61	Reach 1	286.2	n	0.026	0.024	0.026
62	Reach 1	285.9	n	0.026	0.024	0.026
63	Reach 1	285.6	n	0.026	0.024	0.026
64	Reach 1	285.3	n	0.026	0.024	0.026
65	Reach 1	285.0	n	0.026	0.024	0.026
66	Reach 1	284.6	n	0.026	0.024	0.026
67	Reach 1	284.3	n	0.026	0.024	0.026
68	Reach 1	284.0	n	0.026	0.024	0.026
69	Reach 1	283.6	n	0.026	0.024	0.026
70	Reach 1	283.3	n	0.026	0.024	0.026
71	Reach 1	282.9	n	0.026	0.024	0.026
72	Reach 1	282.5	n	0.026	0.024	0.026
73	Reach 1	282.1	n	0.024	0.026	
74	Reach 1	281.8	n	0.026	0.024	0.026
75	Reach 1	281.4	n	0.026	0.024	0.026
76	Reach 1	281.2	n	0.026	0.024	0.026
77	Reach 1	280.8	n	0.026	0.024	0.026
78	Reach 1	280.5	n	0.026	0.024	0.026
79	Reach 1	280.1	n	0.026	0.024	0.026

80	Reach 1	279.8	n	0.026	0.024	0.026
81	Reach 1	279.4	n	0.026	0.024	0.026
82	Reach 1	279.1	n	0.026	0.024	0.026
83	Reach 1	278.8	n	0.026	0.024	0.026
84	Reach 1	278.5	n	0.024	0.026	
85	Reach 1	278.2	n	0.024	0.026	
86	Reach 1	277.9	n	0.024	0.026	
87	Reach 1	277.6	n	0.026	0.024	0.026
88	Reach 1	277.3	n	0.026	0.024	0.026
89	Reach 1	277.0	n	0.026	0.024	0.026
90	Reach 1	276.7	n	0.026	0.024	0.026
91	Reach 1	276.4	n	0.026	0.024	0.026
92	Reach 1	276.1	n	0.026	0.024	0.026
93	Reach 1	275.8	n	0.026	0.024	0.026
94	Reach 1	275.5	n	0.026	0.024	0.026
95	Reach 1	275.2	n	0.026	0.024	0.026
96	Reach 1	274.9	n	0.026	0.024	0.026
97	Reach 1	274.6	n	0.026	0.024	0.026
98	Reach 1	274.3	n	0.026	0.024	0.026
99	Reach 1	274.1	n	0.026	0.024	0.026
100	Reach 1	273.7	n	0.026	0.024	0.026
101	Reach 1	273.5	n	0.026	0.024	0.026
102	Reach 1	273.2	n	0.026	0.024	0.026
103	Reach 1	272.9	n	0.026	0.024	0.026
104	Reach 1	272.6	n	0.024	0.026	
105	Reach 1	272.3	n	0.024	0.026	
106	Reach 1	271.8	n	0.024	0.026	
107	Reach 1	271.4	n	0.024	0.026	
108	Reach 1	271	n	0.024	0.026	
109	Reach 1	270.6	n	0.024	0.026	
110	Reach 1	270.2	n	0.024	0.026	
111	Reach 1	269.9	n	0.024	0.026	
112	Reach 1	269.6	n	0.024	0.026	
113	Reach 1	269.3	n	0.024	0.026	
114	Reach 1	269	n	0.024	0.026	
115	Reach 1	268.7	n	0.024	0.026	
116	Reach 1	268.4	n	0.024	0.026	
117	Reach 1	268.1	n	0.024	0.026	
118	Reach 1	267.8	n	0.024	0.026	
119	Reach 1	267.4	n	0.024	0.026	
120	Reach 1	267.1	n	0.024	0.026	

121	Reach 1	266.8	n	0.024	0.026	
122	Reach 1	266.4	n	0.026	0.024	0.026
123	Reach 1	266	n	0.024	0.026	
124	Reach 1	265.6	n	0.026	0.024	0.026
125	Reach 1	265.1	n	0.026	0.024	0.026
126	Reach 1	264.6	n	0.024	0.026	
127	Reach 1	264.2	n	0.026	0.024	0.026
128	Reach 1	263.8	n	0.026	0.024	0.026
129	Reach 1	263.4	n	0.024	0.026	
130	Reach 1	263.1	n	0.024	0.026	
131	Reach 1	262.7	n	0.026	0.024	0.026
132	Reach 1	262.3	n	0.026	0.024	0.026
133	Reach 1	261.9	n	0.026	0.024	0.026
134	Reach 1	261.5	n	0.026	0.024	0.026
135	Reach 1	261.2	n	0.026	0.024	0.026
136	Reach 1	260.9	n	0.026	0.024	0.026
137	Reach 1	260.6	n	0.026	0.024	0.026
138	Reach 1	260.3	n	0.026	0.024	0.026
139	Reach 1	260	n	0.026	0.024	0.026
140	Reach 1	259.7	n	0.026	0.024	0.026
141	Reach 1	259.3	n	0.026	0.024	0.026
142	Reach 1	259.1	n	0.026	0.024	0.026
143	Reach 1	258.7	n	0.026	0.024	0.026
144	Reach 1	258.4	n	0.026	0.024	0.026
145	Reach 1	258	n	0.024	0.026	
146	Reach 1	257.6	n	0.026	0.024	0.026
147	Reach 1	257.3	n	0.026	0.024	0.026
148	Reach 1	257	n	0.026	0.024	0.026
149	Reach 1	256.6	n	0.026	0.024	0.026
150	Reach 1	256.2	n	0.026	0.024	0.026
151	Reach 1	255.9	n	0.026	0.024	0.026
152	Reach 1	255.6	n	0.026	0.024	0.026
153	Reach 1	255.2	n	0.024	0.026	
154	Reach 1	254.8	n	0.024	0.026	
155	Reach 1	254.5	n	0.024	0.026	
156	Reach 1	254.2	n	0.024	0.026	
157	Reach 1	253.6	n	0.026	0.024	0.026
158	Reach 1	253.3	n	0.026	0.024	0.026
159	Reach 1	253	n	0.026	0.024	0.026
160	Reach 1	252.7	n	0.026	0.024	0.026
161	Reach 1	252.4	n	0.026	0.024	0.026

162	Reach 1	251.9	n	0.026	0.024	0.026
163	Reach 1	251.1	n	0.026	0.024	0.026
164	Reach 1	250.6	n	0.026	0.024	0.026
165	Reach 1	250.2	n	0.026	0.024	0.026
166	Reach 1	249.8	n	0.026	0.024	0.026
167	Reach 1	249.3	n	0.026	0.024	0.026
168	Reach 1	248.8	n	0.024	0.026	
169	Reach 1	248.3	n	0.026	0.024	0.026
170	Reach 1	247.8	n	0.026	0.024	0.026
171	Reach 1	247.5	n	0.026	0.024	0.026
172	Reach 1	247.1	n	0.026	0.024	0.026
173	Reach 1	246.8	n	0.026	0.024	0.026
174	Reach 1	246.5	n	0.026	0.024	0.026
175	Reach 1	246.2	n	0.026	0.024	0.026
176	Reach 1	245.8	n	0.026	0.024	0.026
177	Reach 1	245.6	n	0.026	0.024	0.026
178	Reach 1	245.3	n	0.026	0.024	0.026
179	Reach 1	245.1	n	0.024	0.026	
180	Reach 1	244.9	n	0.024	0.026	
181	Reach 1	244.7	n	0.026	0.024	0.026
182	Reach 1	244.5	n	0.026	0.024	0.026
183	Reach 1	244.2	n	0.026	0.024	0.026
184	Reach 1	244.1	n	0.026	0.024	0.026
185	Reach 1	243.9	n	0.024	0.026	
186	Reach 1	243.7	n	0.026	0.024	0.026
187	Reach 1	243.5	n	0.026	0.024	0.026
188	Reach 1	243.2	n	0.026	0.024	0.026
189	Reach 1	242.9	n	0.026	0.024	0.026
190	Reach 1	242.6	n	0.026	0.024	0.026
191	Reach 1	242.3	n	0.026	0.024	0.026
192	Reach 1	242.1	n	0.026	0.024	0.026
193	Reach 1	241.8	n	0.026	0.024	0.026
194	Reach 1	241.6	n	0.026	0.024	0.026
195	Reach 1	241.4	n	0.026	0.024	0.026
196	Reach 1	241.1	n	0.026	0.024	0.026
197	Reach 1	240.9	n	0.026	0.024	0.026
198	Reach 1	240.6	n	0.026	0.024	0.026
199	Reach 1	240.4	n	0.024	0.026	
200	Reach 1	240.3	n	0.024	0.026	
201	Reach 1	240	n	0.024	0.026	
202	Reach 1	239.8	n	0.026	0.024	0.026

203	Reach 1	239.6	n	0.024	0.026	
204	Reach 1	239.4	n	0.026	0.024	0.026
205	Reach 1	239.1	n	0.024	0.026	
206	Reach 1	238.9	n	0.024	0.026	
207	Reach 1	238.6	n	0.024	0.026	
208	Reach 1	238.3	n	0.026	0.024	0.026
209	Reach 1	238.1	n	0.026	0.024	0.026
210	Reach 1	237.8	n	0.024	0.026	
211	Reach 1	237.5	n	0.024	0.026	
212	Reach 1	237.2	n	0.024	0.026	
213	Reach 1	236.9	n	0.024	0.026	
214	Reach 1	236.5	n	0.024	0.026	
215	Reach 1	236.2	n	0.024	0.026	
216	Reach 1	235.9	n	0.026	0.024	0.026
217	Reach 1	235.7	n	0.024	0.026	
218	Reach 1	235.4	n	0.024	0.026	
219	Reach 1	235.1	n	0.024	0.026	
220	Reach 1	234.8	n	0.024	0.026	
221	Reach 1	234.6	n	0.024	0.026	
222	Reach 1	234.4	n	0.024	0.026	
223	Reach 1	234.2	n	0.024	0.026	
224	Reach 1	234	n	0.024	0.026	
225	Reach 1	233.8	n	0.024	0.026	
226	Reach 1	233.6	n	0.024	0.026	
227	Reach 1	233.4	n	0.024	0.026	
228	Reach 1	233.2	n	0.024	0.026	
229	Reach 1	233	n	0.024	0.026	
230	Reach 1	232.8	n	0.024	0.026	
231	Reach 1	232.5	n	0.024	0.026	
232	Reach 1	232.3	n	0.024	0.026	
233	Reach 1	232	n	0.024	0.026	
234	Reach 1	231.8	n	0.024	0.026	
235	Reach 1	231.5	n	0.024	0.026	
236	Reach 1	231.2	n	0.024	0.026	
237	Reach 1	230.9	n	0.024	0.026	
238	Reach 1	230.6	n	0.024	0.026	
239	Reach 1	230.4	n	0.024	0.026	
240	Reach 1	230.1	n	0.024	0.026	
241	Reach 1	229.8	n	0.024	0.026	
242	Reach 1	229.6	n	0.024	0.026	
243	Reach 1	229.4	n	0.024	0.026	

244	Reach 1	229.2	n	0.026	0.024	0.026
245	Reach 1	229	n	0.024	0.026	
246	Reach 1	228.7	n	0.026	0.024	0.026
247	Reach 1	228.5	n	0.024	0.026	
248	Reach 1	228.3	n	0.024	0.026	
249	Reach 1	228.1	n	0.024	0.026	
250	Reach 1	227.8	n	0.024	0.026	
251	Reach 1	227.6	n	0.026	0.024	0.026
252	Reach 1	227.4	n	0.024	0.026	
253	Reach 1	227.2	n	0.024	0.026	
254	Reach 1	226.9	n	0.026	0.024	0.026
255	Reach 1	226.6	n	0.024	0.026	
256	Reach 1	226.4	n	0.024	0.026	
257	Reach 1	226.1	n	0.024	0.026	
258	Reach 1	225.8	n	0.024	0.026	
259	Reach 1	225.5	n	0.026	0.024	0.026
260	Reach 1	225.2	n	0.026	0.024	0.026
261	Reach 1	225	n	0.026	0.024	0.026
262	Reach 1	224.7	n	0.026	0.024	0.026
263	Reach 1	224.5	n	0.026	0.024	0.026
264	Reach 1	224.2	n	0.026	0.024	0.026
265	Reach 1	223.9	n	0.024	0.026	
266	Reach 1	223.6	n	0.026	0.024	0.026
267	Reach 1	223.3	n	0.026	0.024	0.026
268	Reach 1	223.1	n	0.024	0.026	
269	Reach 1	222.9	n	0.024	0.026	
270	Reach 1	222.6	n	0.024	0.026	
271	Reach 1	222.4	n	0.024	0.026	
272	Reach 1	222.1	n	0.024	0.026	
273	Reach 1	221.8	n	0.026	0.024	0.026
274	Reach 1	221.5	n	0.024	0.026	
275	Reach 1	221.2	n	0.024	0.026	
276	Reach 1	220.9	n	0.024	0.026	
277	Reach 1	220.6	n	0.026	0.024	0.026
278	Reach 1	220.3	n	0.024	0.026	
279	Reach 1	220	n	0.024	0.026	
280	Reach 1	219.7	n	0.024	0.026	
281	Reach 1	219.4	n	0.026	0.024	0.026
282	Reach 1	219.1	n	0.026	0.024	0.026
283	Reach 1	218.8	n	0.024	0.026	
284	Reach 1	218.6	n	0.024	0.026	

285	Reach 1	218.3	n	0.024	0.026	
286	Reach 1	217.9	n	0.024	0.026	
287	Reach 1	217.6	n	0.024	0.026	
288	Reach 1	217.3	n	0.024	0.026	
289	Reach 1	216.9	n	0.024	0.026	
290	Reach 1	216.6	n	0.024	0.026	
291	Reach 1	216.4	n	0.024	0.026	
292	Reach 1	216.1	n	0.024	0.026	
293	Reach 1	215.8	n	0.024	0.026	
294	Reach 1	215.5	n	0.026	0.024	0.026
295	Reach 1	215.3	n	0.024	0.026	
296	Reach 1	215.1	n	0.024	0.026	
297	Reach 1	214.9	n	0.024	0.026	
298	Reach 1	214.7	n	0.024	0.026	
299	Reach 1	214.5	n	0.024	0.026	
300	Reach 1	214.2	n	0.024	0.026	
301	Reach 1	214	n	0.024	0.026	
302	Reach 1	213.7	n	0.024	0.026	
303	Reach 1	213.5	n	0.026	0.024	0.026
304	Reach 1	213.2	n	0.024	0.026	
305	Reach 1	212.9	n	0.024	0.026	
306	Reach 1	212.5	n	0.024	0.026	
307	Reach 1	212.1	n	0.024	0.026	
308	Reach 1	211.8	n	0.026	0.024	0.026
309	Reach 1	211.5	n	0.024	0.026	
310	Reach 1	211.2	n	0.024	0.026	
311	Reach 1	210.9	n	0.024	0.026	
312	Reach 1	210.6	n	0.024	0.026	
313	Reach 1	210.3	n	0.024	0.026	
314	Reach 1	210	n	0.024	0.026	
315	Reach 1	209.7	n	0.026	0.024	0.026
316	Reach 1	209.4	n	0.024	0.026	
317	Reach 1	209.2	n	0.024	0.026	
318	Reach 1	208.9	n	0.024	0.026	
319	Reach 1	208.7	n	0.026	0.024	0.026
320	Reach 1	208.5	n	0.026	0.024	0.026
321	Reach 1	208.2	n	0.026	0.024	0.026
322	Reach 1	208	n	0.024	0.026	
323	Reach 1	207.7	n	0.024	0.026	
324	Reach 1	207.4	n	0.024	0.026	
325	Reach 1	207.1	n	0.024	0.026	

326	Reach 1	206.8	n	0.026	0.024	0.026
327	Reach 1	206.6	n	0.024	0.026	
328	Reach 1	206.4	n	0.024	0.026	
329	Reach 1	206.2	n	0.026	0.024	0.026
330	Reach 1	205.9	n	0.024	0.026	
331	Reach 1	205.6	n	0.024	0.026	
332	Reach 1	205.4	n	0.024	0.026	
333	Reach 1	205.1	n	0.024	0.026	
334	Reach 1	204.8	n	0.024	0.026	
335	Reach 1	204.5	n	0.024	0.026	
336	Reach 1	204.3	n	0.024	0.026	
337	Reach 1	203.9	n	0.024	0.026	
338	Reach 1	203.6	n	0.024	0.026	
339	Reach 1	203.3	n	0.024	0.026	
340	Reach 1	203	n	0.024	0.026	
341	Reach 1	202.7	n	0.024	0.026	
342	Reach 1	202.4	n	0.024	0.026	
343	Reach 1	202.1	n	0.024	0.026	
344	Reach 1	201.9	n	0.024	0.026	
345	Reach 1	201.6	n	0.024	0.026	
346	Reach 1	201.3	n	0.024	0.026	
347	Reach 1	201	n	0.024	0.026	
348	Reach 1	200.7	n	0.024	0.026	
349	Reach 1	200.5	n	0.026	0.024	0.026
350	Reach 1	200.3	n	0.026	0.024	0.026
351	Reach 1	200.1	n	0.026	0.024	0.026
352	Reach 1	199.9	n	0.026	0.024	0.026
353	Reach 1	199.6	n	0.024	0.026	
354	Reach 1	199.4	n	0.024	0.026	
355	Reach 1	199.1	n	0.024	0.026	
356	Reach 1	198.8	n	0.024	0.026	
357	Reach 1	198.5	n	0.024	0.026	
358	Reach 1	198.2	n	0.026	0.024	0.026
359	Reach 1	197.9	n	0.026	0.024	0.026
360	Reach 1	197.6	n	0.026	0.024	0.026
361	Reach 1	197.3	n	0.026	0.024	0.026
362	Reach 1	197.1	n	0.024	0.026	
363	Reach 1	196.9	n	0.024	0.026	
364	Reach 1	196.6	n	0.026	0.024	0.026
365	Reach 1	196.4	n	0.026	0.024	0.026
366	Reach 1	196.1	n	0.024	0.026	

367	Reach 1	195.9	n	0.024	0.026	
368	Reach 1	195.6	n	0.024	0.026	
369	Reach 1	195.4	n	0.024	0.026	
370	Reach 1	195.1	n	0.024	0.026	
371	Reach 1	194.9	n	0.024	0.026	
372	Reach 1	194.6	n	0.024	0.026	
373	Reach 1	194.4	n	0.024	0.026	
374	Reach 1	194.1	n	0.026	0.024	0.026
375	Reach 1	193.9	n	0.024	0.026	
376	Reach 1	193.7	n	0.024	0.026	
377	Reach 1	193.4	n	0.024	0.026	
378	Reach 1	193.3	n	0.024	0.026	
379	Reach 1	193	n	0.024	0.026	
380	Reach 1	192.8	n	0.024	0.026	
381	Reach 1	192.5	n	0.024	0.026	
382	Reach 1	192.2	n	0.024	0.026	
383	Reach 1	191.9	n	0.024	0.026	
384	Reach 1	191.6	n	0.026	0.024	0.026
385	Reach 1	191.3	n	0.024	0.026	
386	Reach 1	191	n	0.024	0.026	
387	Reach 1	190.7	n	0.024	0.026	
388	Reach 1	190.4	n	0.024	0.026	
389	Reach 1	190.1	n	0.024	0.026	
390	Reach 1	189.8	n	0.024	0.026	
391	Reach 1	189.5	n	0.024	0.026	
392	Reach 1	189.3	n	0.024	0.026	
393	Reach 1	189	n	0.024	0.026	
394	Reach 1	188.7	n	0.024	0.026	
395	Reach 1	188.5	n	0.024	0.026	
396	Reach 1	188.2	n	0.024	0.026	
397	Reach 1	187.9	n	0.024	0.026	
398	Reach 1	187.6	n	0.024	0.026	
399	Reach 1	187.2	n	0.024	0.026	
400	Reach 1	186.9	n	0.026	0.024	0.026
401	Reach 1	186.6	n	0.026	0.024	0.026
402	Reach 1	186.3	n	0.024	0.026	
403	Reach 1	185.9	n	0.024	0.026	
404	Reach 1	185.6	n	0.024	0.026	
405	Reach 1	185.3	n	0.024	0.026	
406	Reach 1	185	n	0.024	0.026	
407	Reach 1	184.7	n	0.024	0.026	

408	Reach 1	184.5	n	0.024	0.026	
409	Reach 1	184.2	n	0.026	0.024	0.026
410	Reach 1	184	n	0.024	0.026	
411	Reach 1	183.7	n	0.024	0.026	
412	Reach 1	183.4	n	0.026	0.024	0.026
413	Reach 1	183.1	n	0.026	0.024	0.026
414	Reach 1	182.8	n	0.026	0.024	0.026
415	Reach 1	182.5	n	0.024	0.026	
416	Reach 1	182.3	n	0.024	0.026	
417	Reach 1	182	n	0.026	0.024	0.026
418	Reach 1	181.8	n	0.024	0.026	
419	Reach 1	181.5	n	0.024	0.026	
420	Reach 1	181.3	n	0.024	0.026	
421	Reach 1	181.1	n	0.026	0.024	0.026
422	Reach 1	180.9	n	0.024	0.026	
423	Reach 1	180.6	n	0.024	0.026	
424	Reach 1	180.3	n	0.026	0.024	0.026
425	Reach 1	179.9	n	0.024	0.026	
426	Reach 1	179.7	n	0.026	0.024	0.026
427	Reach 1	179.4	n	0.026	0.024	0.026
428	Reach 1	179.1	n	0.024	0.026	
429	Reach 1	178.7	n	0.026	0.024	0.026
430	Reach 1	178.5	n	0.024	0.026	
431	Reach 1	178.2	n	0.024	0.026	
432	Reach 1	178	n	0.024	0.026	
433	Reach 1	177.8	n	0.024	0.026	
434	Reach 1	177.5	n	0.024	0.026	
435	Reach 1	177.2	n	0.024	0.026	
436	Reach 1	176.9	n	0.024	0.026	
437	Reach 1	176.7	n	0.024	0.026	
438	Reach 1	176.5	n	0.024	0.026	
439	Reach 1	176.3	n	0.024	0.026	
440	Reach 1	176	n	0.024	0.026	
441	Reach 1	175.8	n	0.024	0.026	
442	Reach 1	175.5	n	0.024	0.026	
443	Reach 1	175.2	n	0.024	0.026	
444	Reach 1	174.9	n	0.024	0.026	
445	Reach 1	174.6	n	0.024	0.026	
446	Reach 1	174.3	n	0.024	0.026	
447	Reach 1	174	n	0.024	0.026	
448	Reach 1	173.7	n	0.024	0.026	

449	Reach 1	173.4	n	0.024	0.026	
450	Reach 1	173.2	n	0.024	0.026	
451	Reach 1	172.9	n	0.024	0.026	
452	Reach 1	172.7	n	0.024	0.026	
453	Reach 1	172.5	n	0.024	0.026	
454	Reach 1	172.3	n	0.024	0.026	
455	Reach 1	172.1	n	0.024	0.026	
456	Reach 1	171.9	n	0.024	0.026	
457	Reach 1	171.7	n	0.024	0.026	
458	Reach 1	171.5	n	0.024	0.026	
459	Reach 1	171.1	n	0.024	0.026	
460	Reach 1	170.9	n	0.024	0.026	
461	Reach 1	170.7	n	0.024	0.026	
462	Reach 1	170.5	n	0.024	0.026	
463	Reach 1	170.2	n	0.024	0.026	
464	Reach 1	169.9	n	0.024	0.026	
465	Reach 1	169.7	n	0.026	0.024	0.026
466	Reach 1	169.5	n	0.024	0.026	
467	Reach 1	169.3	n	0.024	0.026	
468	Reach 1	169.1	n	0.024	0.026	
469	Reach 1	168.8	n	0.024	0.026	
470	Reach 1	168.6	n	0.024	0.026	
471	Reach 1	168.4	n	0.024	0.026	
472	Reach 1	168.1	n	0.024	0.026	
473	Reach 1	167.8	n	0.024	0.026	
474	Reach 1	167.5	n	0.024	0.026	
475	Reach 1	167.3	n	0.024	0.026	
476	Reach 1	167	n	0.026	0.024	0.026
477	Reach 1	166.8	n	0.026	0.024	0.026
478	Reach 1	166.6	n	0.024	0.026	
479	Reach 1	166.3	n	0.026	0.024	0.026
480	Reach 1	166.1	n	0.024	0.026	
481	Reach 1	165.8	n	0.024	0.026	
482	Reach 1	165.5	n	0.024	0.026	
483	Reach 1	165.2	n	0.024	0.026	
484	Reach 1	164.9	n	0.024	0.026	
485	Reach 1	164.6	n	0.024	0.026	
486	Reach 1	164.3	n	0.024	0.026	
487	Reach 1	164	n	0.024	0.026	
488	Reach 1	163.7	n	0.024	0.026	
489	Reach 1	163.5	n	0.024	0.026	

490	Reach 1	163.2	n	0.024	0.026	
491	Reach 1	162.9	n	0.024	0.026	
492	Reach 1	162.6	n	0.024	0.026	
493	Reach 1	162.3	n	0.024	0.026	
494	Reach 1	161.9	n	0.024	0.026	
495	Reach 1	161.7	n	0.024	0.026	
496	Reach 1	161.3	n	0.024	0.026	
497	Reach 1	161	n	0.026	0.024	0.026
498	Reach 1	160.8	n	0.024	0.026	
499	Reach 1	160.6	n	0.026	0.024	0.026
500	Reach 1	160.4	n	0.024	0.026	
501	Reach 1	160.1	n	0.024	0.026	
502	Reach 1	159.9	n	0.024	0.026	
503	Reach 1	159.6	n	0.026	0.024	0.026
504	Reach 1	159.4	n	0.024	0.026	
505	Reach 1	159.1	n	0.026	0.024	0.026
506	Reach 1	158.9	n	0.024	0.026	
507	Reach 1	158.6	n	0.024	0.026	
508	Reach 1	158.3	n	0.024	0.026	
509	Reach 1	158	n	0.024	0.026	
510	Reach 1	157.8	n	0.024	0.026	
511	Reach 1	157.5	n	0.024	0.026	
512	Reach 1	157.2	n	0.024	0.026	
513	Reach 1	156.9	n	0.026	0.024	0.026
514	Reach 1	156.7	n	0.024	0.026	
515	Reach 1	156.4	n	0.026	0.024	0.026
516	Reach 1	156.1	n	0.024	0.026	
517	Reach 1	155.8	n	0.024	0.026	
518	Reach 1	155.5	n	0.024	0.026	
519	Reach 1	155.1	n	0.024	0.026	
520	Reach 1	154.8	n	0.024	0.026	
521	Reach 1	154.5	n	0.024	0.026	
522	Reach 1	154.2	n	0.024	0.026	
523	Reach 1	153.9	n	0.024	0.026	
524	Reach 1	153.5	n	0.024	0.026	
525	Reach 1	153.2	n	0.024	0.026	
526	Reach 1	152.8	n	0.024	0.026	
527	Reach 1	152.5	n	0.024	0.026	
528	Reach 1	152.1	n	0.024	0.026	
529	Reach 1	151.9	n	0.024	0.026	
530	Reach 1	151.6	n	0.024	0.026	

531	Reach 1	151.4	n	0.024	0.026	
532	Reach 1	151.1	n	0.024	0.026	
533	Reach 1	150.8	n	0.024	0.026	
534	Reach 1	150.5	n	0.024	0.026	
535	Reach 1	150.2	n	0.024	0.026	
536	Reach 1	149.9	n	0.024	0.026	
537	Reach 1	149.6	n	0.024	0.026	
538	Reach 1	149.3	n	0.024	0.026	
539	Reach 1	149	n	0.024	0.026	
540	Reach 1	148.8	n	0.024	0.026	
541	Reach 1	148.5	n	0.024	0.026	
542	Reach 1	148.2	n	0.024	0.026	
543	Reach 1	147.9	n	0.024	0.026	
544	Reach 1	147.6	n	0.024	0.026	
545	Reach 1	147.3	n	0.024	0.026	
546	Reach 1	146.9	n	0.024	0.026	
547	Reach 1	146.6	n	0.024	0.026	
548	Reach 1	146.4	n	0.024	0.026	
549	Reach 1	146.1	n	0.024	0.026	
550	Reach 1	145.8	n	0.024	0.026	
551	Reach 1	145.5	n	0.024	0.026	
552	Reach 1	145.2	n	0.024	0.026	
553	Reach 1	144.9	n	0.024	0.026	
554	Reach 1	144.6	n	0.024	0.026	
555	Reach 1	144.3	n	0.024	0.026	
556	Reach 1	144	n	0.024	0.026	
557	Reach 1	143.7	n	0.024	0.026	
558	Reach 1	143.3	n	0.024	0.026	
559	Reach 1	143 n	n	0.024	0.026	
560	Reach 1	142.7	n	0.024	0.026	
561	Reach 1	142.3	n	0.024	0.026	
562	Reach 1	142.1	n	0.024	0.026	
563	Reach 1	141.7	n	0.024	0.026	
564	Reach 1	141.4	n	0.024	0.026	
565	Reach 1	141.1	n	0.024	0.026	
566	Reach 1	140.7	n	0.024	0.026	
567	Reach 1	140.4	n	0.024	0.026	
568	Reach 1	140	n	0.024	0.026	
569	Reach 1	139.7	n	0.024	0.026	
570	Reach 1	139.4	n	0.024	0.026	
571	Reach 1	139.1	n	0.024	0.026	

572	Reach 1	138.7	n	0.024	0.026	
573	Reach 1	138.4	n	0.024	0.026	
574	Reach 1	138.1	n	0.024	0.026	
575	Reach 1	137.8	n	0.024	0.026	
576	Reach 1	137.4	n	0.024	0.026	
577	Reach 1	137.1	n	0.024	0.026	
578	Reach 1	136.8	n	0.024	0.026	
579	Reach 1	136.5	n	0.024	0.026	
580	Reach 1	136.1	n	0.024	0.026	
581	Reach 1	135.8	n	0.024	0.026	
582	Reach 1	135.6	n	0.024	0.026	
583	Reach 1	135.3	n	0.024	0.026	
584	Reach 1	135	n	0.024	0.026	
585	Reach 1	134.7	n	0.024	0.026	
586	Reach 1	134.4	n	0.024	0.026	
587	Reach 1	134.1	n	0.024	0.026	
588	Reach 1	133.8	n	0.024	0.026	
589	Reach 1	133.4	n	0.024	0.026	
590	Reach 1	133.1	n	0.024	0.026	
591	Reach 1	132.8	n	0.024	0.026	
592	Reach 1	132.5	n	0.024	0.026	
593	Reach 1	132.2	n	0.024	0.026	
594	Reach 1	131.9	n	0.024	0.026	
595	Reach 1	131.5	n	0.026	0.024	0.026
596	Reach 1	131.3	n	0.024	0.026	
597	Reach 1	131	n	0.024	0.026	
598	Reach 1	130.7	n	0.026	0.024	0.026
599	Reach 1	130.5	n	0.024	0.026	
600	Reach 1	130.2	n	0.024	0.026	
601	Reach 1	130 n	n	0.026	0.024	0.026
602	Reach 1	129.7	n	0.026	0.024	0.026
603	Reach 1	129.5	n	0.024	0.026	
604	Reach 1	129.2	n	0.024	0.026	
605	Reach 1	129	n	0.024	0.026	
606	Reach 1	128.7	n	0.026	0.024	0.026
607	Reach 1	128.6	Lat Struct			
608	Reach 1	128.4	n	0.024	0.026	
609	Reach 1	128.1	n	0.024	0.026	
610	Reach 1	127.8	n	0.026	0.024	0.026
611	Reach 1	127.5	n	0.024	0.026	
612	Reach 1	127.2	n	0.024	0.026	

613	Reach 1	126.9	n	0.024	0.026	
614	Reach 1	126.6	n	0.024	0.026	
615	Reach 1	126.3	n	0.024	0.026	
616	Reach 1	126	n	0.024	0.026	
617	Reach 1	125.8	n	0.024	0.026	
618	Reach 1	125.5	n	0.024	0.026	
619	Reach 1	125.2	n	0.026	0.024	0.026
620	Reach 1	125	n	0.024	0.026	
621	Reach 1	124.7	n	0.026	0.024	0.026
622	Reach 1	124.5	n	0.024	0.026	
623	Reach 1	124.2	n	0.024	0.026	
624	Reach 1	124	n	0.024	0.026	
625	Reach 1	123.8	n	0.024	0.026	
626	Reach 1	123.5	n	0.026	0.024	0.026
627	Reach 1	123.3	n	0.026	0.024	0.026
628	Reach 1	123.1	n	0.024	0.026	
629	Reach 1	122.8	n	0.024	0.026	
630	Reach 1	122.5	n	0.024	0.026	
631	Reach 1	122.2	n	0.024	0.026	
632	Reach 1	121.9	n	0.024	0.026	
633	Reach 1	121.6	n	0.024	0.026	
634	Reach 1	121.3	n	0.024	0.026	
635	Reach 1	120.9	n	0.024	0.026	
636	Reach 1	120.6	n	0.024	0.026	
637	Reach 1	120.2	n	0.024	0.026	
638	Reach 1	119.9	n	0.024	0.026	
639	Reach 1	119.7	n	0.024	0.026	
640	Reach 1	119.4	n	0.024	0.026	
641	Reach 1	119	n	0.024	0.026	
642	Reach 1	118.7	n	0.024	0.026	
643	Reach 1	118.5	n	0.024	0.026	
644	Reach 2	118.2	n	0.026		
645	Reach 2	117.9	n	0.025	0.025	0.026
646	Reach 2	117.6	n	0.026		
647	Reach 2	117.3	n	0.026		
648	Reach 2	117.1	n	0.026		
649	Reach 2	116.8	n	0.026		
650	Reach 2	116.6	n	0.026		
651	Reach 2	116.3	n	0.026		
652	Reach 2	116	n	0.026		
653	Reach 2	115.6	n	0.026		

654	Reach 2	115.3	n	0.026		
655	Reach 2	115	n	0.026		
656	Reach 2	114.8	n	0.026		
657	Reach 2	114.5	n	0.026		
658	Reach 2	114.2	n	0.026		
659	Reach 2	113.8	n	0.026		
660	Reach 2	113.5	n	0.026		
661	Reach 2	113.1	n	0.026		
662	Reach 2	112.8	n	0.026		
663	Reach 2	112.4	n	0.026		
664	Reach 2	112.1	n	0.026		
665	Reach 2	111.9	n	0.026		
666	Reach 2	111.6	n	0.026		
667	Reach 2	111.3	n	0.026		
668	Reach 2	111	n	0.026		
669	Reach 2	110.7	n	0.026		
670	Reach 2	110.4	n	0.026		
671	Reach 2	110.2	n	0.026		
672	Reach 2	109.9	n	0.025	0.025	0.026
673	Reach 2	109.7	n	0.026		
674	Reach 2	109.5	n	0.026		
675	Reach 2	109.2	n	0.026		
676	Reach 2	109	n	0.026		
677	Reach 2	108.8	n	0.026		
678	Reach 2	108.6	n	0.026		
679	Reach 2	108.4	n	0.026		
680	Reach 2	108.2	n	0.026		
681	Reach 2	107.9	n	0.025	0.025	0.026
682	Reach 2	107.6	n	0.026		
683	Reach 2	107.4	n	0.025	0.025	0.026
684	Reach 2	107.1	n	0.025	0.025	0.026
685	Reach 2	106.9	n	0.025	0.025	0.026
686	Reach 2	106.6	n	0.026		
687	Reach 2	106.3	n	0.026		
688	Reach 2	106	n	0.025	0.025	0.026
689	Reach 2	105.7	n	0.026		
690	Reach 2	105.5	n	0.026		
691	Reach 2	105.2	n	0.026		
692	Reach 2	105	n	0.025	0.025	0.026
693	Reach 2	104.8	n	0.026		
694	Reach 2	104.6	n	0.026		

695	Reach 2	104.4	n	0.026		
696	Reach 2	104.2	n	0.026		
697	Reach 2	103.9	n	0.025	0.025	0.026
698	Reach 2	103.7	n	0.026		
699	Reach 2	103.5	n	0.026		
700	Reach 2	103.3	n	0.026		
701	Reach 2	103.1	n	0.026		
702	Reach 2	102.8	n	0.025	0.025	0.026
703	Reach 2	102.7	n	0.026		
704	Reach 2	102.4	n	0.025	0.025	0.026
705	Reach 2	102.2	n	0.026		
706	Reach 2	102	n	0.026		
707	Reach 2	101.8	n	0.026		
708	Reach 2	101.6	n	0.026		
709	Reach 2	101.4	n	0.026		
710	Reach 2	101.3	n	0.026		
711	Reach 2	101.1	n	0.026		
712	Reach 2	100.9	n	0.026		
713	Reach 2	100.7	n	0.026		
714	Reach 2	100.6	n	0.026		
715	Reach 2	100.4	n	0.026		
716	Reach 2	100.1	n	0.026		
717	Reach 2	99.9	n	0.026	0.025	
718	Reach 2	99.6	n	0.026		
719	Reach 2	99.3	n	0.026		
720	Reach 2	99	n	0.026		
721	Reach 2	98.7	n	0.026		
722	Reach 2	98.5	n	0.026		
723	Reach 2	98.2	n	0.026		
724	Reach 3	97.9	n	0.025	0.0201	
725	Reach 3	97.7	n	0.025	0.0201	
726	Reach 3	97.4	n	0.025	0.0201	
727	Reach 3	97.1	n	0.025	0.0201	
728	Reach 3	96.9	n	0.025	0.0201	
729	Reach 3	96.7	n	0.025	0.0201	
730	Reach 3	96.5	n	0.025	0.0201	
731	Reach 3	96.3	n	0.025	0.0201	
732	Reach 3	96.2	n	0.025	0.0201	
733	Reach 3	96	n	0.025	0.0201	
734	Reach 3	95.8	n	0.025	0.0201	
735	Reach 3	95.6	n	0.025	0.024	0.025

736	Reach 3	95.5	n	0.025	0.024	0.025
737	Reach 3	95.4	n	0.025	0.0201	
738	Reach 3	95.2	n	0.025	0.0201	
739	Reach 3	95.1	n	0.025	0.0201	
740	Reach 3	94.9	n	0.025	0.0201	
741	Reach 3	94.7	n	0.025	0.0201	
742	Reach 3	94.6	n	0.025	0.0201	
743	Reach 3	94.4	n	0.025	0.0201	
744	Reach 3	94.2	n	0.025	0.0201	
745	Reach 3	94	n	0.025	0.0201	
746	Reach 3	93.8	n	0.025	0.0201	
747	Reach 3	93.6	n	0.025	0.0201	
748	Reach 3	93.4	n	0.025	0.0201	
749	Reach 3	93.1	n	0.025	0.0201	
750	Reach 3	92.9	n	0.025	0.0201	
751	Reach 3	92.6	n	0.025	0.024	0.025
752	Reach 3	92.3	n	0.025	0.0201	
753	Reach 3	92	n	0.025	0.0201	
754	Reach 3	91.8	n	0.025	0.0201	
755	Reach 3	91.5	n	0.025	0.0201	
756	Reach 3	91.2	n	0.025	0.0201	
757	Reach 3	90.9	n	0.025	0.0201	
758	Reach 3	90.6	n	0.025	0.024	0.025
759	Reach 3	90.4	n	0.025	0.024	0.025
760	Reach 3	90.1	n	0.025	0.0201	
761	Reach 3	89.9	n	0.025	0.0201	
762	Reach 3	89.5	n	0.025	0.0201	
763	Reach 3	89.3	n	0.025	0.0201	
764	Reach 3	88.9	n	0.025	0.0201	
765	Reach 3	88.6	n	0.025	0.0201	
766	Reach 3	88.3	n	0.025	0.024	0.025
767	Reach 3	88.1	n	0.025	0.024	0.025
768	Reach 3	87.8	n	0.025	0.0201	
769	Reach 4	87.5	n	0.024	0.025	
770	Reach 4	87.2	n	0.024	0.025	
771	Reach 4	87	n	0.024	0.025	
772	Reach 4	86.7	n	0.024	0.025	
773	Reach 4	86.3	n	0.024	0.025	
774	Reach 4	86	n	0.024	0.025	
775	Reach 4	85.7	n	0.024	0.025	
776	Reach 4	85.4	n	0.024	0.025	

777	Reach 4	85.1	n	0.024	0.025	
778	Reach 4	84.8	n	0.024	0.025	
779	Reach 4	84.6	n	0.024	0.025	
780	Reach 4	84.2	n	0.024	0.025	
781	Reach 4	83.9	n	0.024	0.025	
782	Reach 4	83.6	n	0.024	0.025	
783	Reach 4	83.3	n	0.024	0.025	
784	Reach 4	83.1	n	0.025	0.024	0.025
785	Reach 4	82.8	n	0.025	0.024	0.025
786	Reach 4	82.6	n	0.025	0.024	0.025
787	Reach 4	82.4	n	0.024	0.025	
788	Reach 4	82.2	n	0.024	0.025	
789	Reach 4	82	n	0.025	0.024	0.025
790	Reach 4	81.8	n	0.025	0.024	0.025
791	Reach 4	81.5	n	0.025	0.024	0.025
792	Reach 5	81.2	n	0.02	0.02	0.02
793	Reach 5	80.9	n	0.02	0.02	
794	Reach 5	80.6	n	0.02	0.02	
795	Reach 5	80.3	n	0.02	0.02	
796	Reach 5	80	n	0.02	0.02	
797	Reach 5	79.7	n	0.02	0.02	
798	Reach 5	79.5	n	0.02	0.02	
799	Reach 5	79.2	n	0.02	0.02	0.02
800	Reach 5	78.9	n	0.02	0.02	
801	Reach 5	78.6	n	0.02	0.02	0.02
802	Reach 5	78.4	n	0.02	0.02	
803	Reach 5	78.1	n	0.02	0.02	0.02
804	Reach 5	77.9	n	0.02	0.02	0.02
805	Reach 5	77.7	n	0.02	0.02	
806	Reach 5	77.5	n	0.02	0.02	0.02
807	Reach 5	77.2	n	0.02	0.02	0.02
808	Reach 5	76.9	n	0.02	0.02	0.02
809	Reach 5	76.7	n	0.02	0.02	
810	Reach 5	76.5	n	0.02	0.02	
811	Reach 5	76.3	n	0.02	0.02	
812	Reach 5	76.2	n	0.02	0.02	
813	Reach 5	76	n	0.02	0.02	
814	Reach 5	75.7	n	0.02	0.02	
815	Reach 5	75.5	n	0.02	0.02	
816	Reach 5	75.3	n	0.02	0.02	
817	Reach 5	75.1	n	0.02	0.02	

818	Reach 5	74.9	n	0.02	0.02	
819	Reach 5	74.6	n	0.02	0.02	
820	Reach 5	74.4	n	0.02	0.02	
821	Reach 5	74.1	n	0.02	0.02	
822	Reach 5	73.8	n	0.02	0.02	
823	Reach 5	73.6	n	0.02	0.02	0.02
824	Reach 5	73.3	n	0.02	0.02	
825	Reach 5	73.2	n	0.02	0.02	
826	Reach 5	73	n	0.02	0.02	
827	Reach 5	72.8	n	0.02	0.02	
828	Reach 5	72.6	n	0.02	0.02	0.02
829	Reach 5	72.3	n	0.02	0.02	0.02
830	Reach 5	72.2	n	0.02	0.02	0.02
831	Reach 5	71.9	n	0.02	0.02	
832	Reach 5	71.7	n	0.02	0.02	
833	Reach 5	71.5	n	0.02	0.02	
834	Reach 5	71.2	n	0.02	0.02	
835	Reach 5	71	n	0.02	0.02	
836	Reach 5	70.8	n	0.02	0.02	0.02
837	Reach 5	70.6	n	0.02	0.02	
838	Reach 5	70.3	n	0.02	0.02	
839	Reach 5	70.1	n	0.02	0.02	
840	Reach 5	69.9	n	0.02	0.02	
841	Reach 5	69.7	n	0.02	0.02	
842	Reach 5	69.4	n	0.02	0.02	
843	Reach 5	69.1	n	0.02	0.02	
844	Reach 5	68.9	n	0.02	0.02	
845	Reach 5	68.6	n	0.02	0.02	
846	Reach 5	68.4	n	0.02	0.02	
847	Reach 5	68.2	n	0.02	0.02	0.02
848	Reach 5	68	n	0.02	0.02	0.02
849	Reach 5	67.8	n	0.02	0.02	0.02
850	Reach 5	67.5	n	0.02	0.02	0.02
851	Reach 5	67.3	n	0.02	0.02	0.02
852	Reach 5	67.1	n	0.02	0.02	0.02
853	Reach 5	66.9	n	0.02	0.02	
854	Reach 5	66.6	n	0.02	0.02	
855	Reach 5	66.4	n	0.02	0.02	
856	Reach 5	66.1	n	0.02	0.02	
857	Reach 5	65.8	n	0.02	0.02	
858	Reach 5	65.6	n	0.02	0.02	

859	Reach 5	65.3	n	0.02	0.02	0.02
860	Reach 5	65	n	0.02	0.02	
861	Reach 5	64.7	n	0.02	0.02	
862	Reach 5	64.5	n	0.02	0.02	
863	Reach 5	64.2	n	0.02	0.02	
864	Reach 5	63.9	n	0.02	0.02	
865	Reach 5	63.6	n	0.02	0.02	
866	Reach 5	63.4	n	0.02	0.02	
867	Reach 5	63.1	n	0.02	0.02	
868	Reach 5	62.9	n	0.02	0.02	
869	Reach 5	62.6	n	0.02	0.02	
870	Reach 5	62.3	n	0.02	0.02	
871	Reach 5	62.1	n	0.02	0.02	
872	Reach 5	61.9	n	0.02	0.02	0.02
873	Reach 5	61.6	n	0.02	0.02	
874	Reach 5	61.3	n	0.02	0.02	
875	Reach 5	61	n	0.02	0.02	0.02
876	Reach 5	60.8	n	0.02	0.02	
877	Reach 5	60.6	n	0.02	0.02	
878	Reach 5	60.4	n	0.02	0.02	
879	Reach 5	60.2	n	0.02	0.02	
880	Reach 5	60	n	0.02	0.02	
881	Reach 5	59.7	n	0.02	0.02	
882	Reach 5	59.5	n	0.02	0.02	
883	Reach 5	59.3	n	0.02	0.02	
884	Reach 5	59.1	n	0.02	0.02	
885	Reach 5	58.8	n	0.02	0.02	0.02
886	Reach 5	58.4	n	0.02	0.02	
887	Reach 5	58.2	n	0.02	0.02	
888	Reach 5	57.9	n	0.02	0.02	
889	Reach 5	57.6	n	0.02	0.02	
890	Reach 5	57.3	n	0.02	0.02	
891	Reach 5	56.9	n	0.02	0.02	
892	Reach 5	56.5	n	0.02	0.02	
893	Reach 5	56.2	n	0.02	0.02	
894	Reach 5	55.8	n	0.02	0.02	
895	Reach 5	55.4	n	0.02	0.02	
896	Reach 5	55.1	n	0.02	0.02	
897	Reach 5	54.8	n	0.02	0.02	
898	Reach 5	54.5	n	0.02	0.02	
899	Reach 5	54.2	n	0.02	0.02	

900	Reach 5	53.9	n	0.02	0.02	
901	Reach 5	53.6	n	0.02	0.02	
902	Reach 5	53.3	n	0.02	0.02	
903	Reach 5	53	n	0.02	0.02	
904	Reach 5	52.6	n	0.02	0.02	
905	Reach 5	52.3	n	0.02	0.02	
906	Reach 5	51.9	n	0.02	0.02	
907	Reach 5	51.6	n	0.02	0.02	
908	Reach 5	51.2	n	0.02	0.02	
909	Reach 5	50.9	n	0.02	0.02	
910	Reach 5	50.5	n	0.02	0.02	
911	Reach 5	50.2	n	0.02	0.02	
912	Reach 5	49.8	n	0.02	0.02	
913	Reach 5	49.5	n	0.02	0.02	
914	Reach 5	49.1	n	0.02	0.02	
915	Reach 5	48.8	n	0.02	0.02	
916	Reach 5	48.5	n	0.02	0.02	
917	Reach 5	48.2	n	0.02	0.02	
918	Reach 5	47.9	n	0.02	0.02	
919	Reach 5	47.6	n	0.02	0.02	
920	Reach 5	47.2	n	0.02	0.02	
921	Reach 5	46.9	n	0.02	0.02	
922	Reach 5	46.5	n	0.02	0.02	0.02
923	Reach 5	46.1	n	0.02	0.02	
924	Reach 5	45.7	n	0.02	0.02	
925	Reach 5	45.3	n	0.02	0.02	
926	Reach 5	45	n	0.02	0.02	
927	Reach 5	44.7	n	0.02	0.02	
928	Reach 5_Mardi_Gr	44.4	n	0.02	0.02	
929	Reach 5_Mardi_Gr	44.1	n	0.02	0.02	0.02
930	Reach 5_DS_Boh_1	43.8	n	0.02	0.02	0.02
931	Reach 5_DS_Boh_1	43.5	n	0.02	0.02	0.02
932	Reach 5_DS_Boh_1	43.2	n	0.02	0.02	0.02
933	Reach 5_DS_Boh_1	42.9	n	0.02	0.02	0.02
934	Reach 5_DS_Boh_1	42.6	n	0.02	0.02	0.02
935	Reach 5_DS_Boh_2	42.3	n	0.02	0.02	0.02
936	Reach 5_DS_Boh_2	42	n	0.02	0.02	0.02
937	Reach 5_DS_Boh_2	41.6	n	0.02	0.02	0.02
938	Reach 5_DS_Boh_3	41.3	n	0.02	0.02	0.02
939	Reach 5_DS_Boh_3	41	n	0.02	0.02	0.02
940	Reach 5_DS_Boh_3	40.7	n	0.02	0.02	0.02

941	Reach 5_DS_Boh_3	40.4	n	0.02	0.02	0.02
942	Reach 5_DS_Boh_3	40.1	n	0.02	0.02	0.02
943	Reach 5_DS_Boh_4	39.8	n	0.02	0.02	0.02
944	Reach 5_DS_Boh_4	39.5	n	0.02	0.02	0.02
945	Reach 5_DS_Boh_4	39.3	n	0.02	0.02	0.02
946	Reach 5_DS_Boh_4	39	n	0.02	0.02	0.02
947	Reach 5_DS_Boh_4	38.7	n	0.02	0.02	0.02
948	Reach 5_DS_Boh_5	38.6	n	0.02	0.02	0.02
949	Reach 5_DS_Boh_5	38.1	n	0.02	0.02	0.02
950	Reach 5_DS_Boh_5	37.8	n	0.02	0.02	
951	Reach 5_DS_Boh_5	37.5	n	0.02	0.02	0.02
952	Reach 5_DS_Boh_5	37.2	n	0.02	0.02	0.02
953	Reach 5_DS_Boh_6	36.9	n	0.02	0.02	0.02
954	Reach 5_DS_Boh_6	36.6	n	0.02	0.02	0.02
955	Reach 5_DS_Boh_6	36.4	n	0.02	0.02	0.02
956	Reach 5_DS_Boh_6	36.1	n	0.02	0.02	0.02
957	Reach 5_DS_Boh_6	35.8	n	0.02	0.02	0.02
958	Reach 5_DS_Boh_6	35.5	n	0.02	0.02	0.02
959	Reach 5_DS_Boh_6	35.2	n	0.02	0.02	0.02
960	Reach 5_DS_Boh_6	34.9	n	0.02	0.02	0.02
961	Reach 5_DS_Boh_6	34.7	n	0.02	0.02	0.02
962	Reach 5_DS_Boh_7	34.3	n	0.02	0.02	0.02
963	Reach 5_DS_Boh_7	33.9	n	0.02	0.02	0.02
964	Reach 5_DS_Boh_7	33.6	n	0.02	0.02	0.02
965	Reach 5_DS_Boh_7	33.3	n	0.02	0.02	0.02
966	Reach 5_DS_Boh_8	32.9	n	0.02	0.02	0.02
967	Reach 5_DS_Boh_8	32.85	n	0.02	0.02	0.02
968	Reach 5_2	32.75	n	0.02	0.02	0.02
969	Reach 5_2	32.05	n	0.02	0.02	0.02
970	Reach 6	32.71	n	0.02	0.02	0.02
971	Reach 6	32.7	n	0.02	0.02	0.02
972	Reach 6	32.41	n	0.02	0.02	
973	Reach 7	32.4	n	0.02	0.02	
974	Reach 7	32.1	n	0.02	0.02	
975	Reach 7	31.9	n	0.02	0.02	
976	Reach 7_2	31.6	n	0.023	0.022	
977	Reach 7_2	31.4	n	0.023	0.022	
978	Reach 7_2	31.2	n	0.023	0.022	
979	Reach 7_2	31	n	0.023	0.022	
980	Reach 7_2	30.8	n	0.023	0.022	
981	Reach 7_2	30.6	n	0.023	0.022	

982	Reach 7_2	30.4	n	0.023	0.022	
983	Reach 7_2	30.1	n	0.023	0.022	
984	Reach 7_2	29.9	n	0.023	0.022	0.023
985	Reach 7_2	29.6	n	0.023	0.022	0.023
986	Reach 7_2	29.5	n	0.023	0.022	0.023
987	Reach 7_2	29.2	n	0.023	0.022	0.023
988	Reach 7_2	29	n	0.023	0.022	0.023
989	Reach 7_2	28.8	n	0.023	0.022	
990	Reach 7_2	28.5	n	0.023	0.022	
991	Reach 7_2	28.3	n	0.023	0.022	
992	Reach 7_2	28	n	0.023	0.022	
993	Reach 7_2	27.7	n	0.023	0.022	
994	Reach 7_2	27.4	n	0.023	0.022	
995	Reach 7_2	27.1	n	0.023	0.022	
996	Reach 7_2	26.7	n	0.023	0.022	
997	Reach 7_2	26.4	n	0.023	0.022	
998	Reach 7_3	26	n	0.023	0.022	
999	Reach 7_3	25.6	n	0.023	0.022	
1000	Reach 7_3	25.2	n	0.023	0.022	
1001	Reach 7_3	24.9	n	0.023	0.022	
1002	Reach 7_3	24.6	n	0.023	0.022	
1003	Reach 7_3	24.2	n	0.023	0.022	
1004	Reach 7_3	23.8	n	0.023	0.022	
1005	Reach 7_3	23.5	n	0.023	0.022	
1006	Reach 7_3	23.1	n	0.023	0.022	
1007	Reach 7_3	22.7	n	0.023	0.022	
1008	Reach 7_3	22.4	n	0.023	0.022	
1009	Reach 7_3	22	n	0.023	0.022	
1010	Reach 7_3	21.7	n	0.023	0.022	
1011	Reach 7_3	21.3	n	0.023	0.022	
1012	Reach 7_3	21	n	0.023	0.022	
1013	Reach 7_3	20.7	n	0.023	0.022	
1014	Reach 7_3	20.5	n	0.023	0.022	
1015	Reach 7_3	20.1	n	0.023	0.022	
1016	Reach 7_3	19.9	n	0.023	0.022	
1017	Reach 7_3	19.6	n	0.023	0.022	
1018	Reach 8	19.4	n	0.019	0.019	
1019	Reach 8	19.1	n	0.019	0.019	0.019
1020	Reach 8	18.8	n	0.019	0.019	0.019
1021	Reach 8	18.6	n	0.019	0.019	0.019
1022	Reach 8	18.3	n	0.019	0.019	0.019

1023	Reach 8	18	n	0.019	0.019	0.019
1024	Reach 8	17.7	n	0.019	0.019	
1025	Reach 8	17.4	n	0.019	0.019	
1026	Reach 8	17.1	n	0.019	0.019	
1027	Reach 8	16.8	n	0.019	0.019	
1028	Reach 8	16.5	n	0.019	0.019	0.019
1029	Reach 8	16.2	n	0.019	0.019	0.019
1030	Reach 8	15.8	n	0.019	0.019	0.019
1031	Reach 8	15.6	n	0.019	0.019	0.019
1032	Reach 8	15.3	n	0.019	0.019	0.019
1033	Reach 8_3	15	n	0.019	0.019	0.019
1034	Reach 8_3	14.7	n	0.019	0.019	0.019
1035	Reach 8_3	14.5	n	0.019	0.019	0.019
1036	Reach 8_3	14.2	n	0.019	0.019	0.019
1037	Reach 8_3	13.8	n	0.019	0.019	0.019
1038	Reach 8_3	13.5	n	0.019	0.019	0.019
1039	Reach 8_3	13.2	n	0.019	0.019	0.019
1040	Reach 8_3	13	n	0.019	0.019	0.019
1041	Reach 8_3	12.8	n	0.019	0.019	0.019
1042	Reach 8_3	12.5	n	0.019	0.019	0.019
1043	Reach 8_3	12.2	n	0.019	0.019	0.019
1044	Reach 8_3	12	n	0.019	0.019	0.019
1045	Reach 8_3	11.7	n	0.019	0.019	0.019
1046	Reach 8_3	11.4	n	0.019	0.019	0.019
1047	Reach 9	11.2	n	0.019	0.019	0.019
1048	Reach 9	11.1	n	0.019	0.019	0.019
1049	Reach 9	10.8	n	0.019	0.019	
1050	Reach 9	10.6	n	0.019	0.019	0.019
1051	Reach 9	10.4	n	0.019	0.019	0.019
1052	Reach 10	10.2	n	0.019	0.019	0.019
1053	Reach 10	9.97	n	0.019	0.019	0.019
1054	Reach 10	9.7	n	0.019	0.019	0.019
1055	Reach 10	9.4	n	0.019	0.019	0.019
1056	Reach 10	9.1	n	0.019	0.019	0.019
1057	Reach 10	8.9	n	0.019	0.019	0.019
1058	Reach 10	8.7	n	0.019	0.019	0.019
1059	Reach 10	8.4	n	0.019	0.019	0.019
1060	Reach 10	8.1	n	0.019	0.019	0.019
1061	Reach 10	7.94	n	0.019	0.019	0.019
1062	Reach 10	7.5	n	0.019	0.019	0.019
1063	Reach 10	7.3	n	0.019	0.019	0.019

1064	Reach 10	6.9	n	0.019	0.019	0.019
1065	Reach 10	6.7	n	0.019	0.019	0.019
1066	Reach 10	6.5	n	0.019	0.019	0.019
1067	Reach 10	6.2	n	0.019	0.019	0.019
1068	Reach 10	6	n	0.019	0.019	0.019
1069	Reach 10	5.8	n	0.019	0.019	0.019
1070	Reach 10	5.5	n	0.019	0.019	0.019
1071	Reach 10	5.3	n	0.019	0.019	0.019
1072	Reach 10	5.1	n	0.019	0.019	0.019
1073	Reach 10	4.9	n	0.019	0.019	0.019
1074	Reach 10	4.7	n	0.019	0.019	0.019
1075	Reach 11	4.46	n	0.019	0.019	0.019
1076	Reach 11	4.26	n	0.019	0.019	0.019
1077	Reach 11	4.04	n	0.019	0.019	0.019
1078	Reach 11	3.83	n	0.019	0.019	0.019
1079	Reach 11	3.6	n	0.019	0.019	0.019
1080	Reach 11	3.36	n	0.019	0.019	0.019
1081	Reach 11	3.15	n	0.019	0.019	0.019
1082	Reach 12	2.95	n	0.019	0.019	0.019
1083	Reach 12	2.75	n	0.019	0.019	0.019
1084	Reach 12	2.65	n	0.019	0.019	0.019
1085	Reach 12	2.46	n	0.019	0.019	0.019
1086	Reach 12	2.28	n	0.019	0.019	0.019
1087	Reach 12	2.08	n	0.019	0.019	0.019
1088	Reach 12	1.7	n	0.019	0.019	0.019
1089	Reach 12	1.53	n	0.019	0.019	0.019
1090	Reach 12	1.4	n	0.019	0.019	0.019
1091	Reach 12	1.25	n	0.019	0.019	0.019
1092	Reach 12	1.1	n	0.019	0.019	0.019
1093	Reach 12	0.98	n	0.019	0.019	0.019
1094	Reach 12	0.7	n	0.019	0.019	0.019
1095	Reach 12	0.58	n	0.019	0.019	0.019
1096	Reach 12	0.35	n	0.019	0.019	0.019
1097	Reach 12	0.2	n	0.019	0.019	0.019
1098	Reach 12	0.07	n	0.019	0.019	0.019

Manning's n values for Southwest Pass						
Number	**Reach**	**River Station**	**Friction (n/K)**	**Left Bank**	**Channel**	**Right Bank**
1	Reach 1	108.0	n	0.02	0.02	0.02
2	Reach 1	107.0	n	0.02	0.02	0.02
3	Reach 1	106.0	n	0.02	0.02	0.02
4	Reach 1	105.0	n	0.02	0.02	0.02
5	Reach 1	104.0	n	0.02	0.02	0.02
6	Reach 1	103.0	n	0.02	0.02	0.02
7	Reach 1	102.0	n	0.02	0.02	0.02
8	Reach 1	101.0	n	0.02	0.02	0.02
9	Reach 1	100.0	n	0.02	0.02	0.02
10	Reach 1	99.0	n	0.02	0.02	0.02
11	Reach 1	98.0	n	0.02	0.02	0.02
12	Reach 1	97.0	n	0.02	0.02	0.02
13	Reach 1	96.0	n	0.02	0.02	0.02
14	Reach 1	95.0	n	0.02	0.02	0.02
15	Reach 1	94.0	n	0.02	0.02	0.02
16	Reach 1	93.0	n	0.02	0.02	0.02
17	Reach 1	92.0	n	0.02	0.02	0.02
18	Reach 1	91.0	n	0.02	0.02	0.02
19	Reach 1	90.0	n	0.02	0.02	0.02
20	Reach 1	89.0	n	0.02	0.02	0.02
21	Reach 1	88.0	n	0.02	0.02	0.02
22	Reach 1	87.0	n	0.02	0.02	0.02
23	Reach 1	86.0	n	0.02	0.02	0.02
24	Reach 1	85.0	n	0.02	0.02	0.02
25	Reach 1	84.0	n	0.02	0.02	0.02
26	Reach 1	83.0	n	0.02	0.02	0.02
27	Reach 1	82.0	n	0.02	0.02	0.02
28	Reach 1	81.0	n	0.02	0.02	0.02
29	Reach 1	80.0	n	0.02	0.02	0.02
30	Reach 1	79.0	n	0.02	0.02	0.02
31	Reach 1	78.0	n	0.02	0.02	0.02
32	Reach 1	77.0	n	0.02	0.02	0.02
33	Reach 1	76.0	n	0.02	0.02	0.02
34	Reach 1	75.0	n	0.02	0.02	0.02
35	Reach 1	74.0	n	0.02	0.02	0.02
36	Reach 1	73.0	n	0.02	0.02	0.02
37	Reach 1	72.0	n	0.02	0.02	0.02
38	Reach 1	71.0	n	0.02	0.02	0.02

39	Reach 1	70.0	n	0.02	0.02	0.02
40	Reach 1	69.0	n	0.02	0.02	0.02
41	Reach 1	68.0	n	0.02	0.02	0.02
42	Reach 1	67.0	n	0.02	0.02	0.02
43	Reach 1	66.0	n	0.02	0.02	0.02
44	Reach 1	65.0	n	0.02	0.02	0.02
45	Reach 1	64.0	n	0.02	0.02	0.02
46	Reach 1	63.0	n	0.02	0.02	0.02
47	Reach 1	62.0	n	0.02	0.02	0.02
48	Reach 1	61.0	n	0.02	0.02	0.02
49	Reach 1	60.0	n	0.02	0.02	0.02
50	Reach 1	59.0	n	0.02	0.02	0.02
51	Reach 1	58.0	n	0.02	0.02	0.02
52	Reach 1	57.0	n	0.02	0.02	0.02
53	Reach 1	56.0	n	0.02	0.02	0.02
54	Reach 1	55.0	n	0.02	0.02	0.02
55	Reach 1	54.0	n	0.02	0.02	0.02
56	Reach 1	53.0	n	0.02	0.02	0.02
57	Reach 1	52.0	n	0.02	0.02	0.02
58	Reach 1	51.0	n	0.02	0.02	0.02
59	Reach 1	50.0	n	0.02	0.02	0.02
60	Reach 1	49.0	n	0.02	0.02	0.02
61	Reach 1	48.0	n	0.02	0.02	0.02
62	Reach 1	47.0	n	0.02	0.02	0.02
63	Reach 1	46.0	n	0.02	0.02	0.02
64	Reach 1	45.0	n	0.02	0.02	0.02
65	Reach 1	44.0	n	0.02	0.02	0.02
66	Reach 1	43.0	n	0.02	0.02	0.02
67	Reach 1	42.0	n	0.02	0.02	0.02
68	Reach 1	41.0	n	0.02	0.02	0.02
69	Reach 1	40.0	n	0.02	0.02	0.02
70	Reach 1	39.0	n	0.02	0.02	0.02
71	Reach 1	38.0	n	0.02	0.02	0.02
72	Reach 1	37.0	n	0.02	0.02	0.02
73	Reach 1	36.0	n	0.02	0.02	0.02
74	Reach 1	35.0	n	0.02	0.02	0.02
75	Reach 1	34.0	n	0.02	0.02	0.02
76	Reach 1	33.0	n	0.02	0.02	0.02
77	Reach 1	32.0	n	0.02	0.02	0.02
78	Reach 1	31.0	n	0.02	0.02	0.02
79	Reach 1	30.0	n	0.02	0.02	0.02

80	Reach 1	29.0	n	0.02	0.02	0.02
81	Reach 1	28.0	n	0.02	0.02	0.02
82	Reach 1	27.0	n	0.02	0.02	0.02
83	Reach 1	26.0	n	0.02	0.02	0.02
84	Reach 1	25.0	n	0.02	0.02	0.02
85	Reach 1	24.0	n	0.02	0.02	0.02
86	Reach 1	23.0	n	0.02	0.02	0.02
87	Reach 1	22.0	n	0.02	0.02	0.02
88	Reach 1	21.0	n	0.02	0.02	0.02
89	Reach 1	20.0	n	0.02	0.02	0.02
90	Reach 1	19.0	n	0.02	0.02	0.02
91	Reach 1	18.0	n	0.02	0.02	0.02
92	Reach 1	17.0	n	0.02	0.02	0.02
93	Reach 1	16.0	n	0.02	0.02	0.02
94	Reach 1	15.0	n	0.02	0.02	0.02
95	Reach 1	14.0	n	0.02	0.02	0.02
96	Reach 1	13.0	n	0.02	0.02	0.02
97	Reach 1	12.0	n	0.02	0.02	0.02
98	Reach 1	11.0	n	0.02	0.02	0.02
99	Reach 1	10.0	n	0.02	0.02	0.02
100	Reach 1	9.0	n	0.02	0.02	0.02
101	Reach 1	8.0	n	0.02	0.02	0.02
102	Reach 1	7.0	n	0.02	0.02	0.02
103	Reach 1	6.0	n	0.02	0.02	0.02
104	Reach 1	5.0	n	0.02	0.02	0.02
105	Reach 1	4.0	n	0.02	0.02	0.02
106	Reach 1	3.0	n	0.02	0.02	0.02
107	Reach 1	2.0	n	0.02	0.02	0.02
108	Reach 1	1.0	n	0.02	0.02	0.02

Number	Reach	River Station	Friction (n/K)	Left Bank	Channel	Right Bank
1	Reach 1	79	n	0.02	0.023	0.02
2	Reach 1	78	n	0.02	0.023	0.02
3	Reach 1	77	n	0.02	0.023	0.02
4	Reach 1	76	n	0.02	0.023	0.02
5	Reach 1	75	n	0.02	0.023	0.02
6	Reach 1	74	n	0.02	0.023	0.02
7	Reach 1	73	n	0.02	0.023	0.02
8	Reach 1	72	n	0.02	0.023	0.02
9	Reach 1	71	n	0.02	0.023	0.02
10	Reach 1	70	n	0.02	0.023	0.02
11	Reach 1	69	n	0.02	0.023	0.02
12	Reach 1	68	n	0.02	0.023	0.02
13	Reach 1	67	n	0.02	0.023	0.02
14	Reach 1	66	n	0.02	0.023	0.02
15	Reach 1	65	n	0.02	0.023	0.02
16	Reach 1	64	n	0.02	0.023	0.02
17	Reach 1	63	n	0.02	0.023	0.02
18	Reach 1	62	n	0.02	0.023	0.02
19	Reach 1	61	n	0.02	0.023	0.02
20	Reach 1	60	n	0.02	0.023	0.02
21	Reach 1	59	n	0.02	0.023	0.02
22	Reach 1	58	n	0.02	0.023	0.02
23	Reach 1	57	n	0.02	0.023	0.02
24	Reach 1	56	n	0.02	0.023	0.02
25	Reach 1	55	n	0.02	0.023	0.02
26	Reach 1	54	n	0.02	0.023	0.02
27	Reach 1	53	n	0.02	0.023	0.02
28	Reach 1	52	n	0.02	0.023	0.02
29	Reach 1	51	n	0.02	0.023	0.02
30	Reach 1	50	n	0.02	0.023	0.02
31	Reach 1	49	n	0.02	0.023	0.02
32	Reach 1	48	n	0.02	0.023	0.02
33	Reach 1	47	n	0.02	0.023	0.02
34	Reach 1	46	n	0.02	0.023	0.02
35	Reach 1	45	n	0.02	0.023	0.02
36	Reach 1	44	n	0.02	0.023	0.02
37	Reach 1	43	n	0.02	0.023	0.02
38	Reach 1	42	n	0.02	0.023	0.02
39	Reach 1	41	n	0.02	0.023	0.02

40	Reach 1	40	n	0.02	0.023	0.02
41	Reach 1	39	n	0.02	0.023	0.02
42	Reach 1	38	n	0.02	0.023	0.02
43	Reach 1	37	n	0.02	0.023	0.02
44	Reach 1	36	n	0.02	0.023	0.02
45	Reach 1	35	n	0.02	0.023	0.02
46	Reach 1	34	n	0.02	0.023	0.02
47	Reach 1	33	n	0.02	0.023	0.02
48	Reach 1	32	n	0.02	0.023	0.02
49	Reach 1	31	n	0.02	0.023	0.02
50	Reach 1	30	n	0.02	0.023	0.02
51	Reach 1	29	n	0.02	0.023	0.02
52	Reach 1	28	n	0.02	0.023	0.02
53	Reach 1	27	n	0.02	0.023	0.02
54	Reach 1	26	n	0.02	0.023	0.02
55	Reach 1	25	n	0.02	0.023	0.02
56	Reach 1	24	n	0.02	0.023	0.02
57	Reach 1	23	n	0.02	0.023	0.02
58	Reach 1	22	n	0.02	0.023	0.02
59	Reach 1	21	n	0.02	0.023	0.02
60	Reach 1	20	n	0.02	0.023	0.02
61	Reach 1	19	n	0.02	0.023	0.02
62	Reach 1	18	n	0.02	0.023	0.02
63	Reach 1	17	n	0.02	0.023	0.02
64	Reach 1	16	n	0.02	0.023	0.02
65	Reach 1	15	n	0.02	0.023	0.02
66	Reach 1	14	n	0.02	0.023	0.02
67	Reach 1	13	n	0.02	0.023	0.02
68	Reach 1	12	n	0.02	0.023	0.02
69	Reach 1	11	n	0.02	0.023	0.02
70	Reach 1	10	n	0.02	0.023	0.02
71	Reach 1	9	n	0.02	0.023	0.02
72	Reach 1	8	n	0.02	0.023	0.02
73	Reach 1	7	n	0.02	0.023	0.02
74	Reach 1	6	n	0.02	0.023	0.02
75	Reach 1	5	n	0.02	0.023	0.02
76	Reach 1	4	n	0.02	0.023	0.02
77	Reach 1	3	n	0.02	0.023	0.02
78	Reach 1	2	n	0.02	0.023	0.02
79	Reach 1	1	n	0.02	0.023	0.02

Manning's n values for Pass A Loutre						
Number	**Reach**	**River Station**	**Friction (n/K)**	**Left Bank**	**Channel**	**Right Bank**
1	Reach 1	29	n	0.02	0.02	0.02
2	Reach 1	28	n	0.02	0.02	0.02
3	Reach 1	27	n	0.02	0.02	0.02
4	Reach 1	26	n	0.02	0.02	0.02
5	Reach 1	25	n	0.02	0.02	0.02
6	Reach 1	24	n	0.02	0.02	0.02
7	Reach 1	23	n	0.02	0.02	0.02
8	Reach 1	22	n	0.02	0.02	0.02
9	Reach 1	21	n	0.02	0.02	0.02
10	Reach 1	20	n	0.02	0.02	0.02
11	Reach 1	19	n	0.02	0.02	0.02
12	Reach 1	18	n	0.02	0.02	0.02
13	Reach 1	17	n	0.02	0.02	0.02
14	Reach 1	16	n	0.02	0.02	0.02
15	Reach 1	15	n	0.02	0.02	0.02
16	Reach 1	14	n	0.02	0.02	0.02
17	Reach 1	13	n	0.02	0.02	0.02
18	Reach 1	12	n	0.02	0.02	0.02
19	Reach 1	11	n	0.02	0.02	0.02
20	Reach 1	10	n	0.02	0.02	0.02
21	Reach 1	9	n	0.02	0.02	0.02
22	Reach 1	8	n	0.02	0.02	0.02
23	Reach 1	7	n	0.02	0.02	0.02
24	Reach 1	6	n	0.02	0.02	0.02
25	Reach 1	5	n	0.02	0.02	0.02
26	Reach 1	4	n	0.02	0.02	0.02
27	Reach 1	3	n	0.02	0.02	0.02
28	Reach 1	2	n	0.02	0.02	0.02
29	Reach 1	1	n	0.02	0.02	0.02

Manning's n values for Main Pass						
Number	**Reach**	**River Station**	**Friction (n/K)**	**Left Bank**	**Channel**	**Right Bank**
1	Reach 1	56	n	0.016	0.016	0.016
2	Reach 1	55	n	0.016	0.016	0.016
3	Reach 1	54	n	0.016	0.016	0.016
4	Reach 1	53	n	0.016	0.016	0.016
5	Reach 1	52	n	0.016	0.016	0.016
6	Reach 1	51	n	0.016	0.016	0.016
7	Reach 1	50	n	0.016	0.016	0.016
8	Reach 1	49	n	0.016	0.016	0.016
9	Reach 1	48	n	0.016	0.016	0.016
10	Reach 1	47	n	0.016	0.016	0.016
11	Reach 1	46	n	0.016	0.016	0.016
12	Reach 1	45	n	0.016	0.016	0.016
13	Reach 1	44	n	0.016	0.016	0.016
14	Reach 1	43	n	0.016	0.016	0.016
15	Reach 1	42	n	0.016	0.016	0.016
16	Reach 1	41	n	0.016	0.016	0.016
17	Reach 1	40	n	0.016	0.016	0.016
18	Reach 1	39	n	0.016	0.016	0.016
19	Reach 1	38	n	0.016	0.016	0.016
20	Reach 1	37	n	0.016	0.016	0.016
21	Reach 1	36	n	0.016	0.016	0.016
22	Reach 1	35	n	0.016	0.016	0.016
23	Reach 1	34	n	0.016	0.016	0.016
24	Reach 1	33	n	0.016	0.016	0.016
25	Reach 1	32	n	0.016	0.016	0.016
26	Reach 1	31	n	0.016	0.016	0.016
27	Reach 1	30	n	0.016	0.016	0.016
28	Reach 1	29	n	0.016	0.016	0.016
29	Reach 1	28	n	0.016	0.016	0.016
30	Reach 1	27	n	0.016	0.016	0.016
31	Reach 1	26	n	0.016	0.016	0.016
32	Reach 1	25	n	0.016	0.016	0.016
33	Reach 1	24	n	0.016	0.016	0.016
34	Reach 1	23	n	0.016	0.016	0.016
35	Reach 1	22	n	0.016	0.016	0.016
36	Reach 1	21	n	0.016	0.016	0.016
37	Reach 1	20	n	0.016	0.016	0.016
38	Reach 1	19	n	0.016	0.016	0.016

39	Reach 1	18	n	0.016	0.016	0.016
40	Reach 1	17	n	0.016	0.016	0.016
41	Reach 1	16	n	0.016	0.016	0.016
42	Reach 1	15	n	0.016	0.016	0.016
43	Reach 1	14	n	0.016	0.016	0.016
44	Reach 1	13	n	0.016	0.016	0.016
45	Reach 1	12	n	0.016	0.016	0.016
46	Reach 1	11	n	0.016	0.016	0.016
47	Reach 1	10	n	0.016	0.016	0.016
48	Reach 1	9	n	0.016	0.016	0.016
49	Reach 1	8	n	0.016	0.016	0.016
50	Reach 1	7.5	n	0.016	0.016	0.016

Manning's n values for Grand Pass						
Number	**Reach**	**River Station**	**Friction (n/K)**	**Left Bank**	**Channel**	**Right Bank**
1	Reach 1	34	n	0.02	0.019	0.02
2	Reach 1	33	n	0.02	0.019	0.02
3	Reach 1	32	n	0.02	0.019	0.02
4	Reach 1	31	n	0.02	0.019	0.02
5	Reach 1	30	n	0.02	0.019	0.02
1	Reach 2	29	n	0.015	0.015	0.015
2	Reach 2	28	n	0.015	0.015	0.015
3	Reach 2	27	n	0.015	0.015	0.015
4	Reach 2	26	n	0.015	0.015	0.015
5	Reach 2	25	n	0.015	0.015	0.015
6	Reach 2	24	n	0.015	0.015	0.015
7	Reach 2	23	n	0.015	0.015	0.015
8	Reach 2	22	n	0.015	0.015	0.015
9	Reach 2	21	n	0.015	0.015	0.015
10	Reach 2	20	n	0.015	0.015	0.015
11	Reach 2	19	n	0.015	0.015	0.015
12	Reach 2	18	n	0.015	0.015	0.015
13	Reach 2	17	n	0.015	0.015	0.015
14	Reach 2	16	n	0.015	0.015	0.015
15	Reach 2	15	n	0.015	0.015	0.015
16	Reach 2	14	n	0.015	0.015	0.015
17	Reach 2	13	n	0.015	0.015	0.015
18	Reach 2	12	n	0.015	0.015	0.015
19	Reach 2	11	n	0.015	0.015	0.015

20	Reach 2	10	n	0.015	0.015	0.015
21	Reach 2	9	n	0.015	0.015	0.015
22	Reach 2	8	n	0.015	0.015	0.015
23	Reach 2	7	n	0.015	0.015	0.015
24	Reach 2	6	n	0.015	0.015	0.015
25	Reach 2	5	n	0.015	0.015	0.015
26	Reach 2	4	n	0.015	0.015	0.015
27	Reach 2	3	n	0.015	0.015	0.015
28	Reach 2	2	n	0.015	0.015	0.015
29	Reach 2	1	n	0.015	0.015	0.015

Manning's n values for Tiger Pass						
Number	**Reach**	**River Station**	**Friction (n/K)**	**Left Bank**	**Channel**	**Right Bank**
1	Reach 1	17	n	0.015	0.015	0.015
2	Reach 1	16	n	0.015	0.015	0.015
3	Reach 1	15	n	0.015	0.015	0.015
4	Reach 1	14	n	0.015	0.015	0.015
5	Reach 1	13	n	0.015	0.015	0.015
6	Reach 1	12	n	0.015	0.015	0.015
7	Reach 1	11	n	0.015	0.015	0.015
8	Reach 1	10	n	0.015	0.015	0.015
9	Reach 1	9	n	0.015	0.015	0.015
10	Reach 1	8	n	0.015	0.015	0.015
11	Reach 1	7	n	0.015	0.015	0.015
12	Reach 1	6	n	0.015	0.015	0.015
13	Reach 1	5	n	0.015	0.015	0.015
14	Reach 1	4	n	0.015	0.015	0.015
15	Reach 1	3	n	0.015	0.015	0.015
16	Reach 1	2	n	0.015	0.015	0.015
17	Reach 1	1	n	0.015	0.015	0.015

Manning's n values for Baptiste Collette						
Number	**Reach**	**River Station**	**Friction (n/K)**	**Left Bank**	**Channel**	**Right Bank**
1	Reach 1	35	n	0.016	0.016	0.016
2	Reach 1	34	n	0.016	0.016	0.016
3	Reach 1	33	n	0.016	0.016	0.016
4	Reach 1	32	n	0.016	0.016	0.016
5	Reach 1	31	n	0.016	0.016	0.016

6	Reach 1	30	n	0.016	0.016	0.016
7	Reach 1	29	n	0.016	0.016	0.016
8	Reach 1	28	n	0.016	0.016	0.016
9	Reach 1	27	n	0.016	0.016	0.016
10	Reach 1	26	n	0.016	0.016	0.016
11	Reach 1	25	n	0.016	0.016	0.016
12	Reach 1	24	n	0.016	0.016	0.016
13	Reach 1	23	n	0.016	0.016	0.016
14	Reach 1	22	n	0.016	0.016	0.016
15	Reach 1	21	n	0.016	0.016	0.016
16	Reach 1	20	n	0.016	0.016	0.016
17	Reach 1	19	n	0.016	0.016	0.016
18	Reach 1	18	n	0.016	0.016	0.016
19	Reach 1	17	n	0.016	0.016	0.016
20	Reach 1	16	n	0.016	0.016	0.016
21	Reach 1	15	n	0.016	0.016	0.016
22	Reach 1	14	n	0.016	0.016	0.016
23	Reach 1	13	n	0.016	0.016	0.016
24	Reach 1	12	n	0.016	0.016	0.016
25	Reach 1	11	n	0.016	0.016	0.016
26	Reach 1	10	n	0.016	0.016	0.016
27	Reach 1	9	n	0.016	0.016	0.016
28	Reach 1	8	n	0.016	0.016	0.016
29	Reach 1	7	n	0.016	0.016	0.016
30	Reach 1	6	n	0.016	0.016	0.016
31	Reach 1	5	n	0.016	0.016	0.016
32	Reach 1	4	n	0.016	0.016	0.016
33	Reach 1	3	n	0.016	0.016	0.016
34	Reach 1	2	n	0.016	0.016	0.016
35	Reach 1	1	n	0.016	0.016	0.016

Manning's n values for 7 Cut Weir						
Number	**Reach**	**River Station**	**Friction (n/K)**	**Left Bank**	**Channel**	**Right Bank**
1	Reach 1	6	n	0.13	0.03	0.13
2	Reach 1	5	n	0.13	0.03	0.13
3	Reach 1	4	n	0.13	0.03	0.13
4	Reach 1	3	n	0.13	0.03	0.13
5	Reach 1	2	n	0.13	0.03	0.13
6	Reach 1	1	n	0.13	0.03	0.13

Manning's n values for Fort St. Philip										
Number	**Reach**	**River Station**	**Friction (n/K)**	**Left Bank**	**FSP 1**	**Mid Bank**	**FSP 2**	**Mid Bank**	**FSP 3**	**Right Bank**
1	Reach 1	3	n	0.13	0.025	0.13	0.025	0.13	0.025	0.13
2	Reach 1	2	n	0.13	0.025	0.13	0.025	0.13	0.025	0.13
3	Reach 1	1	n	0.13	0.025	0.13	0.025	0.13	0.025	0.13

Manning's n values for 7 Cut Weir						
Number	**Reach**	**River Station**	**Friction (n/K)**	**Left Bank**	**Channel**	**Right Bank**
1	Reach 1	5	n	0.13	0.022	0.13
2	Reach 1	4	n	0.13	0.022	0.13
3	Reach 1	3	n	0.13	0.022	0.13
4	Reach 1	2	n	0.13	0.022	0.13
5	Reach 1	1	n	0.13	0.022	0.13

Manning's n values for Bohemia U/S 1,2,3,4,5,6,7 and 8						
Number	**Reach**	**River Station**	**Friction (n/K)**	**Left Bank**	**Channel**	**Right Bank**
1	Reach 1	2	n	0.001	0.001	0.001
2	Reach 1	1.9	n	0.001	0.001	0.001
3	Reach 1	1.8	Inline Structure			
4	Reach 1	1.5	n	0.001	0.001	0.001
5	Reach 1	1	n	0.001	0.001	0.001

Manning's n values for Bohemia Intermediate						
Number	**Reach**	**River Station**	**Friction (n/K)**	**Left Bank**	**Channel**	**Right Bank**
1	Reach 1	2	n	0.001	0.001	0.001
2	Reach 1	1.9	n	0.001	0.001	0.001
3	Reach 1	1.8	Inline Structure			
4	Reach 1	1.5	n	0.001	0.001	0.001
5	Reach 1	1	n	0.001	0.001	0.001

Manning's n values for Bohemia D/S						
Number	**Reach**	**River Station**	**Friction (n/K)**	**Left Bank**	**Channel**	**Right Bank**
1	Reach 1	2	n	0.00005	0.00005	0.00005
2	Reach 1	1.9	n	0.00005	0.00005	0.00005
3	Reach 1	1.8	Inline Structure			
4	Reach 1	1.5	n	0.00005	0.00005	0.00005
5	Reach 1	1	n	0.00005	0.00005	0.00005
Manning's n values for Mardi Gras Pass						
Number	**Reach**	**River Station**	**Friction (n/K)**	**Left Bank**	**Channel**	**Right Bank**
1	Reach 1	31	n	0.07	0.07	0.07
2	Reach 1	30	n	0.07	0.07	0.07
3	Reach 1	29	n	0.07	0.07	0.07
4	Reach 1	28	n	0.07	0.07	0.07
5	Reach 1	27	n	0.07	0.07	0.07
6	Reach 1	26	n	0.07	0.07	0.07
7	Reach 1	25	n	0.07	0.07	0.07
8	Reach 1	24	n	0.07	0.07	0.07
9	Reach 1	23	n	0.07	0.07	0.07
10	Reach 1	22	n	0.07	0.07	0.07
11	Reach 1	21	n	0.07	0.07	0.07
12	Reach 1	20	n	0.026	0.026	0.026
13	Reach 1	19	n	0.026	0.026	0.026
14	Reach 1	18	n	0.026	0.026	0.026
15	Reach 1	17	n	0.026	0.026	0.026
16	Reach 1	16	n	0.026	0.026	0.026
17	Reach 1	15	n	0.026	0.026	0.026
18	Reach 1	14	n	0.026	0.026	0.026
19	Reach 1	13	n	0.026	0.026	0.026
20	Reach 1	12	n	0.026	0.026	0.026
21	Reach 1	11	n	0.026	0.026	0.026
22	Reach 1	10	n	0.026	0.026	0.026
23	Reach 1	9	n	0.026	0.026	0.026
24	Reach 1	8	n	0.026	0.026	0.026
25	Reach 1	7	n	0.026	0.026	0.026
26	Reach 1	6	n	0.026	0.026	0.026
27	Reach 1	5	n	0.026	0.026	0.026
28	Reach 1	4	n	0.026	0.026	0.026
29	Reach 1	3	n	0.026	0.026	0.026
30	Reach 1	2	n	0.026	0.026	0.026
31	Reach 1	1	n	0.026	0.026	0.026

Appendix D

Flow Roughness Factor in HEC-RAS model

Flow/ River Stations	Flow Roughness Factor					
	306 - 240.9	**240.6 - 157.8**	**156.7 - 81.5**	**43.8 - 19.6**	**19.4 - 10.4**	**10.2 - 0**
150000	-	-	-	0.6	0.6	0.6
200000	1.15	1.15	1.15	0.6	0.6	0.6
250000	1.1	1.1	1.1	0.6	0.6	0.6
300000	1.1	1.1	1.1	0.65	0.65	0.6
350000	1.1	1.1	1.1	0.65	0.65	0.6
400000	1.05	1.05	1.05	0.7	0.7	0.6
450000	1.05	1.05	1.05	0.7	0.7	0.6
500000	1	1.05	1	0.7	0.7	0.6
550000	1	1.05	1	0.65	0.75	0.7
600000	1	1	1	0.65	0.8	0.7
650000	0.95	1	1.05	0.65	0.8	0.8
700000	0.95	1	1.05	0.65	0.8	0.8
750000	0.9	1	1.1	0.6	0.8	0.8
800000	0.9	0.95	1.1	0.6	0.85	0.85
850000	0.85	0.95	1.1	0.6	0.85	0.85
900000	0.85	0.95	1	0.6	0.85	0.85
950000	0.8	0.9	0.9	0.65	0.9	0.9
1000000	0.8	0.9	0.9	0.65	0.9	0.9
1050000	0.85	0.85	0.9	0.65	0.9	0.9
1100000	0.85	0.85	0.85	0.65	0.9	0.9
1150000	0.85	0.8	0.85	0.6	0.95	0.95
1200000	0.85	0.75	0.9	0.6	0.95	0.95
1250000	0.9	0.75	0.9	0.6	-	-
1300000	0.9	0.8	0.9	0.6	-	-
1350000	0.9	0.8	0.9	-	-	-
1400000	0.9	0.8	0.9	-	-	-

Appendix E

Strickler's Coefficient Values in CHARIMA model

Mississippi River Main Channel				
Point	**Link**	**River Mile**	**Ks**	**n**
1	101	0.07	60	0.017
2	101	0.2	60	0.017
3	101	0.35	60	0.017
4	101	0.58	60	0.017
5	101	0.7	60	0.017
6	101	0.98	60	0.017
7	101	1.1	60	0.017
8	101	1.25	60	0.017
9	101	1.4	60	0.017
10	101	1.53	60	0.017
11	101	1.7	60	0.017
12	101	2.08	60	0.017
13	101	2.28	60	0.017
14	101	2.46	60	0.017
15	101	2.65	60	0.017
16	101	2.75	60	0.017
1	1	2.95	65	0.015
2	1	3.15	65	0.015
1	3	3.36	65	0.015
2	3	3.6	65	0.015
3	3	3.83	65	0.015
4	3	4.04	65	0.015
5	3	4.26	65	0.015
6	3	4.46	65	0.015
1	5	4.7	65	0.015
2	5	4.9	65	0.015
3	5	5.1	65	0.015
4	5	5.3	65	0.015
5	5	5.5	65	0.015
6	5	5.8	65	0.015
7	5	6	65	0.015
8	5	6.2	65	0.015
9	5	6.5	65	0.015
10	5	6.7	65	0.015
11	5	6.9	65	0.015
12	5	7.3	65	0.015
13	5	7.5	65	0.015
14	5	7.94	65	0.015
15	5	8.1	65	0.015

16	5	8.4	65	0.015
17	5	8.7	65	0.015
18	5	8.9	65	0.015
19	5	9.1	65	0.015
20	5	9.4	65	0.015
21	5	9.7	65	0.015
22	5	9.97	65	0.015
23	5	10.2	65	0.015
1	9	10.35	65	0.015
2	9	10.54	65	0.015
3	9	10.725	65	0.015
4	9	11.07	65	0.015
5	9	11.2	65	0.015
1	11	11.46	65	0.015
2	11	11.72	65	0.015
3	11	11.98	65	0.015
4	11	12.26	65	0.015
5	11	12.5	65	0.015
6	11	12.77	65	0.015
7	11	12.99	65	0.015
8	11	13.25	65	0.015
9	11	13.56	65	0.015
10	11	13.86	65	0.015
11	11	14.21	65	0.015
12	11	14.5	65	0.015
13	11	14.76	65	0.015
14	11	15.05	65	0.015
15	11	15.32	65	0.015
16	11	15.57	65	0.015
1	121	15.86	65	0.015
2	121	16.23	65	0.015
3	121	16.51	65	0.015
4	121	16.8	65	0.015
5	121	17.12	65	0.015
6	121	17.39	65	0.015
7	121	17.72	65	0.015
8	121	18	65	0.015
9	121	18.33	65	0.015
10	121	18.58	65	0.015
11	121	18.85	65	0.015

1	123	19.11	65	0.015
2	123	19.4	65	0.015
1	124	19.6	67	0.015
2	124	19.86	67	0.015
1	126	20.12	67	0.015
2	126	20.48	67	0.015
3	126	20.73	67	0.015
4	126	21.02	67	0.015
5	126	21.3	67	0.015
6	126	21.66	67	0.015
7	126	22	67	0.015
8	126	22.37	67	0.015
9	126	22.7	67	0.015
10	126	23.08	67	0.015
11	126	23.48	67	0.015
12	126	23.83	67	0.015
1	13	24.22	67	0.015
2	13	24.57	67	0.015
3	13	24.89	67	0.015
4	13	25.24	67	0.015
5	13	25.56	67	0.015
6	13	25.98	67	0.015
7	13	26.36	67	0.015
8	13	26.74	67	0.015
9	13	27.06	67	0.015
10	13	27.39	67	0.015
11	13	27.7	67	0.015
12	13	28.03	67	0.015
13	13	28.32	67	0.015
14	13	28.53	67	0.015
15	13	28.79	67	0.015
16	13	28.98	67	0.015
17	13	29.24	67	0.015
18	13	29.46	67	0.015
19	13	29.65	67	0.015
20	13	29.89	67	0.015
21	13	30.15	67	0.015
22	13	30.4	67	0.015
23	13	30.59	67	0.015
24	13	30.78	67	0.015
25	13	30.98	67	0.015

26	13	31.17	67	0.015
27	13	31.37	67	0.015
28	13	31.57	67	0.015
29	13	31.88	67	0.015
30	13	32.13	67	0.015
1	16	32.4	45	0.022
2	16	32.41	45	0.022
1	22	32.45	45	0.022
2	22	32.6	45	0.022
1	26	32.7	45	0.022
2	26	32.8	45	0.022
1	30	32.89	55	0.018
2	30	33.17	55	0.018
3	30	33.53	55	0.018
4	30	33.83	55	0.018
5	30	34.18	55	0.018
6	30	34.53	55	0.018
7	30	34.93	55	0.018
8	30	35.15	55	0.018
9	30	35.45	55	0.018
10	30	35.71	55	0.018
11	30	36.05	55	0.018
12	30	36.33	55	0.018
13	30	36.62	55	0.018
14	30	36.87	55	0.018
15	30	37.17	55	0.018
16	30	37.45	55	0.018
17	30	37.77	55	0.018
18	30	38.08	55	0.018
19	30	38.32	55	0.018
20	30	38.62	55	0.018
1	34	38.92	65	0.015
2	34	39.22	65	0.015
3	34	39.51	65	0.015
4	34	39.77	65	0.015
5	34	40.08	65	0.015
6	34	40.36	65	0.015
7	34	40.64	65	0.015
8	34	40.91	65	0.015
9	34	41.22	65	0.015
10	34	41.51	65	0.015

11	34	41.87	65	0.015
12	34	42.19	65	0.015
13	34	42.5	65	0.015
14	34	42.84	65	0.015
15	34	43.17	65	0.015
16	34	43.46	65	0.015
17	34	43.73	65	0.015
18	34	44.04	65	0.015
19	34	44.31	65	0.015
20	34	44.63	65	0.015
21	34	44.93	65	0.015
22	34	45.23	65	0.015
23	34	45.54	65	0.015
24	34	45.93	65	0.015
25	34	46.32	65	0.015
26	34	46.69	65	0.015
27	34	47.11	65	0.015
28	34	47.44	65	0.015
29	34	47.81	65	0.015
30	34	48.14	65	0.015
31	34	48.46	65	0.015
32	34	48.8	65	0.015
1	35	49.1	65	0.015
2	35	49.5	65	0.015
3	35	49.8	65	0.015
4	35	50.2	65	0.015
5	35	50.5	65	0.015
6	35	50.9	65	0.015
7	35	51.2	65	0.015
8	35	51.6	65	0.015
9	35	51.9	65	0.015
10	35	52.3	65	0.015
11	35	52.6	65	0.015
12	35	53	65	0.015
13	35	53.3	65	0.015
14	35	53.6	65	0.015
15	35	53.9	65	0.015
16	35	54.2	65	0.015
17	35	54.5	65	0.015
18	35	54.8	65	0.015
19	35	55.1	65	0.015

20	35	55.4	65	0.015
21	35	55.8	65	0.015
22	35	56.2	65	0.015
23	35	56.5	65	0.015
24	35	56.9	65	0.015
25	35	57.3	65	0.015
26	35	57.6	65	0.015
27	35	57.9	65	0.015
28	35	58.2	65	0.015
29	35	58.4	65	0.015
30	35	58.8	65	0.015
31	35	59.1	65	0.015
1	36	59.3	65	0.015
2	36	59.5	65	0.015
3	36	59.7	65	0.015
4	36	60	65	0.015
5	36	60.2	65	0.015
6	36	60.4	65	0.015
7	36	60.6	65	0.015
8	36	60.8	65	0.015
9	36	61	65	0.015
10	36	61.3	65	0.015
11	36	61.6	65	0.015
12	36	61.9	65	0.015
13	36	62.1	65	0.015
14	36	62.3	65	0.015
15	36	62.6	65	0.015
16	36	62.9	65	0.015
17	36	63.1	65	0.015
18	36	63.4	65	0.015
19	36	63.6	65	0.015
20	36	63.9	65	0.015
21	36	64.2	65	0.015
22	36	64.5	65	0.015
23	36	64.7	65	0.015
24	36	65	65	0.015
1	37	65.3	65	0.015
2	37	65.6	65	0.015
3	37	65.8	65	0.015
4	37	66.14	65	0.015
5	37	66.4	65	0.015

6	37	66.6	65	0.015
7	37	66.9	65	0.015
8	37	67.1	65	0.015
9	37	67.31	65	0.015
10	37	67.5	65	0.015
11	37	67.78	65	0.015
12	37	68	65	0.015
13	37	68.22	65	0.015
14	37	68.41	65	0.015
15	37	68.64	65	0.015
16	37	68.84	65	0.015
17	37	69.1	65	0.015
18	37	69.4	65	0.015
19	37	69.7	65	0.015
20	37	69.9	65	0.015
21	37	70.1	65	0.015
22	37	70.3	65	0.015
23	37	70.6	65	0.015
24	37	70.8	65	0.015
25	37	71	65	0.015
26	37	71.2	65	0.015
27	37	71.5	65	0.015
28	37	71.7	65	0.015
29	37	71.9	65	0.015
30	37	72.2	65	0.015
31	37	72.3	65	0.015
32	37	72.6	65	0.015
33	37	72.8	65	0.015
34	37	73	65	0.015
35	37	73.2	65	0.015
36	37	73.3	65	0.015
37	37	73.6	65	0.015
38	37	73.8	65	0.015
39	37	74.1	65	0.015
40	37	74.4	65	0.015
41	37	74.6	65	0.015
42	37	74.9	65	0.015
43	37	75.1	65	0.015
44	37	75.3	65	0.015
45	37	75.5	65	0.015
46	37	75.7	65	0.015

47	37	76	65	0.015
48	37	76.3	65	0.015

Southwest Pass				
Point	**Link**	**River Mile**	**Ks**	**n**
1	109	0	40	0.025
2	109	0.19	40	0.025
3	109	0.36	40	0.025
4	109	0.56	40	0.025
5	109	0.74	40	0.025
6	109	0.94	40	0.025
7	109	1.1	40	0.025
8	109	1.29	40	0.025
9	109	1.44	40	0.025
10	109	1.64	40	0.025
11	109	1.84	40	0.025
12	109	1.91	40	0.025
13	109	2.06	40	0.025
14	109	2.27	40	0.025
15	109	2.43	40	0.025
16	109	2.53	40	0.025
17	109	2.69	40	0.025
18	109	2.85	40	0.025
1	107	0	40	0.025
2	107	0.16	40	0.025
3	107	0.22	40	0.025
4	107	0.37	40	0.025
5	107	0.52	40	0.025
6	107	0.68	40	0.025
7	107	0.84	40	0.025
8	107	1	40	0.025
9	107	1.14	40	0.025
10	107	1.23	40	0.025
11	107	1.38	40	0.025
12	107	1.52	40	0.025
13	107	1.67	40	0.025
14	107	1.83	40	0.025
15	107	1.98	40	0.025
16	107	2.13	40	0.025
17	107	2.22	40	0.025
18	107	2.37	40	0.025
19	107	2.53	40	0.025

20	107	2.69	40	0.025
21	107	2.87	40	0.025
22	107	3.05	40	0.025
23	107	3.24	40	0.025
24	107	3.44	40	0.025
25	107	3.61	40	0.025
26	107	3.8	40	0.025
27	107	4	40	0.025
28	107	4.19	40	0.025
29	107	4.37	40	0.025
30	107	4.55	40	0.025
31	107	4.73	40	0.025
32	107	4.93	40	0.025
33	107	5.12	40	0.025
34	107	5.31	40	0.025
35	107	5.48	40	0.025
36	107	5.67	40	0.025
37	107	5.85	40	0.025
38	107	6.04	40	0.025
39	107	6.25	40	0.025
40	107	6.47	40	0.025
41	107	6.68	40	0.025
42	107	6.88	40	0.025
43	107	7.07	40	0.025
44	107	7.25	40	0.025
45	107	7.44	40	0.025
46	107	7.62	40	0.025
47	107	7.8	40	0.025
48	107	7.97	40	0.025
49	107	8.19	40	0.025
50	107	8.36	40	0.025
51	107	8.57	40	0.025
52	107	8.7	40	0.025
53	107	8.88	40	0.025
54	107	9.08	40	0.025
55	107	9.28	40	0.025
56	107	9.48	40	0.025
57	107	9.68	40	0.025
58	107	9.87	40	0.025
1	105	0	40	0.025
2	105	0.15	40	0.025

3	105	0.33	40	0.025
4	105	0.41	40	0.025
5	105	0.55	40	0.025
6	105	0.72	40	0.025
7	105	0.84	40	0.025
8	105	0.92	40	0.025
9	105	1.07	40	0.025
10	105	1.2	40	0.025
11	105	1.35	40	0.025
12	105	1.5	40	0.025
13	105	1.64	40	0.025
14	105	1.8	40	0.025
15	105	1.93	40	0.025
16	105	2.14	40	0.025
17	105	2.28	40	0.025
18	105	2.45	40	0.025
19	105	2.6	40	0.025
20	105	2.76	40	0.025
21	105	2.91	40	0.025
22	105	3.05	40	0.025
23	105	3.22	40	0.025
24	105	3.36	40	0.025
25	105	3.49	40	0.025
26	105	3.65	40	0.025
27	105	3.82	40	0.025
28	105	3.97	40	0.025
29	105	4.13	40	0.025
30	105	4.27	40	0.025
31	105	4.44	40	0.025
32	105	4.59	40	0.025
1	103	0.1	33	0.030
2	103	0.5	33	0.030
Burrwood in Southwest Pass (RM -14.5)				
Point	**Link**	**River Mile**	**Ks**	**n**
1	108	0	5.5	0.182
2	108	0.67	5.5	0.182
Joseph Southwest Pass (RM -4.5)				
Point	**Link**	**River Mile**	**Ks**	**n**
1	106	0	5.5	0.182
2	106	1.7	5.5	0.182

South Pass				
Point	**Link**	**River Mile**	**Ks**	**n**
1	104	0	47	0.021
2	104	0.12	47	0.021
3	104	0.29	47	0.021
4	104	0.44	47	0.021
5	104	0.58	47	0.021
6	104	0.73	47	0.021
7	104	0.89	47	0.021
8	104	1.03	47	0.021
9	104	1.16	47	0.021
10	104	1.33	47	0.021
11	104	1.49	47	0.021
12	104	1.63	47	0.021
13	104	1.8	47	0.021
14	104	1.92	47	0.021
15	104	2.07	47	0.021
16	104	2.24	47	0.021
17	104	2.4	47	0.021
18	104	2.54	47	0.021
19	104	2.68	47	0.021
20	104	2.84	47	0.021
21	104	3	47	0.021
22	104	3.15	47	0.021
23	104	3.3	47	0.021
24	104	3.46	47	0.021
25	104	3.59	47	0.021
26	104	3.74	47	0.021
27	104	3.94	47	0.021
28	104	4.13	47	0.021
29	104	4.26	47	0.021
30	104	4.38	47	0.021
31	104	4.53	47	0.021
32	104	4.67	47	0.021
33	104	4.8	47	0.021
34	104	4.98	47	0.021
35	104	5.13	47	0.021
36	104	5.29	47	0.021
37	104	5.42	47	0.021
38	104	5.58	47	0.021
39	104	5.75	47	0.021

40	104	5.92	47	0.021
41	104	6.06	47	0.021
42	104	6.23	47	0.021
43	104	6.39	47	0.021
44	104	6.53	47	0.021
45	104	6.67	47	0.021
46	104	6.82	47	0.021
47	104	7.01	47	0.021
48	104	7.13	47	0.021
49	104	7.29	47	0.021
50	104	7.43	47	0.021
51	104	7.6	47	0.021
52	104	7.76	47	0.021
53	104	7.92	47	0.021
54	104	8.04	47	0.021
55	104	8.19	47	0.021
56	104	8.33	47	0.021
57	104	8.44	47	0.021
58	104	8.6	47	0.021
59	104	8.78	47	0.021
60	104	8.9	47	0.021
61	104	9.07	47	0.021
62	104	9.24	47	0.021
63	104	9.36	47	0.021
64	104	9.5	47	0.021
65	104	9.67	47	0.021
66	104	9.8	47	0.021
67	104	9.99	47	0.021
68	104	10.15	47	0.021
69	104	10.3	47	0.021
70	104	10.44	47	0.021
71	104	10.56	47	0.021
72	104	10.71	47	0.021
73	104	10.9	47	0.021
74	104	11.05	47	0.021
75	104	11.2	47	0.021
76	104	11	47	0.021
77	104	11.5	47	0.021
78	104	11.66	47	0.021
79	104	11.82	47	0.021

Pass A Loutre				
Point	**Link**	**River Mile**	**Ks**	**n**
1	102	0	35	0.029
2	102	0.5	35	0.029
3	102	1	35	0.029
4	102	1.5	35	0.029
5	102	2	35	0.029
6	102	2.5	35	0.029
7	102	3	35	0.029
8	102	3.5	35	0.029
9	102	4	35	0.029
10	102	4.5	35	0.029
11	102	5	35	0.029
12	102	5.5	35	0.029
13	102	6	35	0.029
14	102	6.5	35	0.029
15	102	7	35	0.029
16	102	7.5	35	0.029
17	102	8	35	0.029
18	102	8.5	35	0.029
19	102	9	35	0.029
20	102	9.5	35	0.029
21	102	10	35	0.029
22	102	10.5	35	0.029
23	102	11	35	0.029
24	102	11.19	35	0.029
25	102	11.3	35	0.029
26	102	11.54	35	0.029
27	102	11.65	35	0.029
28	102	11.78	35	0.029
29	102	11.85	35	0.029

Main Pass				
Point	**Link**	**River Mile**	**Ks**	**n**
1	2	0	32	0.031
2	2	0.23	32	0.031
3	2	0.47	32	0.031
4	2	0.65	32	0.031
5	2	0.84	32	0.031
6	2	1.05	32	0.031
7	2	1.23	32	0.031
8	2	1.41	32	0.031
9	2	1.62	32	0.031
10	2	1.82	32	0.031
11	2	2.02	32	0.031
12	2	2.18	32	0.031
13	2	2.36	32	0.031
14	2	2.6	32	0.031
15	2	2.79	32	0.031
16	2	3.03	32	0.031
17	2	3.23	32	0.031
18	2	3.38	32	0.031
19	2	3.57	32	0.031
20	2	3.77	32	0.031
21	2	3.95	32	0.031
22	2	4.16	32	0.031
23	2	4.37	32	0.031
24	2	4.54	32	0.031
25	2	4.74	32	0.031
26	2	4.91	32	0.031
27	2	5.09	32	0.031
28	2	5.29	32	0.031
29	2	5.47	32	0.031
30	2	5.64	32	0.031
31	2	5.86	32	0.031
32	2	6.06	32	0.031
33	2	6.27	32	0.031
34	2	6.47	32	0.031
35	2	6.65	32	0.031
36	2	6.84	32	0.031
37	2	7.01	32	0.031
38	2	7.17	32	0.031
39	2	7.33	32	0.031

40	2	7.5	32	0.031
41	2	7.73	32	0.031
42	2	7.79	32	0.031
43	2	8.15	32	0.031
44	2	8.46	32	0.031
45	2	8.73	32	0.031
46	2	9	32	0.031
47	2	9.28	32	0.031
48	2	9.55	32	0.031
49	2	9.85	32	0.031
50	2	10.19	32	0.031

West Bay				
Point	**Link**	**River Mile**	**Ks**	**n**
1	4	0	7.5	0.133
2	4	2	7.5	0.133
3	4	1.89	7.5	0.133
4	4	2.1	7.5	0.133
5	4	2.21	7.5	0.133
6	4	2.23	7.5	0.133
7	4	2.24	7.5	0.133
8	4	2.28	7.5	0.133
9	4	2.32	7.5	0.133
10	4	2.34	7.5	0.133
11	4	2.36	7.5	0.133
12	4	2.38	7.5	0.133
13	4	2.4	7.5	0.133

Grand Pass				
Point	**Link**	**River Mile**	**Ks**	**n**
1	6	0	41	0.024
2	6	0.19	41	0.024
3	6	0.39	41	0.024
4	6	0.58	41	0.024
5	6	0.76	41	0.024
1	7	0	41	0.024
2	7	0.13	41	0.024
3	7	0.32	41	0.024
4	7	0.53	41	0.024
5	7	0.73	41	0.024
6	7	0.9	41	0.024
7	7	1.09	41	0.024
8	7	1.29	41	0.024
9	7	1.47	41	0.024
10	7	1.68	41	0.024
11	7	1.83	41	0.024
12	7	2.04	41	0.024
13	7	2.22	41	0.024
14	7	2.44	41	0.024
15	7	2.65	41	0.024
16	7	2.81	41	0.024
17	7	2.96	41	0.024
18	7	3.15	41	0.024
19	7	3.37	41	0.024
20	7	3.54	41	0.024
21	7	3.7	41	0.024
22	7	3.93	41	0.024
23	7	4.1	41	0.024
24	7	4.31	41	0.024
25	7	4.53	41	0.024
26	7	4.69	41	0.024
27	7	4.89	41	0.024
28	7	5.05	41	0.024
29	7	5.2	41	0.024

Tiger Pass				
Point	**Link**	**River Mile**	**Ks**	**n**
1	8	0	41	0.024
2	8	0.19	41	0.024
3	8	0.35	41	0.024
4	8	0.54	41	0.024
5	8	0.71	41	0.024
6	8	0.92	41	0.024
7	8	1.1	41	0.024
8	8	1.28	41	0.024
9	8	1.48	41	0.024
10	8	1.69	41	0.024
11	8	1.86	41	0.024
12	8	2.02	41	0.024
13	8	2.24	41	0.024
14	8	2.43	41	0.024
15	8	2.63	41	0.024
16	8	2.8	41	0.024
17	8	2.99	41	0.024

Baptiste Collette				
Point	**Link**	**River Mile**	**Ks**	**n**
1	10	0	42	0.024
2	10	0.18	42	0.024
3	10	0.37	42	0.024
4	10	0.54	42	0.024
5	10	0.7	42	0.024
6	10	0.91	42	0.024
7	10	1.14	42	0.024
8	10	0.345	42	0.024
9	10	1.52	42	0.024
10	10	1.72	42	0.024
11	10	1.92	42	0.024
12	10	2.1	42	0.024
13	10	2.24	42	0.024
14	10	2.43	42	0.024
15	10	2.61	42	0.024
16	10	2.8	42	0.024
17	10	3	42	0.024
18	10	3.18	42	0.024
19	10	3.36	42	0.024

20	10	3.51	42	0.024
21	10	3.7	42	0.024
22	10	3.84	42	0.024
23	10	4.04	42	0.024
24	10	4.22	42	0.024
25	10	4.42	42	0.024
26	10	4.56	42	0.024
27	10	4.79	42	0.024
28	10	4.95	42	0.024
29	10	5.12	42	0.024
30	10	5.3	42	0.024
31	10	5.54	42	0.024
32	10	5.76	42	0.024
33	10	5.95	42	0.024
34	10	6.14	42	0.024
35	10	6.27	42	0.024

7 Cut weir				
Point	**Link**	**River Mile**	**Ks**	**n**
1	120	0	25	0.04
2	120	0.11	25	0.04
3	120	0.22	25	0.04
4	120	0.33	25	0.04
5	120	0.44	25	0.04
6	120	0.55	25	0.04

Fort St. Philip III				
Point	**Link**	**River Mile**	**Ks**	**n**
1	122	0	35	0.029
2	122	1.6	35	0.029
3	122	4.58	35	0.029
Fort St. Philip II				
Point	**Link**	**River Mile**	**Ks**	**n**
1	122	0	42	0.024
2	122	0.18	42	0.024
3	122	0.37	42	0.024
4	122	0.54	42	0.024
5	122	0.7	42	0.024
6	122	0.91	42	0.024
7	122	1.14	42	0.024

8	122	1.345	42	0.024
9	122	1.52	42	0.024
10	122	1.72	42	0.024
11	122	1.92	42	0.024
12	122	2.1	42	0.024
13	122	2.24	42	0.024
14	122	2.43	42	0.024
15	122	2.61	42	0.024
16	122	2.8	42	0.024
17	122	3	42	0.024
18	122	3.18	42	0.024
19	122	3.36	42	0.024
20	122	3.51	42	0.024
21	122	3.7	42	0.024
22	122	3.84	42	0.024
23	122	4.04	42	0.024
24	122	4.22	42	0.024
25	122	4.42	42	0.024
26	122	4.56	42	0.024
27	122	4.79	42	0.024
28	122	4.95	42	0.024
29	122	5.12	42	0.024
30	122	5.3	42	0.024
31	122	5.54	42	0.024
32	122	5.76	42	0.024
33	122	5.95	42	0.024
34	122	6.14	42	0.024
35	122	6.27	42	0.024
Fort St. Philip I				
Point	**Link**	**River Mile**	**Ks**	**n**
1	125	0	35	0.029
2	125	1.6	35	0.029
3	125	4.58	35	0.029

Ostrica				
Point	**Link**	**River Mile**	**Ks**	**n**
1	132	0	25	0.040
2	132	0.33	25	0.040
3	132	0.66	25	0.040
4	132	0.99	25	0.040
5	132	1.32	25	0.040

Bohemia D/S				
Point	**Link**	**River Mile**	**Ks**	**n**
1	17	0	6	0.167
2	17	0.1	6	0.167
1	14	weir link		
2	14	weir link		
1	15	0	6	0.167
2	15	0.1	6	0.167
Bohemia Intermediate				
Point	**Link**	**River Mile**	**Ks**	**n**
1	23	0	6	0.167
2	23	0.1	6	0.167
1	24	weir link		
2	24	weir link		
1	25	0	6	0.167
2	25	0.1	6	0.167
Bohemia U/S.				
Point	**Link**	**River Mile**	**Ks**	**n**
1	31	0	65	0.015
2	31	0.1	65	0.015
1	32	weir link		
2	32	weir link		
1	33	0	65	0.015
2	33	0.1	65	0.015

Bayou Lamoque South				
Point	**Link**	**River Mile**	**Ks**	**n**
1	18	0.49	55	0.018
2	18	0.5	55	0.018
3	18	0.54	55	0.018
4	18	0.57	55	0.018
1	19	Gate Link		
2	19	Gate Link		
1	20	0	55	0.018
2	20	0.05	55	0.018
3	20	0.09	55	0.018
4	20	0.13	55	0.018
5	20	0.18	55	0.018
6	20	0.22	55	0.018
7	20	0.28	55	0.018
8	20	0.33	55	0.018
9	20	0.38	55	0.018
10	20	0.42	55	0.018
11	20	0.46	55	0.018
12	20	0.47	55	0.018
Bayou Lamoque North				
Point	**Link**	**River Mile**	**Ks**	**n**
1	27	0.52	55	0.018
2	27	0.53	55	0.018
3	27	0.55	55	0.018
4	27	0.585	55	0.018
1	28	Gate Link		
2	28	Gate Link		
1	29	0	55	0.018
2	29	0.05	55	0.018
3	29	0.011	55	0.018
4	29	0.19	55	0.018
5	29	0.25	55	0.018
6	29	0.31	55	0.018
7	29	0.37	55	0.018
8	29	0.4	55	0.018
9	29	0.44	55	0.018
10	29	0.47	55	0.018
11	29	0.5	55	0.018
12	29	0.511	55	0.018

Bayou Lamoque North & South				
Point	**Link**	**River Mile**	**Ks**	**n**
1	21	0	55	0.018
2	21	0.34	55	0.018
3	21	0.63	55	0.018
4	21	0.92	55	0.018
5	21	1.22	55	0.018
6	21	1.5	55	0.018
7	21	1.76	55	0.018
8	21	2.01	55	0.018
9	21	2.21	55	0.018
10	21	2.4	55	0.018
11	21	2.48	55	0.018
12	21	2.55	55	0.018
13	21	2.63	55	0.018
14	21	2.7	55	0.018
15	21	2.77	55	0.018
16	21	2.84	55	0.018
17	21	2.9	55	0.018
18	21	2.96	55	0.018
19	21	3.03	55	0.018
20	21	3.09	55	0.018
21	21	3.13	55	0.018

VITA

Tshering Thindu Gurung was born in Kagbeni, Mustang – Nepal on March 11, 1989. He graduated from high school in 2007. In May 2012, he obtained a 4-year degree of Bachelor in Civil Engineering at the University of New Orleans in New Orleans, LA. In August 2012, he enrolled in the University of New Orleans Master's program in Civil Engineering.

During his master's program, he has been working as a research assistant at the Department of Civil and Environmental Engineering of the University of New Orleans. The focus of his research has been the hydrodynamic numerical modeling applied to the Lower Mississippi River.